

canceling the adverse channel effects. The term pre-emphasis unit is used as another term for the term "equalizer unit" in the following. If a signal passes through both the transmission channel 13 and the pre-emphasis unit 112, the resulting signal shows no frequency dependent loss anymore, and the unwanted inter-symbol interference is reduced to zero in the ideal case. The pre-emphasis unit 112 can also be called predistortion filter.

The pre-emphasis unit 112 comprises an input for setting parameters P. The parameters can also be called coefficients or weights. By means of these parameters P, the frequency dependent gain curve of the pre-emphasis unit 112 is adjusted. In particular, the pre-emphasis unit 112 can be a programmable finite impulse response (FIR) filter having a characteristic such as $V_{out} = c_0 * V_{in1} + c_1 * V_{in2} + \dots$, with c_0, c_1 as adjustable parameters of the pre-emphasis unit.

In order to transmit a pulse via a transmission channel 13 showing a frequency dependent loss in particular at high frequencies, the pre-emphasis unit 13 has to be programmed by parameters such that the initial part of the pulse to be transmitted might be amplified in order to amplify in particular high frequencies characterized by edges of a pulse or vice versa damp the amplitude of low frequency components. By applying the right parameters to the pre-emphasis unit, the joint frequency response of the pre-emphasis unit and the transmission channel can nearly be provoked to show a constant loss over the frequencies of interest.

The sender 11 further comprises a bit pattern sequence generator 111 for generating bit pattern sequences BSP. The fact that the generator is called bit pattern generator does not limit its mode of operation to generate binary digits: Dependent on the way of coding that is used, the bit pattern generator 111 might also provide multilevel patterns or whatever reference signal is needed. In particular, a so called PRBS7 bit pattern sequence is generated and applied during the initialization phase, which PRBS7 bit pattern sequence comprises a defined sequence of 127 bits with around the same number of "0" digits as the number of "1" digits, and which is transmitted repeatedly. The PRBS7 sequence is generated by means of a feedback shift register. Such feedback shift register is also used on the receiver's side for receiving the PRBS7 sequence. These registers are not shown in detail in FIG. 4. In general, every pseudo random bit sequence can be transmitted, as long as this sequence is known at the receiver.

FOR THE PURPOSES OF INFORMATION ONLY

Codes used to identify States party to the PCT on the front pages of pamphlets publishing international applications under the PCT.

AL	Albania	ES	Spain	LS	Lesotho	SI	Slovenia
AM	Armenia	FI	Finland	LT	Lithuania	SK	Slovakia
AT	Austria	FR	France	LU	Luxembourg	SN	Senegal
AU	Australia	GA	Gabon	LV	Latvia	SZ	Swaziland
AZ	Azerbaijan	GB	United Kingdom	MC	Monaco	TD	Chad
BA	Bosnia and Herzegovina	GE	Georgia	MD	Republic of Moldova	TG	Togo
BB	Barbados	GH	Ghana	MG	Madagascar	TJ	Tajikistan
BE	Belgium	GN	Guinea	MK	The former Yugoslav Republic of Macedonia	TM	Turkmenistan
BF	Burkina Faso	GR	Greece			TR	Turkey
BG	Bulgaria	HU	Hungary	ML	Mali	TT	Trinidad and Tobago
BJ	Benin	IE	Ireland	MN	Mongolia	UA	Ukraine
BR	Brazil	IL	Israel	MR	Mauritania	UG	Uganda
BY	Belarus	IS	Iceland	MW	Malawi	US	United States of America
CA	Canada	IT	Italy	MX	Mexico	UZ	Uzbekistan
CF	Central African Republic	JP	Japan	NE	Niger	VN	Viet Nam
CG	Congo	KE	Kenya	NL	Netherlands	YU	Yugoslavia
CH	Switzerland	KG	Kyrgyzstan	NO	Norway	ZW	Zimbabwe
CI	Côte d'Ivoire	KP	Democratic People's Republic of Korea	NZ	New Zealand		
CM	Cameroon			PL	Poland		
CN	China	KR	Republic of Korea	PT	Portugal		
CU	Cuba	KZ	Kazakistan	RO	Romania		
CZ	Czech Republic	LC	Saint Lucia	RU	Russian Federation		
DE	Germany	LI	Liechtenstein	SD	Sudan		
DK	Denmark	LK	Sri Lanka	SE	Sweden		
EE	Estonia	LR	Liberia	SG	Singapore		

METHOD OF DESIGNING AGONISTS AND ANTAGONISTS TO IGF RECEPTOR

Field of the Invention

This invention relates to the field of receptor structure and receptor/ligand interactions. In particular it relates to the field of using
5 receptor structure to predict the structure of related receptors and to the use of the determined structures and predicted structures to select and screen for agonists and antagonists of the polypeptide ligands.

Background of the Invention

Insulin is the peptide hormone that regulates glucose uptake and
10 metabolism. The two types of diabetes mellitus are associated either with an inability to produce insulin because of destruction of the pancreatic islet cells (Homo-Delarche, F. & Boitard, C., 1996, Immunol. Today 10: 456-460) or with poor glucose metabolism resulting from either insulin resistance at the target tissues, or from inadequate insulin secretion by the islets or faulty liver
15 function (Taylor, S. I., et al., 1994, Diabetes, 43: 735-740).

Insulin-like growth factors-1 and 2 (IGF-1 and 2) are structurally related to insulin, but are more important in tissue growth and development than in metabolism. They are primarily produced in the liver in response to growth hormone, but are also produced in most other tissues, where they
20 function as paracrine/autocrine regulators. The IGFs are strong mitogens, and are involved in numerous physiological states and certain cancers (Baserga, R., 1996, TibTech 14: 150-152).

Epidermal growth factor (EGF) is a small polypeptide cytokine that is unrelated to the insulin/IGF family. It stimulates marked proliferation of
25 epithelial tissues, and is a member of a larger family of structurally-related cytokines, such as transforming growth factor α , amphiregulin, betacellulin, heparin-binding EGF and some viral gene products. Abnormal EGF family signalling is a characteristic of certain cancers (Soler, C. & Carpenter, G., 1994 In Nicola, N. (ed) Guidebook to Cytokines and Their receptors", Oxford
30 Univ. Press, Oxford, pp194-197; Walker, F. & Burgess, A. W., 1994, In Nicola, N. (ed) Guidebook to Cytokines and Their receptors", Oxford Univ. Press, Oxford, pp198-201).

Each of these growth factors mediates its biological actions through binding to the corresponding receptor. The IR, IGF-1R and the insulin
35 receptor-related receptor (IRR), for which the ligand is not known, are closely related to each other, and are referred to as the insulin receptor subfamily. A

large body of information is now available concerning the primary structure of these insulin receptor subfamily members (Ebina, Y., et al., 1985 *Cell* 40: 747-758; Ullrich, A., et al., 1985, *Nature* 313: 756-761; Ullrich, A. et al., 1986, *EMBO J* 5: 2503-2512; Shier, P. & Watt, V. M., 1989, *J. Biol. Chem.* 264: 14605-14608) and the identification of some of their functional domains (for reviews see De Meyts, P. 1994, *Diabetologia* 37: 135-148; Lee, J. & Pilch, P. F. 1994 *Amer. J. Physiol.* 266: C319-C334.; Schaffer, L. 1994, *Eur. J. Biochem.* 221: 1127-1132). IGF-1R, IR and IRR are members of the tyrosine kinase receptor superfamily and are closely related to the epidermal growth factor receptor (EGFR) subfamily, with which they share significant sequence identity in the extracellular region as well as in the cytoplasmic kinase domains (Ullrich, A. et al., 1984 *Nature* 309: 418-425; Ward, C. W. et al., 1995 *Proteins: Structure Function & Genetics* 22: 141-153). Both the insulin and EGF receptor subfamilies have a similar arrangement of two homologous domains (L1 and L2) separated by a cys-rich region of approximately 160 amino acids containing 22-24 cys residues (Bajaj, M., et al., 1987 *Biochim. Biophys. Acta* 916: 220-226; Ward, C. W. et al., 1995 *Proteins: Structure Function & Genetics* 22: 141-153). The C-terminal portion of the IGF-1R ectodomain (residues 463 to 906) is comprised of four domains: a connecting domain, two fibronectin type 3 (Fn3) repeats, and an insert domain (O'Bryan, J. P., et al., 1991 *Mol Cell Biol* 11: 5016-5031). The C-terminal portion of the EGFR ectodomain (residues 477-621) consists solely of a second cys-rich region containing 20 cys residues (Ullrich, A. et al., 1984, *Nature* 309: 418-425).

Little is known about the secondary, tertiary and quaternary structure of the ectodomains of these receptor subfamilies. Unlike the members of the EGFR subfamily which are transmembrane monomers which dimerise on binding ligand, the IR subfamily members are homodimers, held together by disulphide bonds. The extracellular region of the IR/IGF-1R/IRR monomers contains an α -chain (~ 703 to 735 amino acid residues) and 192-196 residues of the β -chain. There is a ~23 residue transmembrane segment, followed by the cytoplasmic portion (354 to 408 amino acids), which contains the catalytic tyrosine kinase domain flanked by juxtamembrane and C-tail regulatory regions and is responsible for mediating all receptor-specific functions (White, M. F. & Kahn, C. R. 1994 *J. Biol. Chem.* 269: 1-4). Chemical analyses of the receptor suggest that the α -chains are linked to the β -chains

via a single disulphide bond, with the IR dimer being formed by at least two α - α disulphide linkages (Finn, F. M., et al., 1990, Proc. Natl. Acad. Sci. 87: 419-423; Chiacchia, K. B., 1991, Biochem. Biophys. Res. Commun. 176, 1178-1182; Schaffer, L. & Ljungqvist, L., 1992, Biochem. Biophys. Res. Comm. 189: 650-653; Sparrow, L. G., et al., 1997, J. Biol. Chem. 47: 29460-29467).

Although the three-dimensional (3D) structures of the ligands EGF, TGF- α (Hommel, U., et al., 1992, J. Mol. Biol. 227:271-282), insulin (Dodson, E. J., et al., 1983, Biopolymers 22:281-291), IGF-1 (Sato, A., et al., 1993, Int J Peptide Protein Res 41:433-440) and IGF-2 (Torres, A. M., et al., 1995, J. Mol. Biol. 248:385-401) are known, and numerous analytical and functional studies of ligand binding to EGFR (Soler, C. & Carpenter, G., 1994 In Nicola (ed) Guidebook to Cytokines and Their receptors", Oxford Univ. Press, Oxford, pp194-197), IGF-1R and IR (see De Meyts, P., 1994 Diabetologia, 37:135-148) have been carried out, the mechanisms of ligand binding and subsequent transmembrane signalling have not been resolved.

Ligand-induced, receptor-mediated phosphorylation is the signalling mechanism by which most cytokines, polypeptide hormones and membrane-anchored ligands exert their biological effects. The primary kinase may be part of the intracellular portion of the transmembrane receptor protein, as in the tyrosine kinase receptors (for review see Yarden, Y., et al., 1988, Ann. Rev. Biochem. 57:443-478) or the Ser/Thr kinase receptors (Alevizopoulos, A. & Mermod, N., 1997, BioEssays, 19:581-591) or may be non-covalently associated with the cytoplasmic tail of the transmembrane protein(s) making up the receptor complex, as in the case of the haemopoietic growth factor receptors (Stahl, N., et al., 1995, Science 267:1349-1353). The end result is the same, ligand binding leads to receptor dimerization or oligomerization or a conformational change in pre-existing receptor dimers or oligomers, resulting in activation by transphosphorylation, of the covalently attached or non-covalently associated protein kinase domains (Hunter, T., 1995, Cell, 80:225-236).

Many oncogenes have been shown to be homologous to growth factors, growth factor receptors or molecules in the signal transduction pathways (Baserga, R., 1994 Cell, 79:927-930; Hunter, T., 1997 Cell, 88:333-346). One of the best examples is v-Erb (related to the EGFR). Since overexpression of a number of growth factor receptors results in ligand-dependent transformation, an alternate strategy for oncogenes is to regulate

the expression of growth factor receptors or their ligands or to directly bind to the receptors to stimulate the same effect (Baserga, R., 1994 Cell, 79:927-930). Examples are v-Src, which activates IGF-1 R intracellularly; c-Myb, which transforms cells by enhancing the expression of IGF1R; and SV40 T antigen which interacts with the IGF-1R and enhances the secretion of IGF-1 (see Baserga, R., 1994 Cell, 79:927-930 for review). Cells in which the IGF-1R has been disrupted or deleted cannot be transformed by SV40 T antigen. If oncogenes activate growth factors and their receptors, then tumour suppressor genes should have the opposite effect. One good example of this is the Wilm's tumour suppressor gene, WT1, which suppresses the expression of IGF-1R (Drummond, J. A., et al., 1992, Science, 257:275-277). Cells that are driven to proliferate by oncogenes undergo massive apoptosis when growth factor receptors are ablated, since, unlike normal cells, they appear unable to withdraw from the cell-cycle and enter into the G₀ phase (Baserga, R., 1994 Cell, 79:927-930).

The insulin-like growth factor-1 receptor (IGF-1R) is one of several growth-factor receptors that regulate the proliferation of mammalian cells. However, its ubiquitousness and certain unique aspects of its function make IGF-1R an ideal target for specific therapeutic interventions against abnormal growth, with very little effect on normal cells (see Baserga, R., 1996 TIBTECH, 14:150-152). The receptor is activated by IGF1, IGF2 and insulin, and plays a major role in cellular proliferation in at least three ways: it is essential for optimal growth of cells *in vitro* and *in vivo*; several cell types require IGF-1R to maintain the transformed state; and activated IGF-1R has a protective effect against apoptotic cell death (Baserga, R., 1996 TIBTECH, 14:150-152). These properties alone make it an ideal target for therapeutic interventions. Transgenic experiments have shown that IGF-1R is not an absolute requirement for cell growth, but is essential for the establishment of the transformed state (Baserga, R., 1994 Cell, 79: 927-930). In several cases (human glioblastoma, human melanoma; human breast carcinoma; human lung carcinoma; human ovarian carcinoma; human rhabdomyosarcoma; mouse melanoma, mouse leukaemia; rat glioblastoma; rat rhabdomyosarcoma; hamster mesothelioma) the transformed phenotype can be reversed by decreasing the expression of IGF-1R using antisense to IGF-1R (Baserga, R., 1996 TIBTECH 14:150-152); or by interfering with its function by antibodies to IGF-1R (human breast carcinoma; human

rhabdomyosarcoma) or by dominant negatives of IGF-1R (rat glioblastoma; Baserga, R., 1996 TIBTECH 14:150-152).

Three effects are observed when the function of IGF-1R is impaired: tumour cells undergo massive apoptosis which results in inhibition of tumourogenesis; surviving tumour cells are eliminated by a specific immune response; and such a host response can cause a regression of an established wild-type tumour (Resnicoff, M., et al., 1995, Cancer Res. 54:2218-2222). These effects, plus the fact that interference with IGF-1R function has a limited effect on normal cells (partial inhibition of growth without apoptosis) makes IGF-1R a unique target for therapeutic interventions (Baserga, R., 1996 TIBTECH 14:150-152). In addition IGF-1R is downstream of many other growth factor receptors, which makes it an even more generalised target. The implication of these findings is that if the number of IGF-1Rs on cells can be decreased or their function antagonised, then tumours cease to grow and can be removed immunologically. These studies establish that IGF-1R antagonists will be extremely important therapeutically.

Many cancer cells have constitutively active EGFR (Sandgreen, E. P., et al., 1990, Cell, 61:1121-135; Karnes, W. E. J., et al., 1992, Gastroenterology, 102:474-485) or other EGFR family members (Hines, N. E., 1993, Semin. Cancer Biol. 4:19-26). Elevated levels of activated EGFR occur in bladder, breast, lung and brain tumours (Harris, A. L., et al., 1989, In Furth & Greaves (eds) The Molecular Diagnostics of human cancer. Cold Spring Harbor Lab. Press, CSH, NY, pp353-357). Antibodies to EGFR can inhibit ligand activation of EGFR (Sato, J. D., et al., 1983 Mol. Biol. Med. 1:511-529) and the growth of many epithelial cell lines (Aboud-Pirak E., et al., 1988, J. Natl Cancer Inst. 85:1327-1331). Patients receiving repeated doses of a humanised chimeric anti-EGFR monoclonal antibody showed signs of disease stabilization. The large doses required and the cost of production of humanised monoclonal antibody is likely to limit the application of this type of therapy. These findings indicate that the development of EGF antagonists will be attractive anticancer agents.

Summary of the Invention

The present inventors have now obtained 3D structural information concerning the insulin-like growth factor receptor (IGF-1R). This information can be used to predict the structure of related members of the insulin

receptor family and provides a rational basis for the development of ligands for specific therapeutic applications.

Accordingly, in a first aspect the present invention provides a method of designing a compound able to bind to a molecule of the insulin receptor family and to modulate an activity mediated by the molecule, including the step of assessing the stereochemical complementarity between the compound and the receptor site of the molecule, wherein the receptor site includes:

- (a) amino acids 1 to 462 of the receptor for IGF-1, having the atomic coordinates substantially as shown in Figure 1;
- (b) a subset of said amino acids, or;
- (c) amino acids present in the amino acid sequence of a member of the insulin receptor family, which form an equivalent three-dimensional structure to that of the receptor molecule as depicted in Figure 1.

The phrase "insulin receptor family" encompasses, for example, IGF-1R, IR and IRR. In general, insulin receptor family members show similar domain arrangements and share significant sequence identity (preferably at least 40% identity).

By "stereochemical complementarity" we mean that the biologically active substance or a portion thereof correlates, in the manner of the classic "lock-and-key" visualisation of ligand-receptor interaction, with the groove in the receptor site.

In a preferred embodiment of this aspect of the invention, the compound is selected or modified from a known compound identified from a database.

In a further preferred embodiment, the compound is designed so as to complement the structure of the receptor molecule as depicted in Figure 1.

In a further preferred embodiment, the compound has structural regions able to make close contact with amino acid residues at the surface of the receptor site lining the groove, as depicted in Figure 2.

In a further preferred embodiment, the compound has a stereochemistry such that it can interact with both the L1 and L2 domains of the receptor site.

In a further preferred embodiment, the compound has a stereochemistry such that it can interact with the L1 domain of a first monomer of the receptor homodimer, and with the L2 domain of the other monomer of the receptor homodimer.

In a further preferred embodiment, the interaction of the compound with the receptor site alters the position of at least one of the L1, L2 or cysteine-

rich domains of the receptor molecule relative to the position of at least one of the other of said domains. Preferably, the compound interacts with the β sheet of the L1 domain of the receptor molecule, thereby causing an alteration in the position of the L1 domain relative to the position of the cysteine-rich domain or of the L2 domain. Alternatively, the compound interacts with the receptor site in the region of the interface between the L1 domain and the cysteine-rich domain of the receptor molecule, thereby causing the L1 domain and the cysteine-rich domain to move away from each other. In another preferred embodiment, the compound interacts with the hinge region between the L2 domain and the cysteine-rich domain of the receptor molecule, thereby causing an alteration in the positions of the L2 domain and the cysteine-rich domain relative to each other.

In a further preferred embodiment, the stereochemical complementarity between the compound and the receptor site is such that the compound has a K_b for the receptor site of less than $10^{-6}M$, more preferably is less than $10^{-8}M$.

In a further preferred embodiment or the first aspect of the present invention, the compound has the ability to increase an activity mediated by the receptor molecule.

In a further preferred embodiment, the compound has the ability to decrease an activity mediated by the receptor molecule. Preferably, the stereochemical interaction between the compound and the receptor site is adapted to prevent the binding of a natural ligand of the receptor molecule to the receptor site. It is preferred that the compound has a K_i of less than $10^{-6}M$, more preferably less than $10^{-8}M$ and more preferably less than $10^{-9}M$.

In a further preferred embodiment of the first aspect of the present invention, the receptor is the IGF-1R, or the insulin receptor.

In a second aspect, the present invention provides a computer-assisted method for identifying potential compounds able to bind to a molecule of the insulin receptor family and to modulate an activity mediated by the molecule, using a programmed computer including a processor, an input device, and an output device, including the steps of:

- (a) inputting into the programmed computer, through the input device, data comprising the atomic coordinates of the IGF-1R molecule as shown in Figure 1, or a subset thereof;
- (b) generating, using computer methods, a set of atomic coordinates of a structure that possesses stereochemical complementarity to the atomic

coordinates of the IGF-1R site as shown in Figure 1, or a subset thereof, thereby generating a criteria data set;

(c) comparing, using the processor, the criteria data set to a computer database of chemical structures;

5 (d) selecting from the database, using computer methods, chemical structures which are structurally similar to a portion of said criteria data set; and

(e) outputting, to the output device, the selected chemical structures which are similar to a portion of the criteria data set.

10 In a preferred embodiment of the second aspect, the programmed computer includes a data storage system which includes the database of chemical structures.

In a preferred embodiment of the second aspect, the method is used to identify potential compounds which have the ability to decrease an activity mediated by the receptor.

15 In another preferred embodiment, the computer-assisted method further includes the step of selecting one or more chemical structures from step (e) which interact with the receptor site of the molecule in a manner which prevents the binding of natural ligands to the receptor site.

20 In another preferred embodiment, the computer-assisted method further includes the step of obtaining a compound with a chemical structure selected in steps (d) and (e), and testing the compound for the ability to decrease an activity mediated by the receptor.

25 In a further preferred embodiment, the computer-assisted method is used to identify potential compounds which have the ability to increase an activity mediated by the receptor molecule.

In another preferred embodiment, the computer-assisted method further includes the step of obtaining a molecule with a chemical structure selected in steps (d) and (e), and testing the compound for the ability to increase an activity mediated by the receptor.

30 In a further preferred embodiment of the second aspect of the present invention, the receptor is the IGF-1R, or the insulin receptor.

35 In a third aspect, the present invention provides a method of screening of a putative compound having the ability to modulate the activity of a receptor of the insulin receptor family, including the steps of identifying a putative compound by a method according to the first or second aspects, and testing the

compound for the ability to increase or decrease an activity mediated by the receptor.

In a preferred embodiment of the third aspect, the test is carried out *in vitro*.

5 In a further preferred embodiment of the third aspect, the test is a high throughput assay.

In a preferred embodiment of the third aspect, the test is carried out *in vivo*.

10 Brief Description of the Drawings

Figure 1. IGF-1R residues 1-462, in terms of atomic coordinates refined to a resolution of 2.6 Å (average accuracy $\approx 0.3\text{\AA}$). The coordinates are in relation to a Cartesian system of orthogonal axes.

15

Figure 2. Depiction of the residues lining the groove of the IGF-1R receptor fragment 1-462.

Figure 3. Gel filtration chromatography of affinity-purified IGF-1R/462 protein. The protein was purified on a Superdex S200 column (Pharmacia) fitted to a BioLogic L.C. system (Biorad), equilibrated and eluted at 0.8 ml/min with 40 mM Tris/150 mM NaCl/0.02% NaN₃ adjusted to pH 8.0. (a) Protein eluting in peak 1 contained aggregated IGF-1R/462 protein, peak 2 contained monomeric protein and peak 3 contained the c-myc undecapeptide used for elution from the Mab 9E10 immunoaffinity column. (b) Non-reduced SDS-PAGE of fraction 2 from IGF-1R/462 obtained following Superdex S200 (Fig.1a). Standard proteins are indicated.

Figure 4. Ion exchange chromatography of affinity-purified, truncated IGF-1R ectodomain. A mixture of gradient and isocratic elution chromatography was performed on a Resource Q column (Pharmacia) fitted to a BioLogic System (Biorad), using 20 mM Tris/pH 8.0 as buffer A and the same buffer containing 1M NaCl as buffer B. Protein solution in TBSA was diluted at least 1:2 with water and loaded onto the column at 2 ml/min. Elution was monitored by absorbance (280 nm) and conductivity (mS/cm). Target protein (peak 2) eluted isocratically with 20 mM Tris/0.14 M NaCl pH 8.0. Inset:

Isoelectric focusing gel (pH 3 - 7; Novex Australia Pty Ltd) of fraction 2. The pI was estimated at 5.1 from standard proteins (not shown).

Figure 5. Polypeptide fold for residues 1-462 of IGF-1R. The L1 domain is at the top, viewed from the N-terminal end and L2 is at the bottom. The space at the centre is of sufficient size to accommodate IGF-1. Helices are indicated by curled ribbon and β -strands by arrows. Cysteine side chains are drawn as ball-and-stick with lines showing disulfide bonds. The arrow points in the direction of view for L1 in Figure 7.

Figure 6. Amino acid sequences of IGF-1R and related proteins. a, L1 and L2 domains of human IGF-1R and IR are shown based on a sequence alignment for the two proteins and a structural alignment for the L1 and L2 domains. Positions showing conservation physico-chemical properties of amino acids are boxed, residues used in the structural alignment are shown in Times Italic and residues which form the Trp 176 pocket are in Times Bold. Secondary structure elements for L1 (above the sequences) and L2 (below) are indicated as cylinders for helices and arrows for β -strands. Strands are shaded (pale, medium and dark grey) according to the β -sheet to which they belong. Disulfide bonds are also indicated. b, Cys-rich domains of human IGF-1R, IR and EGFR (domains 2 and 4) are aligned based on sequence and structural considerations. Secondary structural elements and disulfide bonds are indicated above the sequences. The dashed bond is only present in IR. Different types of disulfide bonded modules are labelled below the sequences as open, filled or broken lines. Boxed residues show conservation of physico-chemical properties and structurally conserved residues for modules 4-7 are shown in Times Italic. Residues from EGFR which do not conform to the pattern are in lowercase with probable disulfide bonding indicated below and the conserved Trp 176 and the semi-conserved Gln 182 are in Times Bold.

Figure 7. Stereo view of a superposition of the L1 (white) and L2 (black) domains. Residue numbers above are for L1 and below for L2. The side chain of Trp 176 which protrudes into the core of L1 is drawn as ball-and-stick.

Figure 8. Schematic diagram showing the association of three β -finger motifs. β -strands are drawn as arrows and disulfide bonds as zigzags.

Figure 9: Sequence alignment of hIGF-1R, hIR and hIRR ectodomains, derived by use of the PileUp program in the software package of the Genetics Computer Group, 575 Science Drive, Madison, Wisconsin, USA. For assignment of homologous 3D structures see Figure 6.

Figure 10 Gel filtration chromatography of insulin receptor ectodomain and MFab complexes. hIR -11 ectodomain dimer (5 - 20 mg) was complexed with MFab derivatives (15-25 mg each) of the anti-hIR antibodies 18-44, 83-7 and 83-14 (Soos et al., 1986). Elution profiles were generated from samples loaded on to a Superdex S200 column (Pharmacia), connected to a BioLogic chromatography system (Biorad) and monitored at 280 nm. The column was eluted at 0.8 ml/min with 40 mM Tris/150 mM sodium chloride/0.02% sodium azide buffer adjusted to pH 8.0: Profile 0, hIR -11 ectodomain, Profile 1, ectodomain mixed with MFab 18-44; Profile 2, ectodomain mixed with MFab 18-44 and MFab 83-14; Profile 3, ectodomain mixed with MFab 18-44, MFab 83-14 and MFab 83-7. The apparent mass of each complex was determined from a plot of the following standard proteins: thyroglobulin (660 kDa), ferritin (440 kDa), bovine gamma globulin (158 kDa), bovine serum albumin (67 kDa), chicken ovalbumin (44 kDa) and equine myoglobin (17 kDa).

Figure 11 Schematic representations of electron microscopy images of the hIR ectodomain dimer.

Detailed Description of the Invention

We describe herein the expression, purification, and crystallization of a recombinant truncated IGF-1R fragment (residues 1-462) containing the L1-cysteine-rich-L2 region of the ectodomain. The selected truncation position is just downstream of the exon 6/exon 7 junction (Abbott, A. M., et al., 1992. J Biol Chem., 267:10759-10763), and occurs at a position where the sequences of the IR and EGFR families diverge markedly (Ward, C. W., et al., 1995, Proteins: Struct., Funct., Genet. 22:141-153; Lax, I., et al., 1988, Molec. Cellul. Biol. 8:1970-1978) suggesting it represents a domain boundary. To

limit the effects of glycosylation, the IGF-1R fragment was expressed in Lec8 cells, a glycosylation mutant of Chinese hamster ovary (CHO) cells, whose defined glycosylation defect produces N-linked oligosaccharides truncated at N-acetyl glucosamine residues distal to mannose residues (Stanley, P. 1989, Molec. Cellul. Biol. 9:377-383). Such an approach has facilitated glycoprotein crystallization (Davis, S. J., et al., 1993, Protein Eng. 6:229-232; Liu, J., et al., 1996, J. Biol. Chem. 271:33639-33646).

The IGF-1R construct described herein includes a c-myc peptide tag (Hoogenboom, H. R., et al., 1991, Nucleic Acids Res. 19:4133-4137) that is recognised by the Mab 9E10 (Evan, G. I., et al., 1985, Mol. Cell. Biol. 5:3610-3616) enabling the expressed product to be purified by peptide elution from an antibody affinity column followed by gel filtration over Superdex S200. The purified proteins crystallized under a sparse matrix screen (Jancarik, J. & Kim, S.-H., 1991, J. Appl. Cryst. 24:409-411) but the crystals were of variable quality, with the best diffracting to 3.0-3.5 Å. Isocratic gradient elution by anion-exchange chromatography yielded protein that was less heterogenous and gave crystals of sufficient quality to determine the structure of the first three domains of the human IGF-1R.

The IGF-1R fragment consisted of residues 1-462 of IGF-1R linked via an enterokinase-cleavable pentapeptide sequence to an eleven residue c-myc peptide tag at the C-terminal end. The fragment was expressed in Lec8 cells by continuous media perfusion in a bioreactor using porous carrier disks. It was secreted into the culture medium and purified by peptide elution from an anti-c-myc antibody column followed by Superdex S200 gel filtration. The receptor fragment bound two anti-IGF-1R monoclonal antibodies, 24-31 and 24-60, which recognize conformational epitopes, but could not be shown to bind IGF-1 or IGF-2. Crystals of variable quality were grown as rhombic prisms in 1.7 M ammonium sulfate at pH 7.5 with the best diffracting to 3.0-3.5 Å. Further purification by isocratic elution on an anion-exchange column gave protein which produced better quality crystals, diffracting to 2.6 Å, that were suitable for X-ray structure determination.

The structure of this fragment (IGF-1R residues 1-462; L1-cys rich-L2 domains) has been determined to 2.6 Å resolution by X-ray diffraction. The L domains each adopt a compact shape consisting of a single stranded right-handed β -helix. The cys-rich region is composed of eight disulphide-bonded modules, seven of which form a rod-shaped domain with modules associated

in a novel manner. At the centre of this reasonably extended structure is a space, bounded by all three domains, and of sufficient size to accommodate a ligand molecule. Functional studies on IGF-1R and other members of the insulin receptor family show that the regions primarily responsible for hormone-binding map to this central site. Thus this structure gives a first view of how members of the insulin receptor family might interact with their ligands.

Another group has reported the crystallization of a related receptor, the EGFR, in a complex with its ligand EGF (Weber, W., et al., 1994, J Chromat. 679:181-189). However, difficulties were encountered with these crystals which diffracted to only 6 Å, insufficient for the determination of an atomic resolution structure of this complex (Weber, W., et al., 1994, J Chromat 679:181-189) or the generation of accurate models of structurally related receptor domains such as IGF-1R and IR by homology modelling.

The present inventors have developed 3D structural information about cytokine receptors in order to enable a more accurate understanding of how the binding of ligand leads to signal transduction. Such information provides a rational basis for the development of ligands for specific therapeutic applications, something that heretofore could not have been predicted *de novo* from available sequence data.

The precise mechanisms underlying the binding of agonists and antagonists to the IGF-1R site are not fully clarified. However, the binding of ligands to the receptor site, preferably with an affinity in the order of 10^{-8} M or higher, is understood to arise from enhanced stereochemical complementarity relative to naturally occurring IGF-1 ligands.

Such stereochemical complementarity, pursuant to the present invention, is characteristic of a molecule that matches intra-site surface residues lining the groove of the receptor site as enumerated by the coordinates set out in Figure 1. The residues lining the groove are depicted in Figure 2. By "match" we mean that the identified portions interact with the surface residues, for example, via hydrogen bonding or by enthalpy-reducing Van der Waals interactions which promote desolvation of the biologically active substance within the site, in such a way that retention of the biologically active substance within the groove is favoured energetically.

Substances which are complementary to the shape of the receptor site characterised by amino acids positioned at atomic coordinates set out in

Figure 1 may be able to bind to the receptor site and, when the binding is sufficiently strong, substantially prohibit binding of the naturally occurring ligands to the site.

It will be appreciated that it is not necessary that the
5 complementarity between ligands and the receptor site extend over all residues lining the groove in order to inhibit binding of the natural ligand. Accordingly, agonists or antagonists which bind to a portion of the residues lining the groove are encompassed by the present invention.

In general, the design of a molecule possessing stereochemical
10 complementarity can be accomplished by means of techniques that optimize, either chemically or geometrically, the "fit" between a molecule and a target receptor. Known techniques of this sort are reviewed by Sheridan and Venkataraghavan, *Acc. Chem Res.* 1987 20 322; Goodford, *J. Med. Chem.* 1984 27 557; Beddell, *Chem. Soc. Reviews* 1985, 279; Hol, *Angew. Chem.* 1986 25 767 and Verlinde C.L.M.J & Hol, *W.G.J. Structure* 1994, 2, 577, the
15 respective contents of which are hereby incorporated by reference. See also Blundell et al., *Nature* 1987 326 347 (drug development based on information regarding receptor structure).

Thus, there are two preferred approaches to designing a molecule,
20 according to the present invention, that complements the shape of IGF-1R or a related receptor molecule. By the geometric approach, the number of internal degrees of freedom (and the corresponding local minima in the molecular conformation space) is reduced by considering only the geometric (hard-sphere) interactions of two rigid bodies, where one body (the active
25 site) contains "pockets" or "grooves" that form binding sites for the second body (the complementing molecule, as ligand). The second preferred approach entails an assessment of the interaction of respective chemical groups ("probes") with the active site at sample positions within and around the site, resulting in an array of energy values from which three-dimensional
30 contour surfaces at selected energy levels can be generated.

The geometric approach is illustrated by Kuntz et al., *J. Mol. Biol.* 1982 161 269, the contents of which are hereby incorporated by reference, whose algorithm for ligand design is implemented in a commercial software package distributed by the Regents of the University of California and further
35 described in a document, provided by the distributor, which is entitled "Overview of the DOCK Package, Version 1.0," the contents of which are

hereby incorporated by reference. Pursuant to the Kuntz algorithm, the shape of the cavity represented by the IGF-R1 site is defined as a series of overlapping spheres of different radii. One or more extant data bases of crystallographic data, such as the Cambridge Structural Database System maintained by Cambridge University (University Chemical Laboratory, 5 Lensfield Road, Cambridge CB2 1EW, U.K.) and the Protein Data Bank maintained by Brookhaven National Laboratory (Chemistry Dept. Upton, NY 11973, U.S.A.), is then searched for molecules which approximate the shape thus defined.

10 Molecules identified in this way, on the basis of geometric parameters, can then be modified to satisfy criteria associated with chemical complementarity, such as hydrogen bonding, ionic interactions and Van der Waals interactions.

The chemical-probe approach to ligand design is described, for 15 example, by Goodford, J. Med. Chem. 1985 28 849, the contents of which are hereby incorporated by reference, and is implemented in several commercial software packages, such as GRID (product of Molecular Discovery Ltd., West Way House, Elms Parade, Oxford OX2 9LL, U.K.). Pursuant to this approach, the chemical prerequisites for a site-complementing molecule are identified 20 at the outset, by probing the active site (as represented via the atomic coordinates shown in Fig. 1) with different chemical probes, e.g., water, a methyl group, an amine nitrogen, a carboxyl oxygen, and a hydroxyl. Favored sites for interaction between the active site and each probe are thus determined, and from the resulting three-dimensional pattern of such sites a 25 putative complementary molecule can be generated.

The chemical-probe approach is especially useful in defining variants of a molecule known to bind the target receptor. Accordingly, crystallographic analysis of IGF-1 bound to the receptor site is expected to provide useful information regarding the interaction between the archetype 30 ligand and the active site of interest.

Programs suitable for searching three-dimensional databases to identify molecules bearing a desired pharmacophore include: MACCS-3D and ISIS/3D (Molecular Design Ltd., San Leandro, CA), ChemDBS-3D (Chemical Design Ltd., Oxford, U.K.), and Sybyl/3DB Unity (Tripos Associates, St. 35 Louis, MO).

Programs suitable for pharmacophore selection and design include: DISCO (Abbott Laboratories, Abbott Park, IL), Catalyst (Bio-CAD Corp., Mountain View, CA), and ChemDBS-3D (Chemical Design Ltd., Oxford, U.K.).

5 Databases of chemical structures are available from a number of sources including Cambridge Crystallographic Data Centre (Cambridge, U.K.) and Chemical Abstracts Service (Columbus, OH).

De novo design programs include Ludi (Biosym Technologies Inc., San Diego, CA), Sybyl (Tripos Associates) and Aladdin (Daylight Chemical
10 Information Systems, Irvine, CA).

Those skilled in the art will recognize that the design of a mimetic may require slight structural alteration or adjustment of a chemical structure designed or identified using the methods of the invention.

 The invention may be implemented in hardware or software, or a
15 combination of both. However, preferably, the invention is implemented in computer programs executing on programmable computers each comprising a processor, a data storage system (including volatile and non-volatile memory and/or storage elements), at least one input device, and at least one output device. Program code is applied to input data to perform the
20 functions described above and generate output information. The output information is applied to one or more output devices, in known fashion. The computer may be, for example, a personal computer, microcomputer, or workstation of conventional design.

 Each program is preferably implemented in a high level procedural or
25 object-oriented programming language to communicate with a computer system. However, the programs can be implemented in assembly or machine language, if desired. In any case, the language may be compiled or interpreted language.

 Each such computer program is preferably stored on a storage
30 medium or device (e.g., ROM or magnetic diskette) readable by a general or special purpose programmable computer, for configuring and operating the computer when the storage media or device is read by the computer to perform the procedures described herein. The inventive system may also be considered to be implemented as a computer-readable storage medium,
35 configured with a computer program, where the storage medium so

configured causes a computer to operate in a specific and predefined manner to perform the functions described herein.

Compounds designed according to the methods of the present invention may be assessed by a number of *in vitro* and *in vivo* assays of hormone function. For example, the identification of IGF-1R antagonists of may be undertaken using a solid-phase receptor binding assay. Potential antagonists may be screened for their ability to inhibit the binding of europium-labelled IGF ligands to soluble, recombinant IGF-1R in a microplate-based format. Europium is a lanthanide fluorophore, the presence of which can be measured using time-resolved fluorometry. The sensitivity of this assay matches that achieved by radioisotopes, measurement is rapid and is performed in a microplate format to allow high-sample throughput, and the approach is gaining wide acceptance as the method of choice in the development of screens for receptor agonists/antagonists (see Apell et.al. J. Biomolec. Screening 3:19-27, 1998 : Inglese et. al. Biochemistry 37:2372-2377, 1998).

Binding affinity and inhibitor potency may be measured for candidate inhibitors using biosensor technology.

The IGF-1R antagonists may be tested for their ability to modulate receptor activity using a cell-based assay incorporating a stably transfected, IGF-1-responsive reporter gene [Souriau, C., Fort, P., Roux, P., Hartley, O., LeFranc, M-P. and Weill, M., 1997, Nucleic Acids Res. 25, 1585-1590]. An IGF-1-responsive, luciferase reporter gene has been assembled and transfected in 293 cells. The assay addresses the ability of IGF-1 to activate the reporter gene in the presence of novel ligands. It offers a rapid (results within 6-8 hours of hormone exposure), high-throughput (assay can be conducted in a 96-well format for automated counting) analysis using an extremely sensitive detection system (chemiluminescence). Once candidate compounds have been identified, their ability to antagonise signal transduction via the IGF-1R can be assessed using a number of routine *in vitro* cellular assays such as inhibition of IGF-1-mediated cell proliferation, induction of apoptosis in the presence of IGF-1 and the ablation of IGF-1-driven anchorage-independent cell growth in soft agar [D'Ambrosio, C., Ferber, A., Resnicoff, M. and Baserga, R., 1996, Cancer Res. 56, 4013-4020]. Such assays may be conducted on the P6 cell line, a cell line highly responsive to IGF as a result of the constitutive overexpression of the IGF-1R

(45-50,000 receptors/cell, [Pietrzkowski, Z., Sell, C., Lammers, R., Ullrich, A. and Baserga, R., 1992, Cell Growth Diff. 3, 199-205]). Ultimately, the efficacy of any antagonist as a tumour therapeutic may be tested *in vivo* in animals bearing tumour isografts and xenografts as described [Resnicoff, M., Burgaud, J-L., Rotman, H. L., Abraham, D. and Baserga, R., 1995, Cancer Res. 55, 3739-3741; Resnicoff, M., Sell, C., Rubini, M., Coppola, D., Ambrose, D., Baserga, R. and Rubin, R., 1994 Cancer Res. 54: 2218-2222].

Tumour growth inhibition assays may be designed around a nude mouse xenograft model using a range of cell lines. The effects of the receptor antagonists and inhibitors may be tested on the growth of subcutaneous tumours.

A further use of the structure of the IGF-1R fragment described here is in facilitating structure determination of a related protein, such as a larger fragment of this receptor, another member of the insulin receptor family or a member of the EGF receptor family. This new structure may be either of the protein alone, or in complex with its ligand. For crystallographic analysis this is achieved using the method of molecular replacement (Brunger, Meth. Enzym. 1997 276 558-580, Navaza and Saludjian, *ibid.* 581-594, Tong and Rossmann, *ibid.* 594-611, Bentley, *ibid.* 611-619) in a program such as XPLOR. In this procedure diffraction data is collected from a crystalline protein of unknown structure. A transform of these data (Patterson function) is compared with a Patterson function calculated from a known structure. Firstly, the one Patterson function is rotated on the other to determine the correct orientation of the unknown molecule in the crystal. The translation function is then calculated to determine the location of the molecule with respect to the crystal axes. Once the molecule has been correctly positioned in the unit cell initial phases for the experimental data may be calculated. These phases are necessary for calculation of an electron density map from which structural differences may be observed and for refinement of the structure. Due to limitations in the method the search molecule must be structurally related to that which is to be determined. However it is sufficient for only part of the unknown structure (e.g. < 50%) to be similar to the search molecule. Thus the three dimensional structure of IGF-1R residues 1-462 may be used to solve structures consisting of related receptors, enabling a program of drug design as outlined above.

In summary, the general principles of receptor-based drug design can be applied by persons skilled in the art, using the crystallographic results presented above, to produce ligands of IGF-1R or other related receptors, having sufficient stereochemical complementarity to exhibit high affinity binding to the receptor site.

The present invention is further described below with reference to the following, non-limiting examples.

EXAMPLE 1

Expression, Purification and Crystallization of the IGF-1R Fragment.

Several factors hamper macromolecular crystallization including sample selection, purity, stability, solubility (McPherson, A., et al., 1995, Structure 3:759-768); Gilliland, G. L., & Ladner, J. E., 1996, Curr. Opin. Struct. Biol. 6:595-603), and the nature and extent of glycosylation (Davis, S. J., et al., 1993, Protein Eng. 6:229-232). Initial attempts to obtain structural data from soluble IGF-1R ectodomain (residues 1-906) protein, expressed in Lec8 cells (Stanley, P. 1989, Molec. Cellul. Biol. 9:377-383) and purified by affinity chromatography, produced large, well-formed crystals (1.0 mm x 0.2 mm x 0.2 mm) which gave no discernible X-ray diffraction pattern (unpublished data). Similar difficulties have been encountered with crystals of the structurally-related epidermal growth factor receptor (EGFR) ectodomain, which diffracted to only 6 Å, insufficient for the determination of an atomic resolution structure (Weber, W. et al., 1994, J Chromat 679:181-189). This prompted us to search for a fragment of IGF-1R that was more amenable to X-ray crystallographic studies.

The fragment expressed (residues 1-462) comprises the L1-cysteine-rich-L2 region of the ectodomain. The selected truncation position at Val462 is four residues downstream of the exon 6/exon 7 junction (Abbott, A. M., et al., 1992, J Biol Chem. 267:10759-10763), and occurs at a position where the sequences of the IR and the structurally related EGFR families diverge markedly (Lax, I., et al., 1988, Molec Cell Biol. 8:1970-1978; Ward, C. W., et al., 1995, Proteins: Struct., Funct., Genet. 22:141-153), suggesting that it represents a domain boundary. The expression strategy included use of the pEE14 vector (Bebbington, C. R. & Hentschel, C. C. G., 1987, In: Glover, D. M., ed. DNA Cloning. Academic Press, San Diego. Vol 3, p163) in glycosidase-defective Lec8 cells (Stanley, P., 1989, Molec. Cellul. Biol. 9:377-

383), which produce N-linked oligosaccharides lacking the terminal galactose and N-acetylneuraminic acid residues (Davis, S. J., et al., 1993, Protein Eng. 6:229-232; Liu, T., et al., 1996, J Biol Chem 271:33639-33646.). The construct contained a C-terminal c-myc affinity tag (Hoogenboom, H. R., et al., 1991, Nucl Acids Res. 19:4133-4137), which facilitated immunoaffinity purification by specific peptide elution and avoided aggressive purification conditions. These procedures yielded protein which readily crystallized after a further gel filtration purification step. This provided a general protocol to enhance crystallisation prospects for labile, multidomain glycoproteins.

The structure of this fragment is of considerable interest, since it contains the major determinants governing insulin and IGF-1 binding specificity (Gustafson, T. A. & Rutter, W. J., 1990, J. Biol. Chem. 265:18663-18667; Andersen, A. S., et al., 1990, Biochemistry, 29:7363-7366; Schumacher, R., et al., 1991, J. Biol. Chem. 266:19288-19295; Schumacher, R., et al., 1993, J. Biol. Chem. 268:1087-1094; Schäffer, L., et al., 1993, J. Biol. Chem. 268:3044-3047; Williams, P. F., et al., 1995, J. Biol. Chem. 270:3012-3016), and is very similar to an IGF-1R fragment (residues 1-486) reported to act as a strong dominant negative for several growth functions and which induces apoptosis of tumour cells *in vivo* (D'Ambrosio, C., et al., 1996, Cancer Res. 56:4013-4020). The expression plasmid pEE14/IGF-1R/462 was constructed by inserting the oligonucleotide cassette:

AatII

25 5' GACGTC GACGATGACGATAAG GAACAAAACTCATC

D V D D D D K E Q K L I

(EK cleavage) (c-myc tail)

S E E D L N (Stop)

TCAGAAGAGGATCTGAAT TAGAATTC GACGTC 3'

30 *EcoRI AatII*

encoding an enterokinase cleavage site, c-myc epitope tag (Hoogenboom, H. R., et al., 1991, Nucleic acids Res. 19:4133-4137) and stop codon into the *AatII* site (within codon 462) of Igf-1r cDNA in the mammalian expression vector pECE (Ebina, Y., et al., 1985, Cell, 40:747-758; kindly supplied by W. J. Rutter, UCSF, USA), and introducing the DNA comprising the 5' 1521 bp of

the cDNA (Ullrich, A., et al., 1986, EMBO J. 5:2503-2512) ligated to the oligonucleotide cassette into the EcoRI site of the mammalian plasmid expression vector pEE14 (Bebbington, C. R. & Hentschel, C. C. G., 1987, In: Glover, D. M., ed. DNA Cloning. Academic Press, San Diego. Vol 3, p163; 5 Celltech Ltd., UK). Plasmid pEE14/IGF-1R/462 was transfected into Lec8 mutant CHO cells (Stanley, P. 1989, Molec. Cellul. Biol. 9:377-383) obtained from the American Tissue Culture Collection (CRL:1737), using Lipofectin (Gibco-BRL). Cell lines were maintained after transfection in glutamine-free medium (Glasgow modification of Eagle's medium (GMEM; ICN Biomedicals, 10 Australia) and 10% dialysed FCS (Sigma, Australia) containing 25 µM methionine sulfoximine (MSX; Sigma, Australia) as described (Bebbington, C. R. & Hentschel, C. C. G., 1987, In: Glover, D. M., ed. DNA Cloning. Academic Press, San Diego. Vol 3, p163). Transfectants were screened for protein expression by Western blotting and sandwich enzyme-linked 15 immunosorbent assay (ELISA) (Cosgrove, L., et al., 1995,) using monoclonal antibody (Mab) 9E10 (Evan et al., 1985) as the capture antibody, and either biotinylated anti-IGF-1R Mab 24-60 or 24-31 for detection (Soos et al., 1992; gifts from Ken Siddle, University of Cambridge, UK). Large-scale cultivation of selected clones expressing IGF-1R/462 was carried out in a Celligen Plus 20 bioreactor (New Brunswick Scientific, USA) containing 70 g Fibra-Cel Disks (Sterilin, UK) as carriers in a 1.25 L working volume. Continuous perfusion culture using GMEM medium supplemented with non-essential amino acids, nucleosides, 25 µM MSX and 10% FCS was maintained for 1 to 2 weeks followed by the more enriched DMEM/F12 without glutamine, with the same 25 supplementation for the next 4-5 weeks. The fermentation production run was carried out three times under similar conditions, and resulted in an estimated overall yield of 50 mg of receptor protein from 430 L of harvested medium. Cell growth was poor during the initial stages of the fermentation when GMEM medium was employed, but improved dramatically following the 30 switch to the more enriched medium. Target protein productivity was essentially constant during the period from ~100 to 700 h of the 760 h fermentation, as measured by ELISA using Mab 9E10 as the capture antibody and biotinylated Mab 24-31 as the developing antibody.

Soluble IGF-1R/462 protein was recovered from harvested 35 fermentation medium by affinity chromatography on columns prepared by coupling Mab 9E10 to divinyl sulphone-activated agarose beads (Mini Leak;

Kem En Tec, Denmark) as recommended by the manufacturer. Mini-Leak Low and Medium affinity columns with antibody loadings of 1.5-4.5 mg/ml of hydrated matrix were obtained, with the loading range of 2.5-3 mg/ml giving optimal performance (data not shown). Mab 9E10 was produced by growing
5 hybridoma cells (American Tissue Culture Collection) in serum-free medium in the Celligen Plus bioreactor and recovering the secreted antibody (4 g) using protein A glass beads (Prosep-A, Bioprocessing Limited, USA). Harvested culture medium containing IGF-1R/462 protein was adjusted to pH 8.0 with Tris-HCl (Sigma), made 0.02% (w/v) in sodium azide and passed at
10 3-5 ml/min over 50 ml Mab 9E10 antibody columns at 4° C. Bound protein was recovered by recycling a solution of 2-10 mg of the undecamer c-myc peptide EQKLISEEDLN (Hoogenboom et al., 1991) in 20 ml of Tris-buffered saline containing 0.02% sodium azide (TBSA). Between 65% and 75% of the product was recovered from the medium as estimated by ELISA, with a
15 further 15-25% being recovered by a second pass over the columns. Peptide recirculation (~10 times) through the column eluted bound protein more efficiently than a single, slower elution. Residual bound protein was eluted with sodium citrate buffer at pH 3.0 into 1 M Tris HCl pH 8.0 to neutralize the eluant, and columns were re-equilibrated with TBSA.
20 Gel filtration over Superdex S200 (Pharmacia, Sweden), of affinity-purified material showed a dominant protein peak at ~63 kDa, together with a smaller quantity of aggregated protein (Figure 3a). The peak protein migrated primarily as two closely spaced bands on reduced , sodium dodecyl sulfate polyacrylamide gel electrophoresis (SDS-PAGE; Figure 3b), reacted
25 positively in the ELISA with both Mab 24-60 and Mab 24-31, and gave a single sequence corresponding to the N-terminal 14 residues of IGF-1R. No binding of IGF-1 or IGF-2 could be detected in the solid plate binding assay (Cosgrove et al., 1995, Protein Express Purif. 6:789-798). The IGF-1R/462 fragment was further purified by ion-exchange chromatography on Resource
30 Q (Pharmacia, Sweden). Using shallow salt gradients, protein enriched in the slowest migrating SDS-PAGE band was obtained (data not shown), which formed relatively large, well-formed crystals (see below). Isoelectric focussing showed the presence of one major and two minor isoforms. Protein purified on Resource Q with an isocratic elution step of 0.14 M NaCl in 20
35 mM TrisCl at pH 8.0 (fraction 2, Figure 4) showed less heterogeneity on isoelectric focussing (Figure 4 inset) and SDS-PAGE (data not shown), and

produced crystals of sufficient quality for structure determination (see below).

Crystals were grown by the hanging drop vapour diffusion method using purified protein concentrated in Centricon 10 concentrators (Amicon Inc, USA) to 5-10 mg/ml in 10-20 mM Tris-HCl pH 8.0 and 0.02% (w/v) sodium azide, or 100 mM ammonium sulfate and 0.02% (w/v) sodium azide. Crystallization conditions were initially identified using the factorial screen (Jancarik, J. & Kim, S.-H., 1991, J Appl Cryst 24:409-411), and then optimised. Crystals were examined on an M18XHF rotating anode generator (Siemens, Germany) equipped with Franks mirrors (MSC, USA) and RAXIS IIC and IV image plate detectors (Rigaku, Japan).

From the initial crystallization screen of this protein, crystals of about 0.1 mm in size grew in one week. Upon refining conditions, crystals of up to 0.6 x 0.4 x 0.4 mm could be grown from a solution of 1.7-2.0 M ammonium sulfate, 0.1 M HEPES pH 7.5. The crystals varied considerably in shape and diffraction quality, growing predominantly as rhombic prisms with a length to width ratio of up to 5:1, but sometimes as rhombic bipyramids, the latter form being favoured when using material which had been eluted from the Mab 9E10 column at pH 3.0. Each crystal showed a minor imperfection in the form of very faint lines from the centre to the vertices. Protein from dissolved crystals did not appear to be different from the protein stock solution when run on an isoelectric focusing gel. Upon X-ray examination, the crystals diffracted to 3.0-4.0 Å and were found to belong to the space group $P2_12_12_1$ with $a = 76.8$ Å, $b = 99.0$ Å, $c = 119.6$ Å. In the diffraction pattern, the crystal variability noted above was manifest as a large (1-2°) and anisotropic mosaic spread, with concomitant variation in resolution. To improve the quality of the crystals, they were grown in the presence of various additives or were recrystallized. These methods failed to substantially improve the crystal quality although bigger crystals were obtained by recrystallization. The variability in crystal quality appeared to be due to protein heterogeneity, as demonstrated by the observation that more highly purified protein, eluted isocratically from the Resource Q column and showing one major band on isoelectric focusing (Figure 4 inset), produced crystals of sufficient quality for structure determination. These crystals diffracted to 2.6 Å resolution with cell dimensions, $a = 77.0$ Å, $b = 99.5$ Å, $c = 120.1$ Å and mosaic spread of 0.5°. Heavy metal derivatives of the IGF-

1R/462 crystals have been obtained and are leading to the determination of an atomic resolution structure of this fragment, which contains the L1, cysteine-rich and L2 domains of human IGF-1R.

5

EXAMPLE 2

Structure of the IGF-1R/1-462

Crystals were cryo-cooled to -170°C in a mother liquor containing 20% glycerol, 2.2 M ammonium sulfate and 100 mM Tris at pH 8.0. Native and derivative diffraction data were recorded on Rigaku RAXIS IIC or IV area detectors using copper K α radiation from a Siemens rotating anode generator with Yale/MSO mirroroptics. The space group was P2₁2₁2₁ with a = 77.39 Å, b = 99.72 Å, and c = 120.29 Å. Data were reduced using DENZO and SCALEPACK (Otwinowski, Z. & Minor, W., 1996, *Methods in Enzymology* 276:307-326). Diffraction was notably anisotropic for all crystals examined.

Phasing by multiple isomorphous replacement (MIR) was performed with PROTEIN (Steigeman, W. Dissertation (Technical Univ. Munich, 1974) using anomalous scattering for both UO₂ and PIP derivatives. Statistics for data collection and phasing are given in Table 1. In the initial MIR map regions of protein and solvent could clearly be seen, but the path of the polypeptide was by no means obvious. That map was subject to solvent flattening and histogram matching in DM (Cowtan, K., 1994, *Joint CCP4 and ESF-EACBM newsletter. Protein Crystallogr.* 31:34-38). The structure was traced and rebuilt using O (Jones, T. A., et al., 1991, *Acta Crystallogr.* A47:110-119) and refined with X-PLOR 3.851 (Brunger, A. T., 1996, *X-PLOR Reference Manual 3.851*, Yale Univ., New Haven, CT). After 5 rounds of rebuilding and energy minimisation the R-factor dropped to 0.279 and R_{free} = 0.359 for data 7-2.6 Å resolution. The current model contains 458 amino acids and 3 N-linked carbohydrates but no solvent molecules. For residues with B(Ca) > 70, Å atomic positions are less reliable (37-42, 155-159, 305, 336-341, 404-406, 453-458). There is weak electron density for residues 459-461, but the c-myc tail appears completely disordered.

The 1-462 fragment consists of the N-terminal three domains of IGF-1R (L1, cys-rich, L2), and contains regions of the molecule which dictate ligand specificity (17-23). The molecule adopts a reasonably extended structure (approximately 40 x 48 x 105 Å) with domain 2 (cys-rich region)

making contact along the length of domain 1 (L1) but very little contact with the third domain (L2) (see Figure 5). This leaves a space at the centre of the molecule of approximately 24 Å x 24 Å x 24 Å which is bounded on three sides by the three domains of the molecule. The space is of sufficient size to accommodate the ligand, IGF-1.

Table 1 Summary of Crystallographic data

	Data set ^a	Resol. (Å)	Mean I/s	R _{merge} ^b	Completeness (multiplicity)	No. of sites	R _{cullis} ^c	Phasing power ^d	FOMe
10	Native	2.6	18.7	0.064	0.996 (4.1)				0.47 / 0.71
	PIP	3.0	15.8	0.060	0.982 (2.2)	3	0.66	1.71	
	UO2Ac2	4.5	7.5	0.095	0.989 (2.3)	2	0.82	1.17	
15									
	Refinement resolution (Å)	No of refl. (free)	No. of Atoms	R _{cryst} ^f	R _{free} ^f	Bonds ^e (Å)	Angles ^e (Å)		
20	7.0-2.6	24270 (2693)	3903	0.237	0.304	0.017	0.048		

^a PIP, Di-μ-iodobis(ethylenediamine)diplatinum dinitrate; UO2Ac2, Uranyl acetate.

^b $R_{\text{merge}} = \sum_{\mathbf{h}} \sum_j |I_{\mathbf{h},j} - I_{\mathbf{h}}| / \sum_{\mathbf{h}} \sum_j I_{\mathbf{h}}$, where $I_{\mathbf{h},j}$ is an intensity measurement j and $I_{\mathbf{h}}$ is the mean intensity for that reflection \mathbf{h} .

^c $R_{\text{cullis}} = \sum_{\mathbf{h}} ||\mathbf{F}_{\text{PH}} - \mathbf{F}_{\text{P}}| - |\mathbf{F}_{\text{Hcalc}}|| / \sum_{\mathbf{h}} ||\mathbf{F}_{\text{PH}}| - |\mathbf{F}_{\text{P}}||$, where \mathbf{F}_{PH} , \mathbf{F}_{P} and $\mathbf{F}_{\text{Hcalc}}$ are, respectively, derivative, native and heavy atom structure factors for centric reflections \mathbf{h} .

^d Phasing power = $\sum_{\mathbf{h}} |\mathbf{F}_{\text{Hcalc}}| / \sum_{\mathbf{h}} \epsilon$, where $\mathbf{F}_{\text{Hcalc}}$ is defined above and ϵ is the lack of closure.

^e FOM (figure of merit) = $\langle \cos(\Delta\alpha_{\mathbf{h}}) \rangle$, where $\Delta\alpha_{\mathbf{h}}$ is the error in the phase angle for reflection \mathbf{h} . Values are given before and after density modification at 3.0 and 2.8 Å resolution, respectively.

^f R_{cryst} and R_{free} are defined in Brunger, A.T. *XPLOR* reference manual 3.851 (Yale Univ., New Haven, CT, 1996)

8 r.m.s. deviation from ideal bond and angle-related (1-3) distances.

The L domains

Each of the L domains (residues 1-150 and 300-460) adopts a compact shape (24 x 32 x 37 Å) consisting of a single-stranded right handed β-helix and capped on the ends by short α-helices and disulfide bonds. The body of the domain looks like a loaf of bread, with the base formed from a flat six-stranded β-sheet, 5 residues long and the sides being β-sheets three residues long (Figures 5 & 6). The top is irregular, but in places is similar for the two domains. The two domains are superposable with an rms deviation in Cα positions of 1.6 Å for 109 atoms (Figure 7). Although this fold is reminiscent of other β-helix proteins it is much simpler and smaller with very few elaborations, and thus it represents a new superfamily of domains. One notable difference between the two domains is that the indole ring of Trp 176 from the cys-rich region (Figure 6b) is inserted into the hydrophobic core of L1, and the C-terminal helix is only vestigial (Figure 8). For the insulin receptor family the sequence motif of residues which form the Trp pocket in L1 does not occur in L2 (Figure 6a). However in the EGF receptor, which has an additional cys-rich region after the L2 domain (14, 15), the pocket motif can be found in both L domains and the Trp is conserved in both cys-rich regions (Figure 6b).

The repetitive nature of the β-helix is reflected in the sequence and the first five turns were correctly identified by Bajaj, M., et al. (1987, *Biochim.Biophys. Acta* 916:220-226), the conserved Gly residues being found in turns making one bottom edge of the domain. However, their conclusions about the fold were incorrect. The "helix-like" repeat is actually a pair of bends at the top edge of the domain. In their Motif V, the Gly is not in a bend but is followed by the insertion of a conserved loop of 7-8 residues (see Figure 6a). Glycine is structurally important in the Gly bends as mutation of these residues compromises folding of the receptor [van der Vorm, E.R., et al., 1992, *J. Biol. Chem.* 267, 66-71; Wertheimer, E. et al., 1994, *J. Biol. Chem.* 269, 7587-7592].

Comparison of the L domains with other right-handed β-helix structures such as pectate lyase (Yoder, M. D., et al., 1993, *Structure*, 1:241-251-1507) and the p22 tailspike protein (Steinbacher, S., et al., 1997, *J. Mol. Biol.* 267:865-880) shows some striking similarities as well as differences. In

all cases the ends of the domain are capped by α -helices, but the L domains also have a disulphide bond at each end to hold the termini. The other β -helix domains are considerably longer and have significant twist to their sheets, while the L domains have flat sheets. Although the sizes of the helix repeats are similar (here 24-25 residues vs 22-23 for pectate lyase) the cross-sections are quite different. The L domains have a rectangular cross-section, while pectate lyase and p22 tailspike protein are V-shaped, and have many, and sometimes quite large, insertions (Yoder, M. D., et al., 1993, Structure, 1:241-251-1507; Steinbacher, S., et al., 1997, J.Mol. Biol. 267:865-880). In the hydrophobic core a common feature is the stacking of aliphatic residues from successive turns of the β -helix, and near the C-terminus of each L domain there is also a short Asn ladder, reminiscent of the long Asn ladder observed in pectate lyase (Yoder, M. D., et al., 1993, Structure 1:241-251-1507). On the opposite side of the L domains the Gly bend, as well as the two bends and sheet preceding it, have no counterpart in the other β -helix domains. Thus although the L domains are built on similar principles to the other β -helix domains they constitute a separate superfamily.

The cys-rich domain

The cys-rich domain is composed of eight disulfide-bonded modules (Figure 6b), the first of which sits at the end of L1, while the remainder make a curved rod running diagonally across L1 and reaching to L2 (Figure 5). The strands in modules 2-7 run roughly perpendicular to the axis of the rod in a manner more akin to laminin (Stetefeld, J., et al., 1996, J.Mol.Biol. 257:644-657) than to TNF receptor (Banner, D. W., et al., 1993, Cell, 73:431-445), but the modular arrangement of the cys-rich domain is different to those of other cys-rich proteins for which structures are known. The first 3 modules of IGF-1R have a common core, containing a pair of disulfide bonds, but show considerable variation in the loops (Figure 6b). The connectivity of these modules is the same as in the first half of EGF (Cys 1-3 and 2-4), but their structures do not appear to be closely related to any member of the EGF family. Modules 4 to 7 have a different motif, a β -finger, and best match residues 2152-2168 of fibrillin (Dowling, A. K., et al., 1996, Cell, 85:597-605). Each is composed of three polypeptide strands, the first and third being disulfide bonded and the latter two forming a β -ribbon. The β -ribbon of each β -finger module lines up antiparallel to form a tightly twisted 8-stranded β -sheet (Figures 5 and 8). Module 6 deviates from the common pattern, with

the first segment being replaced by an α -helix followed by a large loop that is likely to have a role in ligand binding (see below). As module 5 is most similar to module 7 it is possible that the four modules arose from serial gene duplications. The final module is a disulfide-linked bend of five residues.

5 The fact that the two major types of cys-rich modules occur separately implies that these are the minimal building blocks of cys-rich domains found in many proteins. Although it can be as short as 16 residues, the motif of modules 4-7 is clearly distinct, and capable of forming a regular extended structure. Thus cys-rich domains such as these can be considered
10 as being made of repeat units each composed of a small number of modules.

Hormone binding

Attempts have been made to locate the IGF-1 (and insulin) binding site by examining natural (Taylor, S. I., 1992, Diabetes, 41:1473-1490) and site-directed mutants (Williams, P. F., et al., 1995, J. Biol. Chem. 270:3012-
15 3016; Mynarcik, D. C et al., 1996, J. Biol. Chem. 271:2439-2442; Mynarcik, D. C., et al., 1997, J. Biol. Chem. 272:2077-2081), chimeric receptors (Andersen, A. S., et al., 1990, Biochemistry 29:7363-7366; Gustafson, T. A., & Rutter, W. J., 1990, J. Biol. Chem. 265:18663-18667; Schäffer, L., et al., 1993, J. Biol. Chem. 268:3044-3047; Schumacher, R., 1993, J. Biol. Chem. 268:1087-1094;
20 Kjeldsen, T., et al., 1991, Proc. Natl Acad. Sci. USA, 88:4404-4408) and by crosslinking studies (Wedekind, F., et al., 1989, Biol. Chem Hoppe-Seyler, 370:251-258; Fabry, M., 1992, J. Biol. Chem. 267:8950-8956; Waugh, S. M., et al., 1989, Biochemistry, 28:3448-3458; Kurose, T., et al., 1994), J. Biol. Chem. 269:29190-29197-34). IGF-1R/IR chimeras not only show which
25 regions of the receptors account for ligand specificity, but also provide an efficient means of identifying some parts of the hormone binding site. Paradoxically, regions controlling specificity are not the same for insulin and IGF-1. Replacing the first 68 residues of IGF-1R with those of IR confers insulin-binding ability on the chimeric IGF-1R (Kjeldsen, T., et al., 1991,
30 Proc. Natl Acad. Sci. USA, 88:4404-4408), and replacing residues 198-300 in the cys-rich region of IR with the corresponding residues 191-290 of IGF-1R allows the chimeric receptor to bind IGF-1 (Schäffer, L., et al., 1993, J. Biol. Chem. 268:3044-3047). Thus a receptor can be constructed which binds both IGF-1 and insulin with near native affinity. From the structure it is clear that
35 if the hormone bound in the central space it could contact both these regions.

From analysis of a series of chimeras examined by Gustafson, T. A., & Rutter, W. J. (J. Biol. Chem. 265:18663-18667, 1990), the specificity determinant in the cys-rich region can be limited further to residues 223-274. This region corresponds to modules 4-6, and includes a large and somewhat mobile loop (residues 255-263, mean B[C α atoms] = 57 Å²) which extends into the central space (see Figure 5). In IR this loop is four residues bigger, and is stabilised by an additional disulfide bond (Schäffer, L. & Hansen, P.H., 1996, Exp. Clin. Endocrinol. Diabetes, 104: Suppl. 2, 89). The larger loop of IR may serve to exclude IGF-1 from the hormone binding site while allowing the smaller insulin molecule to bind. It is interesting to note that mosquito IR homologue, which has a loop two residues larger than the mammalian IRs, also appears to bind insulin but not IGF-1 (Graf, R., et al., 1997, Insect Molec. Biol. 6:151-163). Analysis of the structure indicates that the insulin/IGF-1 specificity is controlled by residues in this loop (amino acids 253-272 in IGF-1R; amino acids 260-283 in IR)

As chimeras only address residues which differ between the two receptors, a more precise analysis of the site can be obtained from single site mutants. In particular, from an alanine-replacement study, four regions of L1 important for insulin binding were identified (Williams, P. F., et al., 1995, J. Biol. Chem. 270:3012-3016). The first three are at similar positions on successive turns of the β -helix and the fourth lies on the conserved bulge on the large β -sheet. Thus there is a footprint for insulin binding to the L1 domain which lies on the first half of the large β -sheet facing into the central space. Residues further along the sheet which are conserved in IGF-1R could also be important. The conservative substitution of leucine for methionine at residue 119 of IR (113 of IGF-1R) causes a mild form of leprechaunism [Hone, J. et al., 1994, J. Med. Genet. 31, 715-716]. This residue is buried, and the mutation could perturb neighbouring residues to affect insulin binding.

The axis of the L2 domain is perpendicular to that of the L1 domain, and the N-terminal end of its β -helix is presented to the hormone-binding site. On this face of the L2 domain the only mutation studied so far is the naturally occurring IR mutant, S323L, which gives rise to Rabson-Mendehall syndrome and severe insulin resistance (Roach, P., 1994, Diabetes 43:1096-1102). As this mutant only affects insulin binding and not cell-surface expression, residue 323 of IR (residue 313 of IGF-1R) is probably at or near the binding site. Structurally this residue lies in the middle of a region

(residues 309-318 of IGF-1R) which is conserved in both IR and IGF-1R, and the surrounding region, 332-345 (of IGF-1R), is also quite well conserved in the these receptors (Figure 6a). Therefore this region is quite likely to form part of the hormone-binding site, but would not have been detected by
5 chimeras. It is interesting to note that in this region IRR is not as well conserved as the other two receptors (Shier, P. & Watt, V.M., 1989, J.Biol.Chem. 264:4605-14608).

The distance from this putative hormone-binding region on L2 to that found on L1 is about 30 Å (Figure 5). Thus L1 and L2 appear too far apart to
10 bind IGF-1 or insulin. However, in the crystal structure there is a deep cleft between part of the cys-rich domain (residue 262) and L2 (residue 305), and this cleft is occupied by a loop from a neighbouring molecule. Thus it seems probable that the position of the L2 domain in the receptor structure or the hormone-receptor complex adopts a different position with respect to the
15 cys-rich domain than that found in the crystal. The movement required to bring L2 sufficiently close to L1 is small, namely a rotation of approximately 25° about residue 298.

A number of IR mutants have been identified which constitutively activate the receptor, and the majority of these are found in the α chain.
20 Curiously all α chain mutants involve changes to or from proline or the deletion of an amino acid, implying that they cause local structural rearrangements. The mutation R86N is similar to wild type, but R86P reduces cell-surface expression and insulin binding while constitutively activating autophosphorylation [Grønskov, K. et al., 1993, Biochem. Biophys. Res. Commun. 192, 905-911]. The proline mutation probably disturbs
25 residues preceding 87 which lie in the interface between the L1 and cys-rich domains, but it could also affect insulin binding. In the cys-rich domain residues 233, 281, 244 and 247 of IR are not conserved in IGF-1R (Figure 6b), yet L233P [Klinkhamer, M.P. et al., 1989, EMBO J. 8, 2503-2507], deletion of
30 N281 [Debois-Mouthon, C. et al., 1996, J. Clin. Endocrinol. Metab. 81, 719-727] or the triple mutant P243R, P244R and H247D [Rafaeloff, R. et al., 1989, J. Biol. Chem. 264, 15900-15904] cause constitutive kinase activation. Due to their locations each of these three mutants appears likely to compromise the folding of a β -finger domain and, in turn, the structural integrity of the rod-
35 like cys-rich domain. The structural ramifications of these mutations could be significant for the whole receptor ectodomain, as disturbing the L1/cys-

rich interface or distorting the rod-like domain could affect the relative position of L1 and the cys-rich domain in this context.

L1 has been further implicated, as deletion of K121 on the opposite side of L1 from the cys-rich domain was also found to cause autophosphorylation [Jospe, N. et al., 1994, J. Clin. Endocrinol. Metab. 79, 1294-1302]. By contrast this mutation does not affect insulin binding. Thus a possible mechanism emerges for insulin binding and signal transduction. When insulin binds between L1 and L2 it modifies the relative position of L1 and the cys-rich domain in the receptor, perhaps by hinge motion between L2 and the cys-rich domain like that suggested above, and the structural rearrangement is transmitted across the plasma membrane. In the absence of insulin the same signal can be initiated by mutations in the cys-rich region or at the L1/cys-rich interface, but at the expense on insulin binding. The signal can also be initiated more directly by mutations on the opposite side of L1 which affect the interaction of L1 with other parts of the ectodomain, possibly the other half of the receptor dimer.

Ligand Studies

Although there is no structural information about an IGF-1/IGF-1R complex a number of studies have probed the nature of this interaction. Results from cross-linking experiments with IGF-1 and insulin and their cognate receptors are consistent with the hormone binding site proposed above. For example B29 of insulin can be cross-linked to the cys-rich region (residues 205-316) (Yip, C. C., et al., 1988, Biochim. Biophys. Res. Commun. 157:321-329) or the L1 domain (Wedekind, F., et al., 1989, Biol. Chem Hoppe-Seyler, 370:251-258). However, these two regions are reasonably well separated, and those studies may indicate that B29 is mobile. Other studies unfortunately do not map the site any more precisely.

Analogues and site-directed mutants of IGF-1 and IGF-2 have been more fruitful. IGF-1 and IGF-2 contain two extra regions relative to insulin, the C region between B and A and a D peptide at the C-terminus. For IGF-1, replacement of the C region by a four Gly linker reduced affinity for IGF-1R by a factor of 40 but increased affinity for IR 5-fold (Bayne, M.L., et al., 1988, J. Biol.Chem. 264:11004-11008). Changes in affinity are consistent with the deletion in IGF-1 complementing differences in the cys-rich regions of IGF-1R and IR noted above. Mutation of residues either side of the C region (residue 24 for IGF-1 [Cascieri, M.A., et al., 1988, Biochemistry 27:3229-

3233], residues 27,43 for IGF-2, [Sakano, K., et al., 1991, J. Biol. Chem. 266:20626-20635]) also has deleterious effects on the affinity of the hormone for IGF-1R, as has truncation of the nearby D peptide in IGF-2 (Roth, B.V., et al., 1991, Biochem. Biophys. Res. Commun. 181:907-914).

5 Insulin has been extensively mutated. Binding studies [summarised in Kristensen, C. et al., 1997, J. Biol. Chem. 272, 12978-12983] indicate that insulin may bind its receptor via a hydrophobic patch (residues A2, A3, A19, B8, B11, B12, B15 and possibly B23 & B24). However this patch is normally buried, and requires the removal of the B chain's C-terminus from the
10 observed position. Assuming IGF-1, IGF-2 and insulin bind their receptors in the same orientation, these data suggest an approximate orientation for the hormone when bound to the receptor.

 One notable feature of IGF-1 and IGF-2 is the large number of charged residues and their uneven distribution over the surface. Basic
15 residues are predominantly found in the C region and, in solution, this region is not well ordered in either IGF-1 or -2 (Sato, A., et al., 1993, Int J Peptide Protein Res. 41:433-440; Torres, A. M., et al., 1995, J. Mol. Biol. 248:385-401). In contrast the binding site of the receptor has a sizable patch of acidic residues in the corner where the cys-rich domain departs from L1. Other
20 acidic residues which are specific to this receptor are found along the inside face of the cys-rich domain and the loop (residues 255-263) extending from module 6. Thus it is possible that electrostatic interactions play an important part in IGF-1 binding, with the C region binding to the acidic patch of the cys-rich region near L1 and the acidic patch on the other side of the
25 hormone directed towards a small patch of basic residues (residues 307-310) on the N-terminal end of L2.

 Although the structure of this fragment gives significant information about the nature of the hormone binding site, residues outside this region have also been shown to affect binding of ligand. A number of studies have
30 implicated residues 704-715 of IR (Mynarcik, D. C et al., 1996, J. Biol. Chem. 271, 2439-2442; Kurose, T., et al., 1994, J. Biol. Chem. 269:29190-29197). These residues could contact insulin on one of the sides left open in the current structure. Using insulin labelled at the B1 residue, Fabry, M., et al., (1992, J. Biol. Chem. 267:8950-8956) cross-linked insulin to the fragment
35 390-488, part of which is not near the site as described. The explanation for this could be either the region 390-488 reaches back to the hormone binding

site, or this region could contact another hormone bound to the other half of the receptor. Further structural information is needed to establish how these other regions contact the hormone and to elucidate how binding of the hormone is communicated to the kinase inside the cell.

5 The structure of the L1-cys-rich-L2 domains of IGF-1R presented here represents the first structural information for the extracellular portion of a member of the insulin receptor family. The L domains display a novel fold which is common to the EGF receptor family, and the modular architecture of the cys-rich domain implies that smaller building blocks should be used to
10 describe the composition of cysteine-rich domains. This fragment contains the major specificity determinants of receptors of this class for their ligands. It has an elongated structure with a space in the middle which could accommodate the ligand. The three sides of this site correspond to regions which have been implicated in hormone binding. Although other sites are
15 present in the receptor ectodomain which interact with the ligand, this structure gives us an initial view of how the insulin, IGF-1 and IGF-2 might interact with their cell surface receptors to control their metabolic and mitogenic effects

Such information will provide valuable insight into the structure of
20 the corresponding domains of the IR and insulin receptor-related receptor as well as members of the related EGFR family (Bajaj, M., et al., 1987, Biochim Biophys Acta 916:220-226; Ward, C. W. et al., 1995, Proteins: Struct Funct Genet 22:141-153).

EXAMPLE 3

Prediction of 3D Structure of the Corresponding Domains of IRR and IR Based on Structure of IGF-1R Fragment.

The sequence identities between the different members of the insulin receptor family are sufficient to allow accurate sequence alignments to facilitate 3D structure predictions by homology modelling. The alignments of
30 the ectodomains of human IGF-1R, IR, and IRR are shown in Figure 9.

EXAMPLE 4

Single-Molecule Imaging of Human Insulin Receptor Ectodomain and its Fab Complexes

Cloning and expression of hIR -11 ectodomain protein

35 A full length clone of the human IR exon -11 form (hIR -11) was prepared by exchanging an Aat II fragment, nucleotides 1195 to 2987 , of the

exon +11 clone (plasmid pET; Ellis et al., 1986; gift from Dr W. J. Rutter, UCSF) of hIR (Ebina et al., 1985, *Cell* 40, 747-758) with the equivalent Aat II fragment from a plasmid (pHIR/P12-1, ATCC 57493) encoding part of the extracellular domain and the entire cytoplasmic domain of hIR -11 (Ullrich et al., 1985, *Nature* 313, 756-761). The ectodomain fragment of hIR -11 (2901 bp, coding for the 27 residue signal sequence and residues His1-Asn914) was produced by Sall and SspI digestion and inserted into the mammalian expression vector pEE6.HCMV-GS (Celltech Limited, Slough, Berkshire, UK) into which a stop codon linker had been inserted, as described previously (Cosgrove et al., 1995, *Protein Expression and Purification* 6, 789-798) for the hIR exon +11 ectodomain.

The resulting recombinant plasmid pHIR II (2 µg) was transfected into glycosylation-deficient Chinese hamster ovary (Lec 8) cells (Stanley, 1989, *Molec. Cellul. Biol.* 9, 377-383) with Lipofectin (Gibco-BRL). After transfection, the cells were maintained in glutamine-free medium GMEM (ICN Biomedicals, Australia) as described previously (Bebbington & Hentschel, 1987, In *DNA Cloning* (Glover, D., ed.), Vol III, Academic Press, San Diego; Cosgrove et al., 1995, *Protein Expression and Purification* 6, 789-798). Expressing cell lines were selected for growth in GMEM with 25 µM methionine sulfoximine (MSX, Sigma). Transfectants were screened for protein expression using sandwich ELISA with anti-IR monoclonal antibodies 83-7 and 83-14. Metabolic labelling of cells, immunoprecipitations, insulin binding assays and Scatchard analyses were performed as described previously for the exon +11 form of hIR ectodomain (Cosgrove et al., 1995, *Protein Expression and Purification* 6, 789-798).

hIR -11 ectodomain production and purification

The selected clone (inoculum of 1.28×10^8 cells) was grown in a spinner flask packed with 10 g of Fibracel disc carriers (Sterilin, U.K.) in 500 ml of GMEM medium containing 10% fetal calf serum (FCS) and 25 µM MSX. Selection pressure was maintained for the duration of the culture.

Ectodomain was recovered from harvested medium by affinity chromatography on immobilized insulin, and further purified by gel filtration chromatography on Superdex S200 (Pharmacia; 1 x 40 cm) in Tris-buffered saline containing 0.02% sodium azide (TBSA) as described previously (Cosgrove et al., 1995, *Protein Expression and Purification* 6, 789-798). Solutions of purified hIR -11 ectodomain were stored at 4° C prior to use.

5 **Production of Fab fragments and their complexes with ectodomain**

Purification of Mabs 83-7, 83-14 and 18-44 from ascites fluid by affinity chromatography using Protein A-Sepharose, and the production of Fabs, were based on the methodologies described in Coligan et al., 1993, Current Protocols in Immunology, Vol 1, pp 2.7.1-2.8.9, Greene Publishing Associates & Wiley - Interscience, John Wiley and Sons. Fab was produced from monoclonal antibody by mercuripapain digestion for 1-4 h, followed by gel filtration on Superdex S200. Products were monitored by reducing and non-reducing SDS-PAGE. For 83-7 Mab, an IgG Type 1 monoclonal antibody, the bivalent (Fab)₂' isolated by this method was reduced to monovalent Fab 83-7 by mild reduction with mM L-cysteine.HCl in 100 mM Tris pH 8.0 (Coligan et al., 1993, Current Protocols in Immunology, Vol 1, pp 2.7.1-2.8.9, Greene Publishing Associates & Wiley - Interscience, John Wiley and Sons).

Complexes of Fab with hIR -11 ectodomain were produced by mixing ~ 2.5 to 3.5 molar excess of Fab with hIR -11 ectodomain at ambient temperature in TBSA at pH 8.0. After 1-3 h, the complex was separated from unbound Fab by gel filtration over a Superdex S200 column in the same buffer.

Electron microscopy

Uncomplexed hIR -11 ectodomain and the Fab complexes described above were diluted in phosphate-buffered saline (PBS) to concentrations of the order of 0.01-0.03 mg/ml. Prior to dilution, 10% glutaraldehyde (Fluka) was added to the PBS to achieve a final concentration of 1% glutaraldehyde. Droplets of ~ 3ml of this solution were applied to thin carbon film on 700-mesh gold grids after glow-discharging in nitrogen for 30 s. After 1 min. the excess protein solution was drawn off and followed by application and withdrawal of 4-5 droplets of negative stain [2% uranyl acetate (Agar), 2% uranyl formate (K and K), 2% potassium phosphotungstate (Probing and Structure) adjusted to pH 6.0 with KOH, or 2% methylamine tungstate (Agar) adjusted to pH 6.8 with NH₄OH]. In the case of both uranyl acetate and uranyl formate staining, an intermediate wash with 2 or 3 droplets of PBS was included prior to application of the stain. The grids were air-dried and

then examined at 60kV accelerating voltage in a JEOL 100B transmission electron microscope at a magnification of 100,000x. It was found that there was a typical thickness of negative stain in which Fabs were most easily seen. Hence areas for photography had to be chosen from particular zones of the grid. Electron micrographs were recorded on Kodak SO-163 film and developed in undiluted Kodak D19 developer. The electron-optical magnification was calibrated under identical imaging conditions by recording single-molecule images of the antigen-antibody complex of influenza virus neuraminidase heads and NC10 MFab (Tulloch et al., 1986, *J. Mol. Biol.* **190**, 215-225; Malby et al., 1994, *Structure*, **2**, 733-746).

Image processing

Electron micrographs showing particles in a limited number of identifiable projections were chosen for digitisation. Micrographs were digitised on a Perkin-Elmer model 1010 GMS PDS flatbed scanning microdensitometer with a scanning aperture (square) size of 20 mm and stepping increment of 20 mm corresponding to a distance of 0.2 nm on the specimen. Particles were selected from the digitised micrograph using the interactive windowing facility of the SPIDER image processing system (Frank et al., 1996, *J. Struct. Biol.* **116**, 190-199). Particles were scaled to an optical density range of 0.0 - 2.0 and aligned by the PSPC reference-free alignment algorithm (Marco et al., 1996, *Ultramicroscopy*, **66**, 5-10). Averages were then calculated over a subset of correctly aligned particles chosen interactively as being representative of a single view of the particle. The final average image presented here is derived from a library of 94 images.

Biochemical characterization of expressed hIR -11 ectodomain

The recombinant protein examined corresponded to the the first 914 residues of the 917 residue ectodomain of the exon -11 form of the human insulin receptor (Ullrich et al., 1986, *Nature* **313**, 756-761). Expressed protein was shown, by SDS-PAGE and autoradiography of immunoprecipitated product from metabolically labelled cells, to exist as a homodimeric complex of ~270 - 320 kDa apparent mass, which dissociated under reducing conditions into monomeric α and β' subunits of respective apparent mass ~120 kDa and ~35 kDa (data not shown).

Purified hIR -11 ectodomain, expressed in Lec8 cells and purified by affinity chromatography on an insulin affinity column, eluted as a symmetrical peak on a Superdex S200 gel filtration column (Figure 10). The

protein eluted with an apparent mass of ~400 kDa, calculated from a standard curve generated by the elution positions of standard proteins (not shown). As expected for protein expressed in Lec 8 cells, whose glycosylation defect produces truncated oligosaccharides (Stanley, 1989, .
5 *Molec. Cellul. Biol.* 9, 377-383), this value is less than the apparent mass (450 - 500 kDa) reported for hIR + 11 ectodomain expressed in wild-type CHO-K1 cells (Johnson et al., 1988, *Proc. Natl Acad. Sci USA* 85, 7516-7520; Cosgrove et al., 1995, *Protein Expression and Purification* 6, 789-798).

Radioassay of insulin binding to purified ectodomain gave linear
10 Scatchard plots and Kd values of $1.5 - 1.8 \times 10^{-9}$ M, similar to the values of $2.4 - 5.0 \times 10^{-9}$ M reported for the hIR -11 ectodomain (Andersen et al., 1990, *Biochemistry* 29, 7363-7366; Markussen et al., 1991, *J. Biol. Chem.* 266, 18814-18818; Schaffer, 1994, *Eur. J. Biochem.* 221, 1127-1132) and the values of $\sim 1.0 - 5.0 \times 10^{-9}$ M reported for the hIR + 11 ectodomain (Schaefer et al.,
15 1992, *J. Biol. Chem.* 267, 23393-23402; Whittaker et al., 1994, *Molec. Endocrinol.* 8, 1521-1527; Cosgrove et al., 1995, *Protein Expression and Purification* 6, 789-798).

Expression of hIGF-1R ectodomain

Cloning, expression and purification of this protein used elements
20 common to those described for hIR -11 ectodomain (Cosgrove et al., 1995, *Protein Expression and Purification* 6, 789-798), and resulted in purified product that was recognised by receptor-specific Mabs 17-69, 24-31 and 24-60 (Soos et al., 1992, *J. Biol. Chem.* 267, 12955-63) and was composed of α and β' subunits of mass similar to those of hIR ectodomain.

25 Preparation of hIR -11 ectodomain/MFab complexes

A complex of hIR -11 ectodomain and Fab from antibody 83-14 eluted as a symmetrical peak of 460 -500 kDa (Figure 10), as did complexes generated from a mixture of hIR -11 ectodomain with Fab from antibody 18-44 and a mixture of hIR -11 ectodomain with Fab 83-7 (not shown). A co-
30 complex of ectodomain with Fabs from antibodies 18-44 and 83-14 eluted at ~ 620 kDa, as did a co-complex with MFabs 83-14/83-7 and another with MFabs 83-7/18-44 (not shown). A complex of hIR -11 ectodomain with all three MFab derivatives, 18-44, 83-7 and 83-14, eluted at an apparent mass of ~ 710 kDa (Figure 10).

35 Electron microscopy

Imaging of hIR -11 and hIGF-1R ectodomains

Single-molecule imaging of uncomplexed dimeric hIR -11 ectodomain was carried out under a variety of negative staining conditions, which emphasised different aspects of the structure of the molecular envelope. Images obtained by this investigation are depicted in Figure 11.

5 The least aggressive or penetrative stain was potassium phosphotungstate (KPT) , which revealed consistent globular particles with very little internal structure other than a suggestion of a division into two parallel bars. Staining with methylamine tungstate also revealed the parallel bar images.

10 Further investigation using progressively more penetrative, but also potentially more disruptive, stains confirmed the observations above. Staining with uranyl acetate and uranyl formate showed the separation of the parallel bars most clearly, but uranyl acetate showed evidence of disrupting the structure of the particles, i.e. a decrease in the consistency of the particle
15 shape and a tendency for particles to look unravelled or denatured despite having been subjected to chemical cross-linking prior to staining. In areas of thicker stain, parallel bars predominated, whereas in more thinly stained regions, U-shaped particles could be identified, sometimes outnumbering the parallel-bar structures (see Figure 11).

20 **Imaging of hIR -11 ectodomain complexed with 83-7 MFab**

 This complex was particularly noteworthy for the consistency of the form of the particles, especially under the gentler staining conditions afforded by stains such as KPT and methylamine tungstate. The particles were interpreted as having been restricted in the views they presented, after
25 air-drying on the carbon support film, by the almost diametrically opposite binding of the two Fab arms to the antigen to form a highly elongated complex structure. Under these conditions three distinct views could be recognised (see Figure 11). Two views (interpreted as top-down/bottom-up) show the Fab arms displaced clockwise or anti-clockwise as extensions of the
30 parallel plates with two-fold symmetry. The third view shows an image with the two Fab arms in line roughly through the centre of the receptor on its opposite sides, interpreted as a side projection of binding half-way up the plates.

 The use of aggressive uranyl stains operating at lower pHs revealed
35 internal structure of the molecular envelope at the expense of consistency of the particle morphology. For example, staining with uranyl acetate or uranyl

formate showed that parallel bars can be seen in particles in which the Fab arms are displaced either clockwise or anticlockwise but not where the intermediate central or axial position of the two Fab arms is presented in projection. These observations show 83-7 MFab binding roughly half-way up the side-edge of each hIR -11 ectodomain plate. The epitope recognised by Mab 83-7 has been mapped to the cys-rich region, residues 191-297, by analysis of chimeric receptors (Zhang and Roth, 1991, *Proc. Natl. Acad. Sci. USA* **88**, 9858-9862).

Imaging of hIR -11 ectodomain complexed with either 83-14 MFab or 18-44 MFab

Complexes were formed with Fabs from the most insulin-mimetic antibody Mab 83-14. Projections showing the Fab arms bound to and extending out from near the base of the U-shaped particles were identified. A second field of particles showed objects composed of two parallel bars as observed for the undecorated ectodomain, with Fab arms projecting obliquely from diametrically opposite extremities (see Figure 11). Similar but less definitive images were also seen when MFab 18-44 was bound to hIR -11 ectodomain. The epitope for Mab 83-14 is between residues 469-592 (Prigent et al., 1990) in the connecting domain. This domain contains one of the disulphide bonds (Cys524-Cys524) between the two monomers in the IR dimer (Schaffer and Ljungqvist, 1992, *Biochem. Biophys. Res. Commun.* **189**, 650-653). The epitope for Mab 18-44 is a linear epitope, residues 765-770 (Prigent et al., 1990, *J. Biol. Chem.* **265**, 9970-9977) in the β -chain, near the end of the insert domain (O'Bryan et al., 1991, *Mol. Cell. Biol.* **11**, 5016-5031). The insert domain contains the second disulphide bond connecting the two monomers in the IR dimer (Sparrow et al., 1997, *J. Biol. Chem.*, **272**, 29460-29467).

Imaging of hIR -11 ectodomain co-complexed with two different MFabs per monomer

The double complex of hIR -11 ectodomain with MFabs 83-7 and 18-44 was stained with 2% KPT at pH 6.0, and revealed the molecular envelopes. The particle appears complex in shape, and can assume a number of different orientations on the carbon support film, giving rise to a number of different projections in the micrograph. The predominant view is of an asymmetric X-shape (some examples circled). It shows the 83-7 MFab arms bound at opposite ends of the parallel bars with the two 18-44 MFabs

appearing as shorter projections extending out from either side of each ectodomain.

Images of the double complex of hIR -11 ectodomain with 83-7 and 83-14 MFabs gave X-shaped images similar to those seen with the 83-7/18-44 double complex. In contrast the double complex of hIR -11 ectodomain with 18-44 and 83-14 MFabs did not present the characteristic asymmetric X-shapes described above. Instead, the molecular envelope appeared to be elongated in many views, with only an occasional X-shaped projection. While a detailed interpretation of these images would be premature, it is clear that MFabs 18-44 and 83-14, two of the more potent insulin mimetic antibodies (Prigent et al., 1990, *J. Biol. Chem.* 265, 9970-9977), can bind simultaneously to the receptor.

Imaging of hIR -11 ectodomain co-complexed with three different MFabs per monomer

A field of particles from a micrograph of hIR -11 ectodomain were complexed simultaneously with MFabs 83-7, 83-14 and 18-44. In the thicker stain regions the molecular envelope was X-shaped, and looked very similar to that of the double complexes of hIR -11 ectodomain with either 83-7 and 18-44 or 83-7 and 83-14. However, in the more thinly stained regions particles of greater complexity were visible, and it was possible occasionally to identify that there are in fact more than four MFabs bound to the ectodomain dimer.

The single-molecule imaging of hIR -11 ectodomain presented here suggests a molecular envelope for this dimeric species significantly different from that of any previously published study. However, an unequivocal determination of the molecular envelope even from the present study is not entirely straightforward. A major complicating factor here has been the relative fragility of the expressed ectodomain when exposed to the rigors of electron microscope preparation by negative staining. For example, staining with potassium phosphotungstate (KPT, pH 6.0-7.0) frequently suggested a denaturation of the dimeric molecules, but when appropriate conditions were satisfied, good seemingly interpretable molecular envelope images were achieved; staining with methylamine tungstate (pH ~7.0) supported the best KPT molecular envelope images, but had the suggestion of a swelling of the molecular structure at neutral pH; and the acid-pH stains of uranyl acetate (pH ~4.2) and uranyl formate (pH~3.0), with their ability to penetrate the

ectodomain structure, appeared to illuminate not so much the molecular envelope as the zones of high projected protein density within the dimer.

An amalgam of impressions from these various staining regimens has led to the following interpretation of single-molecule images of these
5 undecorated, or naked, dimers: the predominant dimeric molecular image encountered here has been that of "parallel bars" of projected protein density. This view is so predominant, indeed, that it suggests there is either a single preferred orientation of the molecules on the glow-discharged carbon support film, or that this impression of parallel bars of density may represent a
10 mixture of superficially similar structure projections, with the subtleties of these different projections being masked by the relatively coarse resolution of this single-molecule direct imaging. The impression of parallel bars of projected protein density is particularly predominant in regions of thicker negative stain. A second view of the molecular envelope, appreciably less
15 well represented in regions of thicker stain but predominant in regions of thin staining, is that of 'open' U's, or V's. These two views of hIR -11 ectodomain were supported by the single-molecule imaging of hIGF-1R, ectodomain under comparable conditions of negative staining.

If the assumption is made that these two recognisable projected
20 views, that of parallel bars and of open U's/V's, are different views of the same dimeric molecule, an assumption strongly supported by the MFab complex imaging, a coarse model of the molecular envelope can be rationalized. The model structure is roughly that of a cube, composed of two almost-parallel plates of high protein density, separated by a deep cleft of low
25 protein main-chain and side-chain density able to be penetrated by stain, and connected by intermediate stain-excluding density near what is assumed here to be their base (that is, nearest the membrane-anchoring region). The width of the low-density cleft appears to be of the order of 30-35Å, sufficient to accommodate the binding of the insulin molecule of diameter ca. 30Å,
30 although we have no electron microscopical evidence to support insulin-binding in this cleft at this stage.

It has been established through imaging of bound 83-7 MFab that there is a dimeric two-fold axis normal to the membrane surface between these plates of density. Occasionally, dimer images display a relative
35 displacement of the bars of density, interpreted here as a limited capacity for a shearing of the interconnecting zone between the two plates along their

horizontal axis parallel to the membrane; other images show bars skewed from parallel, implying a limited capacity for the plates to rotate independently around the two-fold axis, again via this interconnecting zone. These two observations each suggest a relatively flexible connectivity
5 between the dimer plates in the membrane-proximal region of intermediate protein density, which could possibly contribute to the transmembrane signalling process.

The approximate overall measured dimensions of the ectodomain dimer are $110 \times 90 \times 120 \text{ \AA}$, calibrated against the dimensions of imaged
10 influenza neuraminidase heads, known from the solved X-ray structure (Varghese et al., 1983, *Nature* **303**, 35-40). It can be noted that there is a compatibility here between the molecular weights and molecular dimensions of these two molecular species: the compact tetrameric influenza neuraminidase heads of $M_r \sim 200 \text{ kDa}$ occupy a volume almost $100 \times 100 \times 60 \text{ \AA}$;
15 the more open dimeric insulin receptor ectodomains of similar $M_r \sim 240 \text{ kDa}$ imaged here occupy a volume approximately $110 \times 90 \times 120 \text{ \AA}$, roughly twice that of the neuraminidase heads, accommodating the slightly higher molecular weight and substantial central low-density cleft.

The low-resolution roughly cubic compact structure proposed here
20 differs substantially from the T-shaped model proposed by Christiansen et al. (1991, *Proc. Natl. Acad. Sci. U. S. A.* **88**, 249-252) and Trantum-Jensen et al., (1994, *J. Membrane Biol.* **140**, 215-223) for the whole receptor and the elongated model proposed by Schaefer et al. (1992, *J. Biol. Chem.* **267**, 23393-23402) for soluble ectodomain. Significantly, those previous studies did not
25 provide any convincing independent electron microscopical evidence that their imaged objects were in fact insulin receptor.

In the present study, the identity of the imaged molecules as hIR -11 ectodomain has been confirmed by imaging complexes of the dimer with Fabs of the three well-established conformational Mabs against native hIR,
30 83-7, 83-14 and 18-44 (Soos et al., 1986, *Biochem. J.* **235**, 199-208; 1989, *Proc. Natl Acad. Sci. USA* **86**, 5217-5221), bound singly and in combination. In all these instances, virtually every particle in the field of view exhibited MFab decoration through binding to conformational epitopes, establishing not only the identity of the imaged particles but also the conformational integrity of
35 the expressed ectodomains. Furthermore, the cleanliness and uniformity of these hIR -11 ectodomain preparations, both naked and decorated, visualised

here by electron microscopy demonstrate their high suitability for X-ray crystallization trials.

The known flexibility of the Fab arms exacerbates image-to-image variability beyond the limited extent already described for the undecorated dimeric ectodomains, complicating any precise interpretation of these antigen-antibody complexes. Such molecular flexibility also renders largely impractical any single-molecule computer image averaging to facilitate image interpretation, progressively more so with the higher order antigen-antibody complexes studied here.

The most readily interpretable of these images, showing least image-to-image variability, are those of 83-7 MFab bound to dimers where, fortuitously, the antigen-antibody complex is constrained in its degrees of rotational freedom on the carbon support film. Many projected images show the two Fab arms in line roughly through the centre of the antigen on its opposite sides, interpreted as a side projection of binding half-way up the plates from their membrane-proximal base. Other sub-sets of images show the two Fab arms still parallel but displaced clockwise or anticlockwise with 2-fold symmetry, each Fab approximating an extension of one of the parallel bars of antigen density, interpreted here as representing top or bottom projections along the 2-fold axis. The third projection, along the axis of the Fab arms, could not be sampled here because of the constraining geometry of this molecular complex. These observations suggest binding of 83-7 MFab roughly half-way up the side-edge of the hIR -11 ectodomain plate. This then allows an initial attempt at spatially mapping the 83-7 MFab epitope, which has been sequence-mapped to residues 191-297 in the cys-rich region of the insulin receptor (Zhang and Roth, 1991, *Proc. Natl. Acad. Sci. USA* **88**, 9858-9862). The spatial separation and relative orientations of the two binding epitopes of Mab 83-7 on the hIR -11 ectodomain dimer as indicated here appear inconsistent with the proposal that Mab 83-7 could bind intramolecularly to hIR (O'Brien et al., 1987, *Biochem J.* **6**, 4003-4010).

Decoration of the ectodomain dimer with 83-7 MFab established that the two plates of high protein-density are arranged with 2-fold symmetry. Decoration with either 83-14 or 18-44 MFab, on the other hand, allowed sampling of the third projection of the ectodomain dimer precluded by 83-7 MFab binding. Significantly, this third view established unequivocally the U-shaped projection of the hIR -11 ectodomain dimer, something which was

only able to be assumed with the undecorated ectodomain images. Further, this projection has allowed a rough spatial mapping close to the base of the U-shaped dimer for the epitopes recognised by 83-14 MFab (residues 469-592, connecting domain) and 18-44 MFab (residues 765-770, b-chain insert domain; exon 11 plus numbering, Prigent et al., 1990, *J. Biol. Chem.* **265**, 9970-9977).

Inherent in the model structure is the implication that, with the two-fold axis aligned normal to the membrane surface, the mouth of the low-density cleft where insulin binding may occur would lie most distant from the transmembrane anchor, whilst the zone of intermediate density connecting the two high-density plates would be in close proximity to the membrane. It follows, in this model, that the L1/cys-rich/L2 domains (Bajaj et al., 1997, *Biochim. Biophys. Acta* **916**, 220-226; Ward et al., 1995, *Proteins: Struct., Funct., Genet.* **22**, 141-153), which comprise much of the insulin-binding region (see Mynarcik et al., 1997, *J. Biol. Chem.* **272**, 2077-2081), most probably lie in the membrane-distal upper halves of the two plates, whilst the membrane-proximal lower halves contain the connecting domains, the fibronectin-type domains, the insert domains and the interchain disulphide bonds (Schaffer and Ljungqvist, 1992, *Biochem. Biophys. Res. Commun.* **189**, 650-653; Sparrow et al., 1997, *J. Biol. Chem.*, **272**, 29460-29467). Such a disposition of domains is supported by the images seen with the single MFab decoration, the 83-7 MFab epitope in the cys-rich region being spatially mapped roughly half-way up the side-edge of the ectodomain plates, and the 83-14 and 18-44 MFab epitopes (connecting domain and β -chain insert domain, respectively) being mapped near the base of the plates. Our preference is for a single a-b β monomer to occupy a single plate, although the possibility of a single monomer straddling the two plates of protein density cannot be discounted.

The more complex images involving co-binding of two, and even more so of all three, MFabs to each monomer of the ectodomain dimer are not easily interpretable with respect to relative domain arrangements within the monomer at present, not least of all because of the difficulty of finding conditions of negative staining that will simultaneously maintain the integrity of the Fab binding while highlighting recognisable and reproducible details of the internal structure of the dimeric IR ectodomain.

The data presented here demonstrate the ability of single-molecule imaging to give an initial insight into the topology of multidomain structures such as the ectodomain of hIR, and the value of combining this technique with that of either single or multiple monoclonal Fab attachment per monomer as a potential means of epitope, and domain, mapping of the structure. By imaging Fab complexes of other members of the family, such as hIGF-1R ectodomain, and combining available sequence-mapped epitope information with that presented here, a more comprehensive understanding of domain arrangements within the IR family ectodomains should be forthcoming.

EXAMPLE 5

Structure-Based Design of Ligands for the IGF Receptor as Potential Inhibitors of IGF Binding

The structure of IGF receptor can be considered as a filter or screen to design, or evaluate, potential ligands for the receptor. Those skilled in the art can use a number of well known methods for de novo ligand design, such as GRID, GREEN, HSITE, MCSS, HINT, BUCKETS, CLIX, LUDI, CAVEAT, SPLICE, HOOK, NEWLEAD, PRO_LIGAND, ELANA, LEGEND, GenStar, GrowMol, GROW, GEMINI, GroupBuild, SPROUT, and LEAPFROG, to generate potential agonists or antagonists for IGF-1R. In addition, the IGF-1R structure may be used as a query for database searches for potential ligands. The databases searched may be existing eg ACD, Cambridge Crystallographic, NCI, or virtual. Virtual databases, which contain very large numbers (currently up to 10^{12}) of chemically reasonable structures, may be generated by those skilled in the art using techniques such as DBMaker, ChemSpace, TRIAD and ILIAD.

The IGFR structure contains a number of sites into which putative ligands may bind. Search strategies known to those skilled in the art may be used to identify putative ligands for these sites. Examples of two suitable search strategies are described below:

(i) *Database Search*

The properties of key parts of the putative site may be used as a database search query. For example, the Unity 2.x database software may be used. A flexible 3D search can be run in which a "directed tweak" algorithm is used to find low energy conformations of potential ligands which satisfy the query.

(ii) *De novo design of ligands*

The Leapfrog algorithm as incorporated in the software package, Sybyl version 6.4.2 (Tripos Associates, St Louis), may be used to design potential ligands for IGF-1R sites. The coordinates of residues around the site may be taken from the x-ray structure, hydrogens and charges (Kollman all atom dictionary charges) added. From the size, shape and properties of the site, a number of potential ligands may be proposed. Leapfrog may be used to optimize the conformation of ligands and position on the site, to rank the likely strength of binding interactions with IGF-1R, and to suggest modifications to the structures which would have enhanced binding.

It is also possible to design ligands capable of interacting with more than one site. One way in which this may be done is by attaching flexible linkers to ligands designed for specific sites so as to join them. The linkers may be attached in such a way that they do not disrupt the binding to individual sites.

All references cited above are incorporated herein in their entirety by reference.

It will be appreciated by persons skilled in the art that numerous variations and/or modifications may be made to the invention as shown in the specific embodiments without departing from the spirit or scope of the invention as broadly described. The present embodiments are, therefore, to be considered in all respects as illustrative and not restrictive.

Claims:

1. A method of designing a compound able to bind to a molecule of the insulin receptor family and to modulate an activity mediated by the molecule,
5 including the step of assessing the stereochemical complementarity between the compound and the receptor site of the molecule, wherein the receptor site includes:
- (a) amino acids 1 to 462 of the receptor for IGF-1, having the atomic coordinates substantially as shown in Figure 1;
- 10 (b) a subset of said amino acids, or;
- (c) amino acids present in the amino acid sequence of a member of the insulin receptor family, which form an equivalent three-dimensional structure to that of the receptor molecule as depicted in Figure 1.
- 15 2. A method according to claim 1, in which the compound is selected or modified from a known compound identified from a database.
3. A method according to claim 1, in which the compound is designed so as to complement the structure of the receptor molecule as depicted in Figure 1.
- 20 4. A method according to any one of claims 1 to 3, in which the compound has structural regions able to make close contact with amino acid residues at the surface of the receptor site lining the groove, as depicted in Figure 2.
- 25 5. A method according to any one of claims 1 to 4, in which the compound has a stereochemistry such that it can interact with both the L1 and L2 domains of the receptor site.
- 30 6. A method according to any one of claims 1 to 4, in which the compound has a stereochemistry such that it can interact with the L1 domain of a first monomer of the receptor homodimer, and with the L2 domain of the other monomer of the receptor homodimer.
- 35 7. A method according to any one of claims 1 to 4, in which the interaction of the compound with the receptor site alters the position of at least one of the

L1, L2 or cysteine-rich domains of the receptor molecule relative to the position of at least one of the other of said domains.

8. A method according to claim 7, in which the compound interacts with the β sheet of the L1 domain of the receptor molecule, thereby causing an alteration in the position of the L1 domain relative to the position of the cysteine-rich domain or of the L2 domain.
9. A method according to claim 7, in which the compound interacts with the receptor site in the region of the interface between the L1 domain and the cysteine-rich domain of the receptor molecule, thereby causing the L1 domain and the cysteine-rich domain to move away from each other.
10. A method according to claim 7, in which the compound interacts with the hinge region between the L2 domain and the cysteine-rich domain of the receptor molecule, thereby causing an alteration in the positions of the L2 domain and the cysteine-rich domain relative to each other.
11. A method according to any one of claims 1 to 10, in which the stereochemical complementarity between the compound and the receptor site is such that the compound has a K_b for the receptor site of less than $10^{-6}M$.
12. A method according to claim 11, in which the K_b is less than $10^{-8}M$.
13. A method according to any one of claims 1 to 12, in which the compound has the ability to increase an activity mediated by the receptor molecule.
14. A method according to any one of claims 1 to 12, in which the compound has the ability to decrease an activity mediated by the receptor molecule.
15. A method according to claim 14, in which the stereochemical interaction between the compound and the receptor site is adapted to prevent the binding of a natural ligand of the receptor molecule to the receptor site.

16. A method according to claim 14 or claim 15, in which the compound has a K_1 of less than 10^{-6} M.
17. A method according to claim 16, in which the compound has a K_1 of less than 10^{-9} M.
18. A method according to claim 17, in which the compound has a K_1 of less than 10^{-9} M.
19. A method according to any one of claims 1 to 18, in which the receptor is the IGF-1R.
20. A method according to any one of claims 1 to 18, in which the receptor is the insulin receptor.
21. A computer-assisted method for identifying potential compounds able to bind to a molecule of the insulin receptor family and to modulate an activity mediated by the molecule, using a programmed computer including a processor, an input device, and an output device, including the steps of:
- (a) inputting into the programmed computer, through the input device, data comprising the atomic coordinates of the IGF-1R molecule as shown in Figure 1, or a subset thereof;
- (b) generating, using computer methods, a set of atomic coordinates of a structure that possesses stereochemical complementarity to the atomic coordinates of the IGF-1R site as shown in Figure 1, or a subset thereof, thereby generating a criteria data set;
- (c) comparing, using the processor, the criteria data set to a computer database of chemical structures;
- (d) selecting from the database, using computer methods, chemical structures which are structurally similar to a portion of said criteria data set; and
- (e) outputting, to the output device, the selected chemical structures which are similar to a portion of the criteria data set.
22. A computer-assisted method according to claim 21, in which the method is used to identify potential compounds which have the ability to decrease an activity mediated by the receptor.

23. A computer-assisted method according to claim 21 or claim 22, which further includes the step of selecting one or more chemical structures from step (e) which interact with the receptor site of the molecule in a manner which prevents the binding of natural ligands to the receptor site.

24. A computer-assisted method according to any one of claims 21 to 23, which further includes the step of obtaining a compound with a chemical structure selected in steps (d) and (e), and testing the compound for the ability to decrease an activity mediated by the receptor.

25. A computer-assisted method according to claim 21, in which the method is used to identify potential compounds which have the ability to increase an activity mediated by the receptor molecule.

26. A computer-assisted method according to claim 25, further including the step of obtaining a molecule with a chemical structure selected in steps (d) and (e), and testing the compound for the ability to increase an activity mediated by the receptor.

27. A computer-assisted method according to any one of claims 21 to 26, in which the receptor is the IGF-1R.

28. A computer-assisted method according to any one of claims 21 to 26, in which the receptor is the insulin receptor.

29. A method of screening of a putative compound having the ability to modulate the activity of a receptor of the insulin receptor family, including the steps of identifying a putative compound by a method according to any one of claims 1 to 29, and testing the compound for the ability to increase or decrease an activity mediated by the receptor.

30. A method according to claim 29, in which the test is carried out *in vitro*.

31. A method according to claim 29, in which the test is a high throughput assay.

32. A method according to claim 29, in which the test is carried out *in vivo*.
33. A method according to claim 30, in which the test is carried out *in vivo*.

5

Figure 1

ATOM	1	CB	GLU	1	55.967	11.986	66.360	1.00	59.11	AAAA	C
ATOM	2	CG	GLU	1	56.138	11.012	65.162	1.00	79.17	AAAA	C
ATOM	3	CD	GLU	1	57.382	11.319	64.321	1.00	85.10	AAAA	C
ATOM	4	OE1	GLU	1	58.404	10.754	64.796	1.00	86.18	AAAA	O
ATOM	5	OE2	GLU	1	57.424	12.013	63.270	1.00	78.70	AAAA	O
ATOM	6	C	GLU	1	53.508	12.557	66.350	1.00	48.46	AAAA	O
ATOM	7	O	GLU	1	52.685	11.863	65.784	1.00	51.27	AAAA	C
ATOM	10	H	GLU	1	54.256	10.338	67.159	1.00	61.64	AAAA	H
ATOM	12	CA	GLU	1	54.602	11.778	67.081	1.00	54.77	AAAA	C
ATOM	13	H	ILE	2	53.608	13.860	66.375	1.00	37.66	AAAA	H
ATOM	15	CA	ILE	2	52.768	14.699	65.604	1.00	40.87	AAAA	C
ATOM	16	CB	ILE	2	52.925	16.122	66.160	1.00	41.97	AAAA	C
ATOM	17	CG2	ILE	2	52.036	17.122	65.484	1.00	38.50	AAAA	C
ATOM	18	CG1	ILE	2	52.560	16.006	67.663	1.00	46.58	AAAA	C
ATOM	19	CD1	ILE	2	53.150	17.176	68.498	1.00	32.29	AAAA	C
ATOM	20	C	ILE	2	53.122	14.711	64.139	1.00	46.47	AAAA	C
ATOM	21	O	ILE	2	54.258	15.029	63.852	1.00	51.65	AAAA	O
ATOM	22	H	CYS	3	52.235	14.409	63.196	1.00	49.61	AAAA	H
ATOM	24	CA	CYS	3	52.435	14.677	61.773	1.00	38.93	AAAA	C
ATOM	25	C	CYS	3	51.429	15.708	61.302	1.00	42.06	AAAA	C
ATOM	26	O	CYS	3	50.290	15.521	61.690	1.00	42.37	AAAA	O
ATOM	27	CB	CYS	3	52.159	13.415	60.999	1.00	35.66	AAAA	C
ATOM	28	SG	CYS	3	53.019	12.004	61.674	1.00	36.98	AAAA	S
ATOM	29	H	GLY	4	51.851	16.709	60.580	1.00	42.39	AAAA	H
ATOM	31	CA	GLY	4	50.973	17.718	60.003	1.00	47.71	AAAA	C
ATOM	32	C	GLY	4	51.703	18.407	58.869	1.00	48.23	AAAA	C
ATOM	33	O	GLY	4	52.916	18.345	58.884	1.00	55.36	AAAA	O
ATOM	34	H	PRO	5	51.056	19.212	56.048	1.00	49.63	AAAA	H
ATOM	35	CD	PRO	5	51.637	19.947	56.860	1.00	45.28	AAAA	C
ATOM	36	CA	PRO	5	49.605	19.341	58.083	1.00	41.57	AAAA	C
ATOM	37	CB	PRO	5	49.397	20.703	57.474	1.00	44.30	AAAA	C
ATOM	38	CG	PRO	5	50.632	21.036	56.683	1.00	46.43	AAAA	C
ATOM	39	C	PRO	5	48.932	18.217	57.354	1.00	36.40	AAAA	C
ATOM	40	O	PRO	5	49.403	17.094	57.396	1.00	43.35	AAAA	O
ATOM	41	H	GLY	6	47.787	18.438	56.795	1.00	39.15	AAAA	H
ATOM	43	CA	GLY	6	46.896	17.336	56.350	1.00	39.24	AAAA	C
ATOM	44	C	GLY	6	47.710	16.365	55.529	1.00	33.68	AAAA	C
ATOM	45	O	GLY	6	48.510	16.863	54.753	1.00	36.00	AAAA	O
ATOM	46	H	ILE	7	47.586	15.111	55.788	1.00	35.70	AAAA	H
ATOM	48	CA	ILE	7	48.307	14.053	55.141	1.00	37.65	AAAA	C
ATOM	49	CB	ILE	7	48.556	12.797	55.933	1.00	36.31	AAAA	C
ATOM	50	CG2	ILE	7	49.043	11.700	54.988	1.00	34.67	AAAA	C
ATOM	51	CG1	ILE	7	49.561	12.857	57.067	1.00	39.34	AAAA	C
ATOM	52	CD1	ILE	7	49.678	14.249	57.668	1.00	40.22	AAAA	C
ATOM	53	C	ILE	7	47.338	13.762	53.977	1.00	45.00	AAAA	C
ATOM	54	O	ILE	7	46.150	13.843	54.195	1.00	51.52	AAAA	O
ATOM	55	H	ASP	8	47.767	13.631	52.751	1.00	45.60	AAAA	H
ATOM	57	CA	ASP	8	46.938	13.283	51.631	1.00	44.05	AAAA	C
ATOM	58	CB	ASP	8	47.003	14.469	50.651	1.00	44.21	AAAA	C
ATOM	59	CG	ASP	8	45.909	14.379	49.600	1.00	43.48	AAAA	C
ATOM	60	OD1	ASP	8	45.660	13.262	49.096	1.00	51.77	AAAA	O
ATOM	61	OD2	ASP	8	45.253	15.374	49.251	1.00	46.84	AAAA	O
ATOM	62	C	ASP	8	47.428	12.000	50.992	1.00	42.16	AAAA	C
ATOM	63	O	ASP	8	48.423	12.143	50.330	1.00	48.50	AAAA	O
ATOM	64	H	ILE	9	47.096	10.817	51.321	1.00	42.76	AAAA	H
ATOM	66	CA	ILE	9	47.441	9.505	50.939	1.00	44.05	AAAA	C
ATOM	67	CB	ILE	9	47.212	8.483	52.077	1.00	40.82	AAAA	C
ATOM	68	CG2	ILE	9	47.669	7.085	51.653	1.00	36.35	AAAA	C
ATOM	69	CG1	ILE	9	47.888	8.917	53.364	1.00	41.17	AAAA	C
ATOM	70	CD1	ILE	9	49.376	8.947	53.286	1.00	43.78	AAAA	C
ATOM	71	C	ILE	9	46.530	9.137	49.794	1.00	51.48	AAAA	C
ATOM	72	O	ILE	9	45.338	9.420	49.832	1.00	63.05	AAAA	O
ATOM	73	H	ARG	10	47.004	8.417	48.812	1.00	54.87	AAAA	H
ATOM	75	CA	ARG	10	46.283	8.089	47.600	1.00	54.17	AAAA	C
ATOM	76	CB	ARG	10	45.703	9.358	47.023	1.00	48.54	AAAA	C
ATOM	77	CG	ARG	10	46.361	10.169	45.952	1.00	46.55	AAAA	C
ATOM	78	CD	ARG	10	46.002	11.635	46.264	1.00	52.63	AAAA	C
ATOM	79	HE	ARG	10	45.082	12.226	45.284	1.00	59.27	AAAA	H
ATOM	81	CE	ARG	10	44.269	13.262	45.498	1.00	56.22	AAAA	C
ATOM	82	HH1	ARG	10	44.153	13.891	46.666	1.00	55.14	AAAA	H
ATOM	85	HH2	ARG	10	43.455	13.803	44.602	1.00	52.29	AAAA	H
ATOM	88	C	ARG	10	47.019	7.373	46.492	1.00	57.23	AAAA	C
ATOM	89	O	ARG	10	48.240	7.288	46.281	1.00	56.32	AAAA	O
ATOM	90	H	ASU	11	46.248	6.654	45.629	1.00	57.23	AAAA	H
ATOM	92	CA	ASU	11	46.800	5.917	44.494	1.00	50.73	AAAA	C
ATOM	93	CB	ASU	11	47.704	6.798	43.671	1.00	44.65	AAAA	C
ATOM	94	CG	ASU	11	46.878	7.732	42.829	1.00	50.72	AAAA	C
ATOM	95	OD1	ASU	11	45.749	7.451	42.403	1.00	72.59	AAAA	O
ATOM	96	HD2	ASU	11	47.499	8.869	42.587	1.00	54.38	AAAA	H
ATOM	99	C	ASU	11	47.635	4.736	44.915	1.00	53.07	AAAA	C
ATOM	100	O	ASU	11	47.303	3.701	44.347	1.00	51.95	AAAA	O
ATOM	101	H	ASP	12	48.566	4.822	45.878	1.00	50.96	AAAA	H
ATOM	103	CA	ASP	12	49.204	3.570	46.263	1.00	55.44	AAAA	C

2/58

ATOH	104	CB	ASP	12	50.668	3.568	45.758	1.00	66.47	AAAA	C
ATOH	105	CG	ASP	12	50.879	4.026	44.314	1.00	68.25	AAAA	C
ATOH	106	OE1	ASP	12	50.441	3.185	43.457	1.00	58.31	AAAA	O
ATOH	107	OD2	ASP	12	51.391	5.120	43.989	1.00	70.56	AAAA	O
ATOH	108	C	ASP	12	49.061	3.322	47.758	1.00	59.23	AAAA	C
ATOH	109	O	ASP	12	49.687	3.849	48.711	1.00	59.65	AAAA	O
ATOH	110	H	TYR	13	48.411	2.187	48.036	1.00	59.64	AAAA	H
ATOH	112	CA	TYR	13	48.328	1.672	49.397	1.00	64.06	AAAA	C
ATOH	113	CB	TYR	13	47.968	0.196	49.409	1.00	64.56	AAAA	C
ATOH	114	CG	TYR	13	47.467	-0.357	50.721	1.00	69.18	AAAA	C
ATOH	115	CD1	TYR	13	46.216	-0.024	51.248	1.00	72.71	AAAA	C
ATOH	116	CE1	TYR	13	45.746	-0.541	52.450	1.00	71.51	AAAA	C
ATOH	117	CD2	TYR	13	48.233	-1.247	51.457	1.00	70.36	AAAA	C
ATOH	118	CE2	TYR	13	47.788	-1.778	52.661	1.00	71.64	AAAA	C
ATOH	119	CS	TYR	13	46.542	-1.420	53.160	1.00	71.31	AAAA	C
ATOH	120	OH	TYR	13	46.144	-1.977	54.358	1.00	63.25	AAAA	O
ATOH	122	C	TYR	13	49.622	1.839	50.198	1.00	65.99	AAAA	C
ATOH	123	O	TYR	13	49.621	2.321	51.354	1.00	65.01	AAAA	O
ATOH	124	H	GLU	14	50.786	1.541	49.594	1.00	63.51	AAAA	H
ATOH	126	CA	GLU	14	52.078	1.681	50.218	1.00	63.51	AAAA	C
ATOH	127	CB	GLU	14	53.174	1.318	49.219	1.00	68.37	AAAA	C
ATOH	128	CG	GLU	14	52.863	-0.078	48.686	1.00	84.62	AAAA	C
ATOH	129	CD	GLU	14	53.990	-0.515	47.754	1.00	92.28	AAAA	C
ATOH	130	OE1	GLU	14	53.945	-0.161	46.573	1.00	94.82	AAAA	O
ATOH	131	HE2	GLU	14	54.920	-1.254	48.361	1.00	98.03	AAAA	H
ATOH	134	C	GLU	14	52.434	3.058	50.753	1.00	61.62	AAAA	C
ATOH	135	O	GLU	14	53.266	3.292	51.644	1.00	62.09	AAAA	O
ATOH	136	H	GLU	15	51.628	4.038	50.349	1.00	57.02	AAAA	H
ATOH	138	CA	GLU	15	51.724	5.399	50.831	1.00	51.71	AAAA	C
ATOH	139	CB	GLU	15	50.861	6.220	49.911	1.00	43.75	AAAA	C
ATOH	140	CG	GLU	15	51.566	6.605	48.648	1.00	59.65	AAAA	C
ATOH	141	CD	GLU	15	51.554	8.105	48.428	1.00	72.96	AAAA	C
ATOH	142	OE1	GLU	15	51.168	9.005	49.184	1.00	80.58	AAAA	O
ATOH	143	HE2	GLU	15	52.016	8.378	47.211	1.00	74.17	AAAA	H
ATOH	146	C	GLU	15	51.219	5.530	52.258	1.00	50.15	AAAA	C
ATOH	147	O	GLU	15	51.576	6.500	52.940	1.00	48.04	AAAA	O
ATOH	148	H	LEU	16	50.440	4.535	52.688	1.00	46.22	AAAA	H
ATOH	150	CA	LEU	16	49.913	4.449	54.019	1.00	45.52	AAAA	C
ATOH	151	CB	LEU	16	48.950	3.295	54.159	1.00	37.73	AAAA	C
ATOH	152	CG	LEU	16	47.502	3.425	53.707	1.00	41.40	AAAA	C
ATOH	153	CD1	LEU	16	46.837	2.063	53.790	1.00	42.43	AAAA	C
ATOH	154	CD2	LEU	16	46.687	4.424	54.545	1.00	35.93	AAAA	C
ATOH	155	C	LEU	16	51.042	4.280	55.039	1.00	51.52	AAAA	C
ATOH	156	O	LEU	16	50.913	4.601	56.235	1.00	52.53	AAAA	O
ATOH	157	H	LYS	17	52.252	3.936	54.560	1.00	51.01	AAAA	H
ATOH	159	CA	LYS	17	53.422	3.914	55.404	1.00	50.73	AAAA	C
ATOH	160	CB	LYS	17	54.609	3.252	54.737	1.00	56.10	AAAA	C
ATOH	161	CG	LYS	17	54.539	1.733	54.831	1.00	62.40	AAAA	C
ATOH	162	CD	LYS	17	54.768	1.278	53.387	1.00	63.85	AAAA	C
ATOH	163	CE	LYS	17	55.316	-0.141	53.426	1.00	68.40	AAAA	C
ATOH	164	HE	LYS	17	56.537	-0.225	52.554	1.00	73.83	AAAA	H
ATOH	168	C	LYS	17	53.844	5.270	55.852	1.00	44.78	AAAA	C
ATOH	169	O	LYS	17	54.492	5.262	56.933	1.00	39.39	AAAA	O
ATOH	170	H	ARG	18	53.524	6.344	55.201	1.00	41.15	AAAA	H
ATOH	172	CA	ARG	18	53.827	7.673	55.676	1.00	43.01	AAAA	C
ATOH	173	CB	ARG	18	53.250	8.702	54.704	1.00	43.97	AAAA	C
ATOH	174	CG	ARG	18	53.888	8.764	53.333	1.00	53.60	AAAA	C
ATOH	175	CD	ARG	18	52.964	9.362	52.269	1.00	60.34	AAAA	C
ATOH	176	HE	ARG	18	52.528	10.703	52.650	1.00	50.00	AAAA	H
ATOH	178	CE	ARG	18	51.628	11.444	52.021	1.00	48.86	AAAA	C
ATOH	179	HE1	ARG	18	51.068	10.941	50.943	1.00	47.96	AAAA	H
ATOH	182	HE2	ARG	18	51.377	12.656	52.555	1.00	43.72	AAAA	H
ATOH	185	C	ARG	18	53.268	7.924	57.077	1.00	44.03	AAAA	C
ATOH	186	O	ARG	18	53.402	9.010	57.644	1.00	45.53	AAAA	O
ATOH	187	H	LEU	19	52.445	7.069	57.632	1.00	46.36	AAAA	H
ATOH	189	CA	LEU	19	51.653	7.282	58.794	1.00	50.25	AAAA	C
ATOH	190	CB	LEU	19	50.186	6.924	58.674	1.00	50.83	AAAA	C
ATOH	191	CG	LEU	19	49.202	7.371	57.608	1.00	46.43	AAAA	C
ATOH	192	CD1	LEU	19	47.846	6.743	57.852	1.00	22.57	AAAA	C
ATOH	193	CD2	LEU	19	49.018	8.866	57.495	1.00	45.88	AAAA	C
ATOH	194	C	LEU	19	52.210	6.428	59.912	1.00	49.87	AAAA	C
ATOH	195	O	LEU	19	51.870	6.810	61.030	1.00	51.54	AAAA	O
ATOH	196	H	GLU	20	53.270	5.708	59.652	1.00	49.35	AAAA	H
ATOH	198	CA	GLU	20	53.819	4.833	60.679	1.00	49.60	AAAA	C
ATOH	199	CB	GLU	20	54.876	3.960	59.982	1.00	57.91	AAAA	C
ATOH	200	CG	GLU	20	55.893	4.840	59.272	1.00	70.16	AAAA	C
ATOH	201	CD	GLU	20	57.095	4.077	58.757	1.00	69.35	AAAA	C
ATOH	202	OE1	GLU	20	58.123	4.795	58.722	1.00	71.38	AAAA	O
ATOH	203	OE2	GLU	20	56.993	2.885	58.420	1.00	72.84	AAAA	C
ATOH	204	C	GLU	20	54.310	5.417	61.989	1.00	43.55	AAAA	C
ATOH	205	O	GLU	20	54.301	4.652	62.937	1.00	40.01	AAAA	O
ATOH	206	H	ASH	21	54.633	6.659	62.207	1.00	41.06	AAAA	H
ATOH	208	CA	ASH	21	55.054	7.204	63.454	1.00	47.17	AAAA	C
ATOH	209	C	ASH	21	54.066	8.141	64.108	1.00	49.76	AAAA	C
ATOH	210	O	ASH	21	54.228	8.456	65.303	1.00	48.10	AAAA	O

3/58

ATOM	211	CB	ASH	21	56.379	6.093	63.299	1.00	59.11	AAAA	C
ATOM	212	CG	ASH	21	57.413	7.051	63.796	1.00	68.38	AAAA	C
ATOM	213	OD1	ASH	21	57.499	5.855	63.122	1.00	58.51	AAAA	O
ATOM	214	HD2	ASH	21	58.348	7.469	61.890	1.00	77.20	AAAA	H
ATOM	216	H	CYS	22	53.129	8.711	63.351	1.00	47.44	AAAA	H
ATOM	218	CA	CYS	22	52.107	9.614	63.879	1.00	42.99	AAAA	C
ATOM	219	C	CYS	22	51.215	9.089	65.021	1.00	40.43	AAAA	C
ATOM	220	O	CYS	22	50.750	7.923	65.069	1.00	36.07	AAAA	O
ATOM	221	CB	CYS	22	51.182	9.921	62.690	1.00	44.82	AAAA	C
ATOM	222	SG	CYS	22	52.076	10.328	61.148	1.00	39.51	AAAA	S
ATOM	223	H	THR	23	51.287	9.801	66.137	1.00	36.24	AAAA	H
ATOM	225	CA	THR	23	50.339	9.482	67.204	1.00	43.51	AAAA	C
ATOM	226	CE	THR	23	50.944	9.481	68.593	1.00	41.38	AAAA	C
ATOM	227	OG1	THR	23	51.410	10.843	68.822	1.00	51.21	AAAA	O
ATOM	229	CG2	THR	23	52.119	8.571	68.838	1.00	33.83	AAAA	C
ATOM	230	C	THR	23	49.250	10.599	67.116	1.00	44.55	AAAA	C
ATOM	231	O	THR	23	48.085	10.414	67.481	1.00	45.95	AAAA	O
ATOM	232	H	VAL	24	49.646	11.797	66.689	1.00	33.03	AAAA	H
ATOM	234	CA	VAL	24	48.732	12.855	66.442	1.00	35.29	AAAA	C
ATOM	235	CB	VAL	24	48.925	13.979	67.456	1.00	30.60	AAAA	C
ATOM	236	CG1	VAL	24	48.056	15.157	67.082	1.00	27.21	AAAA	C
ATOM	237	CG2	VAL	24	48.656	13.566	68.886	1.00	25.37	AAAA	C
ATOM	238	C	VAL	24	48.895	13.447	65.043	1.00	41.52	AAAA	C
ATOM	239	O	VAL	24	49.987	13.963	64.791	1.00	44.40	AAAA	O
ATOM	240	H	ILE	25	47.855	13.450	64.203	1.00	40.13	AAAA	H
ATOM	242	CA	ILE	25	47.908	14.094	62.882	1.00	32.05	AAAA	C
ATOM	243	CB	ILE	25	47.113	13.299	61.853	1.00	25.85	AAAA	C
ATOM	244	CG2	ILE	25	47.027	14.039	60.542	1.00	18.73	AAAA	C
ATOM	245	CG1	ILE	25	47.677	11.896	61.705	1.00	29.80	AAAA	C
ATOM	246	CD1	ILE	25	47.169	11.155	60.471	1.00	27.41	AAAA	C
ATOM	247	C	ILE	25	47.397	15.490	62.941	1.00	32.92	AAAA	C
ATOM	248	O	ILE	25	46.223	15.776	63.213	1.00	40.91	AAAA	O
ATOM	249	H	GLU	26	48.264	16.472	63.042	1.00	36.60	AAAA	H
ATOM	251	CA	GLU	26	47.832	17.847	63.226	1.00	29.24	AAAA	C
ATOM	252	CB	GLU	26	48.875	18.703	63.856	1.00	29.92	AAAA	C
ATOM	253	CS	GLU	26	48.490	20.144	64.116	1.00	38.06	AAAA	C
ATOM	254	CD	GLU	26	49.561	20.762	65.013	1.00	37.39	AAAA	C
ATOM	255	OE1	GLU	26	50.654	20.937	64.489	1.00	41.56	AAAA	O
ATOM	256	OE2	GLU	26	49.571	21.175	66.182	1.00	49.16	AAAA	O
ATOM	257	C	GLU	26	47.413	18.376	61.869	1.00	37.79	AAAA	C
ATOM	258	O	GLU	26	48.161	19.069	61.181	1.00	39.68	AAAA	O
ATOM	259	H	GLY	27	46.117	18.104	61.582	1.00	37.28	AAAA	H
ATOM	261	CA	GLY	27	45.498	18.503	60.320	1.00	31.17	AAAA	C
ATOM	262	C	GLY	27	44.531	17.400	59.893	1.00	33.72	AAAA	C
ATOM	263	O	GLY	27	43.988	16.715	60.775	1.00	33.29	AAAA	O
ATOM	264	H	TYR	28	44.304	17.209	58.604	1.00	29.24	AAAA	H
ATOM	266	CA	TYR	28	43.318	16.189	58.253	1.00	28.93	AAAA	C
ATOM	267	CB	TYR	28	42.403	16.794	57.217	1.00	31.53	AAAA	C
ATOM	268	CG	TYR	28	43.058	17.256	55.962	1.00	31.79	AAAA	C
ATOM	269	CD1	TYR	28	43.704	16.355	55.116	1.00	36.07	AAAA	C
ATOM	270	CE1	TYR	28	44.361	16.706	53.967	1.00	28.91	AAAA	C
ATOM	271	CD2	TYR	28	43.130	18.572	55.606	1.00	30.98	AAAA	C
ATOM	272	CE2	TYR	28	43.769	18.972	54.428	1.00	28.77	AAAA	C
ATOM	273	CS	TYR	28	44.367	18.021	53.652	1.00	31.53	AAAA	C
ATOM	274	OH	TYR	28	44.971	18.425	52.464	1.00	44.74	AAAA	O
ATOM	276	C	TYR	28	43.953	14.946	57.697	1.00	29.23	AAAA	C
ATOM	277	O	TYR	28	45.119	15.147	57.383	1.00	35.58	AAAA	O
ATOM	278	H	LEU	29	43.250	13.900	57.445	1.00	26.63	AAAA	H
ATOM	280	CA	LEU	29	43.764	12.730	56.803	1.00	29.23	AAAA	C
ATOM	281	CB	LEU	29	43.830	11.611	57.856	1.00	27.09	AAAA	C
ATOM	282	CG	LEU	29	44.212	10.258	57.242	1.00	31.90	AAAA	C
ATOM	283	CD1	LEU	29	45.538	10.396	56.469	1.00	35.03	AAAA	C
ATOM	284	CD2	LEU	29	44.551	9.203	58.290	1.00	25.05	AAAA	C
ATOM	285	C	LEU	29	42.897	12.342	55.616	1.00	33.84	AAAA	C
ATOM	286	O	LEU	29	41.689	12.165	55.806	1.00	43.29	AAAA	O
ATOM	287	H	HIS	30	43.369	12.285	54.395	1.00	35.95	AAAA	H
ATOM	289	CA	HIS	30	42.681	11.891	53.197	1.00	34.92	AAAA	C
ATOM	290	CB	HIS	30	42.893	12.801	52.027	1.00	32.85	AAAA	C
ATOM	291	CG	HIS	30	42.372	14.155	52.046	1.00	25.08	AAAA	C
ATOM	292	CD2	HIS	30	41.519	14.753	52.907	1.00	40.88	AAAA	C
ATOM	293	HD1	HIS	30	42.717	15.120	51.128	1.00	33.66	AAAA	H
ATOM	295	CE1	HIS	30	42.080	16.281	51.444	1.00	31.33	AAAA	C
ATOM	296	HE2	HIS	30	41.329	16.093	52.539	1.00	37.27	AAAA	H
ATOM	298	C	HIS	30	43.173	10.538	52.714	1.00	37.68	AAAA	C
ATOM	299	O	HIS	30	44.357	10.388	52.541	1.00	38.70	AAAA	O
ATOM	300	H	ILE	31	42.308	9.542	52.584	1.00	40.02	AAAA	H
ATOM	302	CA	ILE	31	42.750	8.271	51.992	1.00	39.47	AAAA	C
ATOM	303	CB	ILE	31	42.668	7.204	53.063	1.00	37.95	AAAA	C
ATOM	304	CG2	ILE	31	43.161	5.830	52.651	1.00	23.86	AAAA	C
ATOM	305	CG1	ILE	31	43.481	7.555	54.335	1.00	41.66	AAAA	C
ATOM	306	CD1	ILE	31	43.170	6.575	55.473	1.00	28.22	AAAA	C
ATOM	307	C	ILE	31	41.884	8.044	50.755	1.00	46.52	AAAA	C
ATOM	308	O	ILE	31	40.753	7.589	50.827	1.00	43.56	AAAA	O
ATOM	309	H	LEU	32	42.314	9.489	49.556	1.00	49.89	AAAA	H
ATOM	311	CA	LEU	32	41.484	8.235	48.380	1.00	49.77	AAAA	C

4/58

ATOM	312	CB	LEU	32	41.127	9.515	47.603	1.00	47.48	AAAA	C
ATOM	313	CG	LEU	32	42.091	10.688	47.562	1.00	45.33	AAAA	C
ATOM	314	CD1	LEU	32	41.517	11.812	46.673	1.00	35.77	AAAA	C
ATOM	315	CD2	LEU	32	42.371	11.229	48.960	1.00	49.14	AAAA	C
ATOM	316	C	LEU	32	42.136	7.296	47.353	1.00	51.00	AAAA	C
ATOM	317	O	LEU	32	43.338	7.370	47.186	1.00	41.36	AAAA	O
ATOM	318	H	LEU	33	41.270	6.722	46.497	1.00	50.74	AAAA	H
ATOM	320	CA	LEU	33	41.602	6.175	45.127	1.00	49.92	AAAA	C
ATOM	321	CB	LEU	33	42.091	7.262	44.182	1.00	34.83	AAAA	C
ATOM	322	CG	LEU	33	41.233	8.537	44.164	1.00	33.92	AAAA	C
ATOM	323	CD1	LEU	33	41.892	9.587	43.298	1.00	37.49	AAAA	C
ATOM	324	CD2	LEU	33	39.823	8.313	43.644	1.00	33.01	AAAA	C
ATOM	325	C	LEU	33	42.618	5.073	45.287	1.00	48.35	AAAA	C
ATOM	326	O	LEU	33	43.580	5.077	44.538	1.00	54.14	AAAA	O
ATOM	327	H	ILE	34	42.543	4.212	46.254	1.00	47.61	AAAA	H
ATOM	329	CA	ILE	34	43.523	3.184	46.540	1.00	51.70	AAAA	C
ATOM	330	CB	ILE	34	44.101	3.346	47.963	1.00	57.98	AAAA	C
ATOM	331	CG2	ILE	34	44.538	2.043	48.600	1.00	48.98	AAAA	C
ATOM	332	CG1	ILE	34	45.267	4.371	47.967	1.00	46.70	AAAA	C
ATOM	333	CD1	ILE	34	45.561	4.704	49.439	1.00	66.47	AAAA	C
ATOM	334	C	ILE	34	42.829	1.844	46.408	1.00	59.85	AAAA	C
ATOM	335	O	ILE	34	41.726	1.531	46.856	1.00	60.11	AAAA	O
ATOM	336	H	SER	35	43.622	0.833	46.013	1.00	67.79	AAAA	H
ATOM	338	CA	SER	35	43.048	-0.511	45.922	1.00	68.80	AAAA	C
ATOM	339	CB	SER	35	42.767	-0.882	44.469	1.00	64.16	AAAA	C
ATOM	340	CG	SER	35	41.731	-1.846	44.498	1.00	75.76	AAAA	C
ATOM	342	C	SER	35	43.928	-1.564	46.537	1.00	70.73	AAAA	C
ATOM	343	O	SER	35	44.885	-1.954	45.909	1.00	73.65	AAAA	O
ATOM	344	H	LYS	36	43.687	-2.017	47.740	1.00	74.75	AAAA	H
ATOM	346	CA	LYS	36	44.465	-3.014	48.421	1.00	76.09	AAAA	C
ATOM	347	CB	LYS	36	44.046	-3.131	49.885	1.00	81.22	AAAA	C
ATOM	348	CG	LYS	36	45.147	-3.654	50.775	1.00	78.87	AAAA	C
ATOM	349	CD	LYS	36	44.693	-4.575	51.887	1.00	81.39	AAAA	C
ATOM	350	CE	LYS	36	44.890	-6.025	51.492	1.00	89.38	AAAA	C
ATOM	351	HE	LYS	36	44.371	-6.989	52.506	1.00	91.63	AAAA	H
ATOM	355	C	LYS	36	44.252	-4.362	47.753	1.00	81.41	AAAA	C
ATOM	356	O	LYS	36	43.145	-4.772	47.451	1.00	78.20	AAAA	O
ATOM	357	H	ALA	37	45.371	-5.080	47.615	1.00	88.27	AAAA	H
ATOM	359	CA	ALA	37	45.361	-6.396	46.986	1.00	90.10	AAAA	C
ATOM	360	CB	ALA	37	46.700	-6.655	46.327	1.00	95.49	AAAA	C
ATOM	361	C	ALA	37	45.011	-7.473	47.995	1.00	92.36	AAAA	C
ATOM	362	O	ALA	37	45.668	-7.627	49.012	1.00	92.35	AAAA	O
ATOM	363	H	SER	38	44.031	-8.301	47.622	1.00	94.31	AAAA	H
ATOM	365	CA	SER	38	43.528	-9.352	48.484	1.00	95.70	AAAA	C
ATOM	366	CB	SER	38	42.405	-10.164	47.858	1.00	97.44	AAAA	C
ATOM	367	CG	SER	38	42.061	-11.176	48.814	1.00103.48	AAAA	O	
ATOM	369	C	SER	38	44.702	-10.263	48.821	1.00	96.87	AAAA	C
ATOM	370	O	SER	38	44.761	-10.778	49.924	1.00	98.06	AAAA	O
ATOM	371	H	ASP	39	45.584	-10.415	47.852	1.00	97.59	AAAA	H
ATOM	373	CA	ASP	39	46.821	-11.148	47.980	1.00	99.19	AAAA	C
ATOM	374	CB	ASP	39	47.579	-11.050	46.652	1.00102.13	AAAA	C	
ATOM	375	CG	ASP	39	47.696	-12.387	45.949	0.01101.22	AAAA	C	
ATOM	376	OD1	ASP	39	46.644	-12.978	45.623	0.01101.42	AAAA	O	
ATOM	377	OD2	ASP	39	48.833	-12.848	45.718	0.01101.41	AAAA	O	
ATOM	378	C	ASP	39	47.660	-10.564	49.105	1.00	99.40	AAAA	C
ATOM	379	O	ASP	39	47.692	-11.056	50.224	1.00	99.15	AAAA	O
ATOM	380	H	TYR	40	48.354	-9.479	48.818	1.00100.96	AAAA	H	
ATOM	382	CA	TYR	40	49.120	-8.706	49.802	1.00101.16	AAAA	C	
ATOM	383	CB	TYR	40	49.511	-7.393	49.130	1.00103.67	AAAA	C	
ATOM	384	CG	TYR	40	50.159	-6.281	49.887	1.00107.81	AAAA	C	
ATOM	385	CD1	TYR	40	50.931	-5.325	49.228	1.00109.56	AAAA	C	
ATOM	386	CE1	TYR	40	51.540	-4.280	49.910	1.00109.67	AAAA	C	
ATOM	387	CD2	TYR	40	50.044	-6.115	51.254	1.00109.28	AAAA	C	
ATOM	388	CE2	TYR	40	50.618	-5.102	51.976	1.00109.83	AAAA	C	
ATOM	389	CG	TYR	40	51.372	-4.181	51.276	1.00110.16	AAAA	C	
ATOM	390	OH	TYR	40	51.999	-3.127	51.893	1.00109.84	AAAA	O	
ATOM	392	C	TYR	40	48.343	-8.529	51.100	1.00	99.10	AAAA	C
ATOM	393	O	TYR	40	47.168	-8.182	51.183	1.00	99.05	AAAA	O
ATOM	394	H	LYS	41	49.041	-8.653	52.218	1.00	98.62	AAAA	H
ATOM	396	CA	LYS	41	48.443	-8.549	53.546	1.00100.30	AAAA	C	
ATOM	397	CB	LYS	41	49.385	-9.160	54.599	1.00104.42	AAAA	C	
ATOM	398	CG	LYS	41	49.218	-10.649	54.814	0.01101.06	AAAA	C	
ATOM	399	CD	LYS	41	47.776	-11.107	54.919	0.01100.66	AAAA	C	
ATOM	400	CE	LYS	41	47.205	-10.880	56.308	0.01	99.86	AAAA	C
ATOM	401	HE	LYS	41	47.982	-11.728	57.328	0.01	99.62	AAAA	H
ATOM	405	C	LYS	41	48.035	-7.136	53.947	1.00	98.99	AAAA	C
ATOM	406	O	LYS	41	47.615	-6.371	53.057	1.00103.33	AAAA	O	
ATOM	407	H	SER	42	48.198	-6.754	55.221	1.00	91.75	AAAA	H
ATOM	409	CA	SER	42	47.825	-5.412	55.604	1.00	85.06	AAAA	C
ATOM	410	CB	SER	42	46.385	-5.520	56.147	1.00	95.33	AAAA	C
ATOM	411	CG	SER	42	46.547	-6.140	57.426	1.00104.63	AAAA	O	
ATOM	413	C	SER	42	48.628	-4.715	56.687	1.00	80.78	AAAA	C
ATOM	414	O	SER	42	49.326	-5.259	57.538	1.00	81.03	AAAA	O
ATOM	415	H	TYR	43	48.495	-5.395	56.673	1.00	73.03	AAAA	H
ATOM	417	CA	TYR	43	49.069	-2.488	57.635	1.00	67.25	AAAA	C

5/58

ATOH	418	CH	TYR	43	49.065	-1.119	56.865	1.00	65.37	AAAA	C
ATOH	419	CG	TYR	43	49.953	-1.021	55.727	1.00	63.22	AAAA	C
ATOH	420	CD1	TYR	43	50.931	-1.925	55.408	1.00	63.87	AAAA	C
ATOH	421	CE1	TYR	43	51.698	-1.781	54.274	1.00	66.09	AAAA	C
ATOH	422	CD2	TYR	43	49.770	0.050	54.870	1.00	63.30	AAAA	C
ATOH	423	CE2	TYR	43	50.536	0.214	53.728	1.00	67.62	AAAA	C
ATOH	424	CG	TYR	43	51.508	-0.712	53.432	1.00	66.94	AAAA	C
ATOH	425	OH	TYR	43	52.262	-0.563	52.305	1.00	65.23	AAAA	O
ATOH	427	C	TYR	43	48.248	-2.381	58.925	1.00	64.88	AAAA	C
ATOH	428	O	TYR	43	47.088	-2.851	59.030	1.00	62.90	AAAA	O
ATOH	429	H	ARG	44	48.782	-1.567	59.825	1.00	57.88	AAAA	H
ATOH	431	CA	ARG	44	48.019	-1.285	61.039	1.00	56.45	AAAA	C
ATOH	432	CB	ARG	44	47.842	-2.611	61.760	1.00	46.51	AAAA	C
ATOH	433	CG	ARG	44	47.815	-2.375	63.244	1.00	54.66	AAAA	C
ATOH	434	CD	ARG	44	46.885	-3.327	63.986	1.00	58.54	AAAA	C
ATOH	435	HE	ARG	44	47.090	-2.927	65.403	1.00	68.56	AAAA	C
ATOH	437	CS	ARG	44	46.464	-3.536	66.395	1.00	64.82	AAAA	H
ATOH	438	HH1	ARG	44	45.644	-4.529	66.132	1.00	61.53	AAAA	C
ATOH	441	HH2	ARG	44	46.674	-3.139	67.628	1.00	66.03	AAAA	H
ATOH	444	C	ARG	44	48.811	-0.285	61.845	1.00	55.50	AAAA	C
ATOH	445	O	ARG	44	49.916	-0.552	62.320	1.00	58.43	AAAA	O
ATOH	446	H	PHE	45	48.276	0.866	62.139	1.00	51.13	AAAA	H
ATOH	448	CA	PHE	45	48.865	1.944	62.863	1.00	45.94	AAAA	C
ATOH	449	CB	PHE	45	48.774	3.249	61.978	1.00	35.89	AAAA	C
ATOH	450	CG	PHE	45	49.106	2.937	60.554	1.00	30.29	AAAA	C
ATOH	451	CD1	PHE	45	50.373	3.051	59.998	1.00	45.72	AAAA	C
ATOH	452	CD2	PHE	45	48.127	2.428	59.728	1.00	35.95	AAAA	C
ATOH	453	CE1	PHE	45	50.653	2.715	58.672	1.00	47.76	AAAA	C
ATOH	454	CE2	PHE	45	48.358	2.096	58.406	1.00	39.92	AAAA	C
ATOH	455	CD	PHE	45	49.612	2.244	57.967	1.00	46.44	AAAA	C
ATOH	456	C	PHE	45	48.181	2.123	64.203	1.00	41.65	AAAA	C
ATOH	457	O	PHE	45	47.708	3.223	64.475	1.00	40.99	AAAA	C
ATOH	458	H	PRO	46	48.494	1.338	65.212	1.00	43.20	AAAA	H
ATOH	459	CD	PRO	46	49.300	0.097	65.132	1.00	47.74	AAAA	C
ATOH	460	CA	PRO	46	48.032	1.530	66.560	1.00	43.34	AAAA	C
ATOH	461	CB	PRO	46	48.514	0.319	67.380	1.00	44.92	AAAA	C
ATOH	462	CG	PRO	46	49.404	-0.464	66.514	1.00	45.48	AAAA	C
ATOH	463	C	PRO	46	48.558	2.768	67.233	1.00	41.30	AAAA	C
ATOH	464	O	PRO	46	48.329	2.830	68.443	1.00	44.57	AAAA	O
ATOH	465	H	LYS	47	49.450	3.533	66.676	1.00	39.33	AAAA	H
ATOH	467	CA	LYS	47	49.991	4.679	67.362	1.00	38.10	AAAA	C
ATOH	468	CB	LYS	47	51.378	4.981	66.852	1.00	48.07	AAAA	C
ATOH	469	CG	LYS	47	52.032	3.995	65.902	1.00	67.95	AAAA	C
ATOH	470	CD	LYS	47	53.563	3.976	65.891	1.00	61.33	AAAA	C
ATOH	471	CE	LYS	47	54.115	4.648	67.147	1.00	72.19	AAAA	C
ATOH	472	HE	LYS	47	54.024	6.132	66.874	1.00	79.29	AAAA	H
ATOH	476	C	LYS	47	49.014	5.848	67.195	1.00	39.76	AAAA	C
ATOH	477	O	LYS	47	49.189	6.827	67.952	1.00	35.45	AAAA	O
ATOH	478	H	LEU	48	48.300	5.886	66.053	1.00	38.45	AAAA	H
ATOH	480	CA	LEU	48	47.370	7.004	65.800	1.00	40.40	AAAA	C
ATOH	481	CB	LEU	48	46.823	6.919	64.389	1.00	28.59	AAAA	C
ATOH	482	CG	LEU	48	45.947	7.967	63.787	1.00	31.04	AAAA	C
ATOH	483	CD1	LEU	48	46.637	9.310	63.878	1.00	36.86	AAAA	C
ATOH	484	CD2	LEU	48	45.591	7.738	62.294	1.00	34.49	AAAA	C
ATOH	485	C	LEU	48	46.186	7.022	66.807	1.00	42.21	AAAA	C
ATOH	486	O	LEU	48	45.271	6.187	66.863	1.00	36.48	AAAA	O
ATOH	487	H	THR	49	46.138	8.041	67.673	1.00	38.95	AAAA	H
ATOH	489	CA	THR	49	45.045	8.151	68.574	1.00	37.96	AAAA	C
ATOH	490	CB	THR	49	45.548	8.207	70.034	1.00	48.69	AAAA	C
ATOH	491	CG1	THR	49	46.396	9.340	70.225	1.00	35.90	AAAA	O
ATOH	493	CG2	THR	49	46.230	6.957	70.529	1.00	31.99	AAAA	C
ATOH	494	C	THR	49	44.230	9.425	68.321	1.00	39.48	AAAA	C
ATOH	495	O	THR	49	43.111	9.451	68.837	1.00	34.49	AAAA	O
ATOH	496	H	VAL	50	44.735	10.415	67.605	1.00	37.32	AAAA	H
ATOH	498	CA	VAL	50	43.995	11.664	67.418	1.00	38.72	AAAA	C
ATOH	499	CB	VAL	50	44.293	12.708	68.503	1.00	37.24	AAAA	C
ATOH	500	CG1	VAL	50	43.630	14.066	68.208	1.00	29.96	AAAA	C
ATOH	501	CG2	VAL	50	43.884	12.311	69.913	1.00	32.52	AAAA	C
ATOH	502	C	VAL	50	44.271	12.305	66.048	1.00	37.03	AAAA	C
ATOH	503	O	VAL	50	45.195	11.863	65.431	1.00	37.96	AAAA	O
ATOH	504	H	ILE	51	43.319	12.939	65.415	1.00	37.49	AAAA	H
ATOH	506	CA	ILE	51	43.301	13.575	64.133	1.00	32.48	AAAA	C
ATOH	507	CB	ILE	51	42.346	12.864	63.152	1.00	34.51	AAAA	C
ATOH	508	CG2	ILE	51	41.995	13.802	61.978	1.00	32.31	AAAA	C
ATOH	509	CG1	ILE	51	43.026	11.611	62.671	1.00	30.78	AAAA	C
ATOH	510	CD1	ILE	51	42.358	10.559	61.815	1.00	19.69	AAAA	C
ATOH	511	C	ILE	51	42.659	14.939	64.431	1.00	34.14	AAAA	C
ATOH	512	O	ILE	51	41.546	14.830	64.923	1.00	29.08	AAAA	O
ATOH	513	H	THR	52	43.342	16.058	64.238	1.00	33.93	AAAA	H
ATOH	515	CA	THR	52	42.806	17.305	64.719	1.00	33.83	AAAA	C
ATOH	516	CB	THR	52	43.961	18.338	64.939	1.00	35.39	AAAA	C
ATOH	517	CG1	THR	52	44.726	18.567	63.781	1.00	41.28	AAAA	O
ATOH	519	CG2	THR	52	44.775	17.926	66.134	1.00	22.01	AAAA	C
ATOH	520	C	THR	52	41.741	17.961	63.863	1.00	39.02	AAAA	C
ATOH	521	O	THR	52	41.202	19.030	64.243	1.00	38.88	AAAA	O

6/58

ATOM	522	H	GLU	53	41.524	17.477	62.639	1.00	36.93	AAAA	H
ATOM	524	CA	GLU	53	40.434	17.953	61.785	1.00	38.38	AAAA	C
ATOM	525	CB	GLU	53	41.064	18.512	60.483	1.00	29.76	AAAA	C
ATOM	526	CG	GLU	53	42.061	19.552	60.034	1.00	30.48	AAAA	C
ATOM	527	CD	GLU	53	42.517	20.396	59.697	1.00	40.82	AAAA	C
ATOM	528	OE1	GLU	53	42.638	19.908	58.556	1.00	57.56	AAAA	O
ATOM	529	OE2	GLU	53	42.799	21.559	59.931	1.00	35.74	AAAA	O
ATOM	530	C	GLU	53	39.506	16.789	61.388	1.00	39.19	AAAA	C
ATOM	531	O	GLU	53	38.922	16.311	62.386	1.00	38.95	AAAA	O
ATOM	532	H	TYR	54	39.639	16.353	60.102	1.00	30.60	AAAA	H
ATOM	534	CA	TYR	54	38.666	15.342	59.713	1.00	35.96	AAAA	C
ATOM	535	CB	TYR	54	37.654	15.802	58.636	1.00	30.71	AAAA	C
ATOM	536	CG	TYR	54	38.247	16.476	57.388	1.00	21.18	AAAA	C
ATOM	537	CD1	TYR	54	38.487	15.733	56.305	1.00	20.22	AAAA	C
ATOM	538	CE1	TYR	54	38.980	16.743	55.086	1.00	21.04	AAAA	C
ATOM	539	CD2	TYR	54	38.577	17.844	57.307	1.00	23.97	AAAA	C
ATOM	540	CE2	TYR	54	39.049	18.384	56.124	1.00	24.69	AAAA	C
ATOM	541	CZ	TYR	54	39.263	17.569	55.032	1.00	26.72	AAAA	C
ATOM	542	OH	TYR	54	39.763	18.047	53.847	1.00	37.55	AAAA	O
ATOM	544	C	TYR	54	39.405	14.115	59.142	1.00	33.87	AAAA	C
ATOM	545	O	TYR	54	40.513	14.360	58.678	1.00	30.40	AAAA	O
ATOM	546	H	LEU	55	38.683	13.021	59.004	1.00	23.24	AAAA	H
ATOM	548	CA	LEU	55	39.111	11.812	58.454	1.00	30.08	AAAA	C
ATOM	549	CB	LEU	55	39.011	10.663	59.510	1.00	14.78	AAAA	C
ATOM	550	CG	LEU	55	39.349	9.314	58.818	1.00	26.98	AAAA	C
ATOM	551	CD1	LEU	55	40.668	9.477	58.040	1.00	26.66	AAAA	C
ATOM	552	CD2	LEU	55	39.496	8.093	59.705	1.00	14.45	AAAA	C
ATOM	553	C	LEU	55	38.201	11.548	57.238	1.00	37.43	AAAA	C
ATOM	554	O	LEU	55	36.995	11.632	57.427	1.00	39.55	AAAA	O
ATOM	555	H	LEU	56	38.700	11.348	56.035	1.00	41.83	AAAA	H
ATOM	557	CA	LEU	56	37.955	11.201	54.799	1.00	36.98	AAAA	C
ATOM	558	CB	LEU	56	37.998	12.446	53.949	1.00	33.29	AAAA	C
ATOM	559	CG	LEU	56	37.984	12.514	52.416	1.00	30.35	AAAA	C
ATOM	560	CD1	LEU	56	37.076	11.460	51.821	1.00	47.95	AAAA	C
ATOM	561	CD2	LEU	56	37.286	13.807	51.985	1.00	33.47	AAAA	C
ATOM	562	C	LEU	56	38.595	10.047	54.008	1.00	39.75	AAAA	C
ATOM	563	O	LEU	56	39.714	10.205	53.547	1.00	44.38	AAAA	O
ATOM	564	H	LEU	57	37.846	9.008	53.800	1.00	36.68	AAAA	H
ATOM	566	CA	LEU	57	38.133	7.832	53.034	1.00	41.53	AAAA	C
ATOM	567	CB	LEU	57	37.944	6.588	53.916	1.00	37.00	AAAA	C
ATOM	568	CG	LEU	57	39.064	6.534	55.026	1.00	36.13	AAAA	C
ATOM	569	CD1	LEU	57	38.513	6.890	56.417	1.00	33.26	AAAA	C
ATOM	570	CD2	LEU	57	39.630	5.162	55.039	1.00	24.11	AAAA	C
ATOM	571	C	LEU	57	37.203	7.825	51.838	1.00	46.03	AAAA	C
ATOM	572	O	LEU	57	35.985	7.993	51.969	1.00	44.78	AAAA	O
ATOM	573	H	PHE	58	37.792	7.898	50.642	1.00	47.07	AAAA	H
ATOM	575	CA	PHE	58	36.895	8.002	49.467	1.00	48.75	AAAA	C
ATOM	576	CB	PHE	58	36.704	9.448	49.102	1.00	46.67	AAAA	C
ATOM	577	CG	PHE	58	36.447	9.815	47.692	1.00	54.66	AAAA	C
ATOM	578	CD1	PHE	58	37.413	9.706	46.697	1.00	55.19	AAAA	C
ATOM	579	CD2	PHE	58	35.200	10.301	47.326	1.00	53.86	AAAA	C
ATOM	580	CE1	PHE	59	37.124	10.063	45.396	1.00	50.36	AAAA	C
ATOM	581	CE2	PHE	58	34.885	10.655	46.011	1.00	41.84	AAAA	C
ATOM	582	CO	PHE	58	35.877	10.521	45.037	1.00	46.50	AAAA	C
ATOM	583	C	PHE	58	37.351	7.052	48.379	1.00	49.71	AAAA	C
ATOM	584	O	PHE	58	38.487	7.073	47.934	1.00	52.16	AAAA	O
ATOM	585	H	ARG	59	36.471	6.118	47.944	1.00	44.26	AAAA	H
ATOM	587	CA	ARG	59	36.753	5.281	46.815	1.00	40.80	AAAA	C
ATOM	588	CB	ARG	59	36.911	5.993	45.427	1.00	23.79	AAAA	C
ATOM	589	CG	ARG	59	35.869	7.020	45.121	1.00	46.53	AAAA	C
ATOM	590	CD	ARG	59	35.921	7.562	43.706	1.00	37.64	AAAA	C
ATOM	591	NE	ARG	59	35.822	6.422	42.806	1.00	49.23	AAAA	H
ATOM	593	CE	ARG	59	34.950	5.832	42.036	1.00	41.36	AAAA	C
ATOM	594	HH1	ARG	59	33.702	6.277	41.931	1.00	47.00	AAAA	H
ATOM	597	HH2	ARG	59	35.237	4.729	41.327	1.00	42.58	AAAA	H
ATOM	600	C	ARG	59	38.037	4.494	47.049	1.00	42.25	AAAA	C
ATOM	601	O	ARG	59	38.981	4.513	46.232	1.00	44.11	AAAA	O
ATOM	602	H	VAL	60	38.001	3.625	48.023	1.00	40.84	AAAA	H
ATOM	604	CA	VAL	60	39.101	2.743	48.341	1.00	39.14	AAAA	C
ATOM	605	CB	VAL	60	39.624	3.066	49.751	1.00	40.12	AAAA	C
ATOM	606	CG1	VAL	60	40.407	1.872	50.296	1.00	35.05	AAAA	C
ATOM	607	CG2	VAL	60	40.425	4.352	49.893	1.00	28.86	AAAA	C
ATOM	608	C	VAL	60	38.539	1.337	48.368	1.00	43.56	AAAA	C
ATOM	609	O	VAL	60	37.535	1.224	49.072	1.00	47.66	AAAA	O
ATOM	610	H	ALA	61	39.094	0.371	47.659	1.00	41.92	AAAA	H
ATOM	612	CA	ALA	61	38.617	-0.992	47.749	1.00	42.05	AAAA	C
ATOM	613	CB	ALA	61	38.302	-1.483	46.364	1.00	52.40	AAAA	C
ATOM	614	C	ALA	61	39.613	-1.934	48.386	1.00	43.08	AAAA	C
ATOM	615	O	ALA	61	40.757	-1.602	48.670	1.00	50.59	AAAA	O
ATOM	616	H	GLY	62	39.200	-3.105	48.849	1.00	45.71	AAAA	H
ATOM	618	CA	GLY	62	40.136	-4.079	49.385	1.00	45.39	AAAA	C
ATOM	619	C	GLY	62	40.262	-3.902	50.872	1.00	48.04	AAAA	C
ATOM	620	O	GLY	62	40.587	-4.835	51.604	1.00	52.34	AAAA	O
ATOM	621	H	LEU	63	39.985	-2.734	51.383	1.00	46.90	AAAA	H
ATOM	623	CA	LEU	63	40.003	-2.443	52.805	1.00	49.11	AAAA	C

7/58

ATOH	624	CB	LEU	63	40.274	-0.953	53.027	1.00	41.41	AAAA	C
ATOH	625	CG	LEU	63	40.265	-0.423	54.443	1.00	53.41	AAAA	C
ATOH	626	CD1	LEU	63	41.172	-1.164	55.416	1.00	48.27	AAAA	C
ATOH	627	CD2	LEU	63	40.637	1.047	54.246	1.00	50.51	AAAA	C
ATOH	628	C	LEU	63	38.643	-2.881	53.323	1.00	54.20	AAAA	C
ATOH	629	O	LEU	63	37.587	-2.430	52.837	1.00	57.73	AAAA	O
ATOH	630	H	GLU	64	38.658	-3.852	54.190	1.00	53.97	AAAA	H
ATOH	632	CA	GLU	64	37.462	-4.448	54.749	1.00	56.96	AAAA	C
ATOH	633	CB	GLU	64	37.689	-5.956	54.734	1.00	65.33	AAAA	C
ATOH	634	CG	GLU	64	37.832	-6.484	53.293	1.00	75.14	AAAA	C
ATOH	635	CD	GLU	64	37.104	-7.940	53.128	1.00	78.10	AAAA	C
ATOH	636	OE1	GLU	64	37.424	-8.699	54.132	1.00	63.93	AAAA	O
ATOH	637	OE2	GLU	64	37.036	-8.320	51.978	1.00	88.77	AAAA	O
ATOH	638	C	GLU	64	37.096	-4.007	56.163	1.00	57.12	AAAA	C
ATOH	639	O	GLU	64	35.986	-4.332	56.600	1.00	59.82	AAAA	O
ATOH	640	H	SER	65	37.766	-3.042	56.761	1.00	50.64	AAAA	H
ATOH	642	CA	SER	65	37.539	-2.523	58.060	1.00	47.19	AAAA	C
ATOH	643	CB	SER	65	37.743	-3.596	59.139	1.00	49.24	AAAA	C
ATOH	644	OG	SER	65	37.501	-2.971	60.429	1.00	50.90	AAAA	O
ATOH	646	C	SER	65	38.516	-1.405	58.432	1.00	48.35	AAAA	C
ATOH	647	O	SER	65	39.716	-1.692	58.374	1.00	52.75	AAAA	O
ATOH	648	H	LEU	66	38.054	-0.289	58.984	1.00	41.03	AAAA	H
ATOH	650	CA	LEU	66	38.956	0.758	59.405	1.00	41.94	AAAA	C
ATOH	651	CB	LEU	66	38.247	2.083	59.498	1.00	25.25	AAAA	C
ATOH	652	CG	LEU	66	37.283	2.476	58.402	1.00	34.49	AAAA	C
ATOH	653	CD1	LEU	66	36.974	3.951	58.512	1.00	30.81	AAAA	C
ATOH	654	CD2	LEU	66	37.767	2.200	56.994	1.00	34.34	AAAA	C
ATOH	655	C	LEU	66	39.646	0.462	60.734	1.00	45.39	AAAA	C
ATOH	656	O	LEU	66	40.762	0.947	60.927	1.00	41.05	AAAA	O
ATOH	657	H	GLY	67	39.000	-0.346	61.593	1.00	45.21	AAAA	H
ATOH	659	CA	GLY	67	39.773	-0.672	62.799	1.00	48.14	AAAA	C
ATOH	660	C	GLY	67	40.998	-1.508	62.445	1.00	44.51	AAAA	C
ATOH	661	O	GLY	67	41.855	-1.724	63.287	1.00	45.42	AAAA	O
ATOH	662	H	ASP	68	41.013	-2.189	61.309	1.00	47.60	AAAA	H
ATOH	664	CA	ASP	68	42.194	-2.834	60.738	1.00	50.99	AAAA	C
ATOH	665	CB	ASP	68	42.012	-3.417	59.361	1.00	39.43	AAAA	C
ATOH	666	CG	ASP	68	41.205	-4.678	59.311	1.00	45.82	AAAA	C
ATOH	667	OD1	ASP	68	40.912	-5.341	60.320	1.00	44.69	AAAA	O
ATOH	668	OD2	ASP	68	40.819	-5.065	58.187	1.00	47.23	AAAA	O
ATOH	669	C	ASP	68	43.363	-1.837	60.596	1.00	45.89	AAAA	C
ATOH	670	O	ASP	68	44.436	-2.269	60.903	1.00	44.84	AAAA	O
ATOH	671	H	LEU	69	43.145	-0.609	60.247	1.00	42.49	AAAA	H
ATOH	673	CA	LEU	69	44.175	0.352	60.048	1.00	45.80	AAAA	C
ATOH	674	CB	LEU	69	43.920	1.393	58.945	1.00	45.25	AAAA	C
ATOH	675	CG	LEU	69	43.902	0.882	57.494	1.00	54.25	AAAA	C
ATOH	676	CD1	LEU	69	43.541	2.037	56.565	1.00	47.26	AAAA	C
ATOH	677	CD2	LEU	69	45.211	0.200	57.113	1.00	50.76	AAAA	C
ATOH	678	C	LEU	69	44.347	1.107	61.350	1.00	49.50	AAAA	C
ATOH	679	O	LEU	69	45.470	1.210	61.851	1.00	54.51	AAAA	O
ATOH	680	H	PHE	70	43.296	1.737	61.869	1.00	44.60	AAAA	H
ATOH	682	CA	PHE	70	43.423	2.564	63.046	1.00	39.67	AAAA	C
ATOH	683	CB	PHE	70	42.987	3.973	62.700	1.00	26.08	AAAA	C
ATOH	684	CG	PHE	70	43.465	4.501	61.390	1.00	45.32	AAAA	C
ATOH	685	CD1	PHE	70	42.532	4.748	60.384	1.00	47.41	AAAA	C
ATOH	686	CD2	PHE	70	44.815	4.767	61.130	1.00	48.77	AAAA	C
ATOH	687	CE1	PHE	70	42.945	5.263	59.159	1.00	56.16	AAAA	C
ATOH	688	CE2	PHE	70	45.229	5.256	59.895	1.00	47.24	AAAA	C
ATOH	689	CC	PHE	70	44.293	5.506	58.896	1.00	49.54	AAAA	C
ATOH	690	C	PHE	70	42.655	1.999	64.219	1.00	40.09	AAAA	C
ATOH	691	O	PHE	70	41.874	2.734	64.838	1.00	35.74	AAAA	O
ATOH	692	H	PRO	71	43.053	0.852	64.768	1.00	39.19	AAAA	H
ATOH	693	CD	PRO	71	44.269	0.058	64.411	1.00	39.94	AAAA	C
ATOH	694	CA	PRO	71	42.444	0.237	65.899	1.00	35.30	AAAA	C
ATOH	695	CB	PRO	71	43.308	-0.983	66.246	1.00	38.03	AAAA	C
ATOH	696	CG	PRO	71	44.669	-0.564	65.717	1.00	38.36	AAAA	C
ATOH	697	C	PRO	71	42.453	1.089	67.126	1.00	33.72	AAAA	C
ATOH	698	O	PRO	71	42.005	0.630	68.159	1.00	39.32	AAAA	O
ATOH	699	H	ASH	72	43.058	2.220	67.231	1.00	36.55	AAAA	H
ATOH	701	CA	ASH	72	43.204	3.032	68.401	1.00	32.60	AAAA	C
ATOH	702	CB	ASH	72	44.637	2.916	68.962	1.00	36.89	AAAA	C
ATOH	703	CG	ASH	72	44.735	1.638	69.761	1.00	47.03	AAAA	C
ATOH	704	OD1	ASH	72	44.644	1.619	70.979	1.00	64.42	AAAA	O
ATOH	705	HD2	ASH	72	44.880	0.475	69.169	1.00	63.17	AAAA	O
ATOH	708	C	ASH	72	42.875	4.477	68.135	1.00	30.11	AAAA	C
ATOH	709	O	ASH	72	43.099	5.201	69.104	1.00	36.53	AAAA	O
ATOH	710	H	LEU	73	42.309	4.809	66.978	1.00	27.62	AAAA	H
ATOH	712	CA	LEU	73	41.940	6.207	66.730	1.00	34.07	AAAA	C
ATOH	713	CB	LEU	73	41.476	6.373	65.292	1.00	28.37	AAAA	C
ATOH	714	CG	LEU	73	40.819	7.713	64.882	1.00	29.33	AAAA	C
ATOH	715	CD1	LEU	73	41.918	8.721	64.963	1.00	31.86	AAAA	C
ATOH	716	CD2	LEU	73	40.202	7.518	63.478	1.00	32.07	AAAA	C
ATOH	717	C	LEU	73	40.929	6.569	67.817	1.00	32.14	AAAA	C
ATOH	718	O	LEU	73	40.073	5.737	68.081	1.00	35.02	AAAA	O
ATOH	719	H	THR	74	41.081	7.585	68.592	1.00	29.47	AAAA	H
ATOH	721	CA	THR	74	40.150	7.826	69.683	1.00	34.86	AAAA	C

8/58

ATOM	722	CB	THR	74	41.028	7.744	70.852	1.00	46.09	AAAA	C
ATOM	723	CG1	THR	74	41.729	6.485	70.880	1.00	46.30	AAAA	O
ATOM	725	CG2	THR	74	40.262	7.831	72.253	1.00	39.45	AAAA	C
ATOM	726	C	THR	74	39.424	9.155	69.602	1.00	35.40	AAAA	C
ATOM	727	O	THR	74	38.270	9.322	70.077	1.00	35.32	AAAA	O
ATOM	728	H	VAL	75	40.047	10.198	69.073	1.00	29.80	AAAA	H
ATOM	730	CA	VAL	75	39.351	11.474	68.892	1.00	34.91	AAAA	C
ATOM	731	CB	VAL	75	39.856	12.445	69.955	1.00	26.03	AAAA	C
ATOM	732	CG1	VAL	75	39.173	13.801	69.934	1.00	24.51	AAAA	C
ATOM	733	CG2	VAL	75	39.675	11.910	71.366	1.00	19.87	AAAA	C
ATOM	734	C	VAL	75	39.613	12.045	67.494	1.00	37.57	AAAA	C
ATOM	735	O	VAL	75	40.724	11.808	67.022	1.00	35.99	AAAA	O
ATOM	736	H	ILE	76	38.600	12.555	66.796	1.00	35.91	AAAA	H
ATOM	738	CA	ILE	76	38.696	13.340	65.592	1.00	31.48	AAAA	C
ATOM	739	CB	ILE	76	37.831	12.769	64.492	1.00	29.60	AAAA	C
ATOM	740	CG2	ILE	76	37.856	13.630	63.208	1.00	19.54	AAAA	C
ATOM	741	CG1	ILE	76	38.222	11.314	64.277	1.00	28.52	AAAA	C
ATOM	742	CD1	ILE	76	37.149	10.556	63.479	1.00	28.85	AAAA	C
ATOM	743	C	ILE	76	38.157	14.718	66.000	1.00	33.84	AAAA	C
ATOM	744	O	ILE	76	36.987	14.777	66.274	1.00	38.84	AAAA	O
ATOM	745	H	ARG	77	38.906	15.733	66.230	1.00	39.32	AAAA	H
ATOM	747	CA	ARG	77	38.605	16.901	67.021	1.00	30.82	AAAA	C
ATOM	748	CB	ARG	77	39.961	17.475	67.461	1.00	26.62	AAAA	C
ATOM	749	CG	ARG	77	39.993	18.836	68.058	1.00	52.42	AAAA	C
ATOM	750	CD	ARG	77	41.290	18.957	68.908	1.00	49.10	AAAA	C
ATOM	751	NE	ARG	77	41.411	17.817	69.773	1.00	39.23	AAAA	H
ATOM	753	CC	ARG	77	40.977	18.016	71.064	1.00	48.79	AAAA	C
ATOM	754	HH1	ARG	77	40.440	19.104	71.610	1.00	30.34	AAAA	H
ATOM	757	HH2	ARG	77	41.061	17.012	71.941	1.00	40.38	AAAA	H
ATOM	760	C	ARG	77	37.643	17.733	66.225	1.00	31.75	AAAA	C
ATOM	761	O	ARG	77	36.944	18.637	66.664	1.00	31.40	AAAA	O
ATOM	762	H	GLY	78	37.688	17.661	64.884	1.00	32.87	AAAA	H
ATOM	764	CA	GLY	78	36.982	18.409	63.950	1.00	16.23	AAAA	C
ATOM	765	C	GLY	78	37.199	19.880	64.063	1.00	31.58	AAAA	C
ATOM	766	O	GLY	78	36.363	20.775	63.674	1.00	34.03	AAAA	O
ATOM	767	H	TRP	79	38.439	20.321	64.304	1.00	31.21	AAAA	H
ATOM	769	CA	TRP	79	38.757	21.740	64.337	1.00	30.80	AAAA	C
ATOM	770	CB	TRP	79	40.177	21.943	64.845	1.00	39.07	AAAA	C
ATOM	771	CG	TRP	79	40.626	23.343	65.164	1.00	36.64	AAAA	C
ATOM	772	CD2	TRP	79	41.691	24.001	64.433	1.00	28.52	AAAA	C
ATOM	773	CE2	TRP	79	41.826	25.288	65.002	1.00	36.49	AAAA	C
ATOM	774	CE3	TRP	79	42.473	23.625	63.370	1.00	37.96	AAAA	C
ATOM	775	CD1	TRP	79	40.199	24.235	66.113	1.00	29.59	AAAA	C
ATOM	776	HE1	TRP	79	40.917	25.413	66.054	1.00	27.67	AAAA	H
ATOM	778	CE2	TRP	79	42.770	26.213	64.543	1.00	31.83	AAAA	C
ATOM	779	CE3	TRP	79	43.389	24.548	62.876	1.00	46.14	AAAA	C
ATOM	780	CH2	TRP	79	43.525	25.794	63.470	1.00	35.31	AAAA	C
ATOM	781	C	TRP	79	38.606	22.418	62.986	1.00	28.75	AAAA	C
ATOM	782	O	TRP	79	38.585	23.624	62.961	1.00	23.61	AAAA	O
ATOM	783	H	LYS	80	38.659	21.684	61.895	1.00	31.84	AAAA	H
ATOM	785	CA	LYS	80	38.305	22.153	60.573	1.00	32.78	AAAA	C
ATOM	786	CB	LYS	80	39.453	22.498	59.689	1.00	41.17	AAAA	C
ATOM	787	CG	LYS	80	39.838	23.211	59.470	1.00	34.68	AAAA	C
ATOM	788	CD	LYS	80	41.025	24.350	60.306	1.00	44.77	AAAA	C
ATOM	789	CE	LYS	80	41.276	25.811	59.898	1.00	50.41	AAAA	C
ATOM	790	NE	LYS	80	42.530	25.752	59.092	1.00	67.26	AAAA	H
ATOM	791	C	LYS	80	37.585	20.960	59.917	1.00	34.52	AAAA	C
ATOM	792	O	LYS	80	37.950	19.843	60.237	1.00	37.62	AAAA	O
ATOM	793	H	LEU	81	36.477	21.267	59.207	1.00	31.77	AAAA	H
ATOM	795	CA	LEU	81	35.742	20.157	58.600	1.00	31.02	AAAA	C
ATOM	796	CB	LEU	81	34.290	20.315	59.092	1.00	31.20	AAAA	C
ATOM	797	CG	LEU	81	34.115	20.319	60.632	1.00	36.97	AAAA	C
ATOM	798	CD1	LEU	81	32.832	21.080	60.954	1.00	27.98	AAAA	C
ATOM	799	CD2	LEU	81	34.089	18.955	61.297	1.00	28.77	AAAA	C
ATOM	800	C	LEU	81	35.733	20.023	57.104	1.00	29.86	AAAA	C
ATOM	801	O	LEU	81	36.082	20.947	56.368	1.00	29.34	AAAA	O
ATOM	802	H	PHE	82	35.430	18.813	56.594	1.00	27.78	AAAA	H
ATOM	804	CA	PHE	82	35.176	16.653	55.182	1.00	28.68	AAAA	C
ATOM	805	CB	PHE	82	35.513	17.226	51.795	1.00	32.78	AAAA	C
ATOM	806	CG	PHE	82	35.348	16.901	53.357	1.00	30.48	AAAA	C
ATOM	807	CD1	PHE	82	36.378	17.130	52.447	1.00	32.86	AAAA	C
ATOM	808	CD2	PHE	82	34.142	16.361	52.914	1.00	30.93	AAAA	C
ATOM	809	CE1	PHE	82	36.217	16.769	51.104	1.00	43.27	AAAA	C
ATOM	810	CE2	PHE	82	33.963	16.061	51.538	1.00	26.30	AAAA	C
ATOM	811	CG	PHE	82	35.005	16.238	50.672	1.00	37.73	AAAA	C
ATOM	812	C	PHE	82	33.670	18.911	54.993	1.00	30.06	AAAA	C
ATOM	813	O	PHE	82	32.830	18.045	55.278	1.00	27.36	AAAA	O
ATOM	814	H	TYR	83	33.301	20.148	54.770	1.00	31.68	AAAA	H
ATOM	815	CA	TYR	83	31.911	20.605	54.633	1.00	40.76	AAAA	C
ATOM	816	C	TYR	83	31.043	19.977	55.726	1.00	44.00	AAAA	C
ATOM	817	O	TYR	83	30.075	19.210	55.487	1.00	50.47	AAAA	O
ATOM	818	CB	TYR	83	31.359	20.199	53.269	1.00	31.55	AAAA	C
ATOM	819	CG	TYR	83	32.196	20.742	52.117	0.01	20.00	AAAA	C
ATOM	820	CD1	TYR	83	33.254	19.982	51.609	0.01	20.00	AAAA	C
ATOM	821	CD2	TYR	83	31.906	21.998	51.575	0.01	20.00	AAAA	C

9/58

ATOM	822	CE1	TYR	83	34.027	20.480	50.556	0.01	20.00	AAAA	C
ATOM	823	CE2	TYR	83	32.679	22.496	50.521	0.01	20.00	AAAA	C
ATOM	824	CS	TYR	83	33.740	21.737	50.012	0.01	20.00	AAAA	C
ATOM	825	OH	TYR	83	34.492	22.222	48.989	0.01	20.00	AAAA	O
ATOM	826	H	ASH	84	31.043	20.461	56.924	1.00	40.91	AAAA	H
ATOM	827	CA	ASH	84	30.250	20.057	58.056	1.00	36.54	AAAA	C
ATOM	828	CB	ASH	84	28.763	20.046	57.700	1.00	47.84	AAAA	C
ATOM	829	CG	ASH	84	28.274	21.164	56.797	1.00	60.75	AAAA	C
ATOM	830	OD1	ASH	84	28.319	22.343	57.119	1.00	45.55	AAAA	O
ATOM	831	HD2	ASH	84	27.839	20.876	55.552	1.00	65.98	AAAA	H
ATOM	832	C	ASH	84	30.686	18.679	58.556	1.00	36.33	AAAA	C
ATOM	833	O	ASH	84	30.137	18.206	59.580	1.00	38.24	AAAA	O
ATOM	834	H	TYR	85	31.455	17.900	57.800	1.00	32.78	AAAA	H
ATOM	836	CA	TYR	85	31.617	16.504	58.222	1.00	35.45	AAAA	C
ATOM	837	CB	TYR	85	31.473	15.579	57.000	1.00	35.54	AAAA	C
ATOM	838	CG	TYR	85	30.078	15.733	56.453	1.00	41.35	AAAA	C
ATOM	839	CD1	TYR	85	29.868	16.291	55.199	1.00	38.22	AAAA	C
ATOM	840	CE1	TYR	85	28.611	16.445	54.704	1.00	40.83	AAAA	C
ATOM	841	CD2	TYR	85	28.954	15.371	57.200	1.00	47.42	AAAA	C
ATOM	842	CE2	TYR	85	27.661	15.533	56.705	1.00	45.91	AAAA	C
ATOM	843	CD	TYR	85	27.497	16.072	55.445	1.00	46.06	AAAA	C
ATOM	844	OH	TYR	85	26.258	16.315	54.886	1.00	46.05	AAAA	O
ATOM	846	C	TYR	85	32.977	16.367	58.891	1.00	32.08	AAAA	C
ATOM	847	O	TYR	85	33.943	16.977	58.495	1.00	37.44	AAAA	O
ATOM	848	H	ALA	86	33.027	15.691	59.979	1.00	30.21	AAAA	H
ATOM	850	CA	ALA	86	34.257	15.325	60.670	1.00	34.10	AAAA	C
ATOM	851	CB	ALA	86	33.999	15.370	62.157	1.00	25.48	AAAA	C
ATOM	852	C	ALA	86	34.729	13.962	60.216	1.00	32.67	AAAA	C
ATOM	853	O	ALA	86	35.795	13.481	60.577	1.00	35.10	AAAA	O
ATOM	854	H	LEU	87	33.832	13.173	59.597	1.00	28.56	AAAA	H
ATOM	856	CA	LEU	87	34.188	11.805	59.323	1.00	29.26	AAAA	C
ATOM	857	CB	LEU	87	33.798	10.860	60.471	1.00	13.64	AAAA	C
ATOM	858	CG	LEU	87	33.801	9.363	60.188	1.00	25.77	AAAA	C
ATOM	859	CD1	LEU	87	35.140	8.915	59.571	1.00	27.21	AAAA	C
ATOM	860	CD2	LEU	87	33.637	8.432	61.393	1.00	23.52	AAAA	C
ATOM	861	C	LEU	87	33.530	11.429	58.021	1.00	35.60	AAAA	C
ATOM	862	O	LEU	87	32.320	11.421	58.001	1.00	38.97	AAAA	O
ATOM	863	H	VAL	88	34.174	11.300	56.875	1.00	37.86	AAAA	H
ATOM	865	CA	VAL	88	33.438	11.032	55.628	1.00	33.32	AAAA	C
ATOM	866	CB	VAL	88	33.666	12.085	54.553	1.00	22.38	AAAA	C
ATOM	867	CG1	VAL	88	32.974	11.675	53.261	1.00	19.24	AAAA	C
ATOM	868	CG2	VAL	88	33.165	13.402	55.042	1.00	13.27	AAAA	C
ATOM	869	C	VAL	88	33.898	9.684	55.114	1.00	31.79	AAAA	C
ATOM	870	O	VAL	88	35.069	9.407	55.117	1.00	33.57	AAAA	O
ATOM	871	H	ILE	89	33.078	8.728	54.822	1.00	31.08	AAAA	H
ATOM	873	CA	ILE	89	33.361	7.433	54.280	1.00	30.45	AAAA	C
ATOM	874	CB	ILE	89	32.941	6.384	55.296	1.00	30.17	AAAA	C
ATOM	875	CG2	ILE	89	32.858	4.954	54.821	1.00	37.24	AAAA	C
ATOM	876	CG1	ILE	89	33.893	6.420	56.500	1.00	24.92	AAAA	C
ATOM	877	CD1	ILE	89	33.424	5.613	57.675	1.00	23.96	AAAA	C
ATOM	878	C	ILE	89	32.509	7.206	53.027	1.00	40.64	AAAA	C
ATOM	879	O	ILE	89	31.330	6.881	53.205	1.00	38.69	AAAA	O
ATOM	880	H	PHE	90	33.082	7.464	51.845	1.00	41.45	AAAA	H
ATOM	882	CA	PHE	90	32.346	7.371	50.591	1.00	37.67	AAAA	C
ATOM	883	CB	PHE	90	32.347	8.776	50.110	1.00	32.17	AAAA	C
ATOM	884	CG	PHE	90	31.591	9.081	48.865	1.00	39.77	AAAA	C
ATOM	885	CD1	PHE	90	30.387	9.772	49.025	1.00	32.02	AAAA	C
ATOM	886	CD2	PHE	90	32.052	8.721	47.620	1.00	29.28	AAAA	C
ATOM	887	CE1	PHE	90	29.611	10.111	47.938	1.00	33.30	AAAA	C
ATOM	888	CE2	PHE	90	31.290	9.086	46.534	1.00	43.09	AAAA	C
ATOM	889	CD	PHE	90	30.083	9.764	46.687	1.00	50.24	AAAA	C
ATOM	890	C	PHE	90	32.856	6.384	49.557	1.00	40.72	AAAA	C
ATOM	891	O	PHE	90	34.027	6.296	49.203	1.00	46.15	AAAA	O
ATOM	892	H	GLU	91	32.024	5.519	49.001	1.00	39.16	AAAA	H
ATOM	894	CA	GLU	91	32.248	4.601	47.954	1.00	42.45	AAAA	C
ATOM	895	CB	GLU	91	32.479	5.231	46.583	1.00	38.08	AAAA	C
ATOM	896	CG	GLU	91	31.136	5.865	46.250	1.00	58.86	AAAA	C
ATOM	897	CD	GLU	91	30.955	5.776	44.757	1.00	63.55	AAAA	C
ATOM	898	OE1	GLU	91	31.473	6.651	44.082	1.00	64.10	AAAA	O
ATOM	899	OE2	GLU	91	30.058	4.813	44.573	1.00	63.64	AAAA	O
ATOM	900	C	GLU	91	33.422	3.734	48.313	1.00	42.06	AAAA	C
ATOM	901	O	GLU	91	34.298	3.411	47.587	1.00	44.71	AAAA	O
ATOM	902	H	HET	92	33.352	3.209	49.482	1.00	46.52	AAAA	H
ATOM	904	CA	HET	92	34.409	2.401	50.088	1.00	42.26	AAAA	C
ATOM	905	CB	HET	92	34.299	2.659	51.584	1.00	38.37	AAAA	C
ATOM	906	CG	HET	92	35.412	2.156	52.420	1.00	59.29	AAAA	C
ATOM	907	SD	HET	92	36.802	3.306	52.401	1.00	57.67	AAAA	S
ATOM	908	CE	HET	92	36.340	4.405	51.108	1.00	38.36	AAAA	C
ATOM	909	C	HET	92	34.012	1.005	49.745	1.00	43.37	AAAA	C
ATOM	910	O	HET	92	33.335	0.298	50.523	1.00	45.58	AAAA	O
ATOM	911	H	THR	93	34.449	0.518	48.602	1.00	47.09	AAAA	H
ATOM	913	CA	THR	93	34.175	-0.900	48.273	1.00	47.32	AAAA	C
ATOM	914	CB	THR	93	34.666	-1.281	46.868	1.00	55.28	AAAA	C
ATOM	915	CG1	THR	93	34.013	-0.488	45.892	1.00	57.01	AAAA	O
ATOM	917	CG2	THR	93	34.322	-2.715	46.516	1.00	44.71	AAAA	C

10/58

ATOM	918	C	THR	93	34.885	-1.074	49.186	1.00	51.83	AAAA	C
ATOM	919	O	THR	93	36.115	-1.777	49.361	1.00	57.91	AAAA	O
ATOM	920	H	ASH	94	34.237	-2.983	49.493	1.00	49.85	AAAA	H
ATOM	922	CA	ASH	94	34.747	-4.069	50.285	1.00	45.64	AAAA	C
ATOM	923	CB	ASH	94	36.241	-4.315	50.001	1.00	59.01	AAAA	C
ATOM	924	CG	ASH	94	36.494	-4.849	48.599	1.00	75.44	AAAA	C
ATOM	925	OD1	ASH	94	36.847	-4.081	47.688	1.00	77.49	AAAA	O
ATOM	926	HD2	ASH	94	36.308	-6.153	48.408	1.00	79.63	AAAA	H
ATOM	929	C	ASH	94	34.522	-3.838	51.763	1.00	42.58	AAAA	C
ATOM	930	O	ASH	94	34.752	-4.814	52.501	1.00	46.36	AAAA	O
ATOM	931	H	LEU	95	34.308	-2.609	52.132	1.00	37.28	AAAA	H
ATOM	933	CA	LEU	95	34.324	-2.277	53.621	1.00	39.96	AAAA	C
ATOM	934	CB	LEU	95	34.185	-0.786	53.051	1.00	34.05	AAAA	C
ATOM	935	CG	LEU	95	34.323	-0.296	55.269	1.00	35.81	AAAA	C
ATOM	936	CD1	LEU	95	35.785	-0.537	55.598	1.00	35.48	AAAA	C
ATOM	937	CD2	LEU	95	33.847	1.177	55.344	1.00	25.46	AAAA	C
ATOM	938	C	LEU	95	33.163	-2.986	54.275	1.00	43.75	AAAA	C
ATOM	939	O	LEU	95	32.048	-2.936	53.772	1.00	44.04	AAAA	O
ATOM	940	H	LYS	96	33.451	-3.863	55.213	1.00	46.50	AAAA	H
ATOM	942	CA	LYS	96	32.364	-4.648	55.770	1.00	42.76	AAAA	C
ATOM	943	CB	LYS	96	32.801	-6.075	55.995	1.00	41.41	AAAA	C
ATOM	944	CG	LYS	96	32.760	-6.976	54.788	1.00	49.78	AAAA	C
ATOM	945	CD	LYS	96	32.984	-8.446	55.127	1.00	58.09	AAAA	C
ATOM	946	CE	LYS	96	33.772	-9.160	54.027	1.00	73.43	AAAA	C
ATOM	947	HE	LYS	96	34.098	-10.556	54.489	1.00	79.13	AAAA	H
ATOM	951	C	LYS	96	31.970	-4.055	57.122	1.00	45.29	AAAA	C
ATOM	952	O	LYS	96	30.978	-4.502	57.691	1.00	46.23	AAAA	O
ATOM	953	H	ASP	97	32.685	-3.071	57.645	1.00	45.15	AAAA	H
ATOM	955	CA	ASP	97	32.299	-2.384	58.861	1.00	42.15	AAAA	C
ATOM	956	CB	ASP	97	32.294	-3.292	60.058	1.00	45.39	AAAA	C
ATOM	957	CG	ASP	97	33.662	-3.562	60.624	1.00	56.95	AAAA	C
ATOM	958	OD1	ASP	97	34.579	-2.825	61.012	1.00	59.88	AAAA	O
ATOM	959	OD2	ASP	97	33.931	-4.782	60.714	1.00	56.01	AAAA	O
ATOM	960	C	ASP	97	33.209	-1.224	59.201	1.00	41.25	AAAA	C
ATOM	961	O	ASP	97	34.160	-1.074	58.437	1.00	47.03	AAAA	O
ATOM	962	H	ILE	98	32.822	-0.366	60.129	1.00	40.41	AAAA	H
ATOM	964	CA	ILE	98	33.675	0.820	60.340	1.00	37.83	AAAA	C
ATOM	965	CB	ILE	98	32.983	2.006	61.006	1.00	38.99	AAAA	C
ATOM	966	CG2	ILE	98	34.007	3.133	61.207	1.00	38.95	AAAA	C
ATOM	967	CG1	ILE	98	31.835	2.488	60.092	1.00	34.84	AAAA	C
ATOM	968	CD1	ILE	98	31.629	3.958	59.948	1.00	39.29	AAAA	C
ATOM	969	C	ILE	98	34.854	0.322	61.114	1.00	35.11	AAAA	C
ATOM	970	O	ILE	98	35.970	0.669	60.841	1.00	43.05	AAAA	O
ATOM	971	H	GLY	99	34.618	-0.393	62.192	1.00	34.22	AAAA	H
ATOM	973	CA	GLY	99	35.477	-0.972	63.121	1.00	33.74	AAAA	C
ATOM	974	C	GLY	99	36.279	-0.084	64.024	1.00	35.90	AAAA	C
ATOM	975	O	GLY	99	37.023	-0.572	64.899	1.00	38.21	AAAA	O
ATOM	976	H	LEU	100	36.190	1.221	63.913	1.00	33.35	AAAA	H
ATOM	978	CA	LEU	100	36.763	2.215	64.771	1.00	31.65	AAAA	C
ATOM	979	CB	LEU	100	36.496	3.636	64.294	1.00	29.87	AAAA	C
ATOM	980	CG	LEU	100	36.943	3.980	62.835	1.00	32.13	AAAA	C
ATOM	981	CD1	LEU	100	36.710	5.479	62.610	1.00	21.32	AAAA	C
ATOM	982	CD2	LEU	100	38.412	3.599	62.644	1.00	37.66	AAAA	C
ATOM	983	C	LEU	100	36.312	1.976	66.194	1.00	31.94	AAAA	C
ATOM	984	O	LEU	100	35.950	2.863	66.979	1.00	31.95	AAAA	O
ATOM	985	H	TYR	101	36.704	0.851	66.779	1.00	31.87	AAAA	H
ATOM	987	CA	TYR	101	36.329	0.395	68.071	1.00	33.33	AAAA	C
ATOM	988	CB	TYR	101	36.491	-1.104	68.264	1.00	41.03	AAAA	C
ATOM	989	CG	TYR	101	37.919	-1.559	68.369	1.00	46.66	AAAA	C
ATOM	990	CD1	TYR	101	38.571	-1.380	69.587	1.00	51.20	AAAA	C
ATOM	991	CE1	TYR	101	39.901	-1.743	69.749	1.00	49.44	AAAA	C
ATOM	992	CD2	TYR	101	38.615	-2.112	67.322	1.00	45.15	AAAA	C
ATOM	993	CE2	TYR	101	39.927	-2.505	67.479	1.00	47.08	AAAA	C
ATOM	994	C2	TYR	101	40.548	-2.321	68.688	1.00	49.43	AAAA	C
ATOM	995	OH	TYR	101	41.834	-2.662	68.997	1.00	55.82	AAAA	O
ATOM	997	C	TYR	101	36.989	1.059	69.214	1.00	33.46	AAAA	C
ATOM	998	O	TYR	101	36.630	0.813	70.375	1.00	43.00	AAAA	O
ATOM	999	H	ASH	102	37.752	2.091	69.068	1.00	38.12	AAAA	H
ATOM	1001	CA	ASH	102	38.093	2.979	70.223	1.00	30.78	AAAA	C
ATOM	1002	CB	ASH	102	39.603	2.911	70.363	1.00	48.63	AAAA	C
ATOM	1003	CG	ASH	102	40.112	1.804	71.268	1.00	54.01	AAAA	C
ATOM	1004	OD1	ASH	102	39.738	1.864	72.454	1.00	47.22	AAAA	O
ATOM	1005	HD2	ASH	102	40.864	0.845	70.767	1.00	43.08	AAAA	H
ATOM	1008	C	ASH	102	37.673	4.385	69.947	1.00	33.82	AAAA	C
ATOM	1009	O	ASH	102	38.047	5.364	70.592	1.00	39.84	AAAA	O
ATOM	1010	H	LEU	103	36.845	4.640	68.882	1.00	35.28	AAAA	H
ATOM	1012	CA	LEU	103	36.473	6.040	68.621	1.00	36.57	AAAA	C
ATOM	1013	CB	LEU	103	35.948	6.140	67.213	1.00	34.77	AAAA	C
ATOM	1014	CG	LEU	103	35.525	7.482	66.612	1.00	30.32	AAAA	C
ATOM	1015	CD1	LEU	103	36.606	8.513	66.646	1.00	23.20	AAAA	C
ATOM	1016	CD2	LEU	103	35.199	7.169	65.146	1.00	37.10	AAAA	C
ATOM	1017	C	LEU	103	35.484	6.508	69.691	1.00	37.31	AAAA	C
ATOM	1018	O	LEU	103	34.449	5.874	69.837	1.00	34.24	AAAA	O
ATOM	1019	H	ARG	104	35.810	7.456	70.563	1.00	33.31	AAAA	H
ATOM	1021	CA	ARG	104	34.920	7.841	71.605	1.00	29.66	AAAA	C

11/58

ATOH	1022	CB	ARG	104	35.568	7.657	73.018	1.00	38.17	AAAA	C
ATOH	1023	CG	ARG	104	36.356	6.375	73.165	1.00	48.37	AAAA	C
ATOH	1024	CD	ARG	104	35.425	5.183	73.248	1.00	50.71	AAAA	C
ATOH	1025	HE	ARG	104	34.582	5.320	74.413	1.00	52.38	AAAA	H
ATOH	1027	CC	ARG	104	34.900	4.847	75.621	1.00	72.73	AAAA	C
ATOH	1028	NH1	ARG	104	36.047	4.214	75.800	1.00	81.87	AAAA	H
ATOH	1031	NH2	ARG	104	33.990	5.070	76.577	1.00	78.27	AAAA	H
ATOH	1034	C	ARG	104	34.466	9.273	71.540	1.00	32.58	AAAA	C
ATOH	1035	O	ARG	104	33.553	9.743	72.223	1.00	39.89	AAAA	O
ATOH	1036	H	ASH	105	34.992	10.065	70.637	1.00	33.47	AAAA	H
ATOH	1038	CA	ASH	105	34.549	11.450	70.590	1.00	30.97	AAAA	C
ATOH	1044	C	ASH	105	34.907	12.149	69.310	1.00	31.00	AAAA	C
ATOH	1045	O	ASH	105	36.086	12.067	69.050	1.00	37.79	AAAA	O
ATOH	1039	CB	ASH	105	35.203	12.199	71.721	1.00	12.28	AAAA	C
ATOH	1040	CG	ASH	105	34.786	13.568	71.756	1.00	24.93	AAAA	C
ATOH	1041	OD1	ASH	105	35.125	14.549	71.127	1.00	38.14	AAAA	O
ATOH	1042	HD2	ASH	105	33.828	13.985	72.649	1.00	35.96	AAAA	H
ATOH	1046	H	ILE	106	33.969	12.669	68.576	1.00	31.90	AAAA	H
ATOH	1048	CA	ILE	106	34.129	13.551	67.469	1.00	23.38	AAAA	C
ATOH	1049	CB	ILE	106	33.239	13.185	66.307	1.00	16.54	AAAA	C
ATOH	1050	CG2	ILE	106	33.132	14.408	65.374	1.00	20.38	AAAA	C
ATOH	1051	CG1	ILE	106	33.928	12.034	65.558	1.00	18.30	AAAA	C
ATOH	1052	CD1	ILE	106	33.055	11.293	64.643	1.00	25.48	AAAA	C
ATOH	1053	C	ILE	106	33.803	14.909	68.009	1.00	27.40	AAAA	C
ATOH	1054	O	ILE	106	32.628	15.106	68.243	1.00	32.86	AAAA	O
ATOH	1055	H	THR	107	34.719	15.789	68.350	1.00	30.43	AAAA	H
ATOH	1057	CA	THR	107	34.532	16.983	69.145	1.00	28.27	AAAA	C
ATOH	1058	CB	THR	107	35.902	17.607	69.579	1.00	35.78	AAAA	C
ATOH	1059	OG1	THR	107	36.819	16.503	69.738	1.00	40.26	AAAA	O
ATOH	1061	CG2	THR	107	35.954	18.411	70.855	1.00	28.13	AAAA	C
ATOH	1062	C	THR	107	33.728	17.950	69.332	1.00	27.95	AAAA	C
ATOH	1063	O	THR	107	33.392	19.060	68.831	1.00	32.99	AAAA	O
ATOH	1064	H	ARG	108	33.669	17.777	67.019	1.00	30.28	AAAA	H
ATOH	1066	CA	ARG	108	33.046	18.809	66.180	1.00	31.25	AAAA	C
ATOH	1067	CB	ARG	108	33.965	20.011	65.951	1.00	25.13	AAAA	C
ATOH	1068	CG	ARG	108	33.105	21.174	65.543	1.00	30.68	AAAA	C
ATOH	1069	CD	ARG	108	33.917	22.444	65.529	1.00	17.12	AAAA	C
ATOH	1070	HE	ARG	108	33.511	23.376	64.451	1.00	33.40	AAAA	H
ATOH	1072	CC	ARG	108	34.045	23.608	63.266	1.00	46.41	AAAA	C
ATOH	1073	NH1	ARG	108	35.162	22.929	62.868	1.00	40.30	AAAA	H
ATOH	1076	NH2	ARG	108	33.454	24.543	62.494	1.00	39.82	AAAA	H
ATOH	1079	C	ARG	108	32.701	18.328	64.784	1.00	31.50	AAAA	C
ATOH	1080	O	ARG	108	33.379	17.381	64.430	1.00	32.67	AAAA	O
ATOH	1081	H	GLY	109	31.567	18.809	64.284	1.00	32.60	AAAA	H
ATOH	1083	CA	GLY	109	31.082	18.385	62.983	1.00	28.87	AAAA	C
ATOH	1084	C	GLY	109	30.470	17.008	63.001	1.00	32.32	AAAA	C
ATOH	1085	O	GLY	109	30.471	16.306	64.006	1.00	38.03	AAAA	O
ATOH	1086	H	ALA	110	29.920	16.560	61.894	1.00	34.11	AAAA	H
ATOH	1088	CA	ALA	110	29.086	15.371	61.833	1.00	36.77	AAAA	C
ATOH	1089	CB	ALA	110	27.708	15.721	61.223	1.00	15.32	AAAA	C
ATOH	1090	C	ALA	110	29.745	14.335	60.957	1.00	32.12	AAAA	C
ATOH	1091	O	ALA	110	30.921	14.332	60.687	1.00	34.11	AAAA	O
ATOH	1092	H	ILE	111	29.030	13.337	60.557	1.00	26.55	AAAA	H
ATOH	1094	CA	ILE	111	29.569	12.273	59.771	1.00	32.90	AAAA	C
ATOH	1095	CB	ILE	111	29.669	10.967	60.591	1.00	38.07	AAAA	C
ATOH	1096	CG2	ILE	111	30.091	11.140	62.036	1.00	34.05	AAAA	C
ATOH	1097	CG1	ILE	111	28.345	10.237	60.684	1.00	26.54	AAAA	C
ATOH	1098	CD1	ILE	111	28.437	8.872	61.407	1.00	27.11	AAAA	C
ATOH	1099	C	ILE	111	28.738	11.928	58.521	1.00	33.98	AAAA	C
ATOH	1100	O	ILE	111	27.533	12.179	58.532	1.00	32.15	AAAA	O
ATOH	1101	H	ARG	112	29.432	11.423	57.501	1.00	30.54	AAAA	H
ATOH	1103	CA	ARG	112	28.773	11.107	56.247	1.00	27.48	AAAA	C
ATOH	1104	CB	ARG	112	29.186	12.085	55.169	1.00	26.35	AAAA	C
ATOH	1105	CG	ARG	112	28.548	11.653	53.816	1.00	25.83	AAAA	C
ATOH	1106	CD	ARG	112	28.659	12.912	52.992	1.00	32.92	AAAA	C
ATOH	1107	HE	ARG	112	27.950	12.726	51.770	1.00	50.34	AAAA	H
ATOH	1109	CC	ARG	112	27.778	13.503	50.720	1.00	47.61	AAAA	C
ATOH	1110	NH1	ARG	112	28.334	14.695	50.696	1.00	44.92	AAAA	H
ATOH	1113	NH2	ARG	112	27.012	12.925	49.789	1.00	46.00	AAAA	H
ATOH	1116	C	ARG	112	29.200	9.738	55.791	1.00	29.74	AAAA	C
ATOH	1117	O	ARG	112	30.343	9.611	55.406	1.00	36.52	AAAA	O
ATOH	1118	H	ILE	113	28.326	9.754	55.986	1.00	33.99	AAAA	H
ATOH	1120	CA	ILE	113	28.612	7.376	55.555	1.00	36.26	AAAA	C
ATOH	1121	CB	ILE	113	28.457	6.461	56.760	1.00	33.27	AAAA	C
ATOH	1122	CG2	ILE	113	28.850	5.021	56.449	1.00	15.85	AAAA	C
ATOH	1123	CG1	ILE	113	29.374	7.012	57.874	1.00	31.92	AAAA	C
ATOH	1124	CD1	ILE	113	29.324	6.250	59.176	1.00	42.34	AAAA	C
ATOH	1125	C	ILE	113	27.729	6.959	54.398	1.00	39.26	AAAA	C
ATOH	1126	O	ILE	113	26.637	6.482	54.664	1.00	50.72	AAAA	O
ATOH	1127	H	GLU	114	28.175	7.199	53.190	1.00	35.86	AAAA	H
ATOH	1129	CA	GLU	114	27.491	7.103	51.935	1.00	38.76	AAAA	C
ATOH	1130	CB	GLU	114	27.471	8.443	51.216	1.00	25.58	AAAA	C
ATOH	1131	CG	GLU	114	26.567	8.402	49.969	1.00	27.97	AAAA	C
ATOH	1132	CD	GLU	114	26.349	9.840	49.578	1.00	36.85	AAAA	C
ATOH	1133	OE1	GLU	114	26.763	10.662	50.414	1.00	45.57	AAAA	O

12/58

ATOM	1134	OE2	GLU	114	25.787	10.106	48.488	1.00	35.53	AAAA	C
ATOM	1135	C	GLU	114	28.039	6.072	50.844	1.00	44.17	AAAA	C
ATOM	1136	O	GLU	114	29.120	5.538	51.090	1.00	49.97	AAAA	C
ATOM	1137	H	LYS	115	27.191	5.556	50.096	1.00	40.55	AAAA	H
ATOM	1139	CA	LYS	115	27.219	4.440	49.242	1.00	41.16	AAAA	C
ATOM	1140	CB	LYS	115	27.275	4.764	47.718	1.00	23.62	AAAA	C
ATOM	1141	CG	LYS	115	27.019	6.194	47.411	1.00	18.39	AAAA	C
ATOM	1142	CD	LYS	115	26.537	6.355	45.982	1.00	24.74	AAAA	C
ATOM	1143	CE	LYS	115	26.751	7.804	45.622	1.00	41.86	AAAA	C
ATOM	1144	NE	LYS	115	27.165	8.045	44.196	1.00	60.91	AAAA	H
ATOM	1148	C	LYS	115	28.287	3.421	49.611	1.00	42.39	AAAA	C
ATOM	1149	O	LYS	115	29.102	3.103	48.749	1.00	46.68	AAAA	C
ATOM	1150	H	ASH	116	28.137	2.677	50.665	1.00	40.99	AAAA	H
ATOM	1152	CA	ASH	116	29.022	1.570	50.976	1.00	37.33	AAAA	C
ATOM	1153	CB	ASH	116	29.534	1.868	52.381	1.00	46.12	AAAA	C
ATOM	1154	CG	ASH	116	30.372	3.153	52.345	1.00	48.92	AAAA	C
ATOM	1155	OD1	ASH	116	31.337	3.016	51.583	1.00	38.59	AAAA	C
ATOM	1156	HD2	ASH	116	29.927	4.174	53.056	1.00	37.35	AAAA	H
ATOM	1159	C	ASH	116	28.275	0.277	50.974	1.00	42.52	AAAA	C
ATOM	1160	O	ASH	116	28.067	-0.361	52.033	1.00	48.24	AAAA	C
ATOM	1161	H	ALA	117	27.989	-0.188	49.772	1.00	40.94	AAAA	H
ATOM	1163	CA	ALA	117	27.195	-1.376	49.542	1.00	43.35	AAAA	C
ATOM	1164	CB	ALA	117	27.494	-1.884	48.156	1.00	47.63	AAAA	C
ATOM	1165	C	ALA	117	27.294	-2.504	50.529	1.00	46.55	AAAA	C
ATOM	1166	O	ALA	117	26.211	-2.998	50.890	1.00	51.24	AAAA	C
ATOM	1167	H	ASP	118	28.484	-2.823	51.005	1.00	47.43	AAAA	H
ATOM	1169	CA	ASP	118	28.559	-3.980	51.920	1.00	45.74	AAAA	C
ATOM	1170	CB	ASP	118	29.659	-4.945	51.477	1.00	55.39	AAAA	C
ATOM	1171	CG	ASP	118	29.684	-5.119	49.958	1.00	59.40	AAAA	C
ATOM	1172	OD1	ASP	118	28.870	-5.976	49.608	1.00	64.40	AAAA	C
ATOM	1173	OD2	ASP	118	30.448	-4.447	49.207	1.00	66.73	AAAA	C
ATOM	1174	C	ASP	118	28.818	-3.586	53.353	1.00	37.29	AAAA	C
ATOM	1175	O	ASP	118	29.127	-4.536	54.026	1.00	42.89	AAAA	C
ATOM	1176	H	LEU	119	28.670	-2.327	53.685	1.00	36.46	AAAA	H
ATOM	1178	CA	LEU	119	28.986	-1.885	55.047	1.00	40.58	AAAA	C
ATOM	1179	CB	LEU	119	29.159	-0.389	55.145	1.00	34.31	AAAA	C
ATOM	1180	CG	LEU	119	29.640	0.331	56.378	1.00	36.58	AAAA	C
ATOM	1181	CD1	LEU	119	30.950	-0.101	56.948	1.00	35.77	AAAA	C
ATOM	1182	CD2	LEU	119	29.791	1.830	56.104	1.00	29.68	AAAA	C
ATOM	1183	C	LEU	119	27.937	-2.376	56.007	1.00	43.67	AAAA	C
ATOM	1184	O	LEU	119	26.748	-2.248	55.743	1.00	45.32	AAAA	C
ATOM	1185	N	CYS	120	28.361	-2.967	57.110	1.00	43.53	AAAA	H
ATOM	1187	CA	CYS	120	27.378	-3.407	58.089	1.00	38.93	AAAA	C
ATOM	1188	C	CYS	120	27.881	-2.921	59.426	1.00	41.91	AAAA	C
ATOM	1189	O	CYS	120	28.660	-1.960	59.446	1.00	43.66	AAAA	C
ATOM	1190	CB	CYS	120	27.285	-4.907	58.100	1.00	37.59	AAAA	C
ATOM	1191	SG	CYS	120	26.568	-5.622	56.639	1.00	58.32	AAAA	S
ATOM	1192	H	TYR	121	27.328	-3.456	60.509	1.00	38.05	AAAA	H
ATOM	1194	CA	TYR	121	27.795	-3.010	61.927	1.00	39.68	AAAA	C
ATOM	1195	CB	TYR	121	29.189	-3.572	62.130	1.00	34.61	AAAA	C
ATOM	1196	CG	TYR	121	28.950	-5.032	62.519	1.00	36.52	AAAA	C
ATOM	1197	CD1	TYR	121	29.087	-6.045	61.582	1.00	33.58	AAAA	C
ATOM	1198	CE1	TYR	121	28.852	-7.350	61.980	1.00	41.21	AAAA	C
ATOM	1199	CD2	TYR	121	28.560	-5.337	63.817	1.00	36.31	AAAA	C
ATOM	1200	CE2	TYR	121	28.297	-6.630	64.201	1.00	39.48	AAAA	C
ATOM	1201	CE	TYR	121	28.432	-7.641	63.270	1.00	46.07	AAAA	C
ATOM	1202	OH	TYR	121	28.161	-8.924	63.730	1.00	49.20	AAAA	C
ATOM	1204	C	TYR	121	27.674	-1.523	61.789	1.00	38.83	AAAA	C
ATOM	1205	O	TYR	121	28.445	-0.778	62.369	1.00	43.22	AAAA	C
ATOM	1206	H	LEU	122	26.587	-1.045	61.180	1.00	39.58	AAAA	H
ATOM	1208	CA	LEU	122	26.361	0.405	61.090	1.00	44.82	AAAA	C
ATOM	1209	CB	LEU	122	25.990	0.715	59.634	1.00	46.48	AAAA	C
ATOM	1210	CG	LEU	122	26.497	2.014	59.108	1.00	44.44	AAAA	C
ATOM	1211	CD1	LEU	122	25.778	2.448	57.859	1.00	32.19	AAAA	C
ATOM	1212	CD2	LEU	122	26.136	3.057	60.170	1.00	47.76	AAAA	C
ATOM	1213	C	LEU	122	25.212	0.910	61.935	1.00	44.85	AAAA	C
ATOM	1214	O	LEU	122	25.269	1.759	62.839	1.00	47.66	AAAA	C
ATOM	1215	H	SER	123	24.104	0.137	61.843	1.00	40.12	AAAA	H
ATOM	1217	CA	SER	123	22.949	0.435	62.703	1.00	33.98	AAAA	C
ATOM	1218	CB	SER	123	21.754	-0.330	62.239	1.00	19.26	AAAA	C
ATOM	1219	CG	SER	123	21.964	-1.762	62.402	1.00	34.35	AAAA	C
ATOM	1221	C	SER	123	23.165	0.060	64.159	1.00	37.43	AAAA	C
ATOM	1222	O	SER	123	22.326	0.280	65.025	1.00	35.33	AAAA	C
ATOM	1223	H	THR	124	24.242	-0.698	64.432	1.00	39.03	AAAA	H
ATOM	1225	CA	THR	124	24.554	-1.165	65.753	1.00	37.79	AAAA	C
ATOM	1226	CB	THR	124	25.368	-2.461	65.719	1.00	42.39	AAAA	C
ATOM	1227	CG1	THR	124	26.502	-2.020	64.924	1.00	47.70	AAAA	C
ATOM	1229	CG2	THR	124	24.677	-3.622	65.006	1.00	40.93	AAAA	C
ATOM	1230	C	THR	124	25.522	-0.206	66.445	1.00	39.29	AAAA	C
ATOM	1231	O	THR	124	25.948	-0.642	67.499	1.00	41.41	AAAA	C
ATOM	1232	H	VAL	125	25.737	1.001	65.985	1.00	37.80	AAAA	H
ATOM	1234	CA	VAL	125	26.594	1.964	66.661	1.00	41.06	AAAA	C
ATOM	1235	CB	VAL	125	27.683	2.542	65.714	1.00	39.50	AAAA	C
ATOM	1236	CG1	VAL	125	28.570	3.599	66.352	1.00	28.36	AAAA	C
ATOM	1237	CG2	VAL	125	28.693	1.565	65.110	1.00	33.07	AAAA	C

13/58

ATOH	1238	C	VAL	125	25.759	3.127	67.175	1.00	41.17	AAAA	C
ATOH	1239	O	VAL	125	24.941	3.750	66.531	1.00	41.22	AAAA	O
ATOH	1240	H	ASP	126	26.072	3.636	68.367	1.00	44.54	AAAA	H
ATOH	1242	CA	ASP	126	25.310	4.734	68.967	1.00	37.44	AAAA	C
ATOH	1243	CB	ASP	126	24.862	4.335	70.342	1.00	34.73	AAAA	C
ATOH	1244	CG	ASP	126	23.879	5.303	70.983	1.00	45.53	AAAA	C
ATOH	1245	OD1	ASP	126	23.699	6.520	70.685	1.00	27.71	AAAA	O
ATOH	1246	OD2	ASP	126	23.220	4.865	71.964	1.00	52.32	AAAA	O
ATOH	1247	C	ASP	126	26.146	5.985	68.872	1.00	40.83	AAAA	C
ATOH	1248	O	ASP	126	26.740	6.400	69.888	1.00	42.78	AAAA	O
ATOH	1249	H	TRP	127	26.029	6.649	67.704	1.00	35.42	AAAA	H
ATOH	1251	CA	TRP	127	26.777	7.856	67.410	1.00	33.02	AAAA	C
ATOH	1252	CB	TRP	127	26.568	8.296	65.930	1.00	24.89	AAAA	C
ATOH	1253	CG	TRP	127	27.195	7.372	64.907	1.00	34.36	AAAA	C
ATOH	1254	CD2	TRP	127	28.987	7.208	64.518	1.00	28.60	AAAA	C
ATOH	1255	CE2	TRP	127	28.631	6.186	63.579	1.00	29.06	AAAA	C
ATOH	1256	CE3	TRP	127	29.778	7.845	64.873	1.00	35.51	AAAA	C
ATOH	1257	CD1	TRP	127	26.465	6.450	64.188	1.00	18.67	AAAA	C
ATOH	1258	HE1	TRP	127	27.311	5.712	63.394	1.00	42.87	AAAA	H
ATOH	1260	CE2	TRP	127	29.792	5.783	62.954	1.00	32.53	AAAA	C
ATOH	1261	CE3	TRP	127	30.972	7.445	64.285	1.00	31.51	AAAA	C
ATOH	1262	CH2	TRP	127	30.937	6.405	63.336	1.00	37.86	AAAA	C
ATOH	1263	C	TRP	127	26.558	9.010	68.367	1.00	36.09	AAAA	C
ATOH	1264	O	TRP	127	27.382	9.977	68.497	1.00	40.87	AAAA	O
ATOH	1265	H	SER	128	25.493	8.931	69.171	1.00	31.24	AAAA	H
ATOH	1267	CA	SER	128	25.201	10.041	70.081	1.00	34.04	AAAA	C
ATOH	1268	CB	SER	128	23.757	10.042	70.603	1.00	36.87	AAAA	C
ATOH	1269	CG	SER	128	23.433	8.917	71.424	1.00	28.96	AAAA	C
ATOH	1271	C	SER	128	26.133	9.975	71.292	1.00	32.39	AAAA	O
ATOH	1272	O	SER	128	26.212	10.957	72.134	1.00	30.91	AAAA	O
ATOH	1273	H	LEU	129	26.662	8.792	71.549	1.00	27.18	AAAA	H
ATOH	1275	CA	LEU	129	27.701	8.607	72.526	1.00	36.73	AAAA	C
ATOH	1276	CB	LEU	129	27.920	7.132	72.741	1.00	32.53	AAAA	C
ATOH	1277	CG	LEU	129	26.795	6.324	73.371	1.00	39.28	AAAA	C
ATOH	1278	CD1	LEU	129	27.292	5.024	73.975	1.00	32.54	AAAA	C
ATOH	1279	CD2	LEU	129	26.237	7.117	74.560	1.00	32.12	AAAA	C
ATOH	1280	C	LEU	129	29.054	9.226	72.113	1.00	38.04	AAAA	C
ATOH	1281	O	LEU	129	29.645	10.001	72.874	1.00	34.50	AAAA	O
ATOH	1282	H	ILE	130	29.316	9.217	70.807	1.00	42.09	AAAA	H
ATOH	1284	CA	ILE	130	30.480	9.743	70.144	1.00	41.35	AAAA	C
ATOH	1285	CB	ILE	130	30.793	8.886	68.901	1.00	41.73	AAAA	C
ATOH	1286	CG2	ILE	130	31.992	9.434	68.176	1.00	31.95	AAAA	C
ATOH	1287	CG1	ILE	130	30.969	7.413	69.347	1.00	26.64	AAAA	C
ATOH	1288	CD1	ILE	130	31.053	6.457	68.165	1.00	42.65	AAAA	C
ATOH	1289	C	ILE	130	30.305	11.178	69.679	1.00	46.49	AAAA	C
ATOH	1290	O	ILE	130	31.224	11.985	69.966	1.00	38.46	AAAA	O
ATOH	1291	H	LEU	131	29.089	11.495	69.193	1.00	45.14	AAAA	H
ATOH	1293	CA	LEU	131	28.895	12.865	68.651	1.00	41.45	AAAA	C
ATOH	1294	CB	LEU	131	28.499	12.616	67.259	1.00	46.81	AAAA	C
ATOH	1295	CG	LEU	131	28.823	12.805	65.878	1.00	36.79	AAAA	C
ATOH	1296	CD1	LEU	131	29.128	11.405	65.324	1.00	30.15	AAAA	C
ATOH	1297	CD2	LEU	131	27.625	13.581	65.334	1.00	19.92	AAAA	C
ATOH	1298	C	LEU	131	27.661	13.525	69.285	1.00	39.28	AAAA	C
ATOH	1299	O	LEU	131	26.599	12.867	69.311	1.00	37.75	AAAA	O
ATOH	1300	H	ASP	132	27.742	14.811	69.518	1.00	33.73	AAAA	H
ATOH	1302	CA	ASP	132	26.610	15.542	70.003	1.00	38.20	AAAA	C
ATOH	1303	CB	ASP	132	27.017	16.944	70.381	1.00	43.17	AAAA	C
ATOH	1304	CG	ASP	132	27.349	17.137	71.834	1.00	43.29	AAAA	C
ATOH	1305	OD1	ASP	132	27.536	16.122	72.521	1.00	47.12	AAAA	O
ATOH	1306	OD2	ASP	132	27.413	18.331	72.208	1.00	60.58	AAAA	O
ATOH	1307	C	ASP	132	25.520	15.659	68.946	1.00	43.46	AAAA	C
ATOH	1308	O	ASP	132	24.481	15.032	68.939	1.00	49.32	AAAA	O
ATOH	1309	H	ALA	133	25.754	16.398	67.900	1.00	45.03	AAAA	H
ATOH	1311	CA	ALA	133	24.947	16.776	66.773	1.00	38.62	AAAA	C
ATOH	1312	CB	ALA	133	25.628	17.987	66.092	1.00	33.82	AAAA	C
ATOH	1313	C	ALA	133	24.694	15.669	65.775	1.00	33.33	AAAA	C
ATOH	1314	O	ALA	133	24.777	15.791	64.517	1.00	33.71	AAAA	O
ATOH	1315	H	VAL	134	24.115	14.565	66.219	1.00	27.88	AAAA	H
ATOH	1317	CA	VAL	134	23.813	13.440	65.377	1.00	29.90	AAAA	C
ATOH	1318	CB	VAL	134	23.202	12.241	66.120	1.00	40.63	AAAA	C
ATOH	1319	CG1	VAL	134	24.265	11.441	66.855	1.00	35.20	AAAA	C
ATOH	1320	CG2	VAL	134	22.095	12.761	67.068	1.00	30.84	AAAA	C
ATOH	1321	C	VAL	134	22.735	13.732	64.353	1.00	36.98	AAAA	C
ATOH	1322	O	VAL	134	22.616	13.106	63.292	1.00	32.95	AAAA	O
ATOH	1323	H	SER	135	21.920	14.777	64.626	1.00	39.65	AAAA	H
ATOH	1325	CA	SER	135	20.886	15.139	63.692	1.00	43.12	AAAA	C
ATOH	1326	CB	SER	135	20.093	16.277	64.305	1.00	45.19	AAAA	C
ATOH	1327	CG	SER	135	20.882	17.369	64.684	1.00	39.25	AAAA	O
ATOH	1329	C	SER	135	21.396	15.516	62.309	1.00	41.15	AAAA	C
ATOH	1330	O	SER	135	20.615	15.642	61.359	1.00	43.81	AAAA	O
ATOH	1331	H	ASH	136	22.615	15.911	62.165	1.00	41.11	AAAA	H
ATOH	1333	CA	ASH	136	23.298	16.353	60.978	1.00	37.21	AAAA	C
ATOH	1334	CB	ASH	136	24.324	17.372	61.399	1.00	39.66	AAAA	C
ATOH	1335	CG	ASH	136	23.724	19.709	61.717	1.00	36.59	AAAA	C
ATOH	1336	OD1	ASH	136	22.695	19.079	61.149	1.00	50.81	AAAA	O

14/58

ATOM	1337	HD2	ASH	136	24.379	19.441	62.585	1.00	47.85	AAAA	H
ATOM	1340	C	ASH	136	24.031	15.230	60.259	1.00	35.31	AAAA	C
ATOM	1341	O	ASH	136	24.535	15.484	59.194	1.00	38.70	AAAA	O
ATOM	1342	H	ASH	137	24.057	14.035	60.793	1.00	29.11	AAAA	H
ATOM	1344	CA	ASH	137	24.721	12.959	60.126	1.00	32.98	AAAA	C
ATOM	1345	CB	ASH	137	24.737	11.703	61.033	1.00	24.45	AAAA	C
ATOM	1346	CG	ASH	137	25.631	11.965	62.217	1.00	26.63	AAAA	C
ATOM	1347	OD1	ASH	137	26.070	13.121	62.369	1.00	30.22	AAAA	O
ATOM	1348	HD2	ASH	137	25.830	10.923	63.000	1.00	18.90	AAAA	H
ATOM	1351	C	ASH	137	23.950	12.749	58.817	1.00	35.89	AAAA	C
ATOM	1352	O	ASH	137	22.716	12.755	58.855	1.00	38.57	AAAA	O
ATOM	1353	H	TYR	138	24.592	12.251	57.785	1.00	32.86	AAAA	H
ATOM	1355	CA	TYR	138	24.693	11.983	56.489	1.00	30.25	AAAA	C
ATOM	1356	CB	TYR	138	24.682	12.861	55.421	1.00	27.10	AAAA	C
ATOM	1357	CG	TYR	138	24.618	12.741	54.078	1.00	37.89	AAAA	C
ATOM	1358	CD1	TYR	138	23.083	13.671	53.648	1.00	39.22	AAAA	C
ATOM	1359	CE1	TYR	138	22.510	13.579	52.392	1.00	37.65	AAAA	C
ATOM	1360	CD2	TYR	138	24.357	11.717	53.195	1.00	44.28	AAAA	C
ATOM	1361	CE2	TYR	138	23.801	11.615	51.951	1.00	41.97	AAAA	C
ATOM	1362	CS	TYR	138	22.868	12.562	51.564	1.00	39.42	AAAA	C
ATOM	1363	OH	TYR	136	22.296	12.504	50.318	1.00	45.48	AAAA	O
ATOM	1365	C	TYR	138	24.373	10.578	56.051	1.00	31.33	AAAA	C
ATOM	1366	O	TYR	138	25.505	10.317	55.797	1.00	37.76	AAAA	O
ATOM	1367	H	ILE	139	23.461	9.660	56.116	1.00	35.40	AAAA	H
ATOM	1369	CA	ILE	139	23.637	8.249	55.935	1.00	34.04	AAAA	C
ATOM	1370	CB	ILE	139	23.234	7.450	57.171	1.00	28.66	AAAA	C
ATOM	1371	CG2	ILE	139	23.640	5.984	57.093	1.00	21.99	AAAA	C
ATOM	1372	CG1	ILE	139	23.711	8.057	58.469	1.00	42.81	AAAA	C
ATOM	1373	CD1	ILE	139	24.455	7.100	59.389	1.00	52.23	AAAA	C
ATOM	1374	C	ILE	139	22.729	7.708	54.930	1.00	35.73	AAAA	C
ATOM	1375	O	ILE	139	21.538	7.890	54.757	1.00	42.61	AAAA	O
ATOM	1376	H	VAL	140	23.286	6.997	53.873	1.00	35.29	AAAA	H
ATOM	1378	CA	VAL	140	22.533	6.481	52.755	1.00	32.39	AAAA	C
ATOM	1379	CB	VAL	140	21.967	7.627	51.881	1.00	36.05	AAAA	C
ATOM	1380	CG1	VAL	140	22.800	8.375	50.881	1.00	25.88	AAAA	C
ATOM	1381	CG2	VAL	140	20.807	7.034	51.047	1.00	34.96	AAAA	C
ATOM	1382	C	VAL	140	23.422	5.670	51.874	1.00	41.96	AAAA	C
ATOM	1383	O	VAL	140	24.537	6.172	51.637	1.00	44.03	AAAA	O
ATOM	1384	H	GLY	141	22.899	4.562	51.402	1.00	42.66	AAAA	H
ATOM	1386	CA	GLY	141	23.381	3.805	50.278	1.00	30.94	AAAA	C
ATOM	1387	C	GLY	141	24.265	2.696	50.835	1.00	38.98	AAAA	C
ATOM	1388	O	GLY	141	25.132	2.003	50.176	1.00	35.87	AAAA	O
ATOM	1389	H	ASH	142	23.985	2.418	52.116	1.00	38.92	AAAA	H
ATOM	1391	CA	ASH	142	24.858	1.390	52.746	1.00	44.32	AAAA	C
ATOM	1392	CB	ASH	142	25.257	1.774	54.187	1.00	43.12	AAAA	C
ATOM	1393	CG	ASH	142	26.131	3.022	54.152	1.00	42.00	AAAA	C
ATOM	1394	OD1	ASH	142	26.984	3.077	53.269	1.00	40.47	AAAA	O
ATOM	1395	HD2	ASH	142	25.945	4.022	55.019	1.00	41.98	AAAA	H
ATOM	1398	C	ASH	142	24.153	0.066	52.687	1.00	45.84	AAAA	C
ATOM	1399	O	ASH	142	23.113	-0.015	52.055	1.00	49.65	AAAA	O
ATOM	1400	H	LYS	143	24.574	-0.990	53.272	1.00	45.23	AAAA	H
ATOM	1402	CA	LYS	143	24.073	-2.299	53.195	1.00	49.14	AAAA	C
ATOM	1403	CB	LYS	143	25.166	-3.328	53.433	1.00	41.49	AAAA	C
ATOM	1404	CG	LYS	143	24.750	-4.686	53.832	1.00	44.96	AAAA	C
ATOM	1405	CD	LYS	143	25.512	-5.743	53.100	1.00	48.66	AAAA	C
ATOM	1406	CE	LYS	143	25.643	-7.131	53.558	1.00	38.35	AAAA	C
ATOM	1407	HD2	LYS	143	26.080	-8.093	53.040	1.00	53.83	AAAA	H
ATOM	1411	C	LYS	143	22.902	-2.431	54.169	1.00	52.85	AAAA	C
ATOM	1412	O	LYS	143	22.960	-2.099	55.360	1.00	55.21	AAAA	O
ATOM	1413	H	PRO	144	21.806	-3.047	53.731	1.00	52.39	AAAA	H
ATOM	1414	CD	PRO	144	21.617	-3.469	52.315	1.00	52.58	AAAA	C
ATOM	1415	CA	PRO	144	20.559	-3.118	54.489	1.00	48.30	AAAA	C
ATOM	1416	CB	PRO	144	19.549	-3.602	53.455	1.00	51.41	AAAA	C
ATOM	1417	CG	PRO	144	20.134	-3.299	52.099	1.00	50.41	AAAA	C
ATOM	1418	C	PRO	144	20.621	-4.050	55.659	1.00	44.65	AAAA	C
ATOM	1419	O	PRO	144	20.904	-5.236	55.501	1.00	36.84	AAAA	O
ATOM	1420	H	PRO	145	20.318	-3.533	56.859	1.00	45.12	AAAA	H
ATOM	1421	CD	PRO	145	20.123	-2.054	57.094	1.00	38.17	AAAA	C
ATOM	1422	CA	PRO	145	20.448	-4.233	58.128	1.00	40.19	AAAA	C
ATOM	1423	CB	PRO	145	19.704	-3.288	59.099	1.00	37.08	AAAA	C
ATOM	1424	CG	PRO	145	20.040	-1.910	58.602	1.00	33.65	AAAA	C
ATOM	1425	C	PRO	145	19.993	-5.655	58.155	1.00	47.17	AAAA	C
ATOM	1426	O	PRO	145	20.556	-6.592	58.768	1.00	48.05	AAAA	O
ATOM	1427	H	LYS	146	18.979	-5.924	57.489	1.00	53.72	AAAA	H
ATOM	1429	CA	LYS	146	18.268	-7.229	57.295	1.00	56.94	AAAA	C
ATOM	1430	CB	LYS	146	16.994	-7.050	56.647	1.00	65.44	AAAA	C
ATOM	1431	CG	LYS	146	16.220	-8.232	55.982	1.00	64.32	AAAA	C
ATOM	1432	CD	LYS	146	14.797	-8.422	56.451	0.01	62.75	AAAA	C
ATOM	1433	CE	LYS	146	14.194	-9.717	55.934	0.01	62.14	AAAA	C
ATOM	1434	HD2	LYS	146	12.720	-9.610	55.753	0.01	61.38	AAAA	H
ATOM	1438	C	LYS	146	19.138	-8.138	56.446	1.00	61.40	AAAA	C
ATOM	1439	O	LYS	146	19.237	-9.346	56.732	1.00	66.22	AAAA	O
ATOM	1440	H	GLU	147	19.779	-7.649	55.389	1.00	62.92	AAAA	H
ATOM	1442	CA	GLU	147	20.927	-8.446	54.742	1.00	67.60	AAAA	C
ATOM	1443	CB	GLU	147	21.101	-8.070	53.294	1.00	62.32	AAAA	C

15/58

ATOM	1444	CH	GLU	147	19.967	-7.579	52.567	1.00	73.15	AAAA	C
ATOM	1445	CD	GLU	147	20.164	-7.413	51.093	1.00	85.90	AAAA	C
ATOM	1446	OE1	GLU	147	21.339	-7.636	50.701	1.00	95.25	AAAA	O
ATOM	1447	OE2	GLU	147	19.201	-7.053	50.376	1.00	87.47	AAAA	O
ATOM	1448	C	GLU	147	22.136	-8.470	55.541	1.00	69.40	AAAA	C
ATOM	1449	H	GLU	147	22.883	-9.437	55.361	1.00	72.86	AAAA	G
ATOM	1450	H	CYS	148	22.506	-7.484	56.355	1.00	66.76	AAAA	H
ATOM	1452	CA	CYS	148	23.693	-7.588	57.183	1.00	64.65	AAAA	C
ATOM	1453	C	CYS	148	23.598	-8.702	58.196	1.00	65.56	AAAA	C
ATOM	1454	O	CYS	148	24.473	-9.524	58.414	1.00	65.89	AAAA	O
ATOM	1455	CB	CYS	148	23.952	-6.301	58.001	1.00	57.29	AAAA	C
ATOM	1456	SG	CYS	148	24.565	-5.091	56.808	1.00	59.22	AAAA	S
ATOM	1457	H	GLY	149	22.514	-8.743	58.977	1.00	67.88	AAAA	H
ATOM	1459	CA	GLY	149	22.387	-9.744	60.029	1.00	62.15	AAAA	C
ATOM	1460	C	GLY	149	23.443	-9.627	61.120	1.00	59.18	AAAA	C
ATOM	1461	O	GLY	149	23.925	-10.603	61.699	1.00	61.11	AAAA	O
ATOM	1462	H	ASP	150	23.717	-8.426	61.596	1.00	54.88	AAAA	H
ATOM	1464	CA	ASP	150	24.794	-8.198	62.533	1.00	55.78	AAAA	C
ATOM	1465	CB	ASP	150	25.041	-6.703	62.750	1.00	49.10	AAAA	C
ATOM	1466	CG	ASP	150	25.320	-6.034	61.410	1.00	58.50	AAAA	C
ATOM	1467	OD1	ASP	150	25.726	-6.796	60.480	1.00	57.73	AAAA	O
ATOM	1468	OD2	ASP	150	25.102	-4.819	61.363	1.00	49.69	AAAA	O
ATOM	1469	C	ASP	150	24.519	-8.854	63.855	1.00	59.36	AAAA	C
ATOM	1470	O	ASP	150	23.392	-8.820	64.377	1.00	67.48	AAAA	O
ATOM	1471	H	LEU	151	25.532	-9.369	64.524	1.00	54.39	AAAA	H
ATOM	1473	CA	LEU	151	25.314	-9.908	65.853	1.00	52.79	AAAA	C
ATOM	1474	CB	LEU	151	25.208	-11.409	65.806	1.00	58.55	AAAA	C
ATOM	1475	CG	LEU	151	24.063	-12.101	65.092	1.00	69.45	AAAA	C
ATOM	1476	CD1	LEU	151	24.515	-13.421	64.489	1.00	65.26	AAAA	C
ATOM	1477	CD2	LEU	151	22.937	-12.372	65.951	1.00	65.43	AAAA	C
ATOM	1478	C	LEU	151	26.409	-9.454	66.805	1.00	51.93	AAAA	C
ATOM	1479	O	LEU	151	27.598	-9.734	66.634	1.00	55.59	AAAA	O
ATOM	1480	H	CYS	152	26.024	-8.773	67.849	1.00	48.60	AAAA	H
ATOM	1482	CA	CYS	152	26.992	-8.189	68.740	1.00	56.73	AAAA	C
ATOM	1483	C	CYS	152	27.650	-9.325	69.493	1.00	63.58	AAAA	C
ATOM	1484	O	CYS	152	27.074	-10.405	69.575	1.00	62.40	AAAA	O
ATOM	1485	CB	CYS	152	26.358	-7.144	69.657	1.00	41.99	AAAA	C
ATOM	1486	SG	CYS	152	25.985	-5.635	68.703	1.00	55.83	AAAA	S
ATOM	1487	H	PRO	153	28.826	-9.072	70.059	1.00	68.05	AAAA	H
ATOM	1488	CD	PRO	153	29.618	-7.838	69.903	1.00	66.66	AAAA	C
ATOM	1489	CA	PRO	153	29.497	-10.094	70.851	1.00	70.60	AAAA	C
ATOM	1490	CB	PRO	153	30.601	-9.323	71.557	1.00	69.98	AAAA	C
ATOM	1491	CG	PRO	153	30.861	-8.159	70.690	1.00	70.58	AAAA	C
ATOM	1492	C	PRO	153	28.543	-10.734	71.850	1.00	69.64	AAAA	C
ATOM	1493	O	PRO	153	27.859	-10.075	72.615	1.00	69.58	AAAA	O
ATOM	1494	H	GLY	154	28.444	-12.049	71.843	1.00	71.23	AAAA	H
ATOM	1496	CA	GLY	154	27.610	-12.804	72.745	1.00	78.07	AAAA	C
ATOM	1497	C	GLY	154	26.245	-13.230	72.223	1.00	81.75	AAAA	C
ATOM	1498	O	GLY	154	25.786	-14.318	72.547	1.00	80.26	AAAA	O
ATOM	1499	H	THR	155	25.549	-12.468	71.314	1.00	84.54	AAAA	H
ATOM	1501	CA	THR	155	24.314	-12.683	70.828	1.00	89.38	AAAA	C
ATOM	1502	CB	THR	155	24.916	-11.661	69.705	1.00	85.07	AAAA	C
ATOM	1503	OG1	THR	155	24.063	-10.417	70.420	1.00	84.51	AAAA	O
ATOM	1505	CG2	THR	155	22.686	-11.995	69.092	1.00	82.27	AAAA	C
ATOM	1506	C	THR	155	24.060	-14.094	70.353	1.00	93.69	AAAA	C
ATOM	1507	O	THR	155	23.005	-14.664	70.617	1.00	95.92	AAAA	O
ATOM	1508	H	HET	156	25.003	-14.655	69.617	1.00	97.23	AAAA	H
ATOM	1510	CA	HET	156	24.884	-15.973	69.024	1.00	99.05	AAAA	C
ATOM	1511	CB	HET	156	25.907	-16.190	67.896	1.00	100.40	AAAA	C
ATOM	1512	CG	HET	156	25.456	-15.675	66.542	0.01	99.75	AAAA	C
ATOM	1513	SD	HET	156	23.687	-15.857	66.255	0.01	99.72	AAAA	S
ATOM	1514	CE	HET	156	23.664	-17.214	65.087	0.01	99.59	AAAA	C
ATOM	1515	C	HET	156	25.027	-17.106	70.032	1.00	100.57	AAAA	C
ATOM	1516	O	HET	156	24.353	-18.122	69.835	1.00	101.64	AAAA	O
ATOM	1517	H	ALA	157	25.974	-17.057	70.967	1.00	100.53	AAAA	H
ATOM	1519	CA	ALA	157	26.022	-18.102	71.986	1.00	101.00	AAAA	C
ATOM	1520	CB	ALA	157	27.317	-18.158	72.766	1.00	103.42	AAAA	C
ATOM	1521	C	ALA	157	24.856	-17.890	72.959	1.00	101.10	AAAA	C
ATOM	1522	O	ALA	157	23.993	-18.654	72.921	1.00	104.59	AAAA	O
ATOM	1523	H	GLU	158	24.984	-16.906	73.841	1.00	98.39	AAAA	H
ATOM	1525	CA	GLU	158	23.935	-16.629	74.781	1.00	97.43	AAAA	C
ATOM	1526	CB	GLU	158	23.128	-17.865	75.208	1.00	105.93	AAAA	C
ATOM	1527	CG	GLU	158	21.687	-17.546	75.560	1.00	113.87	AAAA	C
ATOM	1528	CD	GLU	158	21.347	-16.081	75.302	1.00	119.34	AAAA	C
ATOM	1529	OE1	GLU	158	21.284	-15.733	74.096	1.00	126.27	AAAA	O
ATOM	1530	OE2	GLU	158	21.199	-15.317	76.282	1.00	117.79	AAAA	O
ATOM	1531	C	GLU	158	24.434	-15.915	76.025	1.00	95.00	AAAA	C
ATOM	1532	O	GLU	158	23.988	-16.117	77.145	1.00	95.89	AAAA	O
ATOM	1533	H	SER	159	25.276	-14.942	75.769	1.00	93.30	AAAA	H
ATOM	1535	CA	SER	159	25.810	-14.119	76.848	1.00	92.28	AAAA	C
ATOM	1536	CB	SER	159	26.989	-14.805	77.517	1.00	97.37	AAAA	C
ATOM	1537	OG	SER	159	26.972	-14.427	78.886	1.00	98.08	AAAA	O
ATOM	1539	C	SER	159	26.228	-12.793	76.226	1.00	91.47	AAAA	C
ATOM	1540	O	SER	159	27.368	-12.592	75.910	1.00	92.75	AAAA	O
ATOM	1541	H	PRO	160	25.196	-12.007	75.932	1.00	88.65	AAAA	H

16/58

ATOM	1542	CD	PRO	160	23.789	-12.122	76.395	1.00	86.67	AAAA	C
ATOM	1543	CA	PRO	160	25.463	-10.701	75.361	1.00	84.74	AAAA	C
ATOM	1544	CB	PRO	160	24.125	-9.978	75.456	1.00	84.79	AAAA	C
ATOM	1545	CG	PRO	160	23.370	-10.671	76.515	1.00	84.62	AAAA	C
ATOM	1546	C	PRO	160	26.503	-10.025	76.236	1.00	79.60	AAAA	C
ATOM	1547	O	PRO	160	26.319	-9.934	77.456	1.00	79.70	AAAA	O
ATOM	1548	H	HET	161	27.563	-9.522	75.596	1.00	74.45	AAAA	H
ATOM	1550	CA	HET	161	28.530	-8.735	76.378	1.00	67.04	AAAA	C
ATOM	1551	CB	HET	161	29.924	-9.178	76.038	1.00	69.93	AAAA	C
ATOM	1552	CG	HET	161	30.118	-10.630	75.706	1.00	71.43	AAAA	C
ATOM	1553	SD	HET	161	30.716	-11.621	77.094	1.00	85.25	AAAA	S
ATOM	1554	CE	HET	161	29.841	-10.905	78.471	1.00	69.31	AAAA	C
ATOM	1555	C	HET	161	28.358	-7.234	76.189	1.00	61.76	AAAA	C
ATOM	1556	O	HET	161	28.788	-6.443	77.034	1.00	58.60	AAAA	O
ATOM	1557	H	CYS	162	27.681	-6.819	75.095	1.00	54.81	AAAA	H
ATOM	1559	CA	CYS	162	27.493	-5.384	74.938	1.00	49.76	AAAA	C
ATOM	1560	C	CYS	162	26.306	-4.777	75.670	1.00	51.50	AAAA	C
ATOM	1561	O	CYS	162	25.224	-5.324	75.928	1.00	53.89	AAAA	O
ATOM	1562	CB	CYS	162	27.422	-5.099	73.459	1.00	48.31	AAAA	C
ATOM	1563	SG	CYS	162	28.533	-6.064	72.432	1.00	54.02	AAAA	S
ATOM	1564	H	GLU	163	26.409	-3.522	76.031	1.00	46.31	AAAA	H
ATOM	1566	CA	GLU	163	25.355	-2.675	76.538	1.00	47.19	AAAA	C
ATOM	1567	CB	GLU	163	26.051	-1.412	77.027	1.00	49.95	AAAA	C
ATOM	1568	CG	GLU	163	26.476	-1.364	78.465	1.00	62.30	AAAA	C
ATOM	1569	CD	GLU	163	25.817	-0.135	79.116	1.00	81.67	AAAA	C
ATOM	1570	OE1	GLU	163	26.470	0.473	80.016	1.00	73.22	AAAA	O
ATOM	1571	OE2	GLU	163	24.646	0.208	78.721	1.00	80.93	AAAA	O
ATOM	1572	C	GLU	163	24.299	-2.340	75.472	1.00	49.05	AAAA	C
ATOM	1573	O	GLU	163	24.488	-2.423	74.234	1.00	45.90	AAAA	O
ATOM	1574	H	LYS	164	23.142	-1.815	75.880	1.00	47.43	AAAA	H
ATOM	1576	CA	LYS	164	22.011	-1.499	75.081	1.00	43.92	AAAA	C
ATOM	1577	CB	LYS	164	20.714	-2.244	75.450	1.00	44.48	AAAA	C
ATOM	1578	CG	LYS	164	20.560	-3.639	74.870	1.00	48.65	AAAA	C
ATOM	1579	CD	LYS	164	19.480	-4.432	75.622	1.00	49.04	AAAA	C
ATOM	1580	CE	LYS	164	18.409	-5.012	74.720	1.00	49.21	AAAA	C
ATOM	1581	HC	LYS	164	17.951	-6.372	75.134	1.00	37.67	AAAA	H
ATOM	1585	C	LYS	164	21.615	-0.040	75.204	1.00	45.01	AAAA	C
ATOM	1586	O	LYS	164	21.466	0.484	76.282	1.00	45.69	AAAA	O
ATOM	1587	H	THR	165	21.333	0.570	74.034	1.00	44.94	AAAA	H
ATOM	1589	CA	THR	165	20.775	1.943	74.077	1.00	43.13	AAAA	C
ATOM	1590	CB	THR	165	21.831	2.952	73.553	1.00	47.81	AAAA	C
ATOM	1591	OG1	THR	165	22.053	2.689	72.127	1.00	39.13	AAAA	O
ATOM	1593	CG2	THR	165	23.119	2.842	74.362	1.00	40.40	AAAA	C
ATOM	1594	C	THR	165	19.532	1.881	73.189	1.00	40.92	AAAA	C
ATOM	1595	O	THR	165	19.346	0.897	72.414	1.00	35.91	AAAA	O
ATOM	1596	H	THR	166	18.781	2.985	73.173	1.00	39.18	AAAA	H
ATOM	1598	CA	THR	166	17.689	2.991	72.182	1.00	42.97	AAAA	C
ATOM	1599	CB	THR	166	16.297	3.096	72.833	1.00	55.99	AAAA	C
ATOM	1600	OG1	THR	166	15.662	4.385	72.819	1.00	41.42	AAAA	O
ATOM	1602	CG2	THR	166	16.157	2.740	74.313	1.00	42.83	AAAA	C
ATOM	1603	C	THR	166	17.983	4.051	71.137	1.00	40.17	AAAA	C
ATOM	1604	O	THR	166	18.219	5.206	71.509	1.00	35.72	AAAA	O
ATOM	1605	H	ILE	167	17.912	3.725	69.866	1.00	42.21	AAAA	H
ATOM	1607	CA	ILE	167	18.182	4.672	68.777	1.00	41.05	AAAA	C
ATOM	1608	CB	ILE	167	19.437	4.335	67.904	1.00	39.50	AAAA	C
ATOM	1609	CG2	ILE	167	19.589	5.346	66.716	1.00	15.26	AAAA	C
ATOM	1610	CG1	ILE	167	20.722	4.305	68.724	1.00	36.20	AAAA	C
ATOM	1611	CD1	ILE	167	21.899	3.665	67.966	1.00	35.70	AAAA	C
ATOM	1612	C	ILE	167	16.937	4.524	67.882	1.00	40.94	AAAA	C
ATOM	1613	O	ILE	167	16.655	3.435	67.394	1.00	35.51	AAAA	O
ATOM	1614	H	ASH	168	16.318	5.635	67.537	1.00	42.29	AAAA	H
ATOM	1616	CA	ASH	168	15.112	5.633	66.713	1.00	45.22	AAAA	C
ATOM	1617	CB	ASH	168	15.526	5.253	65.292	1.00	45.69	AAAA	C
ATOM	1618	CG	ASH	168	14.497	5.696	64.244	1.00	51.19	AAAA	C
ATOM	1619	OD1	ASH	168	14.344	5.112	63.150	1.00	41.75	AAAA	O
ATOM	1620	HD2	ASH	168	13.749	6.763	64.522	1.00	48.89	AAAA	H
ATOM	1623	C	ASH	168	13.954	4.739	67.141	1.00	46.55	AAAA	C
ATOM	1624	O	ASH	168	13.544	3.879	66.326	1.00	45.95	AAAA	O
ATOM	1625	H	ASH	169	13.644	4.728	68.433	1.00	45.12	AAAA	H
ATOM	1627	CA	ASH	169	12.717	3.759	69.007	1.00	43.67	AAAA	C
ATOM	1628	CB	ASH	169	11.315	4.106	68.540	1.00	36.84	AAAA	C
ATOM	1629	CG	ASH	169	10.943	5.487	69.093	1.00	42.75	AAAA	C
ATOM	1630	OD1	ASH	169	10.917	5.779	70.280	1.00	36.67	AAAA	O
ATOM	1631	HD2	ASH	169	10.658	6.448	68.213	1.00	40.74	AAAA	H
ATOM	1634	C	ASH	169	13.003	2.306	68.719	1.00	44.69	AAAA	C
ATOM	1635	O	ASH	169	12.100	1.544	68.383	1.00	45.72	AAAA	O
ATOM	1636	H	GLU	170	14.226	1.907	68.862	1.00	41.64	AAAA	H
ATOM	1638	CA	GLU	170	14.655	0.513	68.850	1.00	45.88	AAAA	C
ATOM	1639	CB	GLU	170	15.283	0.278	67.524	1.00	55.92	AAAA	C
ATOM	1640	CG	GLU	170	15.028	-0.953	66.702	1.00	67.08	AAAA	C
ATOM	1641	CD	GLU	170	14.517	-0.605	65.294	1.00	74.56	AAAA	C
ATOM	1642	OE1	GLU	170	13.969	0.466	65.049	1.00	77.75	AAAA	O
ATOM	1643	OE2	GLU	170	14.763	-1.437	64.389	1.00	70.71	AAAA	O
ATOM	1644	C	GLU	170	15.647	0.379	70.010	1.00	47.10	AAAA	C
ATOM	1645	O	GLU	170	16.582	1.172	70.213	1.00	49.92	AAAA	O

17/58

ATOH	1646	H	TYR	171	15.344	-0.462	70.957	1.00	42.10	AAAA	H
ATOH	1648	CA	TYR	171	15.231	-0.688	70.097	1.00	51.51	AAAA	C
ATOH	1649	CB	TYR	171	15.434	-0.861	73.359	1.00	49.94	AAAA	C
ATOH	1650	CG	TYR	171	16.175	-1.168	74.620	1.00	48.90	AAAA	C
ATOH	1651	CD1	TYR	171	16.980	-0.210	75.237	1.00	46.46	AAAA	C
ATOH	1652	CE1	TYR	171	17.634	-0.469	76.467	1.00	41.17	AAAA	C
ATOH	1653	CD2	TYR	171	16.065	-2.429	75.194	1.00	43.62	AAAA	C
ATOH	1654	CE2	TYR	171	16.734	-2.675	76.366	1.00	44.44	AAAA	C
ATOH	1655	CO	TYR	171	17.516	-1.718	76.973	1.00	43.58	AAAA	C
ATOH	1656	OH	TYR	171	18.174	-2.017	78.146	1.00	40.16	AAAA	O
ATOH	1658	C	TYR	171	17.058	-1.938	71.833	1.00	51.41	AAAA	C
ATOH	1659	O	TYR	171	16.519	-3.024	71.889	1.00	52.59	AAAA	O
ATOH	1660	H	ASH	172	18.331	-1.750	71.493	1.00	53.70	AAAA	H
ATOH	1662	CA	ASH	172	19.203	-2.898	71.193	1.00	52.36	AAAA	C
ATOH	1663	CB	ASH	172	19.085	-3.278	69.709	1.00	55.43	AAAA	C
ATOH	1664	CG	ASH	172	18.939	-4.766	69.499	1.00	61.75	AAAA	C
ATOH	1665	OD1	ASH	172	19.233	-5.646	70.304	1.00	61.61	AAAA	O
ATOH	1666	HD2	ASH	172	18.449	-5.048	68.295	1.00	57.97	AAAA	H
ATOH	1669	C	ASH	172	20.665	-2.712	71.560	1.00	43.81	AAAA	C
ATOH	1670	O	ASH	172	21.163	-1.760	72.213	1.00	39.38	AAAA	O
ATOH	1671	H	TYR	173	21.373	-3.796	71.393	1.00	43.20	AAAA	H
ATOH	1673	CA	TYR	173	22.794	-3.929	71.699	1.00	44.76	AAAA	C
ATOH	1674	CB	TYR	173	23.223	-5.374	71.514	1.00	41.66	AAAA	C
ATOH	1675	CG	TYR	173	22.759	-6.274	72.630	1.00	45.18	AAAA	C
ATOH	1676	CD1	TYR	173	21.931	-7.316	72.237	1.00	46.48	AAAA	C
ATOH	1677	CE1	TYR	173	21.438	-8.181	73.193	1.00	51.36	AAAA	C
ATOH	1678	CD2	TYR	173	23.081	-6.132	73.978	1.00	44.86	AAAA	C
ATOH	1679	CE2	TYR	173	22.583	-7.016	74.916	1.00	46.92	AAAA	C
ATOH	1680	CO	TYR	173	21.757	-8.036	74.535	1.00	50.33	AAAA	C
ATOH	1691	OH	TYR	173	21.171	-9.006	75.328	1.00	50.64	AAAA	O
ATOH	1693	C	TYR	173	23.673	-3.099	70.762	1.00	46.94	AAAA	C
ATOH	1684	O	TYR	173	23.389	-2.883	69.567	1.00	49.76	AAAA	O
ATOH	1685	H	ARG	174	24.579	-2.318	71.366	1.00	47.79	AAAA	H
ATOH	1687	CA	ARG	174	25.517	-1.496	70.577	1.00	49.13	AAAA	C
ATOH	1688	CB	ARG	174	25.537	-0.132	71.233	1.00	44.32	AAAA	C
ATOH	1689	CG	ARG	174	24.210	0.623	71.234	1.00	48.14	AAAA	C
ATOH	1690	CD	ARG	174	23.372	0.344	70.003	1.00	51.47	AAAA	C
ATOH	1691	HE	ARG	174	21.974	0.760	70.039	1.00	48.35	AAAA	H
ATOH	1693	CO	ARG	174	21.144	0.570	69.017	1.00	48.23	AAAA	C
ATOH	1694	HH1	ARG	174	21.477	0.022	67.864	1.00	38.96	AAAA	H
ATOH	1697	HH2	ARG	174	19.909	1.022	69.197	1.00	54.65	AAAA	H
ATOH	1700	C	ARG	174	26.921	-2.094	70.461	1.00	45.98	AAAA	O
ATOH	1701	O	ARG	174	27.548	-2.557	71.406	1.00	44.97	AAAA	O
ATOH	1702	H	CYS	175	27.493	-2.183	69.294	1.00	46.21	AAAA	H
ATOH	1704	CA	CYS	175	28.787	-2.758	68.997	1.00	45.60	AAAA	C
ATOH	1705	C	CYS	175	29.407	-2.395	67.665	1.00	46.23	AAAA	C
ATOH	1706	O	CYS	175	28.755	-2.018	66.665	1.00	44.78	AAAA	O
ATOH	1707	CB	CYS	175	28.576	-4.253	69.167	1.00	35.62	AAAA	O
ATOH	1708	SG	CYS	175	27.812	-5.181	67.827	1.00	51.92	AAAA	S
ATOH	1709	H	TRP	176	30.764	-2.517	67.583	1.00	48.16	AAAA	H
ATOH	1711	CA	TRP	176	31.430	-2.091	66.325	1.00	42.48	AAAA	C
ATOH	1712	CB	TRP	176	32.769	-1.409	66.564	1.00	36.38	AAAA	C
ATOH	1713	CG	TRP	176	32.689	-0.069	67.203	1.00	25.56	AAAA	C
ATOH	1714	CD2	TRP	176	32.588	1.186	66.480	1.00	23.71	AAAA	C
ATOH	1715	CE2	TRP	176	32.559	2.217	67.422	1.00	32.40	AAAA	C
ATOH	1716	CE3	TRP	176	32.535	1.520	65.141	1.00	24.31	AAAA	C
ATOH	1717	CD1	TRP	176	32.730	0.257	68.525	1.00	28.37	AAAA	C
ATOH	1718	HE1	TRP	176	32.636	1.636	68.678	1.00	37.21	AAAA	H
ATOH	1720	CD2	TRP	176	32.441	3.565	67.088	1.00	28.51	AAAA	C
ATOH	1721	CE3	TRP	176	32.447	2.822	64.789	1.00	22.23	AAAA	C
ATOH	1722	CH2	TRP	176	32.406	3.817	65.745	1.00	29.51	AAAA	C
ATOH	1723	C	TRP	176	31.631	-3.268	65.409	1.00	39.30	AAAA	C
ATOH	1724	O	TRP	176	31.703	-3.121	64.199	1.00	39.15	AAAA	O
ATOH	1725	H	THR	177	31.682	-4.460	66.005	1.00	41.33	AAAA	H
ATOH	1728	CA	THR	177	31.964	-5.644	65.161	1.00	49.28	AAAA	C
ATOH	1729	OG1	THR	177	33.480	-6.062	65.162	1.00	43.66	AAAA	C
ATOH	1731	CG2	THR	177	34.309	-5.025	64.613	1.00	47.85	AAAA	O
ATOH	1732	C	THR	177	33.676	-7.271	64.283	1.00	58.51	AAAA	C
ATOH	1733	O	THR	177	31.290	-6.814	65.859	1.00	48.76	AAAA	C
ATOH	1734	H	THR	178	30.982	-6.539	67.001	1.00	51.53	AAAA	O
ATOH	1736	CA	THR	178	31.269	-8.000	65.331	1.00	51.96	AAAA	H
ATOH	1737	CB	THR	178	30.924	-9.236	65.946	1.00	58.95	AAAA	C
ATOH	1738	OG1	THR	178	31.253	-10.500	65.092	1.00	66.55	AAAA	C
ATOH	1740	CG2	THR	178	31.505	-10.066	63.734	1.00	75.70	AAAA	O
ATOH	1741	C	THR	178	30.104	-11.489	65.149	1.00	74.23	AAAA	C
ATOH	1742	O	THR	178	31.714	-9.539	67.213	1.00	60.25	AAAA	C
ATOH	1743	H	ASH	179	31.204	-10.102	68.135	1.00	66.05	AAAA	O
ATOH	1745	CA	ASH	179	32.977	-9.130	67.253	1.00	57.56	AAAA	H
ATOH	1746	CB	ASH	179	33.793	-9.392	68.443	1.00	53.39	AAAA	C
ATOH	1747	CG	ASH	179	35.130	-10.024	68.068	1.00	48.46	AAAA	C
ATOH	1748	OD1	ASH	179	34.997	-11.218	67.126	1.00	56.25	AAAA	C
ATOH	1749	HD2	ASH	179	34.412	-12.294	67.555	1.00	51.38	AAAA	O
ATOH	1752	C	ASH	179	35.229	-11.063	65.963	1.00	48.10	AAAA	H
ATOH	1753	O	ASH	179	34.096	-8.120	69.295	1.00	50.78	AAAA	C
ATOH					34.556	-8.377	70.406	1.00	57.97	AAAA	O

18/58

ATOH	1754	H	ARG	180	33.626	-7.022	68.913	1.00	47.06	AAAA	H
ATOH	1756	CA	ARG	180	33.808	-5.820	69.691	1.00	48.25	AAAA	C
ATOH	1757	CB	ARG	180	34.925	-4.962	69.074	1.00	49.72	AAAA	C
ATOH	1758	CG	ARG	180	36.324	-5.501	69.285	1.00	60.92	AAAA	C
ATOH	1759	CD	ARG	180	37.288	-4.948	68.279	1.00	70.83	AAAA	C
ATOH	1760	HE	ARG	180	38.569	-5.605	68.203	1.00	76.18	AAAA	H
ATOH	1762	CE	ARG	180	39.298	-5.895	69.276	1.00	76.59	AAAA	C
ATOH	1763	HH1	ARG	180	38.877	-5.608	70.498	1.00	80.82	AAAA	H
ATOH	1766	HH2	ARG	180	40.474	-6.478	69.180	1.00	79.33	AAAA	H
ATOH	1769	C	ARG	180	32.530	-4.977	69.821	1.00	48.10	AAAA	C
ATOH	1770	O	ARG	180	31.862	-4.476	68.905	1.00	46.99	AAAA	O
ATOH	1771	H	CYS	181	32.230	-4.728	71.063	1.00	44.80	AAAA	H
ATOH	1773	CA	CYS	181	31.199	-3.924	71.619	1.00	45.20	AAAA	C
ATOH	1774	C	CYS	181	31.646	-2.463	71.692	1.00	44.50	AAAA	C
ATOH	1775	O	CYS	181	32.835	-2.227	71.724	1.00	47.09	AAAA	O
ATOH	1776	CB	CYS	181	30.940	-4.282	73.110	1.00	43.88	AAAA	C
ATOH	1777	SG	CYS	181	30.363	-5.944	73.346	1.00	56.08	AAAA	S
ATOH	1778	H	GLU	182	30.659	-1.600	71.690	1.00	39.30	AAAA	H
ATOH	1780	CA	GLU	182	30.948	-0.177	71.690	1.00	43.43	AAAA	C
ATOH	1781	CB	GLU	182	29.749	0.619	71.196	1.00	23.99	AAAA	C
ATOH	1782	CG	GLU	182	29.809	2.085	71.435	1.00	28.57	AAAA	C
ATOH	1783	CD	GLU	182	28.757	2.867	70.733	1.00	29.35	AAAA	C
ATOH	1784	OE1	GLU	182	27.898	2.304	70.033	1.00	38.55	AAAA	O
ATOH	1785	HE2	GLU	182	28.857	4.164	70.912	1.00	28.14	AAAA	H
ATOH	1788	C	GLU	182	31.218	0.089	73.162	1.00	46.07	AAAA	C
ATOH	1789	O	GLU	182	30.458	-0.327	74.041	1.00	47.01	AAAA	O
ATOH	1790	H	LYS	183	32.213	0.866	73.524	1.00	46.98	AAAA	H
ATOH	1792	CA	LYS	183	32.479	1.064	74.934	1.00	45.26	AAAA	C
ATOH	1793	CB	LYS	183	33.966	1.275	75.185	1.00	48.68	AAAA	C
ATOH	1794	CG	LYS	183	34.865	0.267	74.482	1.00	47.95	AAAA	C
ATOH	1795	CD	LYS	183	36.337	0.734	74.523	1.00	48.06	AAAA	C
ATOH	1796	CE	LYS	183	37.178	-0.208	73.684	1.00	46.78	AAAA	C
ATOH	1797	HE	LYS	183	38.499	-0.654	74.158	1.00	44.00	AAAA	H
ATOH	1801	C	LYS	183	31.659	2.205	75.477	1.00	48.13	AAAA	C
ATOH	1802	O	LYS	183	31.679	3.305	74.946	1.00	48.84	AAAA	O
ATOH	1803	H	HET	184	31.165	2.014	76.698	1.00	52.59	AAAA	H
ATOH	1805	CA	HET	184	30.388	3.041	77.413	1.00	53.22	AAAA	C
ATOH	1806	CB	HET	184	28.927	2.613	77.537	1.00	54.27	AAAA	C
ATOH	1807	CG	HET	184	27.855	2.955	76.536	1.00	56.16	AAAA	C
ATOH	1808	SD	HET	184	26.911	1.601	75.912	1.00	57.56	AAAA	S
ATOH	1809	CE	HET	184	26.738	1.855	74.171	1.00	46.57	AAAA	C
ATOH	1810	C	HET	184	31.051	3.200	78.770	1.00	50.55	AAAA	C
ATOH	1811	O	HET	184	31.770	2.292	79.116	1.00	48.82	AAAA	O
ATOH	1812	H	CYS	185	30.796	4.195	79.565	1.00	53.97	AAAA	H
ATOH	1814	CA	CYS	185	31.342	4.365	80.892	1.00	58.63	AAAA	C
ATOH	1815	C	CYS	185	30.297	4.320	81.989	1.00	65.16	AAAA	C
ATOH	1816	O	CYS	185	29.133	4.649	81.761	1.00	65.87	AAAA	O
ATOH	1817	CB	CYS	185	31.965	5.772	81.000	1.00	60.37	AAAA	C
ATOH	1818	SG	CYS	185	33.623	5.771	80.312	1.00	60.09	AAAA	S
ATOH	1819	H	PRO	186	30.688	3.978	83.206	1.00	69.41	AAAA	H
ATOH	1820	CD	PRO	186	32.066	3.777	83.702	1.00	71.11	AAAA	C
ATOH	1821	CA	PRO	186	29.717	3.933	84.304	1.00	69.11	AAAA	C
ATOH	1822	CB	PRO	186	30.523	3.487	85.503	1.00	68.03	AAAA	C
ATOH	1823	CG	PRO	186	31.910	3.920	85.198	1.00	71.02	AAAA	C
ATOH	1824	C	PRO	186	29.120	5.320	84.431	1.00	69.47	AAAA	C
ATOH	1825	O	PRO	186	29.820	6.345	84.507	1.00	65.93	AAAA	O
ATOH	1826	H	SER	187	27.801	5.367	84.546	1.00	68.78	AAAA	H
ATOH	1828	CA	SER	187	27.050	6.592	84.750	1.00	69.29	AAAA	C
ATOH	1829	CB	SER	187	25.594	6.287	85.129	1.00	78.29	AAAA	C
ATOH	1830	CG	SER	187	25.474	4.935	85.566	1.00	91.78	AAAA	O
ATOH	1832	C	SER	187	27.630	7.476	85.836	1.00	67.19	AAAA	C
ATOH	1833	O	SER	187	27.606	8.708	85.803	1.00	63.98	AAAA	O
ATOH	1834	H	THR	188	28.108	6.853	86.908	1.00	68.20	AAAA	H
ATOH	1836	CA	THR	188	28.870	7.507	87.963	1.00	68.39	AAAA	C
ATOH	1837	CB	THR	188	29.805	6.459	88.618	1.00	73.84	AAAA	C
ATOH	1838	OG1	THR	188	28.943	5.365	89.016	1.00	89.33	AAAA	O
ATOH	1840	CG2	THR	188	30.605	7.048	89.759	1.00	73.71	AAAA	C
ATOH	1841	C	THR	188	29.802	8.583	87.429	1.00	67.52	AAAA	C
ATOH	1842	O	THR	188	29.843	9.739	87.834	1.00	68.30	AAAA	O
ATOH	1843	H	CYS	189	30.643	8.247	86.446	1.00	63.89	AAAA	H
ATOH	1845	CA	CYS	189	31.583	9.116	85.917	1.00	57.29	AAAA	C
ATOH	1846	C	CYS	189	30.951	10.331	85.195	1.00	57.70	AAAA	C
ATOH	1847	O	CYS	189	31.648	11.327	85.017	1.00	57.56	AAAA	O
ATOH	1848	CB	CYS	189	32.416	8.372	84.769	1.00	58.67	AAAA	C
ATOH	1849	SG	CYS	189	33.347	7.001	85.535	1.00	53.46	AAAA	S
ATOH	1850	H	GLY	190	29.689	10.322	84.806	1.00	56.91	AAAA	H
ATOH	1852	CA	GLY	190	29.038	11.521	84.323	1.00	57.28	AAAA	C
ATOH	1853	C	GLY	190	29.444	11.834	82.886	1.00	59.62	AAAA	C
ATOH	1854	O	GLY	190	29.609	10.932	82.082	1.00	57.91	AAAA	O
ATOH	1855	H	LYS	191	29.842	13.052	82.624	1.00	62.78	AAAA	H
ATOH	1857	CA	LYS	191	30.359	13.520	81.364	1.00	67.72	AAAA	C
ATOH	1858	CB	LYS	191	30.058	15.035	81.214	1.00	72.76	AAAA	C
ATOH	1859	CG	LYS	191	28.568	15.288	81.002	1.00	84.69	AAAA	C
ATOH	1860	CD	LYS	191	28.207	16.733	80.723	1.00	90.15	AAAA	C
ATOH	1861	CE	LYS	191	26.713	16.806	80.471	1.00	91.85	AAAA	C

19/58

ATOH	1862	HC	LYS	191	26.368	16.182	79.152	1.00	97.62	AAAA	H
ATOH	1866	C	LYS	191	31.868	13.299	91.270	1.00	70.13	AAAA	C
ATOH	1867	O	LYS	191	32.486	13.935	89.415	1.00	71.76	AAAA	O
ATOH	1868	H	ARG	192	32.488	12.441	82.679	1.00	66.29	AAAA	H
ATOH	1870	CA	ARG	192	33.885	12.171	82.044	1.00	59.95	AAAA	C
ATOH	1871	CB	ARG	192	34.505	12.070	83.432	1.00	66.58	AAAA	C
ATOH	1872	CG	ARG	192	34.670	13.400	84.131	1.00	71.59	AAAA	C
ATOH	1873	CD	ARG	192	34.386	13.330	85.625	1.00	73.91	AAAA	C
ATOH	1874	HE	ARG	192	35.622	13.290	86.377	1.00	85.74	AAAA	H
ATOH	1876	CE	ARG	192	35.968	12.407	87.330	1.00	90.67	AAAA	C
ATOH	1877	HH1	ARG	192	35.026	11.486	87.600	1.00	88.49	AAAA	H
ATOH	1880	HH2	ARG	192	37.162	12.463	87.950	1.00	72.95	AAAA	H
ATOH	1883	C	ARG	192	34.221	10.851	91.337	1.00	58.83	AAAA	C
ATOH	1884	O	ARG	192	33.336	10.007	91.176	1.00	55.13	AAAA	O
ATOH	1885	H	ALA	193	35.521	10.795	80.968	1.00	50.19	AAAA	H
ATOH	1887	CA	ALA	193	35.962	9.557	80.355	1.00	46.24	AAAA	C
ATOH	1888	CB	ALA	193	37.167	9.921	79.541	1.00	45.15	AAAA	C
ATOH	1889	C	ALA	193	36.221	8.525	81.451	1.00	48.97	AAAA	C
ATOH	1890	O	ALA	193	36.220	8.908	82.616	1.00	44.80	AAAA	O
ATOH	1891	H	CYS	194	36.544	7.304	81.065	1.00	50.30	AAAA	H
ATOH	1893	CA	CYS	194	36.836	6.302	82.043	1.00	57.50	AAAA	C
ATOH	1894	C	CYS	194	37.834	5.304	81.448	1.00	61.25	AAAA	C
ATOH	1895	O	CYS	194	37.952	5.291	80.216	1.00	61.52	AAAA	O
ATOH	1896	CB	CYS	194	35.510	5.741	82.504	1.00	57.96	AAAA	C
ATOH	1897	SG	CYS	194	34.785	4.524	81.402	1.00	54.49	AAAA	S
ATOH	1898	H	THR	195	38.422	4.499	82.311	1.00	58.51	AAAA	H
ATOH	1900	CA	THR	195	39.462	3.584	81.913	1.00	57.42	AAAA	C
ATOH	1901	CB	THR	195	40.237	3.142	83.188	1.00	65.73	AAAA	C
ATOH	1902	OG1	THR	195	40.288	4.248	84.091	1.00	70.15	AAAA	C
ATOH	1904	OG2	THR	195	41.684	2.864	82.745	1.00	77.91	AAAA	C
ATOH	1905	C	THR	195	38.857	2.404	81.226	1.00	54.59	AAAA	C
ATOH	1906	O	THR	195	37.633	2.315	81.318	1.00	58.75	AAAA	O
ATOH	1907	H	GLU	196	39.610	1.408	80.882	1.00	55.95	AAAA	H
ATOH	1909	CA	GLU	196	39.139	0.145	80.364	1.00	60.07	AAAA	C
ATOH	1910	CB	GLU	196	40.395	-0.612	79.914	1.00	68.06	AAAA	C
ATOH	1911	CG	GLU	196	40.479	-1.146	78.526	1.00	73.96	AAAA	C
ATOH	1912	CD	GLU	196	39.235	-0.983	77.670	1.00	83.08	AAAA	C
ATOH	1913	OE1	GLU	196	38.356	-1.884	77.687	1.00	81.19	AAAA	O
ATOH	1914	OE2	GLU	196	39.060	0.041	76.939	1.00	82.10	AAAA	C
ATOH	1915	C	GLU	196	38.382	-0.579	81.467	1.00	63.91	AAAA	C
ATOH	1916	O	GLU	196	37.690	-1.537	81.159	1.00	63.51	AAAA	O
ATOH	1917	H	ASH	197	38.666	-0.312	82.739	1.00	67.40	AAAA	H
ATOH	1919	CA	ASH	197	38.025	-0.947	83.886	1.00	69.21	AAAA	C
ATOH	1920	CB	ASH	197	39.021	-1.394	84.966	1.00	68.49	AAAA	C
ATOH	1921	CG	ASH	197	39.722	-2.692	84.672	0.01	69.09	AAAA	C
ATOH	1922	OD1	ASH	197	40.364	-3.273	85.551	0.01	69.04	AAAA	O
ATOH	1923	HD2	ASH	197	39.622	-3.183	83.443	0.01	68.97	AAAA	H
ATOH	1926	C	ASH	197	37.033	0.043	84.486	1.00	69.01	AAAA	C
ATOH	1927	O	ASH	197	36.845	0.281	85.664	1.00	68.24	AAAA	O
ATOH	1928	H	ASH	198	36.384	0.795	83.607	1.00	69.91	AAAA	H
ATOH	1930	CA	ASH	198	35.356	1.734	84.048	1.00	68.48	AAAA	C
ATOH	1931	CB	ASH	198	34.120	0.880	84.373	1.00	60.12	AAAA	C
ATOH	1932	CG	ASH	198	33.806	0.095	83.102	1.00	69.29	AAAA	C
ATOH	1933	OD1	ASH	198	33.475	0.654	82.054	1.00	73.20	AAAA	O
ATOH	1934	HD2	ASH	198	33.980	-1.206	83.268	1.00	65.34	AAAA	H
ATOH	1937	C	ASH	198	35.784	2.563	85.228	1.00	64.01	AAAA	C
ATOH	1938	O	ASH	198	34.992	2.827	86.117	1.00	64.20	AAAA	O
ATOH	1939	H	GLU	199	36.955	3.164	85.157	1.00	64.75	AAAA	H
ATOH	1941	CA	GLU	199	37.342	4.054	86.255	1.00	64.64	AAAA	C
ATOH	1942	CB	GLU	199	38.702	3.624	86.744	1.00	66.11	AAAA	C
ATOH	1943	CG	GLU	199	38.846	3.717	88.233	1.00	77.15	AAAA	C
ATOH	1944	CD	GLU	199	39.579	2.532	88.832	1.00	80.24	AAAA	C
ATOH	1945	OE1	GLU	199	39.385	2.406	90.066	1.00	81.65	AAAA	O
ATOH	1946	OE2	GLU	199	40.282	1.821	88.079	1.00	77.94	AAAA	O
ATOH	1947	C	GLU	199	37.314	5.463	85.690	1.00	62.92	AAAA	C
ATOH	1948	O	GLU	199	37.922	5.676	84.632	1.00	63.62	AAAA	O
ATOH	1949	H	CYS	200	36.605	6.393	86.313	1.00	56.16	AAAA	H
ATOH	1951	CA	CYS	200	36.600	7.721	85.740	1.00	55.11	AAAA	C
ATOH	1952	C	CYS	200	37.978	8.315	85.521	1.00	57.77	AAAA	C
ATOH	1953	O	CYS	200	38.884	8.058	86.300	1.00	63.79	AAAA	O
ATOH	1954	CB	CYS	200	35.824	8.664	86.648	1.00	52.70	AAAA	C
ATOH	1955	SG	CYS	200	34.196	8.100	87.098	1.00	55.85	AAAA	S
ATOH	1956	H	CYS	201	38.124	9.192	84.540	1.00	54.50	AAAA	H
ATOH	1958	CA	CYS	201	39.338	9.889	84.202	1.00	48.19	AAAA	C
ATOH	1959	C	CYS	201	39.236	11.287	84.786	1.00	42.34	AAAA	C
ATOH	1960	O	CYS	201	38.165	11.704	85.166	1.00	54.32	AAAA	O
ATOH	1961	CB	CYS	201	39.590	10.070	82.695	1.00	40.90	AAAA	C
ATOH	1962	SG	CYS	201	39.644	8.597	81.747	1.00	51.42	AAAA	S
ATOH	1963	H	HIS	202	40.254	12.075	84.675	1.00	39.12	AAAA	H
ATOH	1965	CA	HIS	202	40.290	13.461	85.128	1.00	41.55	AAAA	C
ATOH	1966	C	HIS	202	39.284	14.184	84.289	1.00	46.59	AAAA	C
ATOH	1967	O	HIS	202	39.176	13.851	83.103	1.00	51.64	AAAA	O
ATOH	1968	CB	HIS	202	41.712	13.952	84.810	1.00	45.20	AAAA	C
ATOH	1969	CG	HIS	202	41.996	15.330	85.267	1.00	38.71	AAAA	C
ATOH	1970	HD1	HIS	202	41.501	16.404	84.550	1.00	51.32	AAAA	H

20/58

ATOH	1971	CE1	HIS	202	41.887	17.528	85.178	1.00	47.62	AAAA	C
ATOH	1972	CE2	HIS	202	42.665	15.813	86.340	1.00	39.59	AAAA	C
ATOH	1973	HE2	HIS	202	42.563	17.207	86.258	1.00	43.48	AAAA	H
ATOH	1975	H	PRO	203	38.738	15.293	84.711	1.00	47.74	AAAA	H
ATOH	1976	CD	PRO	203	38.758	15.840	86.082	1.00	46.97	AAAA	C
ATOH	1977	CA	PRO	203	37.780	15.987	83.879	1.00	46.44	AAAA	C
ATOH	1978	CB	PRO	203	37.248	17.107	84.742	1.00	39.47	AAAA	C
ATOH	1979	CG	PRO	203	38.131	17.210	85.910	1.00	43.37	AAAA	C
ATOH	1980	C	PRO	203	38.440	16.519	82.607	1.00	53.27	AAAA	C
ATOH	1981	O	PRO	203	37.698	17.045	81.731	1.00	53.16	AAAA	O
ATOH	1982	H	GLU	204	39.792	16.535	82.561	1.00	50.34	AAAA	H
ATOH	1984	CA	GLU	204	40.439	17.139	81.381	1.00	50.52	AAAA	C
ATOH	1985	CB	GLU	204	41.727	17.891	81.804	1.00	48.58	AAAA	C
ATOH	1986	CG	GLU	204	41.397	19.251	82.397	1.00	43.74	AAAA	C
ATOH	1987	CD	GLU	204	40.778	20.282	81.501	1.00	55.26	AAAA	C
ATOH	1988	OE1	GLU	204	40.766	20.344	80.248	1.00	64.04	AAAA	O
ATOH	1989	OE2	GLU	204	40.226	21.198	82.141	1.00	57.66	AAAA	O
ATOH	1990	C	GLU	204	40.718	16.084	80.319	1.00	45.71	AAAA	C
ATOH	1991	O	GLU	204	41.238	16.405	79.251	1.00	46.56	AAAA	O
ATOH	1992	H	CYS	205	40.612	14.830	80.735	1.00	42.05	AAAA	H
ATOH	1994	CA	CYS	205	40.997	13.764	79.838	1.00	45.81	AAAA	C
ATOH	1995	C	CYS	205	39.892	13.628	78.819	1.00	49.20	AAAA	C
ATOH	1996	O	CYS	205	38.746	13.920	79.133	1.00	50.34	AAAA	O
ATOH	1997	CB	CYS	205	41.288	12.491	80.572	1.00	51.55	AAAA	C
ATOH	1998	SG	CYS	205	42.923	12.246	81.251	1.00	52.89	AAAA	S
ATOH	1999	H	LEU	206	40.232	13.579	77.520	1.00	49.68	AAAA	H
ATOH	2001	CA	LEU	206	39.169	13.446	76.533	1.00	41.49	AAAA	C
ATOH	2002	CB	LEU	206	39.266	14.505	75.462	1.00	48.66	AAAA	C
ATOH	2003	CG	LEU	206	38.274	14.365	74.305	1.00	47.45	AAAA	C
ATOH	2004	CD	LEU	206	36.879	14.243	74.895	1.00	45.79	AAAA	C
ATOH	2005	CE2	LEU	206	38.331	15.599	73.420	1.00	50.71	AAAA	C
ATOH	2006	C	LEU	206	39.310	12.109	75.912	1.00	38.44	AAAA	C
ATOH	2007	O	LEU	206	40.400	11.568	75.813	1.00	36.59	AAAA	O
ATOH	2008	H	GLY	207	38.264	11.359	75.681	1.00	42.41	AAAA	H
ATOH	2010	CA	GLY	207	38.403	10.098	74.978	1.00	40.57	AAAA	C
ATOH	2011	C	GLY	207	38.466	9.061	76.058	1.00	47.15	AAAA	C
ATOH	2012	O	GLY	207	37.668	8.102	76.057	1.00	45.04	AAAA	O
ATOH	2013	H	SER	208	39.622	9.079	76.760	1.00	50.36	AAAA	H
ATOH	2015	CA	SER	208	39.832	7.898	77.660	1.00	48.27	AAAA	C
ATOH	2016	CB	SER	208	39.909	6.631	76.787	1.00	35.77	AAAA	C
ATOH	2017	CG	SER	208	40.600	5.597	77.461	1.00	61.34	AAAA	O
ATOH	2019	C	SER	208	41.144	8.068	78.377	1.00	49.17	AAAA	C
ATOH	2020	O	SER	208	41.781	9.084	78.163	1.00	48.24	AAAA	O
ATOH	2021	H	CYS	209	41.599	7.123	79.189	1.00	52.04	AAAA	H
ATOH	2023	CA	CYS	209	42.824	7.307	79.964	1.00	55.98	AAAA	C
ATOH	2024	C	CYS	209	43.453	6.035	80.484	1.00	57.41	AAAA	C
ATOH	2025	O	CYS	209	42.862	4.963	80.423	1.00	58.33	AAAA	O
ATOH	2026	CB	CYS	209	42.629	8.258	81.146	1.00	52.51	AAAA	C
ATOH	2027	SG	CYS	209	41.380	7.602	82.261	1.00	58.22	AAAA	S
ATOH	2028	H	SER	210	44.734	6.145	80.883	1.00	59.37	AAAA	H
ATOH	2030	CA	SER	210	45.506	4.950	81.318	1.00	58.10	AAAA	C
ATOH	2031	CP	SER	210	47.022	5.083	81.105	1.00	55.07	AAAA	C
ATOH	2032	CG	SER	210	47.546	6.204	81.818	1.00	64.49	AAAA	O
ATOH	2034	C	SER	210	45.331	4.713	82.826	1.00	56.34	AAAA	C
ATOH	2035	O	SER	210	45.529	3.614	83.326	1.00	54.42	AAAA	O
ATOH	2036	H	ALA	211	45.105	5.806	83.548	1.00	52.79	AAAA	H
ATOH	2038	CA	ALA	211	44.980	5.684	85.004	1.00	56.60	AAAA	C
ATOH	2039	CB	ALA	211	46.333	5.926	85.649	1.00	63.41	AAAA	C
ATOH	2040	C	ALA	211	43.962	6.747	85.395	1.00	56.58	AAAA	C
ATOH	2041	O	ALA	211	43.957	7.792	84.711	1.00	50.78	AAAA	O
ATOH	2042	H	PRO	212	43.117	6.416	86.359	1.00	55.93	AAAA	H
ATOH	2043	CD	PRO	212	43.042	5.166	87.115	1.00	55.86	AAAA	C
ATOH	2044	CA	PRO	212	41.951	7.257	86.575	1.00	55.50	AAAA	C
ATOH	2045	CB	PRO	212	41.104	6.470	87.556	1.00	59.65	AAAA	C
ATOH	2046	CG	PRO	212	42.021	5.483	88.175	1.00	54.56	AAAA	C
ATOH	2047	C	PRO	212	42.409	8.535	87.177	1.00	53.64	AAAA	C
ATOH	2048	O	PRO	212	43.611	8.725	87.393	1.00	57.46	AAAA	O
ATOH	2049	H	ALA	213	41.537	9.492	87.347	1.00	53.87	AAAA	H
ATOH	2051	CA	ALA	213	41.912	10.710	88.057	1.00	59.41	AAAA	C
ATOH	2052	CB	ALA	213	41.783	10.255	89.541	1.00	66.40	AAAA	C
ATOH	2053	C	ALA	213	43.289	11.300	87.907	1.00	61.40	AAAA	C
ATOH	2054	O	ALA	213	43.728	12.202	89.652	1.00	60.03	AAAA	O
ATOH	2055	H	ASH	214	44.068	10.999	86.899	1.00	64.80	AAAA	H
ATOH	2057	CA	ASH	214	45.366	11.551	86.596	1.00	63.36	AAAA	C
ATOH	2063	C	ASH	214	45.300	12.284	85.251	1.00	61.56	AAAA	C
ATOH	2064	O	ASH	214	45.198	11.794	84.117	1.00	58.38	AAAA	O
ATOH	2058	CB	ASH	214	46.336	10.379	86.608	1.00	67.32	AAAA	C
ATOH	2059	CG	ASH	214	47.697	10.896	86.362	1.00	75.48	AAAA	C
ATOH	2060	OD1	ASH	214	48.254	11.105	85.302	1.00	83.64	AAAA	O
ATOH	2061	HD2	ASH	214	48.513	11.170	87.427	1.00	90.05	AAAA	H
ATOH	2065	H	ASP	215	45.666	13.565	85.305	1.00	59.78	AAAA	H
ATOH	2067	CA	ASP	215	45.618	14.432	84.143	1.00	56.47	AAAA	C
ATOH	2068	CB	ASP	215	45.430	15.926	84.446	1.00	40.19	AAAA	C
ATOH	2069	CG	ASP	215	46.671	16.543	84.986	1.00	56.36	AAAA	C
ATOH	2070	OD1	ASP	215	46.590	17.699	85.473	1.00	56.17	AAAA	O

21/58

ATOH	2071	OD2	ASP	215	47.768	15.826	84.941	1.00	50.51	AAAA	O
ATOH	2072	O	ASP	215	46.818	14.315	83.221	1.00	53.70	AAAA	O
ATOH	2073	O	ASP	215	46.998	15.148	82.322	1.00	53.58	AAAA	O
ATOH	2074	H	THR	216	47.719	13.425	83.511	1.00	50.87	AAAA	H
ATOH	2076	CA	THR	216	48.883	13.114	82.734	1.00	45.76	AAAA	C
ATOH	2077	CB	THR	216	50.201	13.176	83.529	1.00	53.46	AAAA	C
ATOH	2078	CG1	THR	216	50.403	11.977	84.335	1.00	45.14	AAAA	O
ATOH	2080	CG2	THR	216	50.436	14.314	84.518	1.00	41.30	AAAA	O
ATOH	2081	O	THR	216	48.681	11.712	82.158	1.00	48.34	AAAA	C
ATOH	2082	O	THR	216	49.596	11.282	81.444	1.00	47.49	AAAA	O
ATOH	2083	H	ALA	217	47.559	11.057	82.476	1.00	49.65	AAAA	H
ATOH	2085	CA	ALA	217	47.259	9.760	81.845	1.00	51.83	AAAA	C
ATOH	2086	CB	ALA	217	46.908	8.775	82.943	1.00	52.62	AAAA	C
ATOH	2087	O	ALA	217	46.207	9.747	80.709	1.00	50.60	AAAA	C
ATOH	2088	O	ALA	217	45.775	8.632	80.335	1.00	49.13	AAAA	O
ATOH	2089	H	CYS	218	45.744	10.905	80.226	1.00	43.56	AAAA	H
ATOH	2091	CA	CYS	218	44.802	11.030	79.157	1.00	48.09	AAAA	C
ATOH	2092	O	CYS	218	45.166	10.331	77.869	1.00	47.06	AAAA	C
ATOH	2093	O	CYS	218	46.300	9.967	77.642	1.00	55.57	AAAA	O
ATOH	2094	CB	CYS	218	44.536	12.501	78.775	1.00	51.54	AAAA	C
ATOH	2095	SG	CYS	218	44.256	13.494	80.302	1.00	56.98	AAAA	S
ATOH	2096	H	VAL	219	44.226	10.085	75.978	1.00	43.40	AAAA	H
ATOH	2098	CA	VAL	219	44.575	9.547	75.654	1.00	35.22	AAAA	C
ATOH	2099	CB	VAL	219	43.693	8.427	75.242	1.00	32.26	AAAA	C
ATOH	2100	CG1	VAL	219	43.952	7.873	73.886	1.00	36.19	AAAA	C
ATOH	2101	CG2	VAL	219	43.811	7.144	76.071	1.00	45.51	AAAA	C
ATOH	2102	O	VAL	219	44.453	10.750	74.735	1.00	32.06	AAAA	C
ATOH	2103	O	VAL	219	45.303	10.897	73.874	1.00	42.27	AAAA	O
ATOH	2104	H	ALA	220	43.728	11.759	75.167	1.00	24.24	AAAA	H
ATOH	2106	CA	ALA	220	43.630	12.985	74.385	1.00	27.09	AAAA	C
ATOH	2107	CB	ALA	220	42.536	12.919	73.331	1.00	28.42	AAAA	C
ATOH	2108	O	ALA	220	43.292	14.071	75.390	1.00	29.21	AAAA	C
ATOH	2109	O	ALA	220	42.846	13.604	76.455	1.00	37.88	AAAA	O
ATOH	2110	H	CYS	221	43.285	15.334	75.058	1.00	30.27	AAAA	H
ATOH	2112	CA	CYS	221	42.753	16.382	75.875	1.00	35.55	AAAA	C
ATOH	2113	O	CYS	221	41.460	17.055	75.452	1.00	47.06	AAAA	C
ATOH	2114	O	CYS	221	41.265	17.598	74.368	1.00	49.57	AAAA	O
ATOH	2115	CB	CYS	221	43.804	17.478	76.063	1.00	47.45	AAAA	C
ATOH	2116	SG	CYS	221	45.494	16.935	76.538	1.00	47.06	AAAA	S
ATOH	2117	H	ARG	222	40.503	17.133	76.396	1.00	51.47	AAAA	H
ATOH	2119	CA	ARG	222	39.291	17.906	76.338	1.00	51.86	AAAA	C
ATOH	2120	CB	ARG	222	38.647	18.074	77.712	1.00	54.53	AAAA	C
ATOH	2121	CG	ARG	222	37.314	18.687	77.854	1.00	45.56	AAAA	C
ATOH	2122	CD	ARG	222	36.538	18.338	79.087	1.00	54.45	AAAA	C
ATOH	2123	HE	ARG	222	36.272	16.947	79.269	1.00	65.53	AAAA	H
ATOH	2125	CG	ARG	222	35.534	16.080	78.617	1.00	67.60	AAAA	C
ATOH	2126	HH1	ARG	222	34.925	16.599	77.533	1.00	70.26	AAAA	H
ATOH	2129	HH2	ARG	222	35.342	14.780	78.901	1.00	54.11	AAAA	H
ATOH	2132	O	ARG	222	39.562	19.286	75.740	1.00	50.66	AAAA	O
ATOH	2133	O	ARG	222	38.737	19.845	75.009	1.00	58.34	AAAA	O
ATOH	2134	H	HIS	223	40.556	19.981	76.120	1.00	45.65	AAAA	H
ATOH	2136	CA	HIS	223	40.988	21.291	75.921	1.00	46.93	AAAA	C
ATOH	2137	CB	HIS	223	41.057	22.251	77.011	1.00	49.51	AAAA	C
ATOH	2138	CG	HIS	223	39.710	22.344	77.647	1.00	58.83	AAAA	C
ATOH	2139	CD2	HIS	223	38.820	23.360	77.556	1.00	61.08	AAAA	C
ATOH	2140	HD1	HIS	223	39.082	21.388	78.425	1.00	63.28	AAAA	H
ATOH	2142	CE1	HIS	223	37.881	21.815	78.759	1.00	58.01	AAAA	C
ATOH	2143	HE2	HIS	223	37.681	23.010	78.232	1.00	48.56	AAAA	H
ATOH	2145	O	HIS	223	42.363	21.260	75.122	1.00	50.78	AAAA	C
ATOH	2146	O	HIS	223	42.506	20.753	74.003	1.00	47.43	AAAA	O
ATOH	2147	H	TYR	224	43.359	21.847	75.769	1.00	49.20	AAAA	H
ATOH	2149	CA	TYR	224	44.712	21.992	75.259	1.00	48.17	AAAA	C
ATOH	2150	CB	TYR	224	45.144	23.430	75.426	1.00	44.07	AAAA	C
ATOH	2151	CG	TYR	224	44.318	24.234	74.417	1.00	51.77	AAAA	C
ATOH	2152	CD1	TYR	224	43.193	24.869	74.904	1.00	48.94	AAAA	C
ATOH	2153	CE1	TYR	224	42.401	25.633	74.089	1.00	48.41	AAAA	C
ATOH	2154	CD2	TYR	224	44.623	24.358	73.065	1.00	54.82	AAAA	C
ATOH	2155	CE2	TYR	224	43.847	25.131	72.233	1.00	56.09	AAAA	C
ATOH	2156	CG	TYR	224	42.739	25.745	72.766	1.00	54.23	AAAA	C
ATOH	2157	OH	TYR	224	41.915	26.522	72.017	1.00	61.70	AAAA	O
ATOH	2159	O	TYR	224	45.725	21.095	75.892	1.00	48.19	AAAA	C
ATOH	2160	O	TYR	224	45.776	20.913	77.111	1.00	55.75	AAAA	O
ATOH	2161	H	TYR	225	46.584	20.514	75.077	1.00	48.79	AAAA	H
ATOH	2163	CA	TYR	225	47.655	19.653	75.555	1.00	43.02	AAAA	C
ATOH	2164	CB	TYR	225	48.020	18.639	74.548	1.00	42.32	AAAA	C
ATOH	2165	CG	TYR	225	49.286	17.926	74.954	1.00	46.95	AAAA	C
ATOH	2166	CD1	TYR	225	49.299	16.858	75.817	1.00	43.57	AAAA	C
ATOH	2167	CE1	TYR	225	50.450	16.221	76.173	1.00	47.26	AAAA	C
ATOH	2168	CD2	TYR	225	50.487	18.407	74.421	1.00	52.82	AAAA	C
ATOH	2169	CE2	TYR	225	51.656	17.791	74.781	1.00	53.94	AAAA	C
ATOH	2170	CG	TYR	225	51.639	16.707	75.644	1.00	52.31	AAAA	C
ATOH	2171	OH	TYR	225	52.886	16.186	75.905	1.00	50.71	AAAA	O
ATOH	2173	O	TYR	225	48.872	20.507	75.793	1.00	47.13	AAAA	C
ATOH	2174	O	TYR	225	49.060	21.514	75.150	1.00	53.97	AAAA	O
ATOH	2175	H	TYR	226	49.634	20.253	76.821	1.00	56.84	AAAA	H

22/58

ATOH	2177	CA	TYR	226	50.814	21.601	77.172	1.00	56.83	AAAA	T
ATOH	2178	CB	TYR	226	50.455	22.343	77.785	1.00	59.51	AAAA	C
ATOH	2179	CG	TYR	226	51.741	23.126	77.941	1.00	65.45	AAAA	C
ATOH	2180	CD1	TYR	226	52.121	23.557	79.197	1.00	69.12	AAAA	C
ATOH	2181	CE1	TYR	226	53.289	24.275	79.400	1.00	70.77	AAAA	C
ATOH	2182	CD2	TYR	226	52.580	23.409	76.864	1.00	69.38	AAAA	C
ATOH	2183	CE2	TYR	226	53.758	24.118	77.020	1.00	70.94	AAAA	C
ATOH	2184	CH	TYR	226	54.099	24.549	78.301	1.00	72.96	AAAA	C
ATOH	2185	OH	TYR	226	55.267	25.254	78.435	1.00	70.84	AAAA	O
ATOH	2187	C	TYR	226	51.784	20.356	78.165	1.00	57.55	AAAA	C
ATOH	2188	O	TYR	226	51.492	20.133	79.350	1.00	56.90	AAAA	O
ATOH	2189	H	ALA	227	52.978	20.080	77.642	1.00	53.82	AAAA	H
ATOH	2191	CA	ALA	227	54.061	19.557	79.440	1.00	51.82	AAAA	C
ATOH	2192	CB	ALA	227	54.528	20.620	79.428	1.00	55.81	AAAA	C
ATOH	2193	C	ALA	227	53.600	18.309	79.170	1.00	53.56	AAAA	C
ATOH	2194	O	ALA	227	53.663	18.218	80.413	1.00	49.63	AAAA	O
ATOH	2195	H	GLY	228	53.076	17.360	78.393	1.00	50.68	AAAA	H
ATOH	2197	CA	GLY	228	52.585	16.135	79.028	1.00	49.02	AAAA	C
ATOH	2198	C	GLY	228	51.312	16.330	79.861	1.00	51.61	AAAA	C
ATOH	2199	O	GLY	228	51.028	15.538	80.776	1.00	51.10	AAAA	O
ATOH	2200	H	VAL	229	50.643	17.495	79.791	1.00	47.09	AAAA	H
ATOH	2202	CA	VAL	229	49.489	17.671	80.635	1.00	51.11	AAAA	C
ATOH	2203	CB	VAL	229	49.908	18.610	81.774	1.00	56.52	AAAA	C
ATOH	2204	CG1	VAL	229	48.627	18.896	82.566	1.00	38.39	AAAA	C
ATOH	2205	CG2	VAL	229	51.002	18.035	82.682	1.00	50.16	AAAA	C
ATOH	2206	C	VAL	229	48.255	18.173	79.873	1.00	51.37	AAAA	C
ATOH	2207	O	VAL	229	48.344	19.279	79.309	1.00	53.71	AAAA	O
ATOH	2208	H	CYS	230	47.100	17.518	80.036	1.00	42.21	AAAA	H
ATOH	2210	CA	CYS	230	45.881	18.117	79.471	1.00	40.32	AAAA	C
ATOH	2211	C	CYS	230	45.456	19.350	80.228	1.00	38.42	AAAA	C
ATOH	2212	O	CYS	230	44.964	19.248	81.321	1.00	41.62	AAAA	O
ATOH	2213	CB	CYS	230	44.746	17.132	79.370	1.00	31.54	AAAA	C
ATOH	2214	SG	CYS	230	45.149	15.753	78.266	1.00	43.61	AAAA	S
ATOH	2215	H	VAL	231	45.637	20.534	79.731	1.00	39.83	AAAA	H
ATOH	2217	CA	VAL	231	45.445	21.769	80.462	1.00	46.57	AAAA	C
ATOH	2218	CB	VAL	231	46.618	22.736	80.088	1.00	50.99	AAAA	C
ATOH	2219	CG1	VAL	231	46.798	23.878	81.053	1.00	50.41	AAAA	C
ATOH	2220	CG2	VAL	231	47.838	21.913	80.506	1.00	44.95	AAAA	C
ATOH	2221	C	VAL	231	44.111	22.321	80.057	1.00	52.59	AAAA	C
ATOH	2222	O	VAL	231	43.599	22.183	78.936	1.00	55.30	AAAA	O
ATOH	2223	H	PRO	232	43.482	23.105	80.913	1.00	54.28	AAAA	H
ATOH	2224	CD	PRO	232	43.830	23.385	82.320	1.00	54.25	AAAA	C
ATOH	2225	CA	PRO	232	42.153	23.625	80.575	1.00	54.39	AAAA	C
ATOH	2226	CB	PRO	232	41.537	23.877	81.928	1.00	53.73	AAAA	C
ATOH	2227	CG	PRO	232	42.683	24.287	82.765	1.00	55.00	AAAA	C
ATOH	2228	C	PRO	232	42.361	24.913	79.795	1.00	56.37	AAAA	C
ATOH	2229	O	PRO	232	41.498	25.482	79.137	1.00	55.79	AAAA	O
ATOH	2230	H	ALA	233	43.615	25.400	79.901	1.00	54.76	AAAA	H
ATOH	2232	CA	ALA	233	43.998	26.569	79.124	1.00	49.93	AAAA	C
ATOH	2233	CB	ALA	233	43.440	27.807	79.746	1.00	35.43	AAAA	C
ATOH	2234	C	ALA	233	45.502	26.662	78.974	1.00	49.79	AAAA	C
ATOH	2235	O	ALA	233	46.195	25.879	79.616	1.00	51.41	AAAA	O
ATOH	2236	H	CYS	234	45.984	27.508	78.072	1.00	45.07	AAAA	H
ATOH	2238	CA	CYS	234	47.430	27.518	77.907	1.00	48.63	AAAA	C
ATOH	2239	C	CYS	234	48.001	28.340	79.076	1.00	50.93	AAAA	C
ATOH	2240	O	CYS	234	47.650	29.513	79.250	1.00	47.57	AAAA	O
ATOH	2241	CB	CYS	234	47.816	28.034	76.511	1.00	43.10	AAAA	C
ATOH	2242	SG	CYS	234	47.608	26.789	75.226	1.00	43.04	AAAA	S
ATOH	2243	H	PRO	235	49.127	27.853	79.599	1.00	49.55	AAAA	H
ATOH	2244	CD	PRO	235	49.692	26.557	79.207	1.00	48.75	AAAA	C
ATOH	2245	CA	PRO	235	49.911	28.569	80.599	1.00	51.69	AAAA	C
ATOH	2246	CB	PRO	235	50.984	27.581	80.975	1.00	50.80	AAAA	C
ATOH	2247	CG	PRO	235	50.912	26.417	80.077	1.00	50.06	AAAA	C
ATOH	2248	C	PRO	235	50.487	29.852	80.050	1.00	57.11	AAAA	C
ATOH	2249	O	PRO	235	50.848	29.957	78.870	1.00	59.60	AAAA	O
ATOH	2250	H	PRO	236	50.676	30.875	80.887	1.00	59.85	AAAA	H
ATOH	2251	CD	PRO	236	50.405	30.822	82.363	1.00	55.85	AAAA	C
ATOH	2252	CA	PRO	236	51.323	32.143	80.493	1.00	52.27	AAAA	C
ATOH	2253	CB	PRO	236	51.695	32.814	81.826	1.00	53.62	AAAA	C
ATOH	2254	CG	PRO	236	50.652	32.277	82.754	1.00	56.73	AAAA	C
ATOH	2255	C	PRO	236	52.545	31.886	79.671	1.00	44.21	AAAA	C
ATOH	2256	O	PRO	236	53.219	30.892	79.928	1.00	43.40	AAAA	O
ATOH	2257	H	ASH	237	52.837	32.757	78.716	1.00	46.54	AAAA	H
ATOH	2259	CA	ASH	237	53.895	32.623	77.716	1.00	45.94	AAAA	C
ATOH	2260	CB	ASH	237	55.259	32.653	78.456	1.00	58.65	AAAA	C
ATOH	2261	CG	ASH	237	55.357	33.855	79.371	1.00	58.51	AAAA	C
ATOH	2262	OD1	ASH	237	56.044	33.783	80.379	1.00	72.25	AAAA	O
ATOH	2263	HD2	ASH	237	54.631	34.910	79.051	1.00	62.99	AAAA	H
ATOH	2266	C	ASH	237	53.897	31.425	76.788	1.00	46.87	AAAA	C
ATOH	2267	O	ASH	237	54.962	30.935	76.325	1.00	54.50	AAAA	O
ATOH	2268	H	THR	238	52.617	30.657	76.692	1.00	42.91	AAAA	H
ATOH	2270	CA	THR	238	52.617	29.567	75.780	1.00	40.20	AAAA	C
ATOH	2271	CB	THR	238	52.461	28.248	76.466	1.00	42.62	AAAA	C
ATOH	2272	CG1	THR	238	51.227	28.343	77.237	1.00	50.88	AAAA	O
ATOH	2274	CG2	THR	238	53.552	27.886	77.424	1.00	34.84	AAAA	C

23/58

ATOH	2275	C	THR	238	51.279	29.875	75.678	1.00	42.59	AAAA	C
ATOH	2276	O	THR	238	50.569	30.864	75.509	1.00	42.51	AAAA	O
ATOH	2277	H	TYR	239	51.051	29.480	73.832	1.00	42.62	AAAA	H
ATOH	2279	CA	TYR	239	49.949	29.959	73.024	1.00	41.87	AAAA	C
ATOH	2280	CB	TYR	239	50.457	30.907	71.931	1.00	44.86	AAAA	C
ATOH	2281	CG	TYR	239	51.099	32.125	72.564	1.00	42.05	AAAA	C
ATOH	2282	CD1	TYR	239	52.467	32.086	72.815	1.00	39.41	AAAA	C
ATOH	2283	CE1	TYR	239	53.092	33.152	73.415	1.00	43.27	AAAA	C
ATOH	2284	CD2	TYR	239	50.376	33.230	72.923	1.00	44.15	AAAA	C
ATOH	2285	CE2	TYR	239	50.972	34.310	73.536	1.00	46.22	AAAA	C
ATOH	2286	CS	TYR	239	52.339	34.243	73.779	1.00	50.49	AAAA	C
ATOH	2287	OH	TYR	239	53.013	35.289	74.387	1.00	55.47	AAAA	O
ATOH	2289	C	TYR	239	19.232	28.813	72.315	1.00	45.54	AAAA	C
ATOH	2290	O	TYR	239	49.922	27.810	72.021	1.00	46.66	AAAA	O
ATOH	2291	H	ARG	240	47.895	28.990	72.126	1.00	40.62	AAAA	H
ATOH	2293	CA	ARG	240	47.177	27.892	71.426	1.00	38.78	AAAA	C
ATOH	2294	CB	ARG	240	45.675	28.127	71.452	1.00	39.77	AAAA	C
ATOH	2295	CG	ARG	240	45.116	28.944	72.588	1.00	43.37	AAAA	C
ATOH	2296	CD	ARG	240	43.573	28.957	72.683	1.00	38.60	AAAA	C
ATOH	2297	HE	ARG	240	43.114	29.683	71.455	1.00	53.98	AAAA	H
ATOH	2299	CS	ARG	240	43.123	31.015	71.530	1.00	48.07	AAAA	C
ATOH	2300	HH1	ARG	240	43.513	31.562	72.668	1.00	47.65	AAAA	H
ATOH	2303	HH2	ARG	240	42.788	31.778	70.533	1.00	51.03	AAAA	H
ATOH	2306	C	ARG	240	47.627	27.737	69.979	1.00	31.72	AAAA	C
ATOH	2307	O	ARG	240	47.937	28.730	69.302	1.00	32.37	AAAA	O
ATOH	2308	H	PHE	241	47.779	26.542	69.549	1.00	27.95	AAAA	H
ATOH	2310	CA	PHE	241	48.182	26.269	68.193	1.00	30.41	AAAA	C
ATOH	2311	CB	PHE	241	49.678	25.940	68.151	1.00	34.83	AAAA	C
ATOH	2312	CG	PHE	241	50.235	25.653	66.773	1.00	26.84	AAAA	C
ATOH	2313	CD1	PHE	241	50.165	26.567	65.753	1.00	25.31	AAAA	C
ATOH	2314	CD2	PHE	241	50.785	24.417	66.573	1.00	27.38	AAAA	C
ATOH	2315	CE1	PHE	241	50.676	26.232	64.509	1.00	37.24	AAAA	C
ATOH	2316	CE2	PHE	241	51.294	24.101	65.320	1.00	38.45	AAAA	C
ATOH	2317	CS	PHE	241	51.281	25.010	64.281	1.00	21.17	AAAA	C
ATOH	2318	C	PHE	241	47.382	25.089	67.621	1.00	35.77	AAAA	C
ATOH	2319	O	PHE	241	47.543	24.013	68.186	1.00	36.77	AAAA	O
ATOH	2320	H	GLU	242	46.738	25.301	66.468	1.00	32.30	AAAA	H
ATOH	2322	CA	GLU	242	45.964	24.269	65.805	1.00	35.43	AAAA	C
ATOH	2323	CB	GLU	242	46.953	23.144	65.472	1.00	37.98	AAAA	C
ATOH	2324	CG	GLU	242	47.867	23.415	64.314	1.00	38.63	AAAA	C
ATOH	2325	CD	GLU	242	47.207	23.965	63.075	1.00	39.27	AAAA	C
ATOH	2326	OE1	GLU	242	46.380	23.205	62.517	1.00	42.79	AAAA	O
ATOH	2327	OE2	GLU	242	47.354	25.109	62.626	1.00	36.36	AAAA	C
ATOH	2328	C	GLU	242	44.752	23.771	66.600	1.00	34.36	AAAA	O
ATOH	2329	O	GLU	242	44.390	22.611	66.511	1.00	28.53	AAAA	O
ATOH	2330	H	GLY	243	44.135	24.589	67.449	1.00	36.94	AAAA	H
ATOH	2332	CA	GLY	243	43.048	24.154	68.303	1.00	34.57	AAAA	C
ATOH	2333	C	GLY	243	43.428	23.107	69.319	1.00	37.76	AAAA	C
ATOH	2334	O	GLY	243	42.474	22.473	69.746	1.00	43.00	AAAA	O
ATOH	2335	H	TRP	244	44.637	22.636	69.611	1.00	39.53	AAAA	H
ATOH	2337	CA	TRP	244	44.797	21.536	70.566	1.00	40.85	AAAA	C
ATOH	2338	CB	TRP	244	44.774	20.271	69.764	1.00	26.76	AAAA	C
ATOH	2339	CG	TRP	244	46.012	19.885	69.028	1.00	43.19	AAAA	C
ATOH	2340	CD2	TRP	244	47.019	18.983	69.498	1.00	39.55	AAAA	C
ATOH	2341	CE2	TRP	244	47.998	18.906	68.489	1.00	36.50	AAAA	C
ATOH	2342	CE3	TRP	244	47.186	18.254	70.692	1.00	32.18	AAAA	C
ATOH	2343	CD1	TRP	244	46.424	20.308	67.779	1.00	43.37	AAAA	C
ATOH	2344	HE1	TRP	244	47.595	19.727	67.469	1.00	38.89	AAAA	H
ATOH	2346	CS2	TRP	244	49.150	18.128	68.620	1.00	39.01	AAAA	C
ATOH	2347	CS3	TRP	244	48.336	17.478	70.815	1.00	43.98	AAAA	C
ATOH	2348	CH2	TRP	244	49.322	17.425	69.784	1.00	42.50	AAAA	C
ATOH	2349	C	TRP	244	45.998	21.517	71.509	1.00	42.98	AAAA	C
ATOH	2350	O	TRP	244	46.253	20.501	72.146	1.00	42.70	AAAA	O
ATOH	2351	H	ARG	245	46.888	22.485	71.435	1.00	44.16	AAAA	H
ATOH	2353	CA	ARG	245	48.168	22.472	72.095	1.00	46.47	AAAA	C
ATOH	2354	CB	ARG	245	49.203	21.602	71.367	1.00	47.30	AAAA	C
ATOH	2355	CG	ARG	245	49.985	22.309	70.203	1.00	48.97	AAAA	C
ATOH	2356	CD	ARG	245	51.129	21.552	69.819	1.00	39.28	AAAA	C
ATOH	2357	HE	ARG	245	51.586	21.665	68.444	1.00	50.86	AAAA	H
ATOH	2359	CS	ARG	245	52.629	21.044	67.895	1.00	46.73	AAAA	C
ATOH	2360	HH1	ARG	245	53.344	20.236	68.653	1.00	50.15	AAAA	H
ATOH	2363	HH2	ARG	245	53.072	21.126	66.638	1.00	41.69	AAAA	H
ATOH	2366	C	ARG	245	48.771	23.863	72.271	1.00	46.01	AAAA	C
ATOH	2367	O	ARG	245	48.394	24.793	71.541	1.00	47.44	AAAA	O
ATOH	2368	H	CYS	246	49.625	23.881	73.317	1.00	42.08	AAAA	H
ATOH	2370	CA	CYS	246	50.246	25.199	73.628	1.00	43.48	AAAA	C
ATOH	2371	C	CYS	246	51.695	25.217	73.183	1.00	43.38	AAAA	C
ATOH	2372	O	CYS	246	52.476	24.239	73.320	1.00	42.51	AAAA	O
ATOH	2373	CB	CYS	246	50.102	25.392	75.138	1.00	48.91	AAAA	C
ATOH	2374	SG	CYS	246	48.386	25.049	75.797	1.00	43.68	AAAA	S
ATOH	2375	H	VAL	247	52.121	26.288	72.564	1.00	41.21	AAAA	H
ATOH	2377	CA	VAL	247	53.417	26.468	71.982	1.00	36.51	AAAA	C
ATOH	2378	CB	VAL	247	53.569	26.357	70.444	1.00	36.87	AAAA	C
ATOH	2379	CG1	VAL	247	53.089	24.988	70.024	1.00	32.71	AAAA	C
ATOH	2380	CG2	VAL	247	53.129	27.602	69.729	1.00	28.20	AAAA	C

24/58

ATOH	2381	C	VAL	247	53.969	27.812	72.373	1.00	39.30	AAAA	C
ATOH	2382	O	VAL	247	53.230	28.770	72.540	1.00	38.80	AAAA	O
ATOH	2383	H	ASP	248	55.291	27.820	72.711	1.00	45.21	AAAA	H
ATOH	2385	CA	ASP	248	55.895	29.115	73.098	1.00	40.19	AAAA	C
ATOH	2386	CB	ASP	248	57.091	28.946	73.953	1.00	42.63	AAAA	C
ATOH	2387	CG	ASP	248	58.126	27.997	73.394	1.00	58.81	AAAA	C
ATOH	2388	OD1	ASP	248	59.067	27.795	74.187	1.00	53.06	AAAA	O
ATOH	2389	OD2	ASP	248	58.167	27.395	72.313	1.00	69.51	AAAA	O
ATOH	2390	C	ASP	248	56.315	29.883	71.839	1.00	36.99	AAAA	C
ATOH	2391	O	ASP	248	56.292	29.288	70.772	1.00	39.70	AAAA	O
ATOH	2392	H	ARG	249	56.545	31.163	71.918	1.00	30.72	AAAA	H
ATOH	2394	CA	ARG	249	56.950	32.057	70.906	1.00	36.17	AAAA	C
ATOH	2395	CB	ARG	249	57.223	33.485	71.491	1.00	21.29	AAAA	C
ATOH	2396	CG	ARG	249	57.594	34.424	70.326	1.00	24.96	AAAA	C
ATOH	2397	CD	ARG	249	57.814	35.811	70.843	1.00	21.23	AAAA	C
ATOH	2398	HE	ARG	249	56.658	36.150	71.689	1.00	39.75	AAAA	H
ATOH	2400	CE	ARG	249	55.632	36.823	71.101	1.00	39.35	AAAA	C
ATOH	2401	HH1	ARG	249	55.642	37.118	69.801	1.00	25.41	AAAA	H
ATOH	2404	HH2	ARG	249	54.641	37.118	71.946	1.00	44.04	AAAA	H
ATOH	2407	C	ARG	249	58.134	31.685	70.010	1.00	40.63	AAAA	C
ATOH	2408	O	ARG	249	58.086	31.923	68.797	1.00	44.79	AAAA	O
ATOH	2409	H	ASP	250	59.149	30.974	70.468	1.00	41.87	AAAA	H
ATOH	2411	CA	ASP	250	60.287	30.739	69.606	1.00	46.90	AAAA	C
ATOH	2412	CB	ASP	250	61.740	30.726	70.154	1.00	53.11	AAAA	C
ATOH	2413	CG	ASP	250	62.421	32.122	70.081	1.00	71.49	AAAA	C
ATOH	2414	OD1	ASP	250	63.124	32.682	69.176	1.00	58.53	AAAA	O
ATOH	2415	OD2	ASP	250	62.272	32.928	71.071	1.00	70.30	AAAA	O
ATOH	2416	C	ASP	250	59.881	29.536	68.771	1.00	41.22	AAAA	C
ATOH	2417	O	ASP	250	60.291	29.443	67.616	1.00	39.06	AAAA	O
ATOH	2418	H	PHE	251	59.116	28.609	69.299	1.00	36.13	AAAA	H
ATOH	2420	CA	PHE	251	58.457	27.601	68.489	1.00	34.88	AAAA	C
ATOH	2421	CB	PHE	251	57.468	26.746	69.256	1.00	29.82	AAAA	C
ATOH	2422	CG	PHE	251	56.701	25.801	68.385	1.00	41.50	AAAA	C
ATOH	2423	CD1	PHE	251	57.101	24.479	68.263	1.00	30.66	AAAA	C
ATOH	2424	CD2	PHE	251	55.559	26.213	67.686	1.00	37.78	AAAA	C
ATOH	2425	CE1	PHE	251	56.414	23.597	67.424	1.00	29.30	AAAA	C
ATOH	2426	CE2	PHE	251	54.847	25.372	66.856	1.00	36.09	AAAA	C
ATOH	2427	CE	PHE	251	55.294	24.070	66.715	1.00	36.21	AAAA	C
ATOH	2428	C	PHE	251	57.624	28.290	67.338	1.00	39.28	AAAA	C
ATOH	2429	O	PHE	251	57.811	28.010	66.144	1.00	30.27	AAAA	O
ATOH	2430	H	CYS	252	56.734	29.225	67.713	1.00	35.13	AAAA	H
ATOH	2432	CA	CYS	252	55.895	29.870	66.728	1.00	38.80	AAAA	C
ATOH	2433	C	CYS	252	56.827	30.598	65.747	1.00	44.73	AAAA	C
ATOH	2434	O	CYS	252	56.552	30.534	64.536	1.00	43.20	AAAA	O
ATOH	2435	CB	CYS	252	54.903	30.778	67.379	1.00	35.65	AAAA	C
ATOH	2436	SG	CYS	252	53.562	21.544	66.459	1.00	39.03	AAAA	S
ATOH	2437	H	ALA	253	57.872	31.256	66.285	1.00	41.53	AAAA	H
ATOH	2439	CA	ALA	253	58.687	32.071	65.415	1.00	40.39	AAAA	C
ATOH	2440	CB	ALA	253	59.529	33.088	66.172	1.00	36.07	AAAA	C
ATOH	2441	C	ALA	253	59.551	31.167	64.539	1.00	42.88	AAAA	C
ATOH	2442	O	ALA	253	60.147	31.735	63.640	1.00	47.42	AAAA	O
ATOH	2443	H	ASH	254	59.657	29.859	64.700	1.00	38.75	AAAA	H
ATOH	2445	CA	ASH	254	60.546	29.073	63.928	1.00	42.94	AAAA	C
ATOH	2446	CB	ASH	254	61.667	28.497	64.847	1.00	48.09	AAAA	C
ATOH	2447	CG	ASH	254	62.696	29.635	65.031	1.00	49.54	AAAA	C
ATOH	2448	OD1	ASH	254	63.468	29.840	64.081	1.00	61.38	AAAA	O
ATOH	2449	ND2	ASH	254	62.607	30.321	66.144	1.00	48.38	AAAA	H
ATOH	2452	C	ASH	254	59.907	27.959	63.135	1.00	53.72	AAAA	C
ATOH	2453	O	ASH	254	60.552	26.965	62.804	1.00	51.19	AAAA	O
ATOH	2454	H	ILE	255	58.612	28.136	62.766	1.00	57.77	AAAA	H
ATOH	2456	CA	ILE	255	57.828	27.107	62.134	1.00	53.28	AAAA	C
ATOH	2457	CB	ILE	255	56.329	27.322	62.304	1.00	50.41	AAAA	C
ATOH	2458	CG2	ILE	255	55.477	26.595	61.246	1.00	51.95	AAAA	C
ATOH	2459	CG1	ILE	255	55.778	26.675	63.553	1.00	40.59	AAAA	C
ATOH	2460	CD1	ILE	255	54.479	27.317	64.006	1.00	38.97	AAAA	C
ATOH	2461	C	ILE	255	58.127	26.886	60.651	1.00	52.62	AAAA	C
ATOH	2462	O	ILE	255	58.196	25.709	60.252	1.00	53.96	AAAA	O
ATOH	2463	H	LEU	256	58.290	27.960	59.918	1.00	49.96	AAAA	H
ATOH	2465	CA	LEU	256	58.680	27.764	58.516	1.00	63.68	AAAA	C
ATOH	2466	CB	LEU	256	58.175	29.012	57.799	1.00	56.80	AAAA	C
ATOH	2467	CG	LEU	256	56.671	29.196	57.864	1.00	59.11	AAAA	C
ATOH	2468	CD1	LEU	256	56.310	30.654	57.645	1.00	43.31	AAAA	C
ATOH	2469	CD2	LEU	256	55.965	29.222	56.928	1.00	55.88	AAAA	C
ATOH	2470	C	LEU	256	60.193	27.622	58.355	1.00	66.23	AAAA	C
ATOH	2471	O	LEU	256	60.691	27.511	57.245	1.00	70.29	AAAA	O
ATOH	2472	H	SER	257	60.942	27.559	59.430	1.00	64.61	AAAA	H
ATOH	2474	CA	SER	257	62.352	27.529	59.534	1.00	69.23	AAAA	C
ATOH	2475	CB	SER	257	62.924	27.318	60.955	1.00	62.45	AAAA	C
ATOH	2476	CG	SER	257	63.381	25.980	61.074	1.00	56.18	AAAA	O
ATOH	2478	C	SER	257	62.973	26.497	58.610	1.00	70.77	AAAA	C
ATOH	2479	O	SER	257	64.127	26.731	59.246	1.00	72.50	AAAA	O
ATOH	2480	H	ALA	258	62.322	25.399	58.300	1.00	74.61	AAAA	H
ATOH	2482	CA	ALA	258	62.933	24.488	57.343	1.00	76.34	AAAA	C
ATOH	2483	CB	ALA	258	62.570	23.039	57.584	1.00	80.82	AAAA	C
ATOH	2484	C	ALA	258	62.663	24.964	55.921	1.00	78.21	AAAA	C

25/58

ATOH	2485	O	ALA	259	62.989	24.139	55.029	1.00	79.60	AAAA	O
ATOH	2486	H	GLU	259	62.969	26.109	55.651	1.00	79.05	AAAA	H
ATOH	2488	CA	GLU	259	61.742	26.621	54.342	1.00	83.84	AAAA	C
ATOH	2489	CB	GLU	259	60.225	26.457	54.135	1.00	86.99	AAAA	C
ATOH	2490	CG	GLU	259	59.687	25.949	54.314	1.00	89.38	AAAA	C
ATOH	2491	CD	GLU	259	58.364	25.032	55.057	1.00	97.77	AAAA	C
ATOH	2492	OE1	GLU	259	58.080	24.088	55.838	1.00	101.45	AAAA	O
ATOH	2493	OE2	GLU	259	57.598	26.002	54.837	1.00	94.58	AAAA	O
ATOH	2494	C	GLU	259	62.117	28.078	54.083	1.00	85.43	AAAA	C
ATOH	2495	O	GLU	259	62.059	29.009	54.903	1.00	88.01	AAAA	O
ATOH	2496	H	SER	260	62.298	28.338	52.799	1.00	84.66	AAAA	H
ATOH	2498	CA	SER	260	62.725	29.625	52.254	1.00	84.03	AAAA	C
ATOH	2499	CB	SER	260	63.753	29.269	51.173	1.00	87.24	AAAA	C
ATOH	2500	CG	SER	260	63.306	29.419	49.835	1.00	93.65	AAAA	O
ATOH	2502	C	SER	260	61.558	30.466	51.789	1.00	80.84	AAAA	C
ATOH	2503	O	SER	260	61.496	30.889	50.635	1.00	81.31	AAAA	O
ATOH	2504	H	SER	261	60.617	30.785	52.685	1.00	78.56	AAAA	H
ATOH	2506	CA	SER	261	59.423	31.540	52.308	1.00	72.13	AAAA	C
ATOH	2507	CB	SER	261	58.179	31.297	53.170	1.00	67.30	AAAA	C
ATOH	2508	CG	SER	261	57.436	30.334	52.451	1.00	74.74	AAAA	C
ATOH	2510	C	SER	261	59.683	33.032	52.318	1.00	66.90	AAAA	C
ATOH	2511	O	SER	261	60.046	33.588	53.334	1.00	63.24	AAAA	O
ATOH	2512	H	ASP	262	59.364	33.659	51.204	1.00	65.30	AAAA	H
ATOH	2515	CA	ASP	262	59.358	35.071	50.915	1.00	58.55	AAAA	C
ATOH	2516	CB	ASP	262	59.268	35.285	49.400	1.00	64.85	AAAA	C
ATOH	2517	CD1	ASP	262	59.389	36.713	48.931	1.00	76.42	AAAA	C
ATOH	2518	OD2	ASP	262	59.473	37.708	49.701	1.00	79.81	AAAA	O
ATOH	2519	C	ASP	262	59.404	36.873	47.671	1.00	80.46	AAAA	C
ATOH	2520	O	ASP	262	58.121	35.706	51.529	1.00	56.88	AAAA	C
ATOH	2521	H	SER	263	57.851	36.918	51.510	1.00	52.48	AAAA	C
ATOH	2523	CA	SER	263	57.259	34.849	52.118	1.00	53.43	AAAA	H
ATOH	2524	CB	SER	263	56.047	35.352	52.734	1.00	52.84	AAAA	C
ATOH	2525	CG	SER	263	55.020	34.245	52.885	1.00	46.60	AAAA	C
ATOH	2527	C	SER	263	55.149	33.348	51.791	1.00	66.80	AAAA	O
ATOH	2528	O	SER	263	56.310	35.965	54.117	1.00	49.52	AAAA	C
ATOH	2529	H	GLU	264	57.396	35.737	54.709	1.00	42.33	AAAA	O
ATOH	2531	CA	GLU	264	55.320	36.783	54.540	1.00	38.93	AAAA	H
ATOH	2532	CB	GLU	264	55.362	37.222	55.921	1.00	36.70	AAAA	C
ATOH	2533	CG	GLU	264	54.359	38.337	56.208	1.00	43.71	AAAA	C
ATOH	2534	CD	GLU	264	54.575	39.482	55.218	1.00	37.74	AAAA	C
ATOH	2535	OE1	GLU	264	55.374	40.632	55.793	1.00	34.36	AAAA	C
ATOH	2536	OE2	GLU	264	55.493	40.600	57.034	1.00	41.55	AAAA	O
ATOH	2537	C	GLU	264	55.832	41.576	55.146	1.00	39.60	AAAA	O
ATOH	2538	O	GLU	264	55.098	36.056	56.827	1.00	35.84	AAAA	C
ATOH	2539	H	GLY	265	54.368	35.151	56.355	1.00	39.60	AAAA	O
ATOH	2541	CA	GLY	265	55.801	35.938	57.962	1.00	35.64	AAAA	H
ATOH	2542	C	GLY	265	55.671	34.690	58.727	1.00	40.30	AAAA	C
ATOH	2543	O	GLY	265	54.622	34.716	59.829	1.00	39.51	AAAA	C
ATOH	2544	H	PHE	266	53.951	35.699	60.135	1.00	37.20	AAAA	O
ATOH	2546	CA	PHE	266	54.537	33.569	60.516	1.00	35.75	AAAA	H
ATOH	2547	CB	PHE	266	53.637	33.434	61.625	1.00	33.70	AAAA	C
ATOH	2548	CG	PHE	266	53.924	32.155	62.396	1.00	28.20	AAAA	C
ATOH	2549	CD1	PHE	266	53.356	30.958	61.671	1.00	37.07	AAAA	C
ATOH	2550	CD2	PHE	266	53.760	30.618	60.377	1.00	34.72	AAAA	C
ATOH	2551	CE1	PHE	266	52.383	30.195	62.313	1.00	25.65	AAAA	C
ATOH	2552	CE2	PHE	266	53.225	29.506	59.760	1.00	37.72	AAAA	C
ATOH	2553	CG	PHE	266	51.879	29.094	61.672	1.00	24.63	AAAA	C
ATOH	2554	C	PHE	266	52.260	28.708	60.402	1.00	23.58	AAAA	C
ATOH	2555	O	PHE	266	53.571	34.570	62.608	1.00	35.82	AAAA	C
ATOH	2556	H	VAL	267	54.446	35.372	62.879	1.00	39.23	AAAA	O
ATOH	2558	CA	VAL	267	52.360	34.763	63.161	1.00	37.10	AAAA	H
ATOH	2559	CB	VAL	267	52.118	35.812	64.113	1.00	36.09	AAAA	C
ATOH	2560	CG1	VAL	267	51.315	36.974	63.567	1.00	39.01	AAAA	C
ATOH	2561	CG2	VAL	267	51.626	37.601	62.220	1.00	31.10	AAAA	C
ATOH	2562	C	VAL	267	49.990	36.400	63.570	1.00	36.88	AAAA	C
ATOH	2563	O	VAL	267	51.506	35.260	65.400	1.00	33.55	AAAA	C
ATOH	2564	H	ILE	268	51.202	34.098	65.515	1.00	32.41	AAAA	O
ATOH	2566	CA	ILE	268	51.539	36.088	66.477	1.00	35.98	AAAA	C
ATOH	2567	CB	ILE	268	50.867	35.573	67.691	1.00	39.79	AAAA	H
ATOH	2568	CG2	ILE	268	51.791	35.232	68.849	1.00	31.17	AAAA	C
ATOH	2569	CG1	ILE	268	50.922	35.253	70.150	1.00	32.66	AAAA	C
ATOH	2570	CD1	ILE	268	52.403	33.866	68.724	1.00	23.56	AAAA	C
ATOH	2571	C	ILE	268	53.421	33.546	69.806	1.00	25.93	AAAA	C
ATOH	2572	O	ILE	268	49.806	36.608	68.060	1.00	42.44	AAAA	C
ATOH	2573	H	HIS	269	50.116	37.767	68.327	1.00	39.99	AAAA	O
ATOH	2575	CA	HIS	269	48.528	36.292	67.864	1.00	44.26	AAAA	H
ATOH	2576	CB	HIS	269	47.491	37.320	68.173	1.00	44.28	AAAA	C
ATOH	2577	CG	HIS	269	46.885	37.876	66.901	1.00	45.48	AAAA	C
ATOH	2578	CD2	HIS	269	45.915	38.986	67.079	1.00	54.33	AAAA	C
ATOH	2579	HD1	HIS	269	44.551	39.014	67.096	1.00	46.61	AAAA	C
ATOH	2581	CE1	HIS	269	46.356	40.280	67.307	1.00	51.86	AAAA	H
ATOH	2582	CE2	HIS	269	45.282	41.057	67.437	1.00	55.17	AAAA	C
ATOH	2584	C	HIS	269	44.175	40.324	67.309	1.00	46.97	AAAA	H
ATOH	2585	O	HIS	269	46.423	36.740	69.074	1.00	45.54	AAAA	C
ATOH	2585	O	HIS	269	46.076	35.552	69.227	1.00	42.94	AAAA	C

26/58

ATOH	2586	H	ASP	270	45.652	37.526	70.059	1.00	49.82	AAAA	H
ATOH	2588	CA	ASP	270	44.948	37.025	71.001	1.00	48.03	AAAA	C
ATOH	2589	CB	ASP	270	43.573	37.014	70.339	1.00	63.63	AAAA	C
ATOH	2590	CG	ASP	270	42.919	38.393	70.294	1.00	80.82	AAAA	C
ATOH	2591	OD1	ASP	270	41.737	38.379	69.835	1.00	90.92	AAAA	O
ATOH	2592	OD2	ASP	270	43.467	39.494	70.652	1.00	86.49	AAAA	O
ATOH	2593	C	ASP	270	45.226	35.667	71.594	1.00	44.66	AAAA	C
ATOH	2594	O	ASP	270	44.357	34.782	71.576	1.00	45.54	AAAA	O
ATOH	2595	H	GLY	271	46.477	35.379	71.924	1.00	41.63	AAAA	H
ATOH	2597	CA	GLY	271	46.839	34.117	72.506	1.00	37.20	AAAA	C
ATOH	2598	C	GLY	271	46.818	32.998	71.537	1.00	39.15	AAAA	C
ATOH	2599	O	GLY	271	46.775	31.865	72.039	1.00	46.56	AAAA	O
ATOH	2600	N	GLU	272	47.015	33.292	70.251	1.00	41.49	AAAA	H
ATOH	2602	CA	GLU	272	47.108	32.092	69.371	1.00	43.56	AAAA	C
ATOH	2603	CB	GLU	272	45.752	31.737	68.876	1.00	37.58	AAAA	C
ATOH	2604	CG	GLU	272	45.778	30.600	67.839	1.00	45.30	AAAA	C
ATOH	2605	CD	GLU	272	44.413	30.528	67.149	1.00	36.92	AAAA	C
ATOH	2606	OE1	GLU	272	43.545	31.345	67.533	1.00	48.41	AAAA	O
ATOH	2607	OE2	GLU	272	44.223	29.696	66.286	1.00	44.10	AAAA	O
ATOH	2608	C	GLU	272	48.211	32.324	68.335	1.00	40.32	AAAA	C
ATOH	2609	O	GLU	272	48.445	33.447	67.896	1.00	37.04	AAAA	O
ATOH	2610	H	CYS	273	48.942	31.237	68.138	1.00	38.83	AAAA	H
ATOH	2612	CA	CYS	273	50.046	31.187	67.188	1.00	40.27	AAAA	C
ATOH	2613	C	CYS	273	49.321	30.810	65.883	1.00	42.16	AAAA	C
ATOH	2614	O	CYS	273	48.713	29.712	65.831	1.00	40.86	AAAA	O
ATOH	2615	CB	CYS	273	51.099	30.148	67.529	1.00	40.21	AAAA	C
ATOH	2616	SG	CYS	273	52.337	29.825	66.260	1.00	39.79	AAAA	S
ATOH	2617	H	HET	274	49.373	31.749	64.933	1.00	33.70	AAAA	H
ATOH	2619	CA	HET	274	48.586	31.351	63.720	1.00	36.68	AAAA	C
ATOH	2620	CB	HET	274	47.136	31.861	63.847	1.00	29.11	AAAA	C
ATOH	2621	CG	HET	274	46.923	33.379	63.691	1.00	36.51	AAAA	C
ATOH	2622	SD	HET	274	45.477	33.921	64.677	1.00	40.00	AAAA	S
ATOH	2623	CE	HET	274	45.659	35.658	64.754	1.00	22.47	AAAA	C
ATOH	2624	C	HET	274	49.426	31.900	62.608	1.00	39.35	AAAA	C
ATOH	2625	O	HET	274	50.167	32.880	62.672	1.00	41.00	AAAA	O
ATOH	2626	N	GLN	275	49.378	31.353	61.428	1.00	42.55	AAAA	H
ATOH	2628	CA	GLN	275	50.041	31.834	60.232	1.00	37.69	AAAA	C
ATOH	2629	CB	GLN	275	49.618	30.765	59.242	1.00	34.01	AAAA	C
ATOH	2630	CG	GLN	275	49.329	31.274	57.864	1.00	56.40	AAAA	C
ATOH	2631	CD	GLN	275	49.275	30.190	56.812	1.00	66.46	AAAA	C
ATOH	2632	OE1	GLN	275	49.941	29.151	56.910	1.00	67.24	AAAA	O
ATOH	2633	NE2	GLN	275	48.451	30.436	55.799	1.00	78.29	AAAA	H
ATOH	2636	C	GLN	275	49.721	33.195	59.720	1.00	35.41	AAAA	C
ATOH	2637	O	GLN	275	50.526	33.831	59.064	1.00	35.95	AAAA	O
ATOH	2638	H	GLU	276	48.566	33.754	60.056	1.00	41.70	AAAA	H
ATOH	2640	CA	GLU	276	48.222	35.080	59.571	1.00	43.96	AAAA	C
ATOH	2641	CB	GLU	276	47.387	34.884	58.245	1.00	42.40	AAAA	C
ATOH	2642	CG	GLU	276	47.154	36.269	57.650	1.00	53.84	AAAA	C
ATOH	2643	CD	GLU	276	48.359	37.198	57.460	1.00	61.37	AAAA	C
ATOH	2644	OE1	GLU	276	49.356	36.595	56.943	1.00	67.32	AAAA	O
ATOH	2645	OE2	GLU	276	48.242	38.411	57.811	1.00	45.10	AAAA	O
ATOH	2646	C	GLU	276	47.444	35.935	60.540	1.00	39.74	AAAA	C
ATOH	2647	O	GLU	276	46.760	35.449	61.444	1.00	45.06	AAAA	O
ATOH	2648	H	CYS	277	47.495	37.235	60.500	1.00	38.69	AAAA	H
ATOH	2650	CA	CYS	277	46.718	38.089	61.332	1.00	46.11	AAAA	C
ATOH	2651	C	CYS	277	45.205	37.938	60.994	1.00	52.70	AAAA	C
ATOH	2652	O	CYS	277	44.760	37.511	59.936	1.00	49.43	AAAA	O
ATOH	2653	CB	CYS	277	47.039	39.537	61.111	1.00	45.56	AAAA	C
ATOH	2654	SG	CYS	277	48.629	40.083	61.645	1.00	52.86	AAAA	S
ATOH	2655	H	PRO	278	44.380	38.261	61.993	1.00	54.63	AAAA	H
ATOH	2656	CD	PRO	278	44.824	38.778	63.311	1.00	57.20	AAAA	C
ATOH	2657	CA	PRO	278	42.946	38.185	61.899	1.00	55.82	AAAA	C
ATOH	2658	CB	PRO	278	42.445	38.635	63.267	1.00	55.61	AAAA	C
ATOH	2659	CG	PRO	278	43.605	38.670	64.153	1.00	55.58	AAAA	C
ATOH	2660	C	PRO	278	42.487	39.116	60.781	1.00	52.55	AAAA	C
ATOH	2661	O	PRO	278	43.083	40.195	60.631	1.00	48.76	AAAA	O
ATOH	2662	H	SER	279	41.370	38.845	60.143	1.00	49.35	AAAA	H
ATOH	2664	CA	SER	279	40.815	39.720	59.140	1.00	52.03	AAAA	C
ATOH	2665	CB	SER	279	39.280	39.572	58.975	1.00	47.62	AAAA	C
ATOH	2666	CG	SER	279	39.320	38.778	57.785	1.00	68.16	AAAA	O
ATOH	2668	C	SER	279	41.003	41.209	59.173	1.00	55.40	AAAA	C
ATOH	2669	O	SER	279	41.225	41.740	58.059	1.00	55.40	AAAA	O
ATOH	2670	H	GLY	280	40.775	41.962	60.247	1.00	55.32	AAAA	H
ATOH	2672	CA	GLY	280	40.968	43.406	59.868	1.00	48.58	AAAA	C
ATOH	2673	C	GLY	280	42.248	43.890	60.479	1.00	55.98	AAAA	C
ATOH	2674	O	GLY	280	42.249	45.097	60.772	1.00	56.00	AAAA	O
ATOH	2675	H	PHE	281	43.213	42.983	60.742	1.00	55.42	AAAA	H
ATOH	2677	CA	PHE	281	44.506	43.411	61.262	1.00	52.94	AAAA	C
ATOH	2678	CB	PHE	281	44.938	42.644	62.523	1.00	61.20	AAAA	C
ATOH	2679	CG	PHE	281	43.958	42.792	63.637	1.00	53.66	AAAA	C
ATOH	2680	CD1	PHE	281	44.142	43.702	64.630	1.00	60.47	AAAA	C
ATOH	2681	CD2	PHE	281	42.939	41.992	63.712	1.00	60.98	AAAA	C
ATOH	2682	CE1	PHE	281	43.272	43.901	65.678	1.00	64.71	AAAA	C
ATOH	2683	CE2	PHE	281	41.931	42.162	64.755	1.00	63.18	AAAA	C
ATOH	2684	CC	PHE	281	42.141	43.115	65.744	1.00	58.88	AAAA	C

27/58

ATOH	2685	PHE	281	45.530	43.217	60.240	1.00	48.00	AAAA	C
ATOH	2686	O	281	45.738	42.395	59.327	1.00	38.84	AAAA	O
ATOH	2687	H	282	46.570	43.990	60.557	1.00	49.55	AAAA	H
ATOH	2689	CA	282	47.907	43.984	59.748	1.00	45.00	AAAA	C
ATOH	2690	CB	282	47.945	45.188	58.799	1.00	30.25	AAAA	C
ATOH	2691	CG2	282	48.041	46.494	59.507	1.00	24.60	AAAA	C
ATOH	2692	CG1	282	49.092	45.022	57.795	1.00	38.71	AAAA	C
ATOH	2693	CD1	282	49.194	45.043	56.669	1.00	33.38	AAAA	C
ATOH	2694	C	282	49.981	43.889	60.673	1.00	44.30	AAAA	C
ATOH	2695	O	282	49.978	44.447	61.759	1.00	48.49	AAAA	O
ATOH	2696	H	283	50.126	43.153	60.298	1.00	48.68	AAAA	H
ATOH	2698	CA	283	51.396	43.094	61.048	1.00	39.30	AAAA	C
ATOH	2699	CB	283	52.300	42.200	60.286	1.00	41.10	AAAA	C
ATOH	2700	CG	283	52.295	40.696	60.515	1.00	29.19	AAAA	C
ATOH	2701	CD	283	53.078	39.986	59.451	1.00	29.85	AAAA	C
ATOH	2702	HE	283	52.923	38.545	59.404	1.00	29.39	AAAA	H
ATOH	2704	CG	283	51.862	38.024	58.646	1.00	37.61	AAAA	C
ATOH	2705	HH1	283	51.065	38.846	57.944	1.00	31.41	AAAA	H
ATOH	2708	HH2	283	51.651	36.722	58.596	1.00	31.97	AAAA	H
ATOH	2711	C	283	51.945	44.498	61.190	1.00	42.27	AAAA	C
ATOH	2712	O	283	51.931	45.228	60.173	1.00	43.42	AAAA	O
ATOH	2713	H	284	52.362	44.886	62.422	1.00	39.49	AAAA	H
ATOH	2715	CA	284	52.733	46.311	62.574	1.00	42.07	AAAA	C
ATOH	2721	C	284	54.078	46.656	61.929	1.00	41.64	AAAA	C
ATOH	2722	O	284	54.431	47.798	61.742	1.00	39.01	AAAA	O
ATOH	2716	CB	284	52.734	46.760	64.032	1.00	37.33	AAAA	C
ATOH	2717	CG	284	53.917	46.028	64.611	1.00	50.21	AAAA	C
ATOH	2718	OD1	284	54.609	45.104	64.192	1.00	44.30	AAAA	O
ATOH	2719	HD2	284	54.323	46.432	65.842	1.00	42.46	AAAA	H
ATOH	2723	H	285	54.931	45.699	61.562	1.00	40.10	AAAA	H
ATOH	2725	CA	285	55.971	45.815	60.593	1.00	26.91	AAAA	C
ATOH	2726	C	285	56.091	44.468	59.848	1.00	33.12	AAAA	C
ATOH	2727	O	285	55.584	43.331	60.187	1.00	29.51	AAAA	O
ATOH	2728	H	286	56.915	44.619	58.766	1.00	26.53	AAAA	H
ATOH	2730	CA	286	57.109	43.385	57.975	1.00	32.67	AAAA	C
ATOH	2731	CB	286	57.944	43.681	56.757	1.00	33.19	AAAA	C
ATOH	2732	CG	286	58.283	42.480	56.014	1.00	31.95	AAAA	O
ATOH	2734	C	286	57.750	42.310	58.836	1.00	34.57	AAAA	C
ATOH	2735	O	286	58.700	42.495	59.607	1.00	44.29	AAAA	O
ATOH	2736	H	287	57.227	41.148	58.940	1.00	34.45	AAAA	H
ATOH	2738	CA	287	57.738	40.005	59.634	1.00	35.25	AAAA	C
ATOH	2739	CB	287	59.139	39.610	59.083	1.00	27.97	AAAA	C
ATOH	2740	CG	287	59.037	39.234	57.664	1.00	26.61	AAAA	C
ATOH	2741	CD	287	58.539	37.963	57.130	1.00	21.25	AAAA	C
ATOH	2742	OE1	287	58.192	37.023	57.845	1.00	28.18	AAAA	O
ATOH	2743	HE2	287	58.492	37.838	55.782	1.00	27.55	AAAA	H
ATOH	2746	C	287	57.773	40.286	61.111	1.00	30.25	AAAA	C
ATOH	2747	O	287	58.163	39.415	61.908	1.00	32.78	AAAA	C
ATOH	2748	H	288	57.021	41.217	61.624	1.00	32.49	AAAA	H
ATOH	2750	CA	288	56.696	41.322	63.043	1.00	28.98	AAAA	C
ATOH	2751	CB	288	56.024	42.675	63.313	1.00	35.79	AAAA	C
ATOH	2752	CG	288	55.639	42.612	64.701	1.00	36.61	AAAA	O
ATOH	2754	C	288	55.665	40.285	63.442	1.00	28.96	AAAA	C
ATOH	2755	O	288	54.993	39.776	62.553	1.00	31.16	AAAA	O
ATOH	2756	H	289	55.774	39.720	64.621	1.00	32.51	AAAA	H
ATOH	2758	CA	289	54.975	38.697	65.105	1.00	34.53	AAAA	C
ATOH	2759	CB	289	55.507	37.823	66.153	1.00	30.31	AAAA	C
ATOH	2760	CG	289	56.571	36.872	65.680	1.00	40.50	AAAA	C
ATOH	2761	SD	289	56.977	35.623	66.881	1.00	31.65	AAAA	S
ATOH	2762	CE	289	55.745	34.315	66.508	1.00	30.47	AAAA	C
ATOH	2763	C	289	53.557	39.286	65.703	1.00	35.55	AAAA	C
ATOH	2764	O	289	52.630	38.512	66.014	1.00	38.37	AAAA	O
ATOH	2765	H	290	53.380	40.565	65.742	1.00	29.54	AAAA	H
ATOH	2767	CA	290	52.363	41.358	66.297	1.00	38.81	AAAA	C
ATOH	2768	CB	290	52.947	42.589	67.042	1.00	36.72	AAAA	C
ATOH	2769	CG	290	53.570	42.184	68.351	1.00	41.94	AAAA	C
ATOH	2770	CD1	290	54.932	41.780	68.350	1.00	37.79	AAAA	C
ATOH	2771	CE1	290	55.548	41.368	69.503	1.00	32.60	AAAA	C
ATOH	2772	CD2	290	52.987	42.157	69.570	1.00	39.93	AAAA	C
ATOH	2773	CE2	290	53.501	41.750	70.748	1.00	36.16	AAAA	C
ATOH	2774	CC	290	54.922	41.355	70.693	1.00	38.85	AAAA	C
ATOH	2775	OH	290	55.581	40.923	71.751	1.00	43.41	AAAA	O
ATOH	2777	C	290	51.361	41.955	65.270	1.00	45.54	AAAA	C
ATOH	2778	O	290	51.733	42.520	64.227	1.00	47.10	AAAA	O
ATOH	2779	H	291	50.071	41.698	65.537	1.00	44.68	AAAA	H
ATOH	2781	CA	291	49.017	42.205	64.685	1.00	47.20	AAAA	C
ATOH	2782	C	291	48.295	43.434	65.194	1.00	46.06	AAAA	C
ATOH	2783	O	291	47.992	43.550	66.343	1.00	49.45	AAAA	O
ATOH	2784	CB	291	47.973	41.103	64.483	1.00	43.44	AAAA	C
ATOH	2785	SG	291	48.766	39.715	63.683	1.00	45.49	AAAA	S
ATOH	2786	H	292	48.136	44.453	64.365	1.00	46.82	AAAA	H
ATOH	2788	CA	292	47.399	45.651	64.755	1.00	50.64	AAAA	C
ATOH	2789	CB	292	48.267	46.932	64.779	1.00	39.19	AAAA	C
ATOH	2790	CG2	292	49.291	46.885	65.861	1.00	44.39	AAAA	C
ATOH	2791	CG1	292	48.920	47.095	63.402	1.00	44.25	AAAA	C

28/58

ATOH	2792	CD1	ILE	292	49.234	48.568	63.109	1.00	32.80	AAAA	C
ATOH	2793	C	ILE	292	46.240	46.003	63.806	1.00	50.01	AAAA	C
ATOH	2794	O	ILE	292	46.165	45.526	62.670	1.00	46.64	AAAA	O
ATOH	2795	H	PRO	293	45.150	46.507	64.385	1.00	51.86	AAAA	H
ATOH	2796	CD	PRO	293	45.009	46.804	65.839	1.00	51.05	AAAA	C
ATOH	2797	CA	PRO	293	43.958	46.930	63.675	1.00	51.40	AAAA	C
ATOH	2798	CB	PRO	293	43.170	47.784	64.681	1.00	49.00	AAAA	C
ATOH	2799	CG	PRO	293	43.533	47.112	65.951	1.00	53.73	AAAA	C
ATOH	2800	C	PRO	293	44.253	47.870	62.525	1.00	51.68	AAAA	C
ATOH	2801	O	PRO	293	45.053	48.788	62.737	1.00	51.92	AAAA	O
ATOH	2802	H	CYS	294	43.607	47.621	61.408	1.00	50.66	AAAA	H
ATOH	2804	CA	CYS	294	43.811	48.464	60.254	1.00	57.90	AAAA	C
ATOH	2805	C	CYS	294	43.219	49.848	60.345	1.00	59.59	AAAA	C
ATOH	2806	O	CYS	294	43.744	50.814	59.785	1.00	60.87	AAAA	O
ATOH	2807	CB	CYS	294	43.229	47.686	59.046	1.00	57.59	AAAA	C
ATOH	2808	SG	CYS	294	44.408	46.460	58.563	1.00	51.12	AAAA	S
ATOH	2809	H	ALA	295	42.009	50.031	60.854	1.00	65.87	AAAA	H
ATOH	2811	CA	ALA	295	41.391	51.386	60.804	1.00	71.19	AAAA	C
ATOH	2812	CB	ALA	295	42.311	52.459	61.393	1.00	63.82	AAAA	C
ATOH	2813	C	ALA	295	40.971	51.770	59.370	1.00	69.17	AAAA	C
ATOH	2814	O	ALA	295	41.421	52.717	58.762	1.00	64.70	AAAA	O
ATOH	2815	H	GLY	296	40.153	50.920	58.775	1.00	71.30	AAAA	H
ATOH	2817	CA	GLY	296	39.640	51.049	57.416	1.00	72.66	AAAA	C
ATOH	2818	C	GLY	296	39.895	49.686	56.769	1.00	74.20	AAAA	C
ATOH	2819	O	GLY	296	40.408	48.819	57.490	1.00	75.04	AAAA	O
ATOH	2820	H	PRO	297	39.561	49.540	55.497	1.00	71.98	AAAA	H
ATOH	2821	CD	PRO	297	38.928	50.561	54.637	1.00	72.15	AAAA	C
ATOH	2822	CA	PRO	297	39.958	48.344	54.777	1.00	68.23	AAAA	C
ATOH	2823	CB	PRO	297	39.488	48.603	53.369	1.00	72.57	AAAA	C
ATOH	2824	CG	PRO	297	38.470	49.687	53.490	1.00	74.04	AAAA	C
ATOH	2825	C	PRO	297	41.480	48.306	54.860	1.00	65.78	AAAA	C
ATOH	2826	O	PRO	297	42.147	49.323	54.997	1.00	62.72	AAAA	O
ATOH	2827	H	CYS	298	42.039	47.135	55.073	1.00	63.85	AAAA	H
ATOH	2829	CA	CYS	298	43.464	46.953	55.248	1.00	54.47	AAAA	C
ATOH	2830	C	CYS	298	44.109	47.303	53.908	1.00	54.56	AAAA	C
ATOH	2831	O	CYS	298	43.621	47.030	52.820	1.00	54.83	AAAA	O
ATOH	2832	CB	CYS	298	43.665	45.544	55.669	1.00	47.65	AAAA	C
ATOH	2833	SG	CYS	298	43.501	45.115	57.371	1.00	46.12	AAAA	S
ATOH	2834	H	PRO	299	45.310	47.876	53.967	1.00	49.83	AAAA	H
ATOH	2835	CD	PRO	299	46.087	48.168	55.194	1.00	48.14	AAAA	C
ATOH	2836	CA	PRO	299	46.055	48.212	52.787	1.00	43.67	AAAA	C
ATOH	2837	CB	PRO	299	47.267	48.965	53.281	1.00	44.08	AAAA	C
ATOH	2838	CG	PRO	299	47.454	48.361	54.628	1.00	51.38	AAAA	C
ATOH	2839	C	PRO	299	46.341	46.969	52.010	1.00	38.86	AAAA	C
ATOH	2840	O	PRO	299	46.372	45.874	52.546	1.00	42.85	AAAA	O
ATOH	2841	H	LYS	300	46.310	47.073	50.712	1.00	38.30	AAAA	H
ATOH	2843	CA	LYS	300	46.484	45.958	49.812	1.00	42.62	AAAA	C
ATOH	2844	CB	LYS	300	45.176	45.226	49.595	1.00	34.28	AAAA	C
ATOH	2845	CG	LYS	300	45.346	43.901	48.920	1.00	41.45	AAAA	C
ATOH	2846	CD	LYS	300	44.013	43.413	48.378	1.00	48.31	AAAA	C
ATOH	2847	CE	LYS	300	44.388	42.027	47.787	1.00	48.57	AAAA	C
ATOH	2848	HC	LYS	300	43.662	42.031	46.478	1.00	63.70	AAAA	H
ATOH	2852	C	LYS	300	46.964	46.479	48.432	1.00	48.72	AAAA	C
ATOH	2853	O	LYS	300	46.413	47.383	47.776	1.00	46.09	AAAA	O
ATOH	2854	H	VAL	301	48.150	45.984	48.054	1.00	48.15	AAAA	H
ATOH	2856	CA	VAL	301	48.802	46.462	46.871	1.00	44.52	AAAA	C
ATOH	2857	CB	VAL	301	50.292	46.729	47.074	1.00	51.52	AAAA	C
ATOH	2858	CG1	VAL	301	51.008	47.200	45.796	1.00	43.07	AAAA	C
ATOH	2859	CG2	VAL	301	50.495	47.794	45.141	1.00	49.50	AAAA	C
ATOH	2860	C	VAL	301	48.526	45.410	45.837	1.00	44.59	AAAA	C
ATOH	2861	O	VAL	301	48.913	44.291	46.060	1.00	43.70	AAAA	O
ATOH	2862	H	CYS	302	47.910	45.816	44.718	1.00	47.98	AAAA	H
ATOH	2864	CA	CYS	302	47.645	44.735	43.739	1.00	55.19	AAAA	C
ATOH	2865	C	CYS	302	48.594	44.968	42.583	1.00	57.64	AAAA	C
ATOH	2866	O	CYS	302	48.852	46.152	42.343	1.00	60.23	AAAA	O
ATOH	2867	CB	CYS	302	46.186	44.630	43.330	1.00	68.30	AAAA	C
ATOH	2868	SG	CYS	302	45.970	44.360	44.751	1.00	70.31	AAAA	S
ATOH	2869	H	GLU	303	49.183	43.921	42.075	1.00	58.15	AAAA	H
ATOH	2871	CA	GLU	303	50.174	43.932	41.034	1.00	62.85	AAAA	C
ATOH	2872	CB	GLU	303	51.503	44.006	41.595	1.00	67.85	AAAA	C
ATOH	2873	CG	GLU	303	51.760	43.487	43.014	0.01	67.46	AAAA	C
ATOH	2874	CD	GLU	303	51.999	41.992	43.097	0.01	67.94	AAAA	C
ATOH	2875	OE1	GLU	303	53.011	41.514	42.561	0.01	67.67	AAAA	O
ATOH	2876	OE2	GLU	303	51.147	41.290	43.697	0.01	67.65	AAAA	O
ATOH	2877	C	GLU	303	50.096	42.662	40.194	1.00	64.12	AAAA	C
ATOH	2878	O	GLU	303	50.162	41.562	40.708	1.00	65.08	AAAA	O
ATOH	2879	H	GLU	304	49.867	42.794	38.904	1.00	67.37	AAAA	H
ATOH	2881	CA	GLU	304	49.672	41.583	38.094	1.00	74.63	AAAA	C
ATOH	2882	CB	GLU	304	48.285	41.596	37.458	1.00	71.71	AAAA	C
ATOH	2883	CG	GLU	304	47.339	42.663	38.031	1.00	84.54	AAAA	C
ATOH	2884	CD	GLU	304	45.930	42.152	36.195	1.00	87.56	AAAA	C
ATOH	2885	OE1	GLU	304	45.438	41.571	37.179	1.00	89.13	AAAA	O
ATOH	2886	OE2	GLU	304	45.249	42.269	39.233	1.00	93.19	AAAA	O
ATOH	2887	C	GLU	304	50.966	41.307	37.190	1.00	76.10	AAAA	C
ATOH	2888	O	GLU	304	51.911	41.962	37.217	1.00	74.78	AAAA	O

29/58

ATOH	2889	H	GLU	305	50.899	40.126	36.586	1.00	77.31	AAAA	H
ATOH	2891	CA	GLU	305	51.932	39.656	35.674	1.00	75.96	AAAA	C
ATOH	2892	CB	GLU	305	51.467	38.380	34.970	1.00	79.95	AAAA	C
ATOH	2893	CG	GLU	305	52.307	37.937	33.807	1.00	87.20	AAAA	C
ATOH	2894	CD	GLU	305	51.758	36.891	32.886	0.01	83.39	AAAA	C
ATOH	2895	OE1	GLU	305	50.762	36.234	33.252	0.01	83.66	AAAA	O
ATOH	2896	OE2	GLU	305	52.310	36.700	31.789	0.01	83.73	AAAA	O
ATOH	2897	C	GLU	305	52.276	40.737	34.666	1.00	75.97	AAAA	C
ATOH	2898	O	GLU	305	53.381	41.268	34.613	1.00	76.54	AAAA	O
ATOH	2899	H	LYS	306	51.291	41.181	33.888	1.00	78.22	AAAA	H
ATOH	2901	CA	LYS	306	51.479	42.329	33.004	1.00	75.99	AAAA	C
ATOH	2902	CB	LYS	306	50.467	42.253	31.855	1.00	79.78	AAAA	C
ATOH	2903	CG	LYS	306	51.208	42.227	30.527	1.00	94.52	AAAA	C
ATOH	2904	CD	LYS	306	50.313	42.191	28.314	1.00	92.78	AAAA	C
ATOH	2905	CE	LYS	306	50.740	43.227	28.261	1.00	97.10	AAAA	C
ATOH	2906	HC	LYS	306	50.938	44.554	28.929	1.00	84.87	AAAA	H
ATOH	2910	C	LYS	306	51.381	43.669	33.703	1.00	73.85	AAAA	C
ATOH	2911	O	LYS	306	50.703	43.862	34.718	1.00	76.08	AAAA	O
ATOH	2912	H	LYS	307	52.000	44.700	33.180	1.00	71.15	AAAA	H
ATOH	2914	CA	LYS	307	51.934	46.053	33.692	1.00	69.45	AAAA	C
ATOH	2915	CB	LYS	307	53.022	46.903	33.008	1.00	79.64	AAAA	C
ATOH	2916	CG	LYS	307	54.419	46.837	33.564	1.00	78.88	AAAA	C
ATOH	2917	CD	LYS	307	55.257	48.084	33.374	1.00	85.84	AAAA	C
ATOH	2918	CE	LYS	307	55.708	48.215	31.924	1.00	97.07	AAAA	C
ATOH	2919	HC	LYS	307	54.649	48.840	31.067	1.00	97.80	AAAA	H
ATOH	2923	C	LYS	307	50.562	46.716	33.525	1.00	67.97	AAAA	C
ATOH	2924	O	LYS	307	50.010	47.369	34.431	1.00	64.46	AAAA	O
ATOH	2925	H	THR	308	49.979	46.661	32.323	1.00	65.84	AAAA	H
ATOH	2927	CA	THR	308	48.709	47.319	32.091	1.00	64.56	AAAA	C
ATOH	2928	CB	THR	308	48.714	47.977	30.711	1.00	59.91	AAAA	C
ATOH	2929	CG1	THR	308	49.834	48.843	30.577	1.00	61.97	AAAA	O
ATOH	2931	CG2	THR	308	47.392	48.742	30.561	1.00	63.64	AAAA	C
ATOH	2932	C	THR	308	47.514	46.379	32.234	1.00	61.82	AAAA	C
ATOH	2933	O	THR	308	47.412	45.415	31.477	1.00	62.05	AAAA	O
ATOH	2934	H	LYS	309	46.675	46.719	33.211	1.00	55.66	AAAA	H
ATOH	2936	CA	LYS	309	45.456	45.926	33.445	1.00	54.67	AAAA	C
ATOH	2937	CB	LYS	309	45.043	45.880	34.904	1.00	56.82	AAAA	C
ATOH	2938	CG	LYS	309	43.601	45.541	35.223	1.00	57.50	AAAA	C
ATOH	2939	CD	LYS	309	43.390	44.039	35.086	1.00	59.50	AAAA	C
ATOH	2940	CE	LYS	309	42.703	43.448	36.324	1.00	57.31	AAAA	C
ATOH	2941	HC	LYS	309	42.758	41.954	36.236	1.00	57.22	AAAA	H
ATOH	2945	C	LYS	309	44.391	46.570	32.548	1.00	51.21	AAAA	C
ATOH	2946	O	LYS	309	44.074	47.763	32.680	1.00	47.23	AAAA	O
ATOH	2947	H	THR	310	43.895	45.772	31.610	1.00	47.67	AAAA	H
ATOH	2949	CA	THR	310	42.862	46.328	30.733	1.00	51.89	AAAA	C
ATOH	2950	CB	THR	310	43.161	46.015	29.266	1.00	54.81	AAAA	C
ATOH	2951	CG1	THR	310	41.909	45.710	28.635	1.00	66.29	AAAA	O
ATOH	2953	CG2	THR	310	44.032	44.791	29.139	1.00	55.18	AAAA	C
ATOH	2954	C	THR	310	41.468	45.841	31.117	1.00	51.15	AAAA	C
ATOH	2955	O	THR	310	41.162	44.680	30.991	1.00	49.27	AAAA	O
ATOH	2956	H	ILE	311	40.684	46.706	31.732	1.00	50.18	AAAA	H
ATOH	2958	CA	ILE	311	39.363	46.453	32.275	1.00	48.67	AAAA	C
ATOH	2959	CB	ILE	311	39.120	47.396	33.462	1.00	49.27	AAAA	C
ATOH	2960	CG2	ILE	311	37.655	47.596	33.789	1.00	50.72	AAAA	C
ATOH	2961	CG1	ILE	311	39.896	46.930	34.699	1.00	41.34	AAAA	C
ATOH	2962	CD1	ILE	311	39.847	48.073	35.739	1.00	52.22	AAAA	C
ATOH	2963	C	ILE	311	38.334	46.729	31.186	1.00	45.37	AAAA	C
ATOH	2964	O	ILE	311	38.132	47.875	30.758	1.00	37.14	AAAA	O
ATOH	2965	H	ASP	312	37.871	45.678	30.524	1.00	50.10	AAAA	H
ATOH	2967	CA	ASP	312	36.991	45.842	29.377	1.00	56.35	AAAA	C
ATOH	2968	CB	ASP	312	37.546	45.152	28.128	1.00	59.45	AAAA	C
ATOH	2969	CG	ASP	312	37.761	43.671	28.382	1.00	65.64	AAAA	C
ATOH	2970	OD1	ASP	312	38.525	43.034	27.635	1.00	72.60	AAAA	O
ATOH	2971	OD2	ASP	312	37.154	43.176	29.348	1.00	66.86	AAAA	O
ATOH	2972	C	ASP	312	35.589	45.337	29.693	1.00	59.39	AAAA	C
ATOH	2973	O	ASP	312	34.729	45.007	28.867	1.00	61.00	AAAA	O
ATOH	2974	H	SER	313	35.278	45.290	30.976	1.00	61.17	AAAA	H
ATOH	2976	CA	SER	313	34.053	44.683	31.459	1.00	55.73	AAAA	C
ATOH	2977	CB	SER	313	34.121	43.201	31.093	1.00	48.22	AAAA	C
ATOH	2978	CG	SER	313	34.373	42.514	32.292	1.00	57.89	AAAA	O
ATOH	2980	C	SER	313	33.998	44.818	32.941	1.00	57.87	AAAA	C
ATOH	2981	O	SER	313	34.802	45.506	33.537	1.00	66.47	AAAA	O
ATOH	2982	H	VAL	314	33.001	44.205	33.545	1.00	64.35	AAAA	H
ATOH	2984	CA	VAL	314	32.840	44.305	35.015	1.00	64.39	AAAA	C
ATOH	2985	CB	VAL	314	31.360	44.340	35.343	1.00	69.57	AAAA	C
ATOH	2986	CG1	VAL	314	31.024	43.693	36.691	1.00	65.60	AAAA	C
ATOH	2987	CG2	VAL	314	30.927	45.823	35.319	1.00	65.27	AAAA	C
ATOH	2988	C	VAL	314	33.492	43.088	35.638	1.00	62.65	AAAA	C
ATOH	2989	O	VAL	314	34.029	43.141	36.704	1.00	63.92	AAAA	O
ATOH	2990	H	THR	315	33.468	42.011	34.878	1.00	61.82	AAAA	H
ATOH	2992	CA	THR	315	34.029	40.752	35.284	1.00	63.44	AAAA	C
ATOH	2993	CB	THR	315	33.618	39.628	34.314	1.00	65.54	AAAA	C
ATOH	2994	CG1	THR	315	32.403	40.004	33.634	1.00	74.65	AAAA	O
ATOH	2996	CG2	THR	315	33.339	38.366	35.104	1.00	64.86	AAAA	C
ATOH	2997	C	THR	315	35.541	40.971	35.323	1.00	65.82	AAAA	C

30/58

ATOM	2998	O	THR	315	36.217	40.239	36.206	1.00	66.41	AAAA	O
ATOM	2999	H	SER	316	36.071	41.593	34.332	1.00	63.28	AAAA	H
ATOM	3001	CA	SER	316	37.500	41.793	34.215	1.00	58.72	AAAA	C
ATOM	3002	CB	SER	316	37.795	42.537	32.900	1.00	52.20	AAAA	C
ATOM	3003	CG	SER	316	37.298	43.859	32.933	1.00	48.04	AAAA	O
ATOM	3005	C	SER	316	38.077	42.573	35.387	1.00	58.91	AAAA	C
ATOM	3006	O	SER	316	39.293	42.522	35.520	1.00	59.86	AAAA	O
ATOM	3007	H	ALA	317	37.310	43.362	36.111	1.00	55.86	AAAA	H
ATOM	3009	CA	ALA	317	37.750	44.184	37.191	1.00	57.17	AAAA	C
ATOM	3010	CB	ALA	317	36.833	45.409	37.269	1.00	54.23	AAAA	C
ATOM	3011	C	ALA	317	37.689	43.487	38.538	1.00	62.05	AAAA	C
ATOM	3012	O	ALA	317	37.702	44.128	39.599	1.00	60.30	AAAA	O
ATOM	3013	H	GLU	318	37.361	47.205	38.523	1.00	67.91	AAAA	H
ATOM	3015	CA	GLU	318	37.185	41.380	39.713	1.00	70.72	AAAA	C
ATOM	3016	CB	GLU	318	36.857	39.956	39.293	1.00	74.48	AAAA	C
ATOM	3017	CG	GLU	318	36.624	38.947	40.383	1.00	89.82	AAAA	C
ATOM	3018	CD	GLU	318	35.265	39.080	41.048	1.00	92.69	AAAA	C
ATOM	3019	OE1	GLU	318	34.256	38.807	40.391	1.00	98.57	AAAA	O
ATOM	3020	HE2	GLU	318	35.356	39.509	42.308	1.00	92.51	AAAA	H
ATOM	3023	C	GLU	318	38.380	41.413	40.653	1.00	72.63	AAAA	C
ATOM	3024	O	GLU	318	38.294	41.855	41.804	1.00	68.92	AAAA	O
ATOM	3025	H	HET	319	39.562	41.062	40.153	1.00	75.10	AAAA	H
ATOM	3027	CA	HET	319	40.846	41.175	40.826	1.00	71.85	AAAA	C
ATOM	3028	CB	HET	319	41.950	40.960	39.772	1.00	82.00	AAAA	C
ATOM	3029	CG	HET	319	41.740	39.644	39.050	1.00	91.16	AAAA	C
ATOM	3030	SD	HET	319	43.123	38.482	39.185	1.00	106.72	AAAA	S
ATOM	3031	CE	HET	319	42.486	37.105	38.231	1.00	97.56	AAAA	C
ATOM	3032	C	HET	319	41.118	42.509	41.471	1.00	67.68	AAAA	C
ATOM	3033	O	HET	319	41.577	42.541	42.612	1.00	69.73	AAAA	O
ATOM	3034	H	LEU	320	40.740	43.639	40.887	1.00	62.95	AAAA	H
ATOM	3036	CA	LEU	320	40.907	44.938	41.531	1.00	62.31	AAAA	C
ATOM	3037	CB	LEU	320	40.440	46.085	40.623	1.00	54.93	AAAA	C
ATOM	3038	CG	LEU	320	41.091	46.163	39.238	1.00	53.48	AAAA	C
ATOM	3039	CD1	LEU	320	41.005	47.552	38.692	1.00	51.31	AAAA	C
ATOM	3040	CD2	LEU	320	42.557	45.709	39.403	1.00	58.43	AAAA	C
ATOM	3041	C	LEU	320	40.209	45.008	42.881	1.00	60.30	AAAA	C
ATOM	3042	O	LEU	320	40.344	45.969	43.661	1.00	58.72	AAAA	O
ATOM	3043	H	GLN	321	39.267	44.106	43.112	1.00	59.62	AAAA	H
ATOM	3045	CA	GLN	321	38.482	44.128	44.343	1.00	63.50	AAAA	C
ATOM	3046	CB	GLN	321	37.373	43.089	44.250	1.00	62.52	AAAA	C
ATOM	3047	CG	GLN	321	36.611	42.854	45.522	1.00	56.83	AAAA	C
ATOM	3048	CD	GLN	321	35.337	42.064	45.291	1.00	68.77	AAAA	C
ATOM	3049	OE1	GLN	321	35.362	40.969	44.718	1.00	70.37	AAAA	O
ATOM	3050	HE2	GLN	321	34.218	42.632	45.764	1.00	63.77	AAAA	H
ATOM	3053	C	GLN	321	39.367	44.030	45.594	1.00	60.97	AAAA	C
ATOM	3054	O	GLN	321	40.262	43.196	45.782	1.00	57.29	AAAA	O
ATOM	3055	H	GLY	322	39.092	44.928	46.546	1.00	57.62	AAAA	H
ATOM	3057	CA	GLY	322	39.855	44.928	47.790	1.00	60.63	AAAA	C
ATOM	3058	C	GLY	322	41.126	45.773	47.812	1.00	61.78	AAAA	C
ATOM	3059	O	GLY	322	41.584	46.198	48.889	1.00	60.16	AAAA	O
ATOM	3060	H	CYS	323	41.719	46.124	46.676	1.00	60.03	AAAA	H
ATOM	3062	CA	CYS	323	42.938	46.845	46.528	1.00	54.20	AAAA	C
ATOM	3063	C	CYS	323	42.924	48.307	46.910	1.00	53.48	AAAA	C
ATOM	3064	O	CYS	323	42.105	49.148	46.503	1.00	56.43	AAAA	O
ATOM	3065	CB	CYS	323	43.458	46.822	45.086	1.00	53.33	AAAA	C
ATOM	3066	SG	CYS	323	43.325	45.222	44.248	1.00	66.22	AAAA	S
ATOM	3067	H	THR	324	43.994	48.718	47.580	1.00	49.83	AAAA	H
ATOM	3069	CA	THR	324	44.164	50.161	47.811	1.00	52.29	AAAA	C
ATOM	3070	CB	THR	324	44.623	50.324	49.264	1.00	52.84	AAAA	C
ATOM	3071	OG1	THR	324	45.245	49.087	49.634	1.00	59.82	AAAA	O
ATOM	3073	CG2	THR	324	43.432	50.517	50.193	1.00	60.00	AAAA	C
ATOM	3074	C	THR	324	45.154	50.802	46.844	1.00	48.91	AAAA	C
ATOM	3075	O	THR	324	45.277	52.016	46.710	1.00	46.90	AAAA	O
ATOM	3076	H	ILE	325	46.021	49.963	46.254	1.00	46.87	AAAA	H
ATOM	3078	CA	ILE	325	47.114	50.511	45.445	1.00	45.10	AAAA	C
ATOM	3079	CB	ILE	325	48.473	50.577	46.183	1.00	43.60	AAAA	C
ATOM	3080	CG2	ILE	325	49.586	50.905	45.163	1.00	47.47	AAAA	C
ATOM	3081	CG1	ILE	325	48.394	51.623	47.294	1.00	34.03	AAAA	C
ATOM	3082	CD1	ILE	325	49.585	52.010	48.028	1.00	41.94	AAAA	C
ATOM	3083	C	ILE	325	47.265	49.642	44.229	1.00	42.88	AAAA	C
ATOM	3084	O	ILE	325	47.406	48.429	44.469	1.00	42.99	AAAA	O
ATOM	3085	H	PHE	326	47.170	50.238	43.042	1.00	41.19	AAAA	H
ATOM	3087	CA	PHE	326	47.312	49.334	41.880	1.00	42.88	AAAA	C
ATOM	3088	CB	PHE	326	46.166	49.437	40.877	1.00	39.15	AAAA	C
ATOM	3089	CG	PHE	326	46.403	48.474	39.738	1.00	38.03	AAAA	C
ATOM	3090	CD1	PHE	326	46.186	47.125	39.951	1.00	39.68	AAAA	C
ATOM	3091	CD2	PHE	326	46.917	48.892	38.525	1.00	37.31	AAAA	C
ATOM	3092	CE1	PHE	326	46.447	46.139	39.023	1.00	36.52	AAAA	C
ATOM	3093	CE2	PHE	326	47.136	47.919	37.551	1.00	45.74	AAAA	C
ATOM	3094	CZ	PHE	326	46.924	46.570	37.787	1.00	39.92	AAAA	C
ATOM	3095	C	PHE	326	48.682	49.673	41.280	1.00	48.78	AAAA	C
ATOM	3096	O	PHE	326	49.024	50.826	40.966	1.00	51.39	AAAA	O
ATOM	3097	H	LYS	327	49.623	48.751	41.379	1.00	50.22	AAAA	H
ATOM	3099	CA	LYS	327	50.964	49.963	40.831	1.00	51.49	AAAA	C
ATOM	3100	CB	LYS	327	52.050	48.091	41.519	1.00	58.64	AAAA	C

31/58

ATOM	3101	CG	LYS	327	53.254	48.897	41.891	1.00	59.15	AAAA	C
ATOM	3102	CD	LYS	327	54.528	48.257	41.617	1.00	63.49	AAAA	C
ATOM	3103	CE	LYS	327	55.400	48.951	40.592	1.00	68.12	AAAA	C
ATOM	3104	H2	LYS	327	56.260	47.889	39.938	1.00	71.97	AAAA	H
ATOM	3108	C	LYS	327	50.895	48.464	39.391	1.00	45.70	AAAA	C
ATOM	3109	O	LYS	327	50.901	47.245	39.127	1.00	49.55	AAAA	O
ATOM	3110	H	GLY	328	50.760	49.397	38.502	1.00	39.68	AAAA	H
ATOM	3112	CA	GLY	328	50.647	49.038	37.080	1.00	39.44	AAAA	C
ATOM	3113	C	GLY	328	49.845	50.161	36.427	1.00	39.49	AAAA	C
ATOM	3114	O	GLY	328	49.858	51.307	36.881	1.00	31.92	AAAA	O
ATOM	3115	H	ASH	329	49.286	49.813	35.289	1.00	41.47	AAAA	H
ATOM	3117	CA	ASH	329	48.467	50.750	34.543	1.00	45.72	AAAA	C
ATOM	3118	CB	ASH	329	49.185	50.942	33.211	1.00	42.50	AAAA	C
ATOM	3119	CG	ASH	329	50.624	51.426	33.357	1.00	42.26	AAAA	C
ATOM	3120	OD1	ASH	329	50.954	52.331	34.156	1.00	34.77	AAAA	O
ATOM	3121	HD2	ASH	329	51.425	50.769	32.530	1.00	30.62	AAAA	H
ATOM	3124	C	ASH	329	47.038	50.207	34.357	1.00	50.37	AAAA	C
ATOM	3125	O	ASH	329	46.736	49.015	34.119	1.00	50.17	AAAA	O
ATOM	3126	H	LEU	330	46.090	51.143	34.413	1.00	47.13	AAAA	H
ATOM	3128	CA	LEU	330	44.691	50.860	34.151	1.00	42.53	AAAA	C
ATOM	3129	CB	LEU	330	43.751	51.530	35.153	1.00	42.84	AAAA	C
ATOM	3130	CG	LEU	330	43.768	50.995	36.598	1.00	38.65	AAAA	C
ATOM	3131	CD1	LEU	330	42.864	51.924	37.417	1.00	38.12	AAAA	C
ATOM	3132	CD2	LEU	330	43.283	49.565	36.669	1.00	38.74	AAAA	C
ATOM	3133	C	LEU	330	44.352	51.377	32.758	1.00	39.10	AAAA	C
ATOM	3134	O	LEU	330	44.509	52.545	32.460	1.00	40.71	AAAA	O
ATOM	3135	H	LEU	331	43.933	50.516	31.904	1.00	36.10	AAAA	H
ATOM	3137	CA	LEU	331	43.367	50.869	30.625	1.00	43.10	AAAA	C
ATOM	3138	CB	LEU	331	43.958	49.894	29.585	1.00	42.29	AAAA	C
ATOM	3139	CG	LEU	331	43.301	49.960	28.221	1.00	40.89	AAAA	C
ATOM	3140	CD1	LEU	331	43.501	51.319	27.627	1.00	46.64	AAAA	C
ATOM	3141	CD2	LEU	331	43.844	48.834	27.567	1.00	48.76	AAAA	C
ATOM	3142	C	LEU	331	41.872	50.568	30.705	1.00	41.12	AAAA	C
ATOM	3143	O	LEU	331	41.562	49.365	30.779	1.00	40.08	AAAA	O
ATOM	3144	H	ILE	332	41.029	51.566	30.862	1.00	41.13	AAAA	H
ATOM	3146	CA	ILE	332	39.606	51.241	31.044	1.00	36.90	AAAA	C
ATOM	3147	CB	ILE	332	38.885	52.085	32.076	1.00	34.77	AAAA	C
ATOM	3148	CG2	ILE	332	37.413	51.612	32.195	1.00	34.66	AAAA	C
ATOM	3149	CG1	ILE	332	39.550	51.895	33.452	1.00	33.64	AAAA	C
ATOM	3150	CD1	ILE	332	39.479	53.152	34.337	1.00	48.21	AAAA	C
ATOM	3151	C	ILE	332	38.959	51.367	29.688	1.00	34.03	AAAA	C
ATOM	3152	O	ILE	332	38.867	52.489	29.200	1.00	35.89	AAAA	O
ATOM	3153	H	ASH	333	38.569	50.273	29.094	1.00	35.25	AAAA	H
ATOM	3155	CA	ASH	333	38.014	50.283	27.737	1.00	40.34	AAAA	C
ATOM	3156	CB	ASH	333	38.960	49.499	26.797	1.00	50.50	AAAA	C
ATOM	3157	CG	ASH	333	38.668	49.493	25.310	1.00	59.29	AAAA	C
ATOM	3158	OD1	ASH	333	37.845	48.711	24.784	1.00	64.54	AAAA	O
ATOM	3159	HD2	ASH	333	39.290	50.350	24.467	1.00	45.83	AAAA	H
ATOM	3162	C	ASH	333	36.666	49.581	27.755	1.00	47.63	AAAA	C
ATOM	3163	O	ASH	333	36.462	48.409	27.398	1.00	44.40	AAAA	O
ATOM	3164	H	ILE	334	35.644	50.213	28.315	1.00	54.13	AAAA	H
ATOM	3166	CA	ILE	334	34.332	49.537	28.460	1.00	59.07	AAAA	C
ATOM	3167	CB	ILE	334	33.788	49.826	29.876	1.00	61.98	AAAA	C
ATOM	3168	CG2	ILE	334	32.362	49.355	30.047	1.00	54.04	AAAA	C
ATOM	3169	CG1	ILE	334	34.737	49.224	30.915	1.00	60.43	AAAA	C
ATOM	3170	CD1	ILE	334	34.346	49.687	32.317	1.00	68.57	AAAA	C
ATOM	3171	C	ILE	334	33.271	50.032	27.476	1.00	59.45	AAAA	C
ATOM	3172	O	ILE	334	32.726	51.136	27.635	1.00	56.22	AAAA	O
ATOM	3173	H	ARG	335	32.919	49.181	26.550	1.00	59.69	AAAA	H
ATOM	3175	CA	ARG	335	31.910	49.567	25.573	1.00	73.93	AAAA	C
ATOM	3176	CB	ARG	335	32.262	48.903	24.240	1.00	74.44	AAAA	C
ATOM	3177	CG	ARG	335	33.729	48.932	23.918	1.00	82.97	AAAA	C
ATOM	3178	CD	ARG	335	34.102	49.289	22.500	1.00	86.49	AAAA	C
ATOM	3179	HE	ARG	335	34.361	48.040	21.777	1.00	89.93	AAAA	H
ATOM	3181	CE	ARG	335	34.011	47.838	20.496	1.00	93.67	AAAA	C
ATOM	3182	HH1	ARG	335	33.409	48.852	19.843	1.00	87.24	AAAA	H
ATOM	3185	HH2	ARG	335	34.256	46.674	19.877	1.00	75.31	AAAA	H
ATOM	3188	C	ARG	335	30.492	49.233	26.021	1.00	81.52	AAAA	C
ATOM	3189	O	ARG	335	29.664	50.115	26.239	1.00	84.11	AAAA	O
ATOM	3190	H	ALA	336	30.208	47.953	26.234	1.00	87.51	AAAA	H
ATOM	3192	CA	ALA	336	28.878	47.484	26.601	1.00	92.40	AAAA	C
ATOM	3193	CB	ALA	336	28.835	45.980	26.633	1.00	94.03	AAAA	C
ATOM	3194	C	ALA	336	28.479	48.058	27.953	1.00	96.61	AAAA	C
ATOM	3195	O	ALA	336	29.316	48.019	28.855	1.00	96.96	AAAA	O
ATOM	3196	H	GLY	337	27.298	48.685	28.039	1.00	99.74	AAAA	H
ATOM	3198	CA	GLY	337	26.986	49.385	29.272	1.00	103.11	AAAA	C
ATOM	3199	C	GLY	337	25.568	49.303	29.763	1.00	105.51	AAAA	C
ATOM	3200	O	GLY	337	24.801	50.267	29.596	1.00	106.64	AAAA	O
ATOM	3201	H	ASH	338	25.243	48.145	30.346	1.00	105.41	AAAA	H
ATOM	3203	CA	ASH	338	23.886	48.017	30.908	1.00	106.92	AAAA	C
ATOM	3204	CB	ASH	338	23.714	46.689	31.624	1.00	109.14	AAAA	C
ATOM	3205	CG	ASH	338	24.403	45.544	30.928	1.00	112.30	AAAA	C
ATOM	3206	OD1	ASH	338	25.598	45.595	30.625	1.00	117.94	AAAA	O
ATOM	3207	HD2	ASH	338	23.604	44.508	30.683	1.00	113.72	AAAA	H
ATOM	3210	C	ASH	338	23.790	49.160	31.931	1.00	105.84	AAAA	C

32/58

ATOM	3211	O	ASH	338	23.544	50.345	31.739	1.00103.87	AAAA	O	
ATOM	3212	H	ASH	339	24.299	48.762	33.093	1.00105.47	AAAA	H	
ATOM	3214	CA	ASH	339	24.529	49.740	34.159	1.00107.19	AAAA	C	
ATOM	3215	CB	ASH	339	23.252	49.915	34.945	1.00109.15	AAAA	C	
ATOM	3216	CG	ASH	339	22.777	51.351	35.003	0.01107.52	AAAA	C	
ATOM	3217	OD1	ASH	339	22.715	51.931	36.088	0.01107.49	AAAA	O	
ATOM	3218	HD2	ASH	339	22.441	51.932	33.859	0.01107.46	AAAA	H	
ATOM	3221	C	ASH	339	25.697	49.237	35.007	1.00106.33	AAAA	C	
ATOM	3222	O	ASH	339	25.520	48.390	35.886	1.00108.82	AAAA	O	
ATOM	3223	H	ILE	340	26.897	49.527	34.510	1.00101.36	AAAA	H	
ATOM	3225	CA	ILE	340	28.136	49.101	35.138	1.00	97.43	AAAA	C
ATOM	3226	CB	ILE	340	29.040	48.354	34.151	1.00	93.63	AAAA	C
ATOM	3227	CG2	ILE	340	28.194	47.252	33.489	1.00	99.38	AAAA	C
ATOM	3228	CG1	ILE	340	29.726	49.158	33.070	1.00	85.50	AAAA	C
ATOM	3229	CD1	ILE	340	28.897	49.634	31.915	1.00	92.53	AAAA	C
ATOM	3230	C	ILE	340	28.783	50.357	35.706	1.00	95.32	AAAA	C
ATOM	3231	O	ILE	340	29.472	51.099	34.997	1.00	97.86	AAAA	O
ATOM	3232	H	ALA	341	28.409	50.739	36.915	1.00	89.89	AAAA	H
ATOM	3234	CA	ALA	341	28.892	52.008	37.450	1.00	88.45	AAAA	C
ATOM	3235	CB	ALA	341	28.068	53.201	37.006	1.00	84.56	AAAA	C
ATOM	3236	C	ALA	341	28.786	51.968	38.970	1.00	85.37	AAAA	C
ATOM	3237	O	ALA	341	28.910	52.935	39.690	1.00	86.09	AAAA	O
ATOM	3238	H	SER	342	28.204	50.877	39.386	1.00	84.24	AAAA	H
ATOM	3240	CA	SER	342	27.910	50.601	40.780	1.00	82.05	AAAA	C
ATOM	3241	CB	SER	342	26.426	50.667	41.112	1.00	85.51	AAAA	C
ATOM	3242	CG	SER	342	26.145	51.271	42.361	1.00	86.02	AAAA	C
ATOM	3244	C	SER	342	28.487	49.196	40.965	1.00	76.62	AAAA	C
ATOM	3245	O	SER	342	29.119	48.966	41.964	1.00	71.76	AAAA	O
ATOM	3246	H	GLU	343	28.373	48.409	39.905	1.00	76.23	AAAA	H
ATOM	3248	CA	GLU	343	29.001	47.109	39.820	1.00	74.59	AAAA	C
ATOM	3249	CB	GLU	343	28.595	46.300	38.616	1.00	78.62	AAAA	C
ATOM	3250	CG	GLU	343	27.118	46.105	38.316	1.00	85.33	AAAA	C
ATOM	3251	CD	GLU	343	26.898	45.121	37.169	1.00	92.76	AAAA	C
ATOM	3252	OE1	GLU	343	27.209	43.911	37.310	1.00	96.41	AAAA	O
ATOM	3253	OE2	GLU	343	26.423	45.517	36.082	1.00	98.55	AAAA	O
ATOM	3254	C	GLU	343	30.525	47.319	39.804	1.00	77.75	AAAA	C
ATOM	3255	O	GLU	343	31.273	46.787	40.637	1.00	75.73	AAAA	O
ATOM	3256	H	LEU	344	31.022	48.237	38.966	1.00	75.65	AAAA	H
ATOM	3258	CA	LEU	344	32.415	48.596	38.839	1.00	72.36	AAAA	C
ATOM	3259	CB	LEU	344	32.760	49.697	37.808	1.00	64.33	AAAA	C
ATOM	3260	CG	LEU	344	32.687	49.397	36.311	1.00	50.12	AAAA	C
ATOM	3261	CD1	LEU	344	33.224	50.577	35.519	1.00	57.00	AAAA	C
ATOM	3262	CD2	LEU	344	33.401	48.127	35.905	1.00	51.62	AAAA	C
ATOM	3263	C	LEU	344	32.963	49.130	40.174	1.00	69.74	AAAA	C
ATOM	3264	O	LEU	344	34.079	48.739	40.551	1.00	69.12	AAAA	O
ATOM	3265	H	GLU	345	32.166	49.959	40.822	1.00	63.10	AAAA	H
ATOM	3267	CA	GLU	345	32.555	50.591	42.061	1.00	65.42	AAAA	C
ATOM	3268	CB	GLU	345	31.592	51.714	42.478	1.00	55.59	AAAA	C
ATOM	3269	CG	GLU	345	32.267	52.607	43.486	1.00	68.78	AAAA	C
ATOM	3270	CD	GLU	345	31.324	53.374	44.376	1.00	81.31	AAAA	C
ATOM	3271	OE1	GLU	345	30.614	54.320	43.976	1.00	85.60	AAAA	O
ATOM	3272	OE2	GLU	345	31.237	53.078	45.595	1.00	88.79	AAAA	O
ATOM	3273	C	GLU	345	32.706	49.652	43.255	1.00	63.31	AAAA	C
ATOM	3274	O	GLU	345	33.501	49.913	44.134	1.00	60.06	AAAA	O
ATOM	3275	H	ASH	346	32.151	48.462	43.202	1.00	62.25	AAAA	H
ATOM	3277	CA	ASH	346	32.285	47.403	44.173	1.00	63.82	AAAA	C
ATOM	3278	CB	ASH	346	31.024	46.498	44.095	1.00	61.66	AAAA	C
ATOM	3279	CG	ASH	346	31.110	45.292	45.006	1.00	58.73	AAAA	C
ATOM	3280	OD1	ASH	346	31.188	45.252	46.224	1.00	69.11	AAAA	O
ATOM	3261	HD2	ASH	346	31.155	44.092	44.444	1.00	51.10	AAAA	H
ATOM	3284	C	ASH	346	33.532	46.580	43.870	1.00	63.71	AAAA	C
ATOM	3285	O	ASH	346	33.636	45.336	43.905	1.00	65.65	AAAA	O
ATOM	3286	H	PHE	347	34.419	47.173	43.066	1.00	63.23	AAAA	H
ATOM	3288	CA	PHE	347	35.540	46.411	42.506	1.00	61.39	AAAA	C
ATOM	3289	CB	PHE	347	35.123	45.854	41.170	1.00	61.38	AAAA	C
ATOM	3290	CG	PHE	347	34.457	44.534	41.142	1.00	65.57	AAAA	C
ATOM	3291	CD1	PHE	347	33.090	44.438	40.982	1.00	75.25	AAAA	C
ATOM	3292	CD2	PHE	347	35.148	43.351	41.267	1.00	77.15	AAAA	C
ATOM	3293	CE1	PHE	347	32.425	43.224	40.951	1.00	75.55	AAAA	C
ATOM	3294	CE2	PHE	347	34.512	42.130	41.249	1.00	72.86	AAAA	C
ATOM	3295	C	PHE	347	33.152	42.051	41.095	1.00	72.74	AAAA	C
ATOM	3296	O	PHE	347	36.712	47.375	42.440	1.00	57.70	AAAA	O
ATOM	3297	H	PHE	347	37.770	46.820	42.354	1.00	59.92	AAAA	H
ATOM	3298	H	HET	348	36.482	48.676	42.319	1.00	50.56	AAAA	H
ATOM	3300	CA	HET	348	37.500	49.630	41.964	1.00	42.86	AAAA	C
ATOM	3301	CB	HET	348	37.402	50.096	40.493	1.00	31.72	AAAA	C
ATOM	3302	CG	HET	348	37.426	48.933	39.471	1.00	33.42	AAAA	C
ATOM	3303	SD	HET	348	37.566	49.448	37.732	1.00	44.79	AAAA	S
ATOM	3304	CE	HET	348	38.408	50.999	37.791	1.00	59.57	AAAA	C
ATOM	3305	C	HET	348	37.368	50.831	42.867	1.00	45.88	AAAA	C
ATOM	3306	O	HET	348	39.210	51.772	42.901	1.00	43.33	AAAA	O
ATOM	3307	H	GLY	349	36.296	50.783	43.683	1.00	45.30	AAAA	H
ATOM	3309	CA	GLY	349	35.998	51.965	44.504	1.00	49.19	AAAA	C
ATOM	3310	C	GLY	349	36.980	52.189	45.620	1.00	52.77	AAAA	C
ATOM	3311	O	GLY	349	37.033	53.299	46.156	1.00	53.43	AAAA	O

33/58

ATOH	3312	H	LEU	350	37.791	51.150	41.921	1.00	56.17	AAAA	H
ATOH	3314	CA	LEU	350	38.735	51.256	47.001	1.00	58.04	AAAA	C
ATOH	3315	CR	LEU	350	38.873	49.949	47.854	1.00	49.00	AAAA	C
ATOH	3316	CG	LEU	350	37.871	50.020	49.031	1.00	50.79	AAAA	C
ATOH	3317	CD1	LEU	350	37.705	48.680	49.760	1.00	52.92	AAAA	C
ATOH	3318	CD2	LEU	350	38.247	51.106	50.038	1.00	56.11	AAAA	C
ATOH	3319	C	LEU	350	40.144	51.727	46.685	1.00	61.34	AAAA	C
ATOH	3320	O	LEU	350	40.931	51.962	47.619	1.00	63.52	AAAA	O
ATOH	3321	H	ILE	351	40.446	51.677	45.372	1.00	57.89	AAAA	H
ATOH	3323	CA	ILE	351	41.729	52.088	44.873	1.00	48.69	AAAA	C
ATOH	3324	CB	ILE	351	41.814	51.912	43.352	1.00	48.19	AAAA	C
ATOH	3325	CG2	ILE	351	43.121	52.416	42.757	1.00	40.01	AAAA	C
ATOH	3326	CG1	ILE	351	41.535	50.418	43.058	1.00	36.87	AAAA	C
ATOH	3327	CD1	ILE	351	41.172	50.351	41.581	1.00	36.46	AAAA	C
ATOH	3328	C	ILE	351	42.031	53.533	45.178	1.00	46.80	AAAA	C
ATOH	3329	O	ILE	351	41.367	54.358	44.626	1.00	42.87	AAAA	O
ATOH	3330	H	GLU	352	43.002	53.866	46.015	1.00	50.61	AAAA	H
ATOH	3332	CA	GLU	352	43.381	55.241	46.248	1.00	51.20	AAAA	C
ATOH	3333	CB	GLU	352	43.907	55.353	47.678	1.00	52.12	AAAA	C
ATOH	3334	CG	GLU	352	42.912	55.769	48.735	1.00	65.55	AAAA	C
ATOH	3335	CD	GLU	352	43.034	54.834	49.947	1.00	71.49	AAAA	C
ATOH	3336	OE1	GLU	352	43.881	55.244	50.765	1.00	66.09	AAAA	O
ATOH	3337	OE2	GLU	352	42.330	53.799	50.009	1.00	76.07	AAAA	O
ATOH	3338	C	GLU	352	44.502	55.751	45.314	1.00	47.43	AAAA	C
ATOH	3339	O	GLU	352	44.798	56.951	45.182	1.00	40.38	AAAA	O
ATOH	3340	H	VAL	353	45.342	54.838	44.852	1.00	43.54	AAAA	H
ATOH	3342	CA	VAL	353	46.512	55.236	44.078	1.00	43.71	AAAA	C
ATOH	3343	CB	VAL	353	47.759	55.540	44.911	1.00	45.01	AAAA	C
ATOH	3344	CG1	VAL	353	47.766	55.261	46.387	1.00	30.84	AAAA	C
ATOH	3345	CG2	VAL	353	48.988	54.844	44.310	1.00	42.55	AAAA	C
ATOH	3346	C	VAL	353	46.829	54.233	42.957	1.00	41.41	AAAA	C
ATOH	3347	O	VAL	353	46.843	53.005	43.172	1.00	39.19	AAAA	O
ATOH	3348	H	VAL	354	47.074	54.855	41.816	1.00	36.31	AAAA	H
ATOH	3350	CA	VAL	354	47.586	54.092	40.651	1.00	43.97	AAAA	C
ATOH	3351	CB	VAL	354	46.725	54.390	39.407	1.00	40.86	AAAA	C
ATOH	3352	CG1	VAL	354	47.347	53.896	36.123	1.00	36.72	AAAA	C
ATOH	3353	CG2	VAL	354	45.293	53.849	39.678	1.00	35.35	AAAA	C
ATOH	3354	C	VAL	354	49.043	54.510	40.388	1.00	44.56	AAAA	C
ATOH	3355	O	VAL	354	49.366	55.718	40.288	1.00	43.32	AAAA	O
ATOH	3356	H	THR	355	49.972	53.561	40.431	1.00	43.83	AAAA	H
ATOH	3358	CA	THR	355	51.392	53.914	40.284	1.00	44.85	AAAA	C
ATOH	3359	CB	THR	355	52.374	52.789	40.653	1.00	42.40	AAAA	C
ATOH	3360	OG1	THR	355	52.273	51.744	39.695	1.00	45.30	AAAA	O
ATOH	3362	CG2	THR	355	52.210	52.194	42.039	1.00	38.13	AAAA	C
ATOH	3363	C	THR	355	51.746	54.339	38.851	1.00	43.84	AAAA	C
ATOH	3364	O	THR	355	52.463	55.334	38.697	1.00	44.26	AAAA	O
ATOH	3365	H	GLY	356	51.127	53.704	37.870	1.00	41.16	AAAA	H
ATOH	3367	CA	GLY	356	51.358	54.073	36.470	1.00	37.91	AAAA	C
ATOH	3368	C	GLY	356	50.505	55.264	35.955	1.00	38.07	AAAA	C
ATOH	3369	O	GLY	356	50.364	56.261	36.615	1.00	34.65	AAAA	O
ATOH	3370	H	TYR	357	49.910	55.004	34.800	1.00	38.47	AAAA	H
ATOH	3372	CA	TYR	357	48.982	55.973	34.205	1.00	38.03	AAAA	C
ATOH	3373	CB	TYR	357	49.557	56.343	32.905	1.00	31.44	AAAA	C
ATOH	3374	CG	TYR	357	49.473	55.219	31.812	1.00	33.04	AAAA	C
ATOH	3375	CD1	TYR	357	48.333	54.842	31.077	1.00	32.86	AAAA	C
ATOH	3376	CE1	TYR	357	48.352	53.779	30.175	1.00	32.83	AAAA	C
ATOH	3377	CD2	TYR	357	50.639	54.465	31.606	1.00	34.28	AAAA	C
ATOH	3378	CE2	TYR	357	50.706	53.402	30.720	1.00	32.51	AAAA	C
ATOH	3379	CG	TYR	357	49.552	53.068	30.007	1.00	37.26	AAAA	C
ATOH	3380	CH	TYR	357	49.726	51.997	29.166	1.00	35.85	AAAA	O
ATOH	3382	C	TYR	357	47.582	55.368	34.150	1.00	38.55	AAAA	C
ATOH	3383	O	TYR	357	47.458	54.127	34.088	1.00	36.11	AAAA	O
ATOH	3384	H	VAL	358	46.593	56.216	33.814	1.00	40.98	AAAA	H
ATOH	3386	CA	VAL	358	45.197	55.798	33.639	1.00	38.90	AAAA	C
ATOH	3387	CB	VAL	358	44.211	56.502	34.610	1.00	49.15	AAAA	C
ATOH	3388	CG1	VAL	358	42.815	55.883	34.484	1.00	33.12	AAAA	C
ATOH	3389	CG2	VAL	358	44.748	56.437	36.043	1.00	29.20	AAAA	C
ATOH	3390	C	VAL	358	44.760	56.194	32.234	1.00	35.64	AAAA	C
ATOH	3391	O	VAL	358	44.792	57.358	31.885	1.00	34.58	AAAA	O
ATOH	3392	H	LYS	359	44.387	55.188	31.461	1.00	36.00	AAAA	H
ATOH	3394	CA	LYS	359	43.898	55.419	30.117	1.00	41.27	AAAA	C
ATOH	3395	CB	LYS	359	44.845	54.707	29.174	1.00	37.40	AAAA	C
ATOH	3396	CG	LYS	359	44.340	54.473	27.770	1.00	45.19	AAAA	C
ATOH	3397	CD	LYS	359	45.040	55.517	26.750	1.00	43.40	AAAA	C
ATOH	3398	CE	LYS	359	45.958	54.402	25.986	1.00	43.56	AAAA	C
ATOH	3399	HE	LYS	359	45.416	53.937	24.680	1.00	47.98	AAAA	H
ATOH	3403	C	LYS	359	42.423	54.979	29.939	1.00	42.14	AAAA	C
ATOH	3404	O	LYS	359	42.056	53.791	30.006	1.00	40.40	AAAA	O
ATOH	3405	H	ILE	360	41.602	55.974	29.572	1.00	37.16	AAAA	H
ATOH	3407	CA	ILE	360	40.164	55.742	29.334	1.00	40.02	AAAA	C
ATOH	3408	CB	ILE	360	39.297	56.804	30.048	1.00	38.10	AAAA	C
ATOH	3409	CG2	ILE	360	37.887	56.277	29.932	1.00	39.42	AAAA	C
ATOH	3410	CG1	ILE	360	39.769	57.111	31.481	1.00	28.54	AAAA	C
ATOH	3411	CD1	ILE	360	39.423	56.037	32.491	1.00	33.16	AAAA	C
ATOH	3412	C	ILE	360	39.888	55.837	27.834	1.00	39.49	AAAA	C

34/58

ATOH	3413	O	ILE	360	40.014	56.942	27.235	1.00	37.32	AAAA	O
ATOH	3414	H	ARG	361	39.567	54.721	27.221	1.00	34.34	AAAA	H
ATOH	3416	CA	ARG	361	39.472	54.782	25.744	1.00	41.24	AAAA	C
ATOH	3417	CB	ARG	361	40.783	54.213	25.140	1.00	47.92	AAAA	C
ATOH	3418	CG	ARG	361	40.805	54.203	23.646	1.00	50.39	AAAA	C
ATOH	3419	CD	ARG	361	41.943	53.357	23.116	1.00	51.36	AAAA	C
ATOH	3420	HE	ARG	361	41.473	51.974	23.263	1.00	50.97	AAAA	H
ATOH	3422	CE	ARG	361	42.297	50.962	23.490	1.00	55.78	AAAA	C
ATOH	3423	HH1	ARG	361	43.612	51.074	23.616	1.00	51.62	AAAA	H
ATOH	3426	HH2	ARG	361	41.834	49.719	23.631	1.00	54.52	AAAA	H
ATOH	3429	C	ARG	361	38.382	53.866	25.246	1.00	42.06	AAAA	C
ATOH	3430	O	ARG	361	38.336	52.661	25.499	1.00	38.93	AAAA	O
ATOH	3431	H	HIS	362	37.514	54.342	24.373	1.00	46.19	AAAA	H
ATOH	3433	CA	HIS	362	36.372	53.555	23.885	1.00	49.34	AAAA	C
ATOH	3434	CB	HIS	362	37.000	52.300	23.266	1.00	49.94	AAAA	C
ATOH	3435	CG	HIS	362	37.849	52.610	22.084	1.00	42.70	AAAA	C
ATOH	3436	CD2	HIS	362	38.049	53.765	21.411	1.00	48.32	AAAA	C
ATOH	3437	HD1	HIS	362	38.628	51.676	21.469	1.00	43.59	AAAA	H
ATOH	3439	CE1	HIS	362	39.256	52.247	20.465	1.00	46.01	AAAA	C
ATOH	3440	HE2	HIS	362	38.923	53.515	20.408	1.00	49.22	AAAA	H
ATOH	3442	C	HIS	362	35.295	53.113	24.913	1.00	50.32	AAAA	C
ATOH	3443	O	HIS	362	34.686	52.030	24.795	1.00	41.31	AAAA	O
ATOH	3444	N	SER	363	35.222	53.875	26.013	1.00	46.96	AAAA	H
ATOH	3446	CA	SER	363	34.402	53.456	27.139	1.00	52.19	AAAA	C
ATOH	3447	CB	SER	363	35.231	53.837	28.400	1.00	53.73	AAAA	C
ATOH	3448	CG	SER	363	35.713	52.558	28.816	1.00	41.72	AAAA	O
ATOH	3450	C	SER	363	33.005	54.072	27.046	1.00	49.08	AAAA	C
ATOH	3451	O	SER	363	32.653	55.040	27.694	1.00	37.49	AAAA	O
ATOH	3452	H	HIS	364	32.243	53.577	26.058	1.00	52.25	AAAA	H
ATOH	3454	CA	HIS	364	30.954	54.173	25.717	1.00	53.66	AAAA	C
ATOH	3455	C	HIS	364	29.879	53.937	26.760	1.00	46.77	AAAA	C
ATOH	3456	O	HIS	364	29.297	54.899	27.280	1.00	51.44	AAAA	O
ATOH	3457	CB	HIS	364	30.485	53.699	24.348	1.00	49.83	AAAA	C
ATOH	3458	CG	HIS	364	31.493	54.182	23.338	1.00	51.51	AAAA	C
ATOH	3459	HD1	HIS	364	31.870	55.502	23.156	1.00	44.83	AAAA	H
ATOH	3460	CE1	HIS	364	32.758	55.533	22.214	1.00	28.57	AAAA	C
ATOH	3461	CD2	HIS	364	32.194	53.393	22.472	1.00	38.62	AAAA	C
ATOH	3462	HE2	HIS	364	32.992	54.274	21.810	1.00	41.44	AAAA	H
ATOH	3464	H	ALA	365	29.949	52.819	27.427	1.00	47.53	AAAA	H
ATOH	3466	CA	ALA	365	29.211	52.488	28.621	1.00	44.41	AAAA	C
ATOH	3467	CB	ALA	365	29.678	51.133	29.150	1.00	40.28	AAAA	C
ATOH	3468	C	ALA	365	29.318	53.473	29.768	1.00	44.70	AAAA	C
ATOH	3469	O	ALA	365	28.576	53.206	30.726	1.00	45.28	AAAA	O
ATOH	3470	H	LEU	366	30.158	54.517	29.762	1.00	40.80	AAAA	H
ATOH	3472	CA	LEU	366	30.415	55.243	30.968	1.00	42.21	AAAA	C
ATOH	3473	CB	LEU	366	31.885	55.241	31.350	1.00	43.78	AAAA	C
ATOH	3474	CG	LEU	366	32.740	54.037	31.667	1.00	51.52	AAAA	C
ATOH	3475	CD1	LEU	366	34.192	54.373	32.043	1.00	51.77	AAAA	C
ATOH	3476	CD2	LEU	366	32.118	53.305	32.834	1.00	51.17	AAAA	C
ATOH	3477	C	LEU	366	29.974	56.687	30.896	1.00	46.36	AAAA	C
ATOH	3478	O	LEU	366	30.305	57.248	29.849	1.00	48.40	AAAA	O
ATOH	3479	H	VAL	367	29.521	57.275	32.015	1.00	43.68	AAAA	H
ATOH	3481	CA	VAL	367	29.072	58.675	31.940	1.00	44.18	AAAA	C
ATOH	3482	CB	VAL	367	27.557	58.727	32.376	1.00	48.80	AAAA	C
ATOH	3483	CG1	VAL	367	26.923	60.073	32.571	1.00	41.69	AAAA	C
ATOH	3484	CG2	VAL	367	26.697	57.949	31.365	1.00	34.00	AAAA	C
ATOH	3485	C	VAL	367	29.923	59.518	32.845	1.00	44.90	AAAA	C
ATOH	3486	O	VAL	367	29.965	60.751	32.720	1.00	44.75	AAAA	O
ATOH	3487	H	SER	368	30.591	58.818	33.757	1.00	48.72	AAAA	H
ATOH	3489	CA	SER	368	31.487	59.465	34.742	1.00	52.70	AAAA	C
ATOH	3490	CB	SER	368	30.658	59.706	36.000	1.00	55.32	AAAA	C
ATOH	3491	CG	SER	368	31.300	60.298	37.091	1.00	64.86	AAAA	O
ATOH	3493	C	SER	368	32.590	58.497	35.179	1.00	52.76	AAAA	C
ATOH	3494	O	SER	368	32.352	57.299	34.976	1.00	48.99	AAAA	O
ATOH	3495	H	LEU	369	33.631	59.012	35.831	1.00	53.86	AAAA	H
ATOH	3497	CA	LEU	369	34.716	58.129	36.274	1.00	60.15	AAAA	C
ATOH	3498	CB	LEU	369	36.073	58.630	35.784	1.00	55.91	AAAA	C
ATOH	3499	CG	LEU	369	36.325	58.736	34.271	1.00	45.96	AAAA	C
ATOH	3500	CD1	LEU	369	37.669	59.428	34.154	1.00	53.97	AAAA	C
ATOH	3501	CD2	LEU	369	36.207	57.384	33.619	1.00	38.77	AAAA	C
ATOH	3502	C	LEU	369	34.645	58.036	37.811	1.00	62.52	AAAA	C
ATOH	3503	O	LEU	369	35.569	57.700	38.595	1.00	59.33	AAAA	O
ATOH	3504	H	SER	370	33.437	58.401	38.285	1.00	56.26	AAAA	H
ATOH	3506	CA	SER	370	33.089	58.431	39.690	1.00	53.88	AAAA	C
ATOH	3507	CB	SER	370	31.673	59.052	39.816	1.00	57.50	AAAA	C
ATOH	3508	CG	SER	370	30.771	58.061	39.261	1.00	69.12	AAAA	O
ATOH	3510	C	SER	370	33.060	57.085	40.412	1.00	47.97	AAAA	C
ATOH	3511	O	SER	370	33.228	56.943	41.596	1.00	41.93	AAAA	O
ATOH	3512	H	PHE	371	32.967	55.936	39.792	1.00	45.48	AAAA	H
ATOH	3514	CA	PHE	371	33.223	54.643	40.356	1.00	46.29	AAAA	C
ATOH	3515	CB	PHE	371	32.952	53.596	39.287	1.00	43.53	AAAA	C
ATOH	3516	CG	PHE	371	33.724	53.629	38.012	1.00	56.45	AAAA	C
ATOH	3517	CD1	PHE	371	34.805	52.807	37.764	1.00	58.95	AAAA	C
ATOH	3518	CD2	PHE	371	33.371	54.515	37.004	1.00	53.92	AAAA	C
ATOH	3519	CE1	PHE	371	35.498	52.842	36.570	1.00	59.50	AAAA	C

35/58

ATOH	3520	CE2	PHE	371	34.040	54.546	35.817	1.00	56.49	AAAA	C
ATOH	3521	CO	PHE	371	35.119	53.716	35.579	1.00	56.39	AAAA	C
ATOH	3522	C	PHE	371	34.654	54.467	40.895	1.00	54.84	AAAA	C
ATOH	3523	O	PHE	371	35.005	53.592	41.728	1.00	52.23	AAAA	C
ATOH	3524	H	LEU	372	35.633	55.305	40.510	1.00	50.17	AAAA	H
ATOH	3526	CA	LEU	372	36.928	55.395	41.109	1.00	46.25	AAAA	C
ATOH	3527	CB	LEU	372	38.171	55.812	40.276	1.00	44.82	AAAA	C
ATOH	3528	CG	LEU	372	38.411	54.800	39.114	1.00	36.78	AAAA	C
ATOH	3529	CD1	LEU	372	38.853	55.643	37.934	1.00	45.04	AAAA	C
ATOH	3530	CD2	LEU	372	39.260	53.657	39.565	1.00	35.55	AAAA	C
ATOH	3531	C	LEU	372	36.715	56.392	42.243	1.00	42.26	AAAA	C
ATOH	3532	O	LEU	372	37.224	57.507	42.364	1.00	38.37	AAAA	O
ATOH	3533	H	LYS	373	35.970	55.862	43.192	1.00	47.06	AAAA	H
ATOH	3535	CA	LYS	373	35.527	56.509	44.415	1.00	50.19	AAAA	C
ATOH	3536	CB	LYS	373	34.546	55.521	45.077	1.00	56.74	AAAA	C
ATOH	3537	CG	LYS	373	33.645	56.162	46.119	1.00	59.64	AAAA	C
ATOH	3538	CD	LYS	373	32.529	56.955	45.441	0.01	60.17	AAAA	C
ATOH	3539	CE	LYS	373	31.674	57.687	46.460	0.01	60.45	AAAA	C
ATOH	3540	HC	LYS	373	31.083	58.933	45.899	0.01	60.38	AAAA	H
ATOH	3544	C	LYS	373	36.646	56.863	45.366	1.00	49.72	AAAA	C
ATOH	3545	O	LYS	373	36.636	57.960	45.907	1.00	42.42	AAAA	O
ATOH	3546	H	ASH	374	37.657	55.986	45.513	1.00	54.43	AAAA	H
ATOH	3548	CA	ASH	374	38.765	56.352	46.410	1.00	59.92	AAAA	C
ATOH	3549	CB	ASH	374	39.080	55.154	47.314	1.00	63.16	AAAA	C
ATOH	3550	CG	ASH	374	38.009	54.978	48.396	1.00	64.53	AAAA	C
ATOH	3551	OD1	ASH	374	37.892	53.972	49.096	1.00	66.40	AAAA	C
ATOH	3552	HD2	ASH	374	37.160	55.965	48.578	1.00	52.88	AAAA	O
ATOH	3555	C	ASH	374	40.043	56.892	45.786	1.00	62.35	AAAA	C
ATOH	3556	O	ASH	374	41.031	57.223	46.479	1.00	63.08	AAAA	O
ATOH	3557	H	LEU	375	40.091	56.893	44.438	1.00	58.34	AAAA	H
ATOH	3559	CA	LEU	375	41.305	57.374	43.795	1.00	54.73	AAAA	C
ATOH	3560	CB	LEU	375	41.099	57.359	42.288	1.00	56.41	AAAA	C
ATOH	3561	CG	LEU	375	42.396	57.422	41.459	1.00	54.12	AAAA	C
ATOH	3562	CD1	LEU	375	43.135	56.112	41.689	1.00	37.88	AAAA	C
ATOH	3563	CD2	LEU	375	42.030	57.796	40.041	1.00	40.97	AAAA	C
ATOH	3564	C	LEU	375	41.712	58.754	44.245	1.00	52.37	AAAA	C
ATOH	3565	O	LEU	375	41.151	59.777	43.877	1.00	52.11	AAAA	O
ATOH	3566	H	ARG	376	42.801	58.874	44.982	1.00	55.16	AAAA	H
ATOH	3568	CA	ARG	376	43.320	60.155	45.434	1.00	55.45	AAAA	C
ATOH	3569	CB	ARG	376	43.706	60.222	46.928	1.00	58.68	AAAA	C
ATOH	3570	CG	ARG	376	44.288	58.907	47.415	1.00	69.10	AAAA	C
ATOH	3571	CD	ARG	376	44.286	58.817	48.944	1.00	81.17	AAAA	C
ATOH	3572	HE	ARG	376	45.377	57.926	49.410	1.00	84.46	AAAA	H
ATOH	3574	CZ	ARG	376	46.618	58.380	49.598	1.00	85.64	AAAA	C
ATOH	3575	HH1	ARG	376	46.966	59.645	49.383	1.00	81.84	AAAA	H
ATOH	3578	HH2	ARG	376	47.571	57.548	50.012	1.00	94.15	AAAA	H
ATOH	3581	C	ARG	376	44.556	60.544	44.633	1.00	50.16	AAAA	C
ATOH	3582	O	ARG	376	44.746	61.728	44.465	1.00	44.25	AAAA	O
ATOH	3583	H	LEU	377	45.375	59.578	44.219	1.00	50.99	AAAA	H
ATOH	3585	CA	LEU	377	46.526	59.942	43.379	1.00	49.40	AAAA	C
ATOH	3586	CB	LEU	377	47.596	60.411	44.329	1.00	64.72	AAAA	C
ATOH	3587	CG	LEU	377	48.806	59.577	44.667	1.00	70.76	AAAA	C
ATOH	3588	CD1	LEU	377	50.031	60.157	43.954	1.00	63.32	AAAA	C
ATOH	3589	CD2	LEU	377	49.010	59.696	46.179	1.00	68.60	AAAA	C
ATOH	3590	C	LEU	377	47.043	59.022	42.311	1.00	46.33	AAAA	C
ATOH	3591	O	LEU	377	46.868	57.788	42.286	1.00	45.17	AAAA	O
ATOH	3592	H	ILE	378	47.448	59.675	41.199	1.00	45.12	AAAA	H
ATOH	3594	CA	ILE	378	48.042	58.976	40.042	1.00	49.10	AAAA	C
ATOH	3595	CB	ILE	378	47.342	59.303	38.724	1.00	46.36	AAAA	C
ATOH	3596	CG2	ILE	378	48.115	58.696	37.574	1.00	34.36	AAAA	C
ATOH	3597	CG1	ILE	378	45.871	58.862	38.829	1.00	38.59	AAAA	C
ATOH	3598	CD1	ILE	378	44.999	59.515	37.765	1.00	37.18	AAAA	C
ATOH	3599	C	ILE	378	49.524	59.381	40.003	1.00	49.87	AAAA	C
ATOH	3600	O	ILE	378	49.801	60.595	40.040	1.00	44.72	AAAA	O
ATOH	3601	H	LEU	379	50.454	58.423	40.067	1.00	49.97	AAAA	H
ATOH	3603	CA	LEU	379	51.866	58.712	40.344	1.00	48.48	AAAA	C
ATOH	3604	CB	LEU	379	52.575	57.531	41.054	1.00	48.44	AAAA	C
ATOH	3605	CG	LEU	379	52.234	57.363	42.554	1.00	50.28	AAAA	C
ATOH	3606	CD1	LEU	379	52.926	56.187	43.217	1.00	39.89	AAAA	C
ATOH	3607	CD2	LEU	379	52.616	58.625	43.300	1.00	42.89	AAAA	C
ATOH	3608	C	LEU	379	52.609	59.019	39.080	1.00	50.94	AAAA	C
ATOH	3609	O	LEU	379	53.576	59.788	39.139	1.00	54.23	AAAA	O
ATOH	3610	H	GLY	380	52.175	58.423	37.972	1.00	48.67	AAAA	H
ATOH	3612	CA	GLY	380	52.931	58.715	36.702	1.00	49.94	AAAA	C
ATOH	3613	C	GLY	380	54.249	58.155	36.624	1.00	52.70	AAAA	C
ATOH	3614	O	GLY	380	55.026	58.657	35.803	1.00	49.94	AAAA	O
ATOH	3615	H	GLU	381	54.549	57.033	37.272	1.00	52.51	AAAA	H
ATOH	3617	CA	GLU	381	55.849	56.386	37.243	1.00	52.33	AAAA	C
ATOH	3618	CB	GLU	381	56.055	55.310	38.323	1.00	45.22	AAAA	C
ATOH	3619	CG	GLU	381	55.402	55.779	39.636	1.00	52.91	AAAA	C
ATOH	3620	CD	GLU	381	56.050	55.192	40.873	1.00	42.11	AAAA	C
ATOH	3621	OE1	GLU	381	56.160	53.966	40.890	1.00	40.26	AAAA	O
ATOH	3622	OE2	GLU	381	56.379	56.014	41.754	1.00	51.32	AAAA	O
ATOH	3623	C	GLU	381	56.078	55.784	35.859	1.00	55.86	AAAA	C
ATOH	3624	O	GLU	381	57.216	55.652	35.345	1.00	54.61	AAAA	O

36/58

ATOM	3625	H	GLU	382	54.980	55.449	35.157	1.00	53.56	AAAA	H
ATOM	3627	CA	GLU	382	55.091	55.018	33.766	1.00	48.15	AAAA	C
ATOM	3628	CB	GLU	382	55.051	53.550	33.532	1.00	35.27	AAAA	C
ATOM	3629	CG	GLU	382	54.739	53.225	32.051	1.00	49.69	AAAA	C
ATOM	3630	CD	GLU	382	54.676	51.719	31.807	1.00	56.45	AAAA	C
ATOM	3631	OE1	GLU	382	55.062	50.924	32.705	1.00	61.66	AAAA	O
ATOM	3632	OE2	GLU	382	54.264	51.201	30.745	1.00	57.69	AAAA	O
ATOM	3633	C	GLU	382	54.006	55.732	32.973	1.00	50.84	AAAA	C
ATOM	3634	O	GLU	382	53.097	56.282	33.598	1.00	49.44	AAAA	O
ATOM	3635	H	GLU	383	54.347	56.256	31.780	1.00	52.25	AAAA	H
ATOM	3637	CA	GLU	383	53.498	57.153	31.016	1.00	40.15	AAAA	C
ATOM	3638	CB	GLU	383	53.914	58.609	31.155	1.00	28.50	AAAA	C
ATOM	3639	CG	GLU	383	54.489	58.909	32.542	1.00	31.10	AAAA	C
ATOM	3640	CD	GLU	383	54.950	60.301	32.752	1.00	33.19	AAAA	C
ATOM	3641	OE1	GLU	383	55.186	60.840	31.683	1.00	40.34	AAAA	O
ATOM	3642	OE2	GLU	383	55.043	60.943	33.934	1.00	36.30	AAAA	H
ATOM	3645	C	GLU	383	53.426	56.744	29.563	1.00	40.45	AAAA	C
ATOM	3646	O	GLU	383	54.131	55.858	29.139	1.00	43.45	AAAA	O
ATOM	3647	H	LEU	384	52.375	57.195	28.860	1.00	42.54	AAAA	H
ATOM	3649	CA	LEU	384	52.257	56.889	27.443	1.00	43.24	AAAA	C
ATOM	3650	CB	LEU	384	50.814	57.011	26.949	1.00	43.79	AAAA	C
ATOM	3651	CG	LEU	384	49.818	56.235	27.061	1.00	41.21	AAAA	C
ATOM	3652	CD1	LEU	384	48.611	57.095	28.221	1.00	33.99	AAAA	C
ATOM	3653	CD2	LEU	384	49.405	54.968	27.149	1.00	33.20	AAAA	C
ATOM	3654	C	LEU	384	53.204	57.809	26.672	1.00	40.51	AAAA	C
ATOM	3655	O	LEU	384	53.582	58.872	27.177	1.00	29.66	AAAA	O
ATOM	3656	H	GLU	385	53.659	57.319	25.531	1.00	45.22	AAAA	H
ATOM	3658	CA	GLU	385	54.410	58.116	24.570	1.00	49.98	AAAA	C
ATOM	3659	CB	GLU	385	54.424	57.475	23.174	1.00	60.50	AAAA	C
ATOM	3660	CG	GLU	385	55.045	56.095	23.106	1.00	68.76	AAAA	C
ATOM	3661	CD	GLU	385	54.195	54.951	23.592	1.00	72.07	AAAA	C
ATOM	3662	OE1	GLU	385	53.150	55.213	24.244	1.00	81.88	AAAA	O
ATOM	3663	OE2	GLU	385	54.565	53.786	23.301	1.00	73.13	AAAA	O
ATOM	3664	C	GLU	385	53.828	59.515	24.450	1.00	47.41	AAAA	C
ATOM	3665	O	GLU	385	52.635	59.706	24.184	1.00	54.43	AAAA	O
ATOM	3666	H	GLY	386	54.614	60.470	24.902	1.00	43.69	AAAA	H
ATOM	3668	CA	GLY	386	54.181	61.870	24.897	1.00	40.34	AAAA	C
ATOM	3669	C	GLY	386	54.286	62.449	26.308	1.00	40.65	AAAA	C
ATOM	3670	O	GLY	386	53.930	63.615	26.491	1.00	39.75	AAAA	O
ATOM	3671	H	ASH	387	54.441	61.537	27.272	1.00	40.75	AAAA	H
ATOM	3673	CA	ASH	387	54.479	61.912	28.675	1.00	49.18	AAAA	C
ATOM	3674	CB	ASH	387	55.500	63.084	28.874	1.00	44.41	AAAA	C
ATOM	3675	CG	ASH	387	56.925	62.541	28.722	1.00	61.51	AAAA	C
ATOM	3676	OD1	ASH	387	57.199	61.313	28.677	1.00	57.85	AAAA	O
ATOM	3677	OD2	ASH	387	58.063	63.251	28.592	1.00	61.96	AAAA	N
ATOM	3680	C	ASH	387	53.095	62.100	29.299	1.00	48.46	AAAA	C
ATOM	3681	O	ASH	387	52.836	62.891	30.218	1.00	48.99	AAAA	O
ATOM	3682	H	TYR	388	52.214	61.116	29.058	1.00	46.29	AAAA	H
ATOM	3684	CA	TYR	388	50.846	61.199	29.540	1.00	45.09	AAAA	C
ATOM	3695	CB	TYR	388	49.823	60.957	28.399	1.00	40.70	AAAA	C
ATOM	3686	CG	TYR	388	49.925	62.056	27.373	1.00	42.24	AAAA	C
ATOM	3687	CD1	TYR	388	50.343	61.854	26.064	1.00	44.39	AAAA	C
ATOM	3688	CE1	TYR	388	50.401	62.885	25.157	1.00	35.51	AAAA	C
ATOM	3689	CD2	TYR	388	49.625	63.356	27.709	1.00	44.67	AAAA	C
ATOM	3690	CE2	TYR	388	49.699	64.428	26.830	1.00	38.14	AAAA	C
ATOM	3691	CZ	TYR	388	50.087	64.148	25.555	1.00	41.27	AAAA	C
ATOM	3692	OH	TYR	388	50.151	65.181	24.604	1.00	50.18	AAAA	O
ATOM	3694	C	TYR	388	50.563	60.288	30.714	1.00	41.88	AAAA	C
ATOM	3695	O	TYR	388	50.727	59.092	30.511	1.00	32.99	AAAA	O
ATOM	3696	H	SER	389	50.020	60.917	31.753	1.00	45.42	AAAA	H
ATOM	3698	CA	SER	389	49.591	60.131	32.931	1.00	50.13	AAAA	C
ATOM	3699	CB	SER	389	49.798	60.894	34.261	1.00	45.57	AAAA	C
ATOM	3700	OG	SER	389	51.185	60.899	34.504	1.00	51.11	AAAA	O
ATOM	3702	C	SER	389	48.097	59.813	32.804	1.00	48.11	AAAA	C
ATOM	3703	O	SER	389	47.686	58.792	33.336	1.00	49.25	AAAA	O
ATOM	3704	H	PHE	390	47.321	60.685	32.196	1.00	42.56	AAAA	H
ATOM	3706	CA	PHE	390	45.867	60.595	32.146	1.00	40.76	AAAA	C
ATOM	3707	CB	PHE	390	45.241	61.581	33.139	1.00	44.80	AAAA	C
ATOM	3708	CG	PHE	390	43.764	61.358	33.328	1.00	40.53	AAAA	C
ATOM	3709	CD1	PHE	390	43.406	60.273	34.089	1.00	40.80	AAAA	C
ATOM	3710	CD2	PHE	390	42.768	62.157	32.748	1.00	35.59	AAAA	C
ATOM	3711	CE1	PHE	390	42.050	59.985	34.312	1.00	47.09	AAAA	C
ATOM	3712	CE2	PHE	390	41.454	61.824	32.965	1.00	44.50	AAAA	C
ATOM	3713	CZ	PHE	390	41.063	60.745	33.739	1.00	34.54	AAAA	C
ATOM	3714	C	PHE	390	45.372	60.829	30.720	1.00	38.54	AAAA	C
ATOM	3715	O	PHE	390	45.542	61.918	30.126	1.00	40.29	AAAA	O
ATOM	3716	H	TYR	391	44.819	59.818	30.096	1.00	33.48	AAAA	H
ATOM	3718	CA	TYR	391	44.596	59.782	28.663	1.00	38.58	AAAA	C
ATOM	3719	CB	TYR	391	45.579	58.871	27.972	1.00	38.95	AAAA	C
ATOM	3720	CG	TYR	391	45.760	59.006	26.503	1.00	44.54	AAAA	C
ATOM	3721	CD1	TYR	391	46.822	59.815	26.052	1.00	47.14	AAAA	C
ATOM	3722	CE1	TYR	391	47.057	59.993	24.722	1.00	46.03	AAAA	C
ATOM	3723	CD2	TYR	391	44.927	58.390	25.584	1.00	46.94	AAAA	C
ATOM	3724	CE2	TYR	391	45.157	58.560	24.242	1.00	47.45	AAAA	C
ATOM	3725	CZ	TYR	391	46.207	59.350	23.830	1.00	45.84	AAAA	C

37/58

ATOM	3726	OH	TFR	391	46.374	59.492	22.481	1.00	44.76	AAAA	O
ATOM	3728	C	TFR	391	43.194	59.232	22.349	1.00	39.74	AAAA	C
ATOM	3729	O	TFR	391	42.841	59.103	22.736	1.00	38.49	AAAA	O
ATOM	3730	H	VAL	392	42.417	60.158	27.779	1.00	37.07	AAAA	H
ATOM	3732	CA	VAL	392	40.958	59.874	27.603	1.00	39.52	AAAA	C
ATOM	3733	CB	VAL	392	40.075	60.800	28.440	1.00	41.12	AAAA	C
ATOM	3734	CG1	VAL	392	38.612	60.464	28.472	1.00	37.96	AAAA	C
ATOM	3735	CG2	VAL	392	40.666	61.041	29.841	1.00	33.19	AAAA	C
ATOM	3736	C	VAL	392	40.531	60.092	26.182	1.00	31.08	AAAA	C
ATOM	3737	O	VAL	392	40.508	61.277	25.804	1.00	34.71	AAAA	O
ATOM	3738	H	LEU	393	40.299	59.113	25.383	1.00	34.62	AAAA	H
ATOM	3740	CA	LEU	393	39.948	59.259	23.977	1.00	38.12	AAAA	C
ATOM	3741	CB	LEU	393	41.200	59.036	23.096	1.00	42.49	AAAA	C
ATOM	3742	CG	LEU	393	41.023	58.649	21.586	1.00	26.48	AAAA	C
ATOM	3743	CD1	LEU	393	41.128	59.879	20.753	1.00	26.57	AAAA	C
ATOM	3744	CD2	LEU	393	42.078	57.589	21.244	1.00	29.98	AAAA	C
ATOM	3745	C	LEU	393	38.821	58.375	23.492	1.00	39.15	AAAA	C
ATOM	3746	O	LEU	393	38.760	57.173	23.799	1.00	37.90	AAAA	O
ATOM	3747	H	ASP	394	38.015	58.973	22.565	1.00	43.38	AAAA	H
ATOM	3749	CA	ASP	394	36.888	59.215	21.975	1.00	44.77	AAAA	C
ATOM	3750	CB	ASP	394	37.445	57.073	21.120	1.00	44.80	AAAA	C
ATOM	3751	CG	ASP	394	36.466	56.477	20.156	1.00	47.14	AAAA	C
ATOM	3752	GD1	ASP	394	36.750	55.577	19.333	1.00	52.91	AAAA	O
ATOM	3753	OD2	ASP	394	35.311	56.948	20.180	1.00	49.27	AAAA	O
ATOM	3754	C	ASP	394	35.936	57.619	23.021	1.00	43.17	AAAA	C
ATOM	3755	O	ASF	394	35.831	56.385	23.212	1.00	43.51	AAAA	O
ATOM	3756	H	ASH	395	35.299	58.495	23.746	1.00	39.90	AAAA	H
ATOM	3758	CA	ASH	395	34.305	58.158	24.776	1.00	46.32	AAAA	C
ATOM	3759	CB	ASH	395	34.804	59.512	26.212	1.00	42.96	AAAA	C
ATOM	3760	CG	ASH	395	35.992	57.619	26.579	1.00	36.92	AAAA	C
ATOM	3761	OD1	ASH	395	36.013	55.394	26.796	1.00	21.65	AAAA	O
ATOM	3762	HD2	ASH	395	37.075	59.409	26.559	1.00	27.87	AAAA	H
ATOM	3765	C	ASH	395	32.932	58.816	24.541	1.00	40.44	AAAA	C
ATOM	3766	O	ASH	395	32.749	59.982	24.882	1.00	37.06	AAAA	O
ATOM	3767	H	GLH	396	32.073	58.055	23.877	1.00	46.74	AAAA	H
ATOM	3769	CA	GLH	396	30.771	58.582	23.421	1.00	52.93	AAAA	C
ATOM	3770	CB	GLH	396	29.848	57.567	22.744	1.00	52.29	AAAA	C
ATOM	3771	CG	GLH	396	30.173	57.405	21.257	1.00	46.42	AAAA	C
ATOM	3772	CD	GLH	396	29.817	55.991	20.840	1.00	55.21	AAAA	C
ATOM	3773	OE1	GLH	396	28.835	55.421	21.312	1.00	61.17	AAAA	O
ATOM	3774	HE2	GLH	396	30.628	55.411	19.971	1.00	55.79	AAAA	H
ATOM	3777	C	GLH	396	29.874	59.224	24.458	1.00	48.64	AAAA	C
ATOM	3778	O	GLH	396	29.407	60.287	24.113	1.00	51.63	AAAA	O
ATOM	3779	H	ASH	397	29.717	58.681	25.633	1.00	48.95	AAAA	H
ATOM	3781	CA	ASH	397	28.783	59.196	26.632	1.00	51.72	AAAA	C
ATOM	3782	CB	ASH	397	27.969	57.959	27.093	1.00	35.94	AAAA	C
ATOM	3783	CG	ASH	397	27.231	57.430	25.860	1.00	49.09	AAAA	C
ATOM	3784	OD1	ASH	397	26.591	58.304	25.229	1.00	49.32	AAAA	O
ATOM	3785	HD2	ASH	397	27.258	56.175	25.431	1.00	43.31	AAAA	H
ATOM	3788	C	ASH	397	29.367	59.945	27.990	1.00	52.99	AAAA	C
ATOM	3789	O	ASH	397	28.586	60.344	28.627	1.00	53.33	AAAA	O
ATOM	3790	H	LEU	398	30.682	59.990	28.001	1.00	55.73	AAAA	H
ATOM	3792	CA	LEU	398	31.312	60.550	29.179	1.00	52.12	AAAA	C
ATOM	3793	CB	LEU	398	32.827	60.388	29.149	1.00	48.47	AAAA	C
ATOM	3794	CG	LEU	398	33.606	60.283	30.460	1.00	41.81	AAAA	C
ATOM	3795	CD1	LEU	398	33.417	58.939	31.136	1.00	40.35	AAAA	C
ATOM	3796	CD2	LEU	398	35.070	60.608	30.982	1.00	39.03	AAAA	C
ATOM	3797	C	LEU	398	30.923	61.995	29.353	1.00	52.35	AAAA	C
ATOM	3798	O	LEU	398	31.422	62.509	28.681	1.00	49.91	AAAA	O
ATOM	3799	H	GLH	399	30.241	62.225	30.469	1.00	58.76	AAAA	H
ATOM	3801	CA	GLH	399	29.688	63.558	30.796	1.00	60.03	AAAA	C
ATOM	3802	CB	GLH	399	28.236	63.331	31.262	1.00	59.55	AAAA	C
ATOM	3803	CG	GLH	399	27.235	63.962	30.316	1.00	73.07	AAAA	C
ATOM	3804	CD	GLH	399	25.944	63.146	30.340	1.00	78.39	AAAA	C
ATOM	3805	OE1	GLH	399	25.097	63.455	31.194	1.00	71.79	AAAA	O
ATOM	3806	HE2	GLH	399	25.856	62.158	29.440	1.00	69.88	AAAA	H
ATOM	3809	C	GLH	399	30.490	64.252	31.888	1.00	54.49	AAAA	C
ATOM	3810	O	GLH	399	30.528	65.477	32.068	1.00	51.96	AAAA	O
ATOM	3811	H	GLH	400	31.058	63.389	32.734	1.00	50.44	AAAA	H
ATOM	3813	CA	GLH	400	31.938	63.948	33.756	1.00	53.83	AAAA	C
ATOM	3814	CB	GLH	400	31.215	64.314	35.649	1.00	54.97	AAAA	C
ATOM	3815	CG	GLH	400	30.717	63.150	35.997	1.00	58.99	AAAA	C
ATOM	3816	CD	GLH	400	30.678	63.430	37.389	1.00	65.82	AAAA	C
ATOM	3817	OE1	GLH	400	30.906	64.502	37.962	1.00	68.10	AAAA	O
ATOM	3818	HE2	GLH	400	30.341	62.444	38.222	1.00	55.35	AAAA	H
ATOM	3821	C	GLH	400	33.113	63.008	34.052	1.00	52.08	AAAA	C
ATOM	3822	O	GLH	400	33.107	61.783	33.942	1.00	51.90	AAAA	O
ATOM	3823	H	LEU	401	34.073	63.580	34.751	1.00	49.58	AAAA	H
ATOM	3825	CA	LEU	401	35.175	62.844	35.334	1.00	49.57	AAAA	C
ATOM	3826	CB	LEU	401	36.378	63.803	35.260	1.00	47.94	AAAA	C
ATOM	3827	CG	LEU	401	36.638	64.237	33.772	1.00	46.61	AAAA	C
ATOM	3828	CD1	LEU	401	37.658	65.326	33.677	1.00	39.09	AAAA	C
ATOM	3829	CD2	LEU	401	36.919	63.069	31.860	1.00	40.72	AAAA	C
ATOM	3830	C	LEU	401	34.866	62.357	36.734	1.00	51.23	AAAA	C
ATOM	3831	O	LEU	401	34.258	61.299	36.692	1.00	49.06	AAAA	O

38/58

ATOH	3832	H	TRP	402	35.297	63.140	37.690	1.00	54.58	AAAA	H
ATOH	3834	CA	TRP	402	34.975	63.090	39.097	1.00	59.76	AAAA	C
ATOH	3835	CB	TRP	402	36.279	62.953	39.933	1.00	59.56	AAAA	C
ATOH	3836	CG	TRP	402	36.971	61.624	39.737	1.00	58.17	AAAA	C
ATOH	3837	CD2	TRP	402	37.981	61.243	38.784	1.00	53.18	AAAA	C
ATOH	3838	CE2	TRP	402	38.286	59.897	39.002	1.00	56.61	AAAA	C
ATOH	3839	CE3	TRP	402	38.643	61.917	37.764	1.00	43.25	AAAA	C
ATOH	3840	CD1	TRP	402	36.712	60.517	40.459	1.00	53.50	AAAA	C
ATOH	3841	HE1	TRP	402	37.488	59.467	40.032	1.00	57.66	AAAA	H
ATOH	3843	CE2	TRP	402	39.212	59.160	38.249	1.00	51.44	AAAA	C
ATOH	3844	CE3	TRP	402	39.546	61.199	37.026	1.00	53.69	AAAA	C
ATOH	3845	CH2	TRP	402	39.820	59.857	37.263	1.00	50.75	AAAA	C
ATOH	3846	C	TRP	402	34.223	64.389	39.429	1.00	64.09	AAAA	C
ATOH	3847	O	TRP	402	34.408	65.449	38.808	1.00	61.98	AAAA	O
ATOH	3848	H	ASP	403	33.503	64.418	40.551	1.00	68.85	AAAA	H
ATOH	3850	CA	ASP	403	32.947	65.668	41.068	1.00	67.83	AAAA	C
ATOH	3851	CB	ASP	403	31.918	65.343	42.151	1.00	72.19	AAAA	C
ATOH	3852	CG	ASP	403	30.853	66.417	42.306	1.00	73.08	AAAA	C
ATOH	3853	OD1	ASP	403	31.177	67.625	42.297	1.00	71.67	AAAA	O
ATOH	3854	OD2	ASP	403	29.693	65.979	42.454	1.00	75.08	AAAA	O
ATOH	3855	C	ASP	403	34.005	66.607	41.607	1.00	66.63	AAAA	C
ATOH	3856	O	ASP	403	34.245	66.672	42.811	1.00	67.18	AAAA	O
ATOH	3857	H	TRP	404	34.449	67.588	40.846	1.00	69.29	AAAA	H
ATOH	3859	CA	TRP	404	35.412	68.588	41.291	1.00	77.11	AAAA	C
ATOH	3860	CB	TRP	404	35.859	69.409	40.063	1.00	79.10	AAAA	C
ATOH	3861	CG	TRP	404	36.504	68.509	39.047	1.00	82.59	AAAA	C
ATOH	3862	CD2	TRP	404	37.294	67.346	39.322	1.00	84.82	AAAA	C
ATOH	3863	CE2	TRP	404	37.686	66.813	38.081	1.00	84.56	AAAA	C
ATOH	3864	CE3	TRP	404	37.703	66.710	40.506	1.00	80.95	AAAA	C
ATOH	3865	CD1	TRP	404	36.460	68.622	37.694	1.00	83.37	AAAA	C
ATOH	3866	HE1	TRP	404	37.165	67.617	37.111	1.00	80.33	AAAA	H
ATOH	3868	CE2	TRP	404	38.477	65.662	37.982	1.00	85.91	AAAA	C
ATOH	3869	CE3	TRP	404	38.471	65.573	40.392	1.00	86.36	AAAA	C
ATOH	3870	CH2	TRP	404	38.860	65.051	39.133	1.00	85.05	AAAA	C
ATOH	3871	C	TRP	404	35.034	69.517	42.420	1.00	81.60	AAAA	C
ATOH	3872	O	TRP	404	35.387	70.709	42.504	1.00	84.57	AAAA	O
ATOH	3873	H	ASP	405	34.281	69.063	43.393	1.00	84.45	AAAA	H
ATOH	3875	CA	ASP	405	33.771	69.861	44.496	1.00	87.48	AAAA	C
ATOH	3876	CB	ASP	405	32.352	70.365	44.262	1.00	88.04	AAAA	C
ATOH	3877	CG	ASP	405	32.274	71.612	43.409	1.00	92.54	AAAA	C
ATOH	3878	OD1	ASP	405	33.306	72.285	43.207	1.00	94.82	AAAA	O
ATOH	3879	OD2	ASP	405	31.130	71.854	42.955	1.00	95.26	AAAA	O
ATOH	3880	C	ASP	405	33.730	68.906	45.693	1.00	87.80	AAAA	C
ATOH	3881	O	ASP	405	34.245	69.224	46.743	1.00	92.18	AAAA	O
ATOH	3882	H	ALA	406	33.239	67.709	45.460	1.00	84.46	AAAA	H
ATOH	3884	CA	ALA	406	33.176	66.671	46.451	1.00	82.87	AAAA	C
ATOH	3885	CB	ALA	406	31.943	65.805	46.133	1.00	76.32	AAAA	C
ATOH	3886	C	ALA	406	34.445	65.840	46.459	1.00	85.77	AAAA	C
ATOH	3887	O	ALA	406	34.470	64.823	47.185	1.00	89.38	AAAA	O
ATOH	3888	H	ARG	407	35.433	66.073	45.577	1.00	83.74	AAAA	H
ATOH	3890	CA	ARG	407	36.541	65.151	45.400	1.00	79.60	AAAA	C
ATOH	3891	CB	ARG	407	36.165	64.140	44.297	1.00	77.84	AAAA	C
ATOH	3892	CG	ARG	407	35.457	62.950	44.921	1.00	81.91	AAAA	C
ATOH	3893	CD	ARG	407	35.362	61.688	44.113	1.00	86.97	AAAA	C
ATOH	3894	HE	ARG	407	36.281	60.660	44.607	1.00	86.94	AAAA	H
ATOH	3896	CG	ARG	407	37.564	60.583	44.279	1.00	92.14	AAAA	C
ATOH	3897	HH1	ARG	407	38.169	61.441	43.469	1.00	97.06	AAAA	H
ATOH	3900	HH2	ARG	407	38.309	59.616	44.770	1.00	96.33	AAAA	H
ATOH	3903	C	ARG	407	37.880	65.749	45.048	1.00	76.72	AAAA	C
ATOH	3904	O	ARG	407	37.989	66.774	44.410	1.00	77.47	AAAA	O
ATOH	3905	H	ASN	408	38.958	65.081	45.453	1.00	75.75	AAAA	H
ATOH	3907	CA	ASN	408	40.311	65.556	45.173	1.00	73.79	AAAA	C
ATOH	3908	CB	ASN	408	40.938	66.240	46.388	1.00	74.46	AAAA	C
ATOH	3909	CG	ASN	408	41.986	67.242	45.947	1.00	82.51	AAAA	C
ATOH	3910	OD1	ASN	408	41.913	68.429	46.240	1.00	90.33	AAAA	O
ATOH	3911	HD2	ASN	408	43.028	66.821	45.253	1.00	84.46	AAAA	H
ATOH	3914	C	ASN	408	41.257	64.468	44.654	1.00	65.97	AAAA	C
ATOH	3915	O	ASN	408	41.251	63.374	45.151	1.00	63.82	AAAA	O
ATOH	3916	H	LEU	409	42.041	64.793	43.650	1.00	61.41	AAAA	H
ATOH	3918	CA	LEU	409	42.895	63.872	42.947	1.00	60.90	AAAA	C
ATOH	3919	CB	LEU	409	42.153	63.250	41.768	1.00	62.98	AAAA	C
ATOH	3920	CG	LEU	409	42.992	62.553	40.704	1.00	59.77	AAAA	C
ATOH	3921	CD1	LEU	409	43.488	61.205	41.197	1.00	54.06	AAAA	C
ATOH	3922	CD2	LEU	409	42.094	62.445	39.486	1.00	55.74	AAAA	C
ATOH	3923	C	LEU	409	44.151	64.599	42.485	1.00	61.19	AAAA	C
ATOH	3924	O	LEU	409	44.141	65.809	42.370	1.00	60.64	AAAA	O
ATOH	3925	H	THR	410	45.281	63.903	42.424	1.00	63.74	AAAA	H
ATOH	3927	CA	THR	410	46.588	64.462	42.131	1.00	60.44	AAAA	C
ATOH	3928	CB	THR	410	47.454	64.676	43.385	1.00	67.08	AAAA	C
ATOH	3929	OG1	THR	410	46.870	65.746	44.157	1.00	74.29	AAAA	O
ATOH	3931	CG2	THR	410	48.909	65.103	43.162	1.00	48.56	AAAA	C
ATOH	3932	C	THR	410	47.426	63.565	41.218	1.00	56.62	AAAA	C
ATOH	3933	O	THR	410	47.382	62.354	41.317	1.00	54.99	AAAA	O
ATOH	3934	H	ILE	411	48.077	64.245	40.288	1.00	53.97	AAAA	H
ATOH	3936	CA	ILE	411	48.897	63.562	39.291	1.00	53.29	AAAA	C

39/58

ATOM	3937	CE	ILE	411	48.409	63.854	37.864	1.00	49.81	AAAA	C
ATOM	3938	CG2	ILE	411	49.216	63.128	36.806	1.00	30.86	AAAA	C
ATOM	3939	CG1	ILE	411	46.911	63.489	37.729	1.00	40.83	AAAA	C
ATOM	3940	CD1	ILE	411	46.322	63.547	36.338	1.00	38.51	AAAA	C
ATOM	3941	C	ILE	411	50.319	64.018	39.568	1.00	55.38	AAAA	C
ATOM	3942	O	ILE	411	50.656	65.179	39.291	1.00	57.59	AAAA	O
ATOM	3943	H	SER	412	51.073	63.182	40.270	1.00	54.26	AAAA	H
ATOM	3945	CA	SER	412	52.434	63.502	40.689	1.00	54.46	AAAA	C
ATOM	3946	CB	SER	412	53.071	62.210	41.248	1.00	55.78	AAAA	C
ATOM	3947	OG	SER	412	53.756	62.536	42.434	1.00	67.12	AAAA	O
ATOM	3949	C	SER	412	53.326	63.910	39.523	1.00	55.52	AAAA	C
ATOM	3950	O	SER	412	54.081	64.876	39.527	1.00	55.04	AAAA	O
ATOM	3951	H	ALA	413	53.254	63.124	38.438	1.00	50.12	AAAA	H
ATOM	3953	CA	ALA	413	54.064	63.402	37.281	1.00	50.01	AAAA	C
ATOM	3954	CB	ALA	413	55.334	62.520	37.365	1.00	34.96	AAAA	C
ATOM	3955	C	ALA	413	53.301	63.078	35.994	1.00	48.71	AAAA	C
ATOM	3956	O	ALA	413	52.495	62.168	35.998	1.00	48.81	AAAA	O
ATOM	3957	H	GLY	414	53.675	63.690	34.895	1.00	47.92	AAAA	H
ATOM	3959	CA	GLY	414	53.057	63.454	33.607	1.00	51.75	AAAA	C
ATOM	3960	C	GLY	414	52.017	64.524	33.294	1.00	52.77	AAAA	C
ATOM	3961	O	GLY	414	51.684	65.370	34.114	1.00	53.23	AAAA	O
ATOM	3962	H	LYS	415	51.385	64.406	32.138	1.00	56.31	AAAA	H
ATOM	3964	CA	LYS	415	50.289	65.317	31.759	1.00	52.49	AAAA	C
ATOM	3965	CB	LYS	415	50.884	66.358	30.833	1.00	50.94	AAAA	C
ATOM	3966	CG	LYS	415	51.198	65.855	29.429	1.00	54.39	AAAA	C
ATOM	3967	CD	LYS	415	52.288	66.691	28.765	1.00	53.96	AAAA	C
ATOM	3968	CE	LYS	415	52.785	66.151	27.441	1.00	56.01	AAAA	C
ATOM	3969	H2	LYS	415	52.426	67.032	26.284	1.00	66.36	AAAA	H
ATOM	3973	C	LYS	415	49.110	64.576	31.155	1.00	50.04	AAAA	C
ATOM	3974	O	LYS	415	49.077	63.337	31.036	1.00	49.77	AAAA	O
ATOM	3975	H	HET	416	48.091	65.353	30.771	1.00	48.34	AAAA	H
ATOM	3977	CA	HET	416	46.890	64.734	30.186	1.00	46.77	AAAA	C
ATOM	3978	CB	HET	416	45.629	65.186	30.949	1.00	42.79	AAAA	C
ATOM	3979	CG	HET	416	45.836	65.880	32.273	1.00	40.91	AAAA	C
ATOM	3980	SD	HET	416	44.511	65.636	33.517	1.00	56.20	AAAA	S
ATOM	3981	CE	HET	416	44.002	67.366	33.690	1.00	35.94	AAAA	C
ATOM	3982	C	HET	416	46.623	65.064	28.728	1.00	40.40	AAAA	C
ATOM	3983	O	HET	416	46.963	66.137	28.247	1.00	34.84	AAAA	O
ATOM	3984	H	TYR	417	45.893	64.169	28.104	1.00	38.49	AAAA	H
ATOM	3986	CA	TYR	417	45.355	64.387	26.765	1.00	39.50	AAAA	C
ATOM	3987	CB	TYR	417	46.156	63.471	25.831	1.00	32.02	AAAA	C
ATOM	3988	CG	TYR	417	45.583	63.430	24.428	1.00	39.48	AAAA	C
ATOM	3989	CD1	TYR	417	45.730	64.501	23.511	1.00	39.29	AAAA	C
ATOM	3990	CE1	TYR	417	45.196	64.429	22.253	1.00	34.56	AAAA	C
ATOM	3991	CD2	TYR	417	44.884	62.321	24.005	1.00	36.81	AAAA	C
ATOM	3992	CE2	TYR	417	44.379	62.241	22.722	1.00	38.80	AAAA	C
ATOM	3993	CE	TYR	417	44.535	63.292	21.872	1.00	44.20	AAAA	C
ATOM	3994	OH	TYR	417	44.053	63.361	20.552	1.00	58.10	AAAA	O
ATOM	3996	C	TYR	417	43.853	64.065	26.698	1.00	44.18	AAAA	C
ATOM	3997	O	TYR	417	43.376	62.974	27.135	1.00	42.19	AAAA	O
ATOM	3998	H	PHE	418	43.068	64.971	26.100	1.00	45.84	AAAA	H
ATOM	4000	CA	PHE	418	41.644	64.701	25.910	1.00	45.67	AAAA	C
ATOM	4001	CB	PHE	418	40.772	65.657	26.720	1.00	47.19	AAAA	C
ATOM	4002	CG	PHE	418	40.675	65.264	28.177	1.00	43.44	AAAA	C
ATOM	4003	CD1	PHE	418	41.552	65.685	29.132	1.00	38.43	AAAA	C
ATOM	4004	CD2	PHE	418	39.638	64.417	28.544	1.00	51.21	AAAA	C
ATOM	4005	CE1	PHE	418	41.402	65.291	30.440	1.00	46.44	AAAA	C
ATOM	4006	CE2	PHE	418	39.486	64.023	29.845	1.00	46.63	AAAA	C
ATOM	4007	CE	PHE	418	40.358	64.454	30.801	1.00	44.68	AAAA	C
ATOM	4008	C	PHE	418	41.251	64.730	24.440	1.00	44.64	AAAA	C
ATOM	4009	O	PHE	418	41.375	65.762	23.812	1.00	47.60	AAAA	O
ATOM	4010	H	ALA	419	40.554	63.713	23.936	1.00	43.06	AAAA	H
ATOM	4012	CA	ALA	419	40.015	63.793	22.607	1.00	39.21	AAAA	C
ATOM	4013	CB	ALA	419	41.090	63.562	21.555	1.00	30.88	AAAA	C
ATOM	4014	C	ALA	419	38.837	62.846	22.366	1.00	41.77	AAAA	C
ATOM	4015	O	ALA	419	38.871	61.628	22.557	1.00	36.08	AAAA	O
ATOM	4016	H	PHE	420	37.829	63.398	21.618	1.00	40.41	AAAA	H
ATOM	4018	CA	PHE	420	36.742	62.621	21.070	1.00	40.03	AAAA	C
ATOM	4019	CB	PHE	420	37.157	61.430	20.180	1.00	45.54	AAAA	C
ATOM	4020	CG	PHE	420	37.832	61.909	18.912	1.00	54.18	AAAA	C
ATOM	4021	CD1	PHE	420	39.221	61.987	18.751	1.00	49.23	AAAA	C
ATOM	4022	CD2	PHE	420	37.006	62.345	17.871	1.00	47.65	AAAA	C
ATOM	4023	CE1	PHE	420	39.783	62.496	17.567	1.00	46.00	AAAA	C
ATOM	4024	CE2	PHE	420	37.572	62.833	16.725	1.00	51.10	AAAA	C
ATOM	4025	CZ	PHE	420	38.964	62.928	16.549	1.00	44.01	AAAA	C
ATOM	4026	C	PHE	420	35.762	62.146	22.126	1.00	41.65	AAAA	C
ATOM	4027	O	PHE	420	35.352	60.991	22.215	1.00	38.35	AAAA	O
ATOM	4028	H	ASU	421	35.459	63.024	23.049	1.00	45.35	AAAA	H
ATOM	4030	CA	ASU	421	34.477	62.960	24.112	1.00	46.86	AAAA	C
ATOM	4031	CB	ASU	421	35.183	63.276	25.449	1.00	43.60	AAAA	C
ATOM	4032	CG	ASU	421	36.407	62.401	25.654	1.00	47.90	AAAA	C
ATOM	4033	OD1	ASU	421	36.426	61.147	25.714	1.00	44.83	AAAA	O
ATOM	4034	HD2	ASU	421	37.541	63.101	25.732	1.00	37.46	AAAA	H
ATOM	4037	C	ASU	421	33.432	64.069	23.835	1.00	47.83	AAAA	C
ATOM	4038	O	ASU	421	33.617	65.233	24.237	1.00	38.95	AAAA	C

40/58

ATOM	4039	H	PRO	422	32.453	63.777	22.268	1.00	47.86	AAAA	H
ATOM	4040	CD	PRO	422	32.213	62.423	22.372	1.00	44.11	AAAA	C
ATOM	4041	CA	PRO	422	31.463	64.776	22.605	1.00	47.85	AAAA	C
ATOM	4042	CB	PRO	422	30.731	64.084	21.446	1.00	44.86	AAAA	C
ATOM	4043	CG	PRO	422	30.947	62.623	21.606	1.00	43.01	AAAA	C
ATOM	4044	C	PRO	422	30.577	65.284	23.735	1.00	51.16	AAAA	C
ATOM	4045	O	PRO	422	30.223	66.406	23.744	1.00	48.54	AAAA	O
ATOM	4046	H	LYS	423	30.320	64.487	24.774	1.00	52.90	AAAA	H
ATOM	4048	CA	LYS	423	29.431	64.908	25.865	1.00	58.82	AAAA	C
ATOM	4049	CB	LYS	423	28.556	63.721	26.360	1.00	52.93	AAAA	C
ATOM	4050	CG	LYS	423	28.209	62.810	25.196	1.00	70.55	AAAA	C
ATOM	4051	CD	LYS	423	26.743	62.448	24.996	1.00	73.79	AAAA	C
ATOM	4052	CE	LYS	423	26.030	63.374	24.021	1.00	77.06	AAAA	C
ATOM	4053	CE	LYS	423	25.949	64.748	24.614	1.00	64.99	AAAA	H
ATOM	4057	C	LYS	423	30.158	65.482	27.071	1.00	57.43	AAAA	C
ATOM	4058	O	LYS	423	29.582	65.478	28.152	1.00	55.22	AAAA	O
ATOM	4059	H	LEU	424	31.425	65.859	26.862	1.00	55.95	AAAA	H
ATOM	4061	CA	LEU	424	32.261	66.162	28.017	1.00	57.07	AAAA	C
ATOM	4062	CB	LEU	424	33.463	65.250	28.237	1.00	49.16	AAAA	C
ATOM	4063	CG	LEU	424	34.390	65.748	29.370	1.00	68.27	AAAA	C
ATOM	4064	CD1	LEU	424	33.821	65.362	30.734	1.00	60.66	AAAA	C
ATOM	4065	CD2	LEU	424	35.825	65.276	29.123	1.00	60.35	AAAA	C
ATOM	4066	C	LEU	424	32.709	67.585	27.878	1.00	56.29	AAAA	C
ATOM	4067	O	LEU	424	33.696	67.861	27.201	1.00	59.98	AAAA	O
ATOM	4068	H	CYS	425	31.995	68.488	28.492	1.00	58.76	AAAA	H
ATOM	4070	CA	CYS	425	32.342	69.916	28.406	1.00	60.39	AAAA	C
ATOM	4071	C	CYS	425	33.771	70.119	28.810	1.00	62.59	AAAA	C
ATOM	4072	O	CYS	425	34.288	69.665	29.231	1.00	64.45	AAAA	O
ATOM	4073	CB	CYS	425	31.249	70.644	29.214	1.00	68.23	AAAA	C
ATOM	4074	SG	CYS	425	29.916	71.303	28.086	1.00	81.03	AAAA	S
ATOM	4075	H	VAL	426	34.529	70.953	28.102	1.00	65.31	AAAA	H
ATOM	4077	CA	VAL	426	35.943	71.149	28.358	1.00	65.49	AAAA	C
ATOM	4078	CB	VAL	426	36.644	72.022	27.310	1.00	66.66	AAAA	C
ATOM	4079	CG1	VAL	426	36.715	71.413	25.925	1.00	62.49	AAAA	C
ATOM	4080	CG2	VAL	426	35.962	73.365	27.239	1.00	60.92	AAAA	C
ATOM	4081	C	VAL	426	36.105	71.711	29.757	1.00	65.99	AAAA	C
ATOM	4082	O	VAL	426	37.180	71.724	30.388	1.00	64.51	AAAA	O
ATOM	4083	H	SER	427	35.090	72.361	30.267	1.00	67.67	AAAA	H
ATOM	4085	CA	SER	427	35.091	72.927	31.599	1.00	66.85	AAAA	C
ATOM	4086	CB	SER	427	33.685	73.499	31.864	1.00	61.16	AAAA	C
ATOM	4087	CG	SER	427	34.088	74.860	32.098	1.00	67.05	AAAA	O
ATOM	4089	C	SER	427	35.515	71.972	32.701	1.00	64.24	AAAA	C
ATOM	4090	O	SER	427	36.332	72.328	33.573	1.00	63.66	AAAA	O
ATOM	4091	H	GLU	428	34.965	70.771	32.618	1.00	58.75	AAAA	H
ATOM	4093	CA	GLU	428	35.384	69.753	33.585	1.00	63.39	AAAA	C
ATOM	4094	CB	GLU	428	34.594	68.485	33.240	1.00	68.67	AAAA	C
ATOM	4095	CG	GLU	428	33.115	68.560	33.537	1.00	66.59	AAAA	C
ATOM	4096	CD	GLU	428	32.785	68.560	35.023	1.00	72.33	AAAA	C
ATOM	4097	OE1	GLU	428	32.729	67.522	35.722	1.00	81.62	AAAA	O
ATOM	4098	OE2	GLU	428	32.501	69.688	35.517	1.00	70.97	AAAA	O
ATOM	4099	C	GLU	428	36.870	69.485	33.429	1.00	61.63	AAAA	C
ATOM	4100	O	GLU	428	37.671	69.696	34.307	1.00	62.03	AAAA	O
ATOM	4101	H	ILE	429	37.265	69.262	32.165	1.00	61.26	AAAA	H
ATOM	4103	CA	ILE	429	38.631	69.038	31.789	1.00	61.09	AAAA	C
ATOM	4104	CB	ILE	429	38.759	68.933	30.263	1.00	59.32	AAAA	C
ATOM	4105	CG2	ILE	429	40.257	68.915	29.895	1.00	45.93	AAAA	C
ATOM	4106	CE1	ILE	429	37.968	67.719	29.794	1.00	57.66	AAAA	C
ATOM	4107	CD1	ILE	429	38.038	67.555	28.225	1.00	53.48	AAAA	C
ATOM	4108	C	ILE	429	39.498	70.166	32.323	1.00	61.90	AAAA	C
ATOM	4109	O	ILE	429	40.592	70.017	32.867	1.00	61.28	AAAA	O
ATOM	4110	H	TYR	430	38.987	71.384	32.200	1.00	65.34	AAAA	H
ATOM	4112	CA	TYR	430	39.729	72.543	32.719	1.00	68.10	AAAA	C
ATOM	4113	CB	TYR	430	39.180	73.822	32.099	1.00	71.02	AAAA	C
ATOM	4114	CG	TYR	430	39.538	74.006	30.639	1.00	75.98	AAAA	C
ATOM	4115	CD1	TYR	430	38.653	73.821	29.599	1.00	77.60	AAAA	C
ATOM	4116	CE1	TYR	430	38.953	73.977	28.270	1.00	75.72	AAAA	C
ATOM	4117	CD2	TYR	430	40.810	74.401	30.260	1.00	75.95	AAAA	C
ATOM	4118	CE2	TYR	430	41.155	74.575	28.937	1.00	74.81	AAAA	C
ATOM	4119	CC	TYR	430	40.221	74.359	27.952	1.00	78.51	AAAA	C
ATOM	4120	OH	TYR	430	40.564	74.542	26.616	1.00	85.40	AAAA	O
ATOM	4122	C	TYR	430	39.779	72.634	34.241	1.00	63.72	AAAA	C
ATOM	4123	O	TYR	430	40.654	73.321	34.758	1.00	58.26	AAAA	O
ATOM	4124	H	ARG	431	38.819	72.017	34.967	1.00	65.53	AAAA	H
ATOM	4126	CA	ARG	431	38.747	72.043	36.356	1.00	68.15	AAAA	C
ATOM	4127	CB	ARG	431	37.348	71.748	36.898	1.00	73.32	AAAA	C
ATOM	4128	CG	ARG	431	37.345	71.815	38.430	1.00	82.99	AAAA	C
ATOM	4129	CD	ARG	431	37.270	73.279	39.860	1.00	88.39	AAAA	C
ATOM	4130	HE	ARG	431	37.698	73.472	40.258	1.00	92.48	AAAA	H
ATOM	4132	CE	ARG	431	36.835	73.258	41.259	1.00	94.93	AAAA	C
ATOM	4133	HH1	ARG	431	35.610	72.872	40.872	1.00	87.40	AAAA	H
ATOM	4136	HH2	ARG	431	37.021	73.371	42.567	1.00	95.17	AAAA	H
ATOM	4139	C	ARG	431	39.718	70.986	36.877	1.00	67.75	AAAA	C
ATOM	4140	O	ARG	431	40.637	71.292	37.629	1.00	66.74	AAAA	O
ATOM	4141	H	NET	432	39.541	69.791	36.305	1.00	63.87	AAAA	H
ATOM	4143	CA	NET	432	40.437	68.703	36.652	1.00	64.40	AAAA	C

41/58

ATOH	4144	CB	HET	432	40.237	67.522	35.719	1.00	54.25	AAAA	C
ATOH	4145	CG	HET	432	41.254	66.426	35.971	1.00	40.18	AAAA	C
ATOH	4146	SD	HET	432	40.829	64.925	35.112	1.00	52.21	AAAA	S
ATOH	4147	CE	HET	432	41.582	63.681	36.137	1.00	54.89	AAAA	C
ATOH	4148	C	HET	432	41.991	69.170	36.626	1.00	64.65	AAAA	C
ATOH	4149	O	HET	432	42.530	68.992	37.655	1.00	65.88	AAAA	O
ATOH	4150	H	GLU	433	42.331	69.811	35.556	1.00	65.78	AAAA	H
ATOH	4152	CA	GLU	433	43.622	70.469	35.510	1.00	69.16	AAAA	C
ATOH	4153	CB	GLU	433	43.704	71.506	34.401	1.00	69.58	AAAA	C
ATOH	4154	CG	GLU	433	44.121	70.967	33.048	1.00	76.91	AAAA	C
ATOH	4155	CD	GLU	433	44.623	72.149	32.242	1.00	82.02	AAAA	C
ATOH	4156	OE1	GLU	433	44.718	73.224	32.874	1.00	86.82	AAAA	O
ATOH	4157	OE2	GLU	433	44.905	72.050	31.042	1.00	88.26	AAAA	O
ATOH	4158	C	GLU	433	44.016	71.219	36.781	1.00	71.29	AAAA	C
ATOH	4159	O	GLU	433	45.133	71.083	37.294	1.00	74.29	AAAA	O
ATOH	4160	H	GLU	434	43.178	72.120	37.280	1.00	72.93	AAAA	H
ATOH	4162	CA	GLU	434	43.505	72.873	38.485	1.00	72.86	AAAA	C
ATOH	4163	CB	GLU	434	42.458	73.916	38.840	1.00	81.36	AAAA	C
ATOH	4164	CG	GLU	434	41.191	73.956	38.032	1.00	83.34	AAAA	C
ATOH	4165	CD	GLU	434	40.181	75.064	38.432	1.00	97.32	AAAA	C
ATOH	4166	OE1	GLU	434	39.521	74.928	39.505	1.00	97.34	AAAA	O
ATOH	4167	OE2	GLU	434	40.080	75.941	37.583	1.00	99.95	AAAA	O
ATOH	4168	C	GLU	434	43.675	71.886	39.632	1.00	71.46	AAAA	C
ATOH	4169	O	GLU	434	44.728	71.858	40.251	1.00	78.49	AAAA	O
ATOH	4170	N	VAL	435	42.670	71.095	39.926	1.00	66.34	AAAA	N
ATOH	4172	CA	VAL	435	42.711	70.129	41.001	1.00	62.49	AAAA	C
ATOH	4173	CB	VAL	435	41.451	69.217	40.972	1.00	60.38	AAAA	C
ATOH	4174	CG1	VAL	435	41.547	68.214	42.104	1.00	52.32	AAAA	C
ATOH	4175	CG2	VAL	435	40.203	70.073	41.029	1.00	50.79	AAAA	C
ATOH	4176	C	VAL	435	43.939	69.253	41.018	1.00	60.74	AAAA	C
ATOH	4177	O	VAL	435	44.607	69.165	42.034	1.00	62.37	AAAA	O
ATOH	4178	H	THR	436	44.282	68.506	39.988	1.00	60.67	AAAA	H
ATOH	4180	CA	THR	436	45.335	67.516	39.936	1.00	56.36	AAAA	C
ATOH	4181	CB	THR	436	45.199	66.565	38.736	1.00	50.92	AAAA	C
ATOH	4182	CG1	THR	436	44.913	67.283	37.503	1.00	47.03	AAAA	O
ATOH	4184	CG2	THR	436	44.108	65.526	38.901	1.00	54.38	AAAA	C
ATOH	4185	C	THR	436	46.701	68.184	39.930	1.00	60.55	AAAA	C
ATOH	4186	O	THR	436	47.714	67.490	40.024	1.00	60.61	AAAA	O
ATOH	4187	H	GLY	437	46.836	69.496	39.835	1.00	60.65	AAAA	N
ATOH	4189	CA	GLY	437	48.102	70.164	39.749	1.00	59.47	AAAA	C
ATOH	4190	C	GLY	437	48.800	69.864	38.424	1.00	64.78	AAAA	C
ATOH	4191	O	GLY	437	49.983	70.254	38.245	1.00	62.70	AAAA	O
ATOH	4192	H	THR	438	48.112	69.387	37.380	1.00	63.79	AAAA	H
ATOH	4194	CA	THR	438	48.731	69.169	36.076	1.00	65.09	AAAA	C
ATOH	4195	CB	THR	438	47.967	68.027	35.411	1.00	66.87	AAAA	C
ATOH	4196	CG1	THR	438	46.600	68.385	35.731	1.00	62.22	AAAA	O
ATOH	4198	CG2	THR	438	48.208	66.659	36.019	1.00	68.74	AAAA	C
ATOH	4199	C	THR	438	48.590	70.415	35.220	1.00	66.14	AAAA	C
ATOH	4200	O	THR	438	49.003	70.543	34.070	1.00	68.05	AAAA	O
ATOH	4201	H	LYS	439	48.089	71.481	35.822	1.00	67.37	AAAA	H
ATOH	4203	CA	LYS	439	47.927	72.757	35.154	1.00	71.08	AAAA	C
ATOH	4204	CB	LYS	439	47.114	73.708	36.034	1.00	69.23	AAAA	C
ATOH	4205	CG	LYS	439	46.677	74.938	35.265	1.00	77.26	AAAA	C
ATOH	4206	CD	LYS	439	45.832	75.942	36.014	1.00	81.65	AAAA	C
ATOH	4207	CE	LYS	439	44.385	75.475	36.182	1.00	87.39	AAAA	C
ATOH	4208	HE	LYS	439	43.667	76.431	37.100	1.00	93.85	AAAA	H
ATOH	4212	C	LYS	439	49.249	73.396	34.752	1.00	73.01	AAAA	C
ATOH	4213	O	LYS	439	49.996	73.986	35.541	1.00	74.60	AAAA	O
ATOH	4214	H	GLY	440	49.517	73.453	33.441	1.00	73.33	AAAA	H
ATOH	4216	CA	GLY	440	50.733	74.167	32.014	1.00	71.39	AAAA	C
ATOH	4217	C	GLY	440	51.716	73.204	32.389	1.00	71.20	AAAA	C
ATOH	4218	O	GLY	440	52.684	73.650	31.822	1.00	72.70	AAAA	O
ATOH	4219	H	ARG	441	51.445	71.908	32.436	1.00	72.99	AAAA	H
ATOH	4221	CA	ARG	441	52.343	70.945	31.831	1.00	74.12	AAAA	C
ATOH	4222	CB	ARG	441	52.617	69.740	32.716	1.00	69.44	AAAA	C
ATOH	4223	CG	ARG	441	51.847	69.695	34.003	1.00	63.34	AAAA	C
ATOH	4224	CD	ARG	441	52.060	68.314	34.595	1.00	67.64	AAAA	C
ATOH	4225	HE	ARG	441	52.244	68.395	36.030	1.00	61.00	AAAA	H
ATOH	4227	CE	ARG	441	52.326	67.357	36.831	1.00	59.21	AAAA	C
ATOH	4228	HE1	ARG	441	52.258	66.117	36.395	1.00	60.57	AAAA	H
ATOH	4231	HE2	ARG	441	52.468	67.596	38.128	1.00	72.94	AAAA	H
ATOH	4234	C	ARG	441	51.760	70.446	30.511	1.00	73.50	AAAA	C
ATOH	4235	O	ARG	441	52.195	69.424	30.012	1.00	74.73	AAAA	O
ATOH	4236	H	GLN	442	50.732	71.114	30.043	1.00	74.68	AAAA	H
ATOH	4238	CA	GLN	442	49.959	70.646	28.914	1.00	75.13	AAAA	C
ATOH	4239	CB	GLN	442	48.457	70.875	29.126	1.00	68.73	AAAA	C
ATOH	4240	CG	GLN	442	47.669	69.576	29.195	1.00	71.20	AAAA	C
ATOH	4241	CD	GLN	442	47.623	69.028	30.607	1.00	70.98	AAAA	C
ATOH	4242	OE1	GLN	442	47.714	67.822	30.868	1.00	78.66	AAAA	O
ATOH	4243	HE2	GLN	442	47.477	69.907	31.584	1.00	66.86	AAAA	H
ATOH	4246	C	GLN	442	50.326	71.359	27.627	1.00	77.69	AAAA	C
ATOH	4247	O	GLN	442	50.227	72.569	27.530	1.00	75.57	AAAA	O
ATOH	4248	H	ALA	443	50.474	70.554	26.575	1.00	81.54	AAAA	H
ATOH	4250	CA	ALA	443	50.643	71.148	25.236	1.00	82.95	AAAA	C
ATOH	4251	CB	ALA	443	51.164	70.118	24.220	1.00	81.69	AAAA	C

42/58

ATOH	4252	C	ALA	443	49.259	71.706	24.952	1.00	83.73	AAAA	C
ATOH	4253	O	ALA	443	48.398	71.744	25.830	1.00	83.87	AAAA	C
ATOH	4254	H	LYS	444	48.914	72.052	23.713	1.00	86.20	AAAA	H
ATOH	4256	CA	LYS	444	47.559	72.524	23.482	1.00	85.88	AAAA	C
ATOH	4257	CB	LYS	444	47.426	73.997	23.128	1.00	83.99	AAAA	C
ATOH	4258	CG	LYS	444	46.673	74.734	24.241	1.00	93.60	AAAA	C
ATOH	4259	CD	LYS	444	45.883	73.841	25.186	1.00	95.14	AAAA	C
ATOH	4260	CE	LYS	444	46.390	73.786	26.614	1.00	97.04	AAAA	C
ATOH	4261	HE	LYS	444	45.368	73.090	27.473	1.00	97.22	AAAA	H
ATOH	4265	C	LYS	444	46.659	71.779	22.508	1.00	84.20	AAAA	C
ATOH	4266	O	LYS	444	45.428	71.901	22.635	1.00	85.63	AAAA	O
ATOH	4267	H	GLY	445	47.214	70.734	21.916	1.00	70.85	AAAA	H
ATOH	4269	CA	GLY	445	46.368	69.786	21.208	1.00	75.06	AAAA	C
ATOH	4270	C	GLY	445	45.803	68.844	22.260	1.00	72.30	AAAA	C
ATOH	4271	O	GLY	445	44.963	67.993	21.940	1.00	74.90	AAAA	O
ATOH	4272	H	ASP	446	46.300	68.981	23.492	1.00	67.97	AAAA	H
ATOH	4274	CA	ASP	446	45.914	68.174	24.642	1.00	62.81	AAAA	C
ATOH	4275	CB	ASP	446	46.754	68.552	25.873	1.00	55.24	AAAA	C
ATOH	4276	CG	ASP	446	48.213	68.169	25.801	1.00	54.07	AAAA	C
ATOH	4277	OD1	ASP	446	48.693	67.385	24.946	1.00	45.08	AAAA	O
ATOH	4278	OD2	ASP	446	49.091	68.595	26.593	1.00	50.12	AAAA	O
ATOH	4279	C	ASP	446	44.438	68.274	25.016	1.00	58.07	AAAA	C
ATOH	4280	O	ASP	446	43.610	67.369	25.127	1.00	55.59	AAAA	O
ATOH	4281	H	ILE	447	44.043	69.527	25.226	1.00	54.13	AAAA	H
ATOH	4283	CA	ILE	447	42.652	69.822	25.510	1.00	54.09	AAAA	C
ATOH	4284	CB	ILE	447	42.505	70.502	26.877	1.00	48.92	AAAA	C
ATOH	4285	CG2	ILE	447	41.030	70.663	27.182	1.00	41.02	AAAA	C
ATOH	4286	CG1	ILE	447	43.211	69.621	27.932	1.00	52.36	AAAA	C
ATOH	4287	CD1	ILE	447	43.468	70.327	29.237	1.00	48.47	AAAA	C
ATOH	4288	C	ILE	447	42.027	70.591	24.364	1.00	53.06	AAAA	C
ATOH	4289	O	ILE	447	41.718	71.772	24.423	1.00	56.08	AAAA	O
ATOH	4290	H	ASH	448	41.625	69.915	23.307	1.00	53.17	AAAA	H
ATOH	4292	CA	ASH	448	41.013	70.642	22.202	1.00	54.61	AAAA	C
ATOH	4293	CB	ASH	448	41.283	69.982	20.863	1.00	49.17	AAAA	C
ATOH	4294	CG	ASH	448	40.415	68.786	20.577	1.00	49.40	AAAA	C
ATOH	4295	OD1	ASH	448	39.287	68.977	20.113	1.00	52.34	AAAA	O
ATOH	4296	OD2	ASH	448	40.990	67.622	20.871	1.00	52.49	AAAA	H
ATOH	4299	C	ASH	448	39.518	70.824	22.402	1.00	56.44	AAAA	C
ATOH	4300	O	ASH	448	38.816	69.974	22.939	1.00	55.83	AAAA	O
ATOH	4301	H	THR	449	39.071	71.917	21.764	1.00	58.52	AAAA	H
ATOH	4303	CA	THR	449	37.682	72.351	21.901	1.00	58.62	AAAA	C
ATOH	4304	CB	THR	449	37.497	73.845	22.169	1.00	55.90	AAAA	C
ATOH	4305	CG1	THR	449	37.913	74.485	20.943	1.00	68.89	AAAA	O
ATOH	4307	CG2	THR	449	38.354	74.352	23.310	1.00	59.06	AAAA	C
ATOH	4308	C	THR	449	36.920	72.053	20.628	1.00	56.82	AAAA	C
ATOH	4309	O	THR	449	35.750	72.381	20.473	1.00	60.87	AAAA	O
ATOH	4310	H	ARG	450	37.539	71.304	19.757	1.00	55.76	AAAA	H
ATOH	4312	CA	ARG	450	36.887	70.935	18.507	1.00	54.66	AAAA	C
ATOH	4313	CB	ARG	450	37.845	71.179	17.377	1.00	48.33	AAAA	C
ATOH	4314	CG	ARG	450	38.385	69.975	16.645	1.00	54.81	AAAA	C
ATOH	4315	CD	ARG	450	39.487	70.561	15.696	1.00	44.92	AAAA	C
ATOH	4316	HE	ARG	450	40.706	70.719	16.488	1.00	52.49	AAAA	H
ATOH	4318	CG	ARG	450	41.544	69.757	16.882	1.00	39.08	AAAA	C
ATOH	4319	HH1	ARG	450	41.176	68.572	16.466	1.00	41.07	AAAA	H
ATOH	4322	HH2	ARG	450	42.601	70.001	17.610	1.00	45.18	AAAA	H
ATOH	4325	C	ARG	450	36.267	69.553	18.557	1.00	56.82	AAAA	C
ATOH	4326	O	ARG	450	35.186	69.303	17.992	1.00	58.15	AAAA	O
ATOH	4327	H	ASH	451	36.800	68.583	19.324	1.00	56.66	AAAA	H
ATOH	4329	CA	ASH	451	36.107	67.311	19.434	1.00	50.27	AAAA	C
ATOH	4330	CB	ASH	451	36.725	66.127	18.760	1.00	48.54	AAAA	C
ATOH	4331	CG	ASH	451	38.243	66.143	18.764	1.00	60.51	AAAA	C
ATOH	4332	OD1	ASH	451	38.779	66.279	19.855	1.00	53.45	AAAA	O
ATOH	4333	OD2	ASH	451	38.707	65.976	17.506	1.00	54.88	AAAA	H
ATOH	4336	C	ASH	451	35.849	66.854	20.869	1.00	52.97	AAAA	C
ATOH	4337	O	ASH	451	35.330	65.750	21.096	1.00	49.71	AAAA	O
ATOH	4338	H	ASH	452	36.126	67.668	21.851	1.00	51.98	AAAA	H
ATOH	4340	CA	ASH	452	35.769	67.485	23.229	1.00	55.88	AAAA	C
ATOH	4341	CB	ASH	452	36.947	67.873	24.136	1.00	54.62	AAAA	C
ATOH	4342	CG	ASH	452	37.936	66.736	24.285	1.00	60.96	AAAA	C
ATOH	4343	OD1	ASH	452	37.646	65.633	24.735	1.00	51.30	AAAA	C
ATOH	4344	OD2	ASH	452	39.153	67.098	23.855	1.00	56.75	AAAA	H
ATOH	4347	C	ASH	452	34.603	68.385	23.688	1.00	58.11	AAAA	C
ATOH	4348	O	ASH	452	34.785	69.629	23.657	1.00	55.07	AAAA	O
ATOH	4349	H	GLY	453	33.444	67.813	23.985	1.00	55.08	AAAA	H
ATOH	4351	CA	GLY	453	32.313	68.658	24.296	1.00	59.47	AAAA	C
ATOH	4352	C	GLY	453	31.500	69.269	23.174	1.00	64.95	AAAA	C
ATOH	4353	O	GLY	453	30.302	69.603	23.276	1.00	65.71	AAAA	O
ATOH	4354	H	GLU	454	31.910	69.109	21.910	1.00	67.44	AAAA	H
ATOH	4356	CA	GLU	454	31.266	69.543	20.690	1.00	63.63	AAAA	C
ATOH	4357	CB	GLU	454	31.739	68.818	19.401	1.00	53.71	AAAA	C
ATOH	4358	CG	GLU	454	32.348	67.430	19.738	1.00	49.50	AAAA	C
ATOH	4359	CD	GLU	454	32.368	66.620	18.454	1.00	54.61	AAAA	C
ATOH	4360	OE1	GLU	454	31.368	66.637	17.702	0.01	54.10	AAAA	O
ATOH	4361	OE2	GLU	454	33.417	66.003	18.160	0.01	54.17	AAAA	O
ATOH	4362	C	GLU	454	29.762	69.301	20.767	1.00	65.41	AAAA	C

43/58

ATOH	4363	G	GLU	454	29.022	70.089	20.169	1.00	67.86	AAAA	G
ATOH	4364	H	ARG	455	29.288	69.187	21.333	1.00	66.45	AAAA	H
ATOH	4366	CA	ARG	455	27.843	67.997	21.371	1.00	69.33	AAAA	C
ATOH	4367	CB	ARG	455	27.448	66.733	20.652	1.00	73.38	AAAA	C
ATOH	4368	CG	ARG	455	28.467	65.912	19.924	1.00	74.27	AAAA	C
ATOH	4369	CD	ARG	455	27.775	64.740	19.240	1.00	79.54	AAAA	C
ATOH	4370	DE	ARG	455	27.301	63.638	20.052	1.00	86.31	AAAA	C
ATOH	4372	CS	ARG	455	27.802	62.412	20.189	1.00	88.60	AAAA	C
ATOH	4373	HH1	ARG	455	28.990	61.997	19.538	1.00	84.51	AAAA	H
ATOH	4376	HH2	ARG	455	27.225	61.523	21.003	1.00	87.36	AAAA	H
ATOH	4379	C	ARG	455	27.213	67.934	22.756	1.00	67.35	AAAA	C
ATOH	4380	O	ARG	455	26.423	67.025	22.961	1.00	66.26	AAAA	O
ATOH	4381	H	ALA	456	27.499	68.879	23.623	1.00	66.50	AAAA	H
ATOH	4383	CA	ALA	456	26.947	68.906	24.964	1.00	72.01	AAAA	C
ATOH	4384	CB	ALA	456	27.832	68.147	25.939	1.00	61.84	AAAA	C
ATOH	4385	C	ALA	456	26.802	70.379	25.371	1.00	75.25	AAAA	C
ATOH	4386	O	ALA	456	27.706	71.219	25.202	1.00	81.30	AAAA	O
ATOH	4387	H	SER	457	25.653	70.720	25.939	0.50	71.91	AAAA	H
ATOH	4389	CA	SER	457	25.431	72.095	26.358	0.50	69.64	AAAA	C
ATOH	4390	CB	SER	457	23.991	72.247	26.836	0.50	73.39	AAAA	C
ATOH	4391	OG	SER	457	23.422	73.294	26.060	0.50	73.31	AAAA	C
ATOH	4393	C	SER	457	26.418	72.510	27.437	0.50	69.27	AAAA	C
ATOH	4394	O	SER	457	26.458	71.957	28.530	0.50	67.32	AAAA	O
ATOH	4395	H	CYS	458	27.197	73.531	27.117	0.50	70.44	AAAA	H
ATOH	4397	CA	CYS	458	28.287	73.960	27.972	0.50	72.57	AAAA	C
ATOH	4398	C	CYS	458	27.949	75.205	28.757	0.50	72.54	AAAA	C
ATOH	4399	O	CYS	458	27.065	75.128	29.606	0.50	76.63	AAAA	O
ATOH	4400	CB	CYS	458	29.527	74.171	27.089	0.50	75.38	AAAA	C
ATOH	4401	SG	CYS	458	30.844	73.032	27.490	0.50	72.18	AAAA	S
ATOH	4402	H	ALA	459	28.607	76.306	28.441	0.50	70.13	AAAA	H
ATOH	4404	CA	ALA	459	28.445	77.572	29.116	0.50	70.05	AAAA	C
ATOH	4405	CB	ALA	459	27.046	78.149	28.996	0.50	70.57	AAAA	C
ATOH	4406	C	ALA	459	28.826	77.461	30.601	0.50	70.13	AAAA	C
ATOH	4407	O	ALA	459	29.080	78.556	31.154	0.50	69.96	AAAA	O
ATOH	4407	OT	ALA	459	28.855	76.301	31.054	0.50	68.22	AAAA	O
ATOH	4522	C1	HAG	461	59.581	7.102	61.119	1.00	88.13	AAAA	C
ATOH	4524	C2	HAG	461	59.964	7.338	59.697	1.00	91.94	AAAA	C
ATOH	4526	H2	HAG	461	58.738	7.699	58.920	1.00	92.72	AAAA	H
ATOH	4528	C7	HAG	461	58.400	9.020	58.999	1.00	96.97	AAAA	C
ATOH	4529	O7	HAG	461	58.879	9.774	59.726	1.00	98.62	AAAA	O
ATOH	4530	C8	HAG	461	57.323	9.390	58.043	1.00	100.60	AAAA	C
ATOH	4534	C3	HAG	461	60.725	6.225	59.085	1.00	94.77	AAAA	C
ATOH	4536	O3	HAG	461	61.417	6.725	57.930	1.00	98.51	AAAA	O
ATOH	4538	C4	HAG	461	61.873	5.869	60.064	1.00	96.01	AAAA	C
ATOH	4540	O4	HAG	461	62.661	4.821	59.484	1.00	99.20	AAAA	O
ATOH	4542	C5	HAG	461	61.359	5.529	61.474	1.00	95.13	AAAA	C
ATOH	4545	C6	HAG	461	62.465	5.321	62.495	1.00	93.66	AAAA	C
ATOH	4548	O6	HAG	461	62.745	6.364	63.354	1.00	92.13	AAAA	O
ATOH	4544	O5	HAG	461	60.625	6.648	61.949	1.00	91.92	AAAA	O
ATOH	4550	C1	HAG	463	33.054	15.249	72.938	1.00	43.58	AAAA	C
ATOH	4552	C2	HAG	463	31.644	15.282	73.412	1.00	43.62	AAAA	C
ATOH	4554	H2	HAG	463	30.709	14.527	72.541	1.00	42.16	AAAA	H
ATOH	4556	C7	HAG	463	29.912	13.584	73.099	1.00	40.84	AAAA	C
ATOH	4557	O7	HAG	463	29.928	13.406	74.222	1.00	40.10	AAAA	O
ATOH	4558	C8	HAG	463	28.975	12.694	72.394	1.00	35.47	AAAA	C
ATOH	4562	C3	HAG	463	31.150	16.675	73.448	1.00	45.40	AAAA	C
ATOH	4564	O3	HAG	463	29.979	16.555	74.196	1.00	45.99	AAAA	O
ATOH	4566	C4	HAG	463	32.117	17.617	74.171	1.00	50.36	AAAA	C
ATOH	4568	O4	HAG	463	31.596	18.919	73.891	1.00	53.97	AAAA	O
ATOH	4569	C5	HAG	463	33.589	17.477	73.725	1.00	48.50	AAAA	C
ATOH	4572	C6	HAG	463	34.490	17.996	74.742	1.00	48.34	AAAA	C
ATOH	4575	O6	HAG	463	34.906	18.739	75.671	1.00	57.11	AAAA	O
ATOH	4571	O5	HAG	463	33.942	16.120	73.583	1.00	48.58	AAAA	O
ATOH	4576	C1	FUC	464	34.544	19.954	76.083	1.00	81.45	AAAA	C
ATOH	4578	C2	FUC	464	35.179	21.173	75.463	1.00	86.35	AAAA	C
ATOH	4579	O2	FUC	464	35.153	21.169	74.021	1.00	92.94	AAAA	O
ATOH	4582	C3	FUC	464	34.252	22.284	75.945	1.00	86.79	AAAA	C
ATOH	4584	O3	FUC	464	34.691	23.613	75.596	1.00	87.83	AAAA	C
ATOH	4586	C4	FUC	464	33.871	22.274	77.412	1.00	86.67	AAAA	O
ATOH	4588	O4	FUC	464	34.598	23.297	78.115	1.00	87.06	AAAA	O
ATOH	4590	C5	FUC	464	33.921	20.894	78.040	1.00	85.85	AAAA	C
ATOH	4593	C6	FUC	464	34.279	20.768	79.512	1.00	83.37	AAAA	C
ATOH	4592	O5	FUC	464	35.042	20.150	77.425	1.00	82.43	AAAA	O
ATOH	4597	C1	HAG	465	31.575	19.813	74.940	1.00	64.68	AAAA	C
ATOH	4599	C2	HAG	465	31.267	21.207	74.437	1.00	69.57	AAAA	C
ATOH	4601	H2	HAG	465	32.480	21.642	73.690	1.00	71.25	AAAA	H
ATOH	4603	C7	HAG	465	32.401	21.953	72.381	1.00	73.86	AAAA	C
ATOH	4604	O7	HAG	465	31.373	21.835	71.881	1.00	74.80	AAAA	O
ATOH	4605	C8	HAG	465	33.679	22.401	71.787	1.00	76.00	AAAA	C
ATOH	4609	C3	HAG	465	31.050	22.214	75.546	1.00	72.71	AAAA	C
ATOH	4611	O3	HAG	465	30.713	23.517	75.108	1.00	71.03	AAAA	O
ATOH	4613	C4	HAG	465	30.035	21.654	76.560	1.00	75.71	AAAA	C
ATOH	4615	O4	HAG	465	29.993	22.409	77.793	1.00	76.79	AAAA	O
ATOH	4617	C5	HAG	465	30.498	20.238	76.977	1.00	75.45	AAAA	C
ATOH	4620	C6	HAG	465	29.461	19.647	77.930	1.00	75.64	AAAA	C

44/58

ATOH	4623	06	HAG	465	28.385	19.238	77.142	1.00	76.25	AAAA	O
ATOH	4619	05	HAG	465	30.514	19.425	75.807	1.00	71.44	AAAA	O
ATOH	4625	C1	HAG	467	49.927	11.058	87.926	1.00	96.51	AAAA	C
ATOH	4627	C2	HAG	467	50.538	11.751	89.100	1.00	99.92	AAAA	C
ATOH	4629	H2	HAG	467	49.662	12.898	89.458	1.00	101.79	AAAA	H
ATOH	4631	C7	HAG	467	49.299	13.021	90.759	1.00	103.63	AAAA	C
ATOH	4632	O7	HAG	467	49.541	12.267	91.586	1.00	105.48	AAAA	O
ATOH	4633	C8	HAG	467	48.526	14.239	91.102	1.00	105.02	AAAA	C
ATOH	4637	C3	HAG	467	51.967	12.134	88.802	1.00	101.03	AAAA	C
ATOH	4639	O3	HAG	467	52.535	12.761	89.949	1.00	100.89	AAAA	O
ATOH	4641	C4	HAG	467	52.643	10.771	88.506	1.00	101.15	AAAA	C
ATOH	4643	O4	HAG	467	54.067	10.834	88.441	1.00	101.35	AAAA	O
ATOH	4645	C5	HAG	467	52.039	10.160	87.218	1.00	100.16	AAAA	C
ATOH	4648	C6	HAG	467	52.746	8.852	86.934	1.00	99.75	AAAA	C
ATOH	4651	O6	HAG	467	52.088	7.704	87.302	1.00	101.54	AAAA	O
ATOH	4647	O5	HAG	467	50.671	9.918	87.503	1.00	98.59	AAAA	O
ATOH	4653	C1	HAG	469	55.375	46.143	66.863	1.00	48.45	AAAA	C
ATOH	4655	C2	HAG	469	56.601	46.993	66.861	1.00	50.42	AAAA	C
ATOH	4657	H2	HAG	469	57.106	47.015	65.451	1.00	51.50	AAAA	H
ATOH	4659	C7	HAG	469	57.535	48.143	64.746	1.00	48.88	AAAA	C
ATOH	4660	O7	HAG	469	56.849	49.101	65.234	1.00	55.62	AAAA	O
ATOH	4661	C8	HAG	469	57.838	48.134	63.394	1.00	43.70	AAAA	C
ATOH	4665	C3	HAG	469	57.608	46.491	67.844	1.00	49.62	AAAA	C
ATOH	4667	O3	HAG	469	58.640	47.461	68.031	1.00	47.76	AAAA	O
ATOH	4669	C4	HAG	469	56.843	46.263	69.172	1.00	48.47	AAAA	C
ATOH	4671	O4	HAG	469	57.826	45.800	70.134	1.00	50.06	AAAA	O
ATOH	4672	C5	HAG	469	55.847	45.130	69.959	1.00	50.81	AAAA	C
ATOH	4675	C6	HAG	469	55.190	44.720	70.239	1.00	53.92	AAAA	C
ATOH	4678	O6	HAG	469	54.829	45.551	71.192	1.00	56.25	AAAA	O
ATOH	4674	O5	HAG	469	54.914	45.599	68.043	1.00	55.45	AAAA	O
ATOH	4679	C1	FUC	470	53.830	46.395	71.203	1.00	61.17	AAAA	C
ATOH	4681	C2	FUC	470	53.642	47.121	72.534	1.00	59.23	AAAA	C
ATOH	4682	O2	FUC	470	54.861	46.876	73.241	1.00	55.14	AAAA	O
ATOH	4685	C3	FUC	470	53.421	48.429	71.757	1.00	58.39	AAAA	C
ATOH	4687	O3	FUC	470	53.381	49.515	72.637	1.00	56.30	AAAA	O
ATOH	4689	C4	FUC	470	52.245	48.255	70.809	1.00	61.24	AAAA	C
ATOH	4691	O4	FUC	470	51.061	47.904	71.544	1.00	63.74	AAAA	O
ATOH	4693	C5	FUC	470	52.455	47.086	69.828	1.00	62.20	AAAA	C
ATOH	4696	C6	FUC	470	51.462	46.723	68.784	1.00	59.15	AAAA	C
ATOH	4695	O5	FUC	470	52.567	45.889	70.781	1.00	64.68	AAAA	O
ATOH	4700	C1	HAG	471	58.034	46.760	71.149	1.00	37.00	AAAA	C
ATOH	4702	C2	HAG	471	58.977	46.225	72.186	1.00	40.30	AAAA	C
ATOH	4704	H2	HAG	471	58.958	44.787	72.509	1.00	36.82	AAAA	H
ATOH	4706	C7	HAG	471	57.856	44.183	72.903	1.00	44.21	AAAA	C
ATOH	4707	O7	HAG	471	56.892	44.744	72.885	1.00	51.50	AAAA	O
ATOH	4708	C8	HAG	471	58.202	42.814	73.323	1.00	46.02	AAAA	C
ATOH	4712	C3	HAG	471	58.901	47.250	73.291	1.00	34.50	AAAA	C
ATOH	4714	O3	HAG	471	59.698	46.917	74.385	1.00	35.84	AAAA	O
ATOH	4716	C4	HAG	471	59.645	48.488	72.694	1.00	38.52	AAAA	C
ATOH	4718	O4	HAG	471	59.754	49.464	73.694	1.00	37.44	AAAA	O
ATOH	4719	C5	HAG	471	59.056	48.958	71.332	1.00	36.94	AAAA	C
ATOH	4722	C6	HAG	471	60.116	49.692	70.525	1.00	36.14	AAAA	C
ATOH	4725	O6	HAG	471	61.166	50.390	71.080	1.00	43.49	AAAA	O
ATOH	4721	O5	HAG	471	58.853	47.785	70.530	1.00	34.98	AAAA	O
ATOH	4727	C1	HAG	472	61.035	49.984	73.959	1.00	53.37	AAAA	C
ATOH	4729	C2	HAG	472	60.920	51.497	74.260	1.00	56.72	AAAA	C
ATOH	4730	O2	HAG	472	59.924	51.584	75.272	1.00	62.11	AAAA	O
ATOH	4733	C3	HAG	472	62.216	52.031	74.842	1.00	60.70	AAAA	C
ATOH	4735	O3	HAG	472	62.028	53.337	75.383	1.00	60.70	AAAA	O
ATOH	4736	C4	HAG	472	62.787	51.161	75.932	1.00	55.46	AAAA	C
ATOH	4738	O4	HAG	472	64.085	51.595	76.171	1.00	57.16	AAAA	O
ATOH	4740	C5	HAG	472	62.797	49.685	75.511	1.00	52.10	AAAA	C
ATOH	4743	C6	HAG	472	63.458	48.905	76.595	1.00	50.32	AAAA	C
ATOH	4746	O6	HAG	472	62.990	48.969	77.885	1.00	51.02	AAAA	O
ATOH	4742	O5	HAG	472	61.443	49.407	75.200	1.00	53.33	AAAA	O
ATOH	4748	C1	HAG	473	62.594	54.401	74.672	1.00	72.61	AAAA	C
ATOH	4750	C2	HAG	473	62.417	55.679	75.569	1.00	75.28	AAAA	C
ATOH	4751	O2	HAG	473	63.378	56.709	75.348	1.00	74.98	AAAA	O
ATOH	4754	C3	HAG	473	60.977	56.163	75.493	1.00	78.65	AAAA	C
ATOH	4756	O3	HAG	473	60.941	57.447	76.148	1.00	79.16	AAAA	O
ATOH	4758	C4	HAG	473	60.344	56.204	74.114	1.00	78.70	AAAA	C
ATOH	4760	O4	HAG	473	58.983	56.571	74.178	1.00	78.93	AAAA	O
ATOH	4762	C5	HAG	473	60.499	54.802	73.474	1.00	76.89	AAAA	C
ATOH	4765	C6	HAG	473	59.968	54.490	72.091	1.00	74.73	AAAA	C
ATOH	4768	O6	HAG	473	60.239	55.469	71.138	1.00	71.39	AAAA	O
ATOH	4764	O5	HAG	473	61.916	54.562	73.463	1.00	74.97	AAAA	O
ATOH	4408	CB	ALA	479	42.462	74.494	16.374	1.00	82.09	BBBB	C
ATOH	4409	C	ALA	479	40.017	74.702	17.001	1.00	91.42	BBBB	C
ATOH	4410	O	ALA	479	40.393	75.108	18.103	1.00	96.11	BBBB	O
ATOH	4413	H	ALA	479	40.696	74.461	14.624	1.00	86.43	BBBB	H
ATOH	4415	CA	ALA	479	41.033	74.108	16.033	1.00	89.85	BBBB	C
ATOH	4416	H	ALA	480	38.749	74.752	16.610	1.00	92.12	BBBB	H
ATOH	4418	CA	ALA	480	37.684	75.264	17.467	1.00	91.26	BBBB	C
ATOH	4419	CB	ALA	480	37.925	76.731	17.769	1.00	86.84	BBBB	C
ATOH	4420	C	ALA	480	36.306	75.030	16.849	1.00	91.39	BBBB	C

45/58

ATOM	4421	O	ALA	480	35.415	74.647	17.610	1.00	93.79	BBBB	O
ATOM	4422	H	GLU	481	36.135	75.304	15.564	0.01	89.69	BBBB	H
ATOM	4424	CA	GLU	481	34.832	75.164	14.915	1.00	87.19	BBBB	C
ATOM	4425	CB	GLU	481	34.471	76.492	14.224	0.01	92.74	BBBB	C
ATOM	4426	CG	GLU	481	34.277	77.627	15.220	1.00	99.93	BBBB	C
ATOM	4427	CD	GLU	481	34.067	79.003	14.626	1.00103.59	BBBB	C	
ATOM	4428	OE1	GLU	481	35.011	79.777	14.381	1.00103.27	BBBB	O	
ATOM	4429	NE2	GLU	481	32.792	79.328	14.398	1.00108.06	BBBB	H	
ATOM	4432	C	GLU	481	34.755	73.947	14.005	1.00	85.31	BBBB	C
ATOM	4433	C	GLU	481	33.736	73.508	13.456	1.00	83.41	BBBB	O
ATOM	4434	H	LYS	482	35.849	73.188	13.908	1.00	82.05	BBBB	H
ATOM	4436	CA	LYS	482	35.982	71.990	13.089	1.00	73.49	BBBB	C
ATOM	4437	CB	LYS	482	37.377	71.930	12.480	1.00	73.13	BBBB	C
ATOM	4438	CG	LYS	482	38.287	73.128	12.494	1.00	76.33	BBBB	C
ATOM	4439	CD	LYS	482	39.413	72.968	11.471	1.00	80.62	BBBB	C
ATOM	4440	CE	LYS	482	39.985	74.310	11.027	0.01	76.66	BBBB	C
ATOM	4441	HC	LYS	482	41.252	74.136	10.262	0.01	76.20	BBBB	H
ATOM	4445	C	LYS	482	35.779	70.701	13.872	1.00	67.70	BBBB	C
ATOM	4446	O	LYS	482	35.879	70.744	15.092	1.00	69.99	BBBB	O
ATOM	4447	H	LEU	483	35.530	69.585	13.199	1.00	61.47	BBBB	H
ATOM	4449	CA	LEU	483	35.193	68.356	13.896	1.00	59.03	BBBB	C
ATOM	4450	CB	LEU	483	34.256	67.529	13.039	1.00	55.20	BBBB	C
ATOM	4451	CG	LEU	483	32.779	67.860	12.875	1.00	61.94	BBBB	C
ATOM	4452	CD1	LEU	483	32.405	69.154	13.595	1.00	44.78	BBBB	C
ATOM	4453	CD2	LEU	483	32.433	67.707	11.395	1.00	44.63	BBBB	C
ATOM	4454	C	LEU	483	36.421	67.509	14.229	1.00	59.73	BBBB	O
ATOM	4455	O	LEU	483	36.465	66.709	15.165	1.00	57.22	BBBB	O
ATOM	4456	H	ILE	484	37.345	67.543	13.262	1.00	56.21	BBBB	H
ATOM	4458	CA	ILE	484	38.597	66.820	13.367	1.00	52.58	BBBB	C
ATOM	4459	CP	ILE	484	38.480	65.390	12.870	1.00	50.27	BBBB	C
ATOM	4460	CG2	ILE	484	37.769	65.319	11.524	1.00	44.85	BBBB	C
ATOM	4461	CG1	ILE	484	39.870	64.766	12.756	1.00	39.79	BBBB	C
ATOM	4462	CD1	ILE	484	39.888	63.291	12.404	1.00	30.43	BBBB	C
ATOM	4463	C	ILE	484	39.623	67.645	12.608	1.00	53.49	BBBB	C
ATOM	4464	O	ILE	484	39.158	68.568	11.942	1.00	48.33	BBBB	O
ATOM	4465	H	SER	485	40.911	67.499	12.887	1.00	50.86	BBBB	H
ATOM	4467	CA	SER	485	41.898	68.335	12.209	1.00	49.78	BBBB	C
ATOM	4468	CB	SER	485	41.969	69.753	12.747	1.00	46.06	BBBB	C
ATOM	4469	CG	SER	485	43.190	70.035	13.376	1.00	63.03	BBBB	O
ATOM	4471	C	SER	485	43.294	67.711	12.240	1.00	50.57	BBBB	O
ATOM	4472	O	SER	485	43.510	66.601	12.740	1.00	46.55	BBBB	O
ATOM	4473	H	GLU	486	44.246	68.389	11.604	1.00	52.16	BBBB	H
ATOM	4475	CA	GLU	486	45.624	67.874	11.509	1.00	59.12	BBBB	C
ATOM	4476	CB	GLU	486	46.547	68.683	10.598	1.00	59.71	BBBB	C
ATOM	4477	CG	GLU	486	46.221	70.162	10.568	1.00	76.75	BBBB	C
ATOM	4478	CD	GLU	486	47.370	71.045	10.983	1.00	80.53	BBBB	C
ATOM	4479	OE1	GLU	486	48.315	70.404	11.472	1.00	91.67	BBBB	O
ATOM	4480	OE2	GLU	486	47.480	72.289	10.897	1.00	86.00	BBBB	O
ATOM	4481	C	GLU	486	46.272	67.773	12.896	1.00	56.50	BBBB	O
ATOM	4482	O	GLU	486	46.768	66.747	13.326	1.00	49.83	BBBB	O
ATOM	4483	H	GLU	487	45.955	68.738	13.732	1.00	58.37	BBBB	H
ATOM	4485	CA	GLU	487	46.129	68.736	15.169	1.00	59.36	BBBB	C
ATOM	4486	CB	GLU	487	45.303	69.887	15.729	1.00	61.32	BBBB	C
ATOM	4487	CG	GLU	487	45.645	70.232	17.159	1.00	79.21	BBBB	C
ATOM	4488	CD	GLU	487	46.397	71.545	17.177	1.00	86.09	BBBB	C
ATOM	4489	OE1	GLU	487	45.768	72.610	17.320	1.00	92.00	BBBB	O
ATOM	4490	OE2	GLU	487	47.637	71.452	17.026	1.00	96.51	BBBB	O
ATOM	4491	C	GLU	487	45.735	67.436	15.841	1.00	58.84	BBBB	C
ATOM	4492	O	GLU	487	46.421	67.018	16.761	1.00	61.93	BBBB	O
ATOM	4493	H	ASP	488	44.748	66.661	15.474	1.00	56.50	BBBB	H
ATOM	4495	CA	ASP	488	44.446	65.347	15.932	1.00	55.61	BBBB	C
ATOM	4496	CB	ASP	488	42.947	64.977	15.699	1.00	51.22	BBBB	C
ATOM	4497	CG	ASP	488	42.047	66.008	16.267	1.00	45.27	BBBB	C
ATOM	4498	OD1	ASP	488	42.114	66.563	17.387	1.00	56.45	BBBB	O
ATOM	4499	OD2	ASP	488	41.154	66.399	15.492	1.00	55.11	BBBB	O
ATOM	4500	C	ASP	488	45.206	64.211	15.238	1.00	58.91	BBBB	C
ATOM	4501	O	ASP	488	44.967	63.042	15.634	1.00	57.00	BBBB	O
ATOM	4502	H	LEU	489	45.933	64.513	14.163	1.00	57.39	BBBB	H
ATOM	4504	CA	LEU	489	46.659	63.426	13.528	1.00	64.03	BBBB	C
ATOM	4505	CB	LEU	489	46.722	63.677	12.024	1.00	62.69	BBBB	C
ATOM	4506	CG	LEU	489	45.746	62.788	11.226	1.00	53.71	BBBB	C
ATOM	4507	CD1	LEU	489	44.324	63.243	11.514	1.00	51.88	BBBB	C
ATOM	4508	CD2	LEU	489	46.072	62.967	9.766	1.00	55.20	BBBB	C
ATOM	4509	C	LEU	489	48.017	63.355	14.210	1.00	68.12	BBBB	C
ATOM	4510	O	LEU	489	48.860	62.560	13.938	1.00	71.57	BBBB	O
ATOM	4511	H	ASH	490	48.306	64.318	15.063	1.00	68.24	BBBB	H
ATOM	4513	CA	ASH	490	49.497	64.424	15.855	1.00	75.04	BBBB	C
ATOM	4514	CB	ASH	490	49.724	65.910	16.187	1.00	84.46	BBBB	C
ATOM	4515	CG	ASH	490	51.191	66.105	16.589	1.00	98.83	BBBB	C
ATOM	4516	OD1	ASH	490	52.082	65.342	16.178	1.00	97.25	BBBB	O
ATOM	4517	HD2	ASH	490	51.459	67.128	17.407	1.00100.47	BBBB	H	
ATOM	4520	C	ASH	490	49.350	63.610	17.139	1.00	80.30	BBBB	C
ATOM	4521	O	ASH	490	49.891	62.484	17.264	1.00	80.97	BBBB	O
ATOM	4521	OT	ASH	490	48.510	64.012	19.001	1.00	89.51	BBBB	O
ATOM	4770	S	SUL	493	37.234	-7.808	65.465	1.00108.87	BBBB	S	

46/58

ATOM	4771	01	SUL	493	38.452	-7.921	66.345	1.00112.65	DDDD	0
ATOM	4772	02	SUL	493	37.611	-7.873	64.029	1.00110.21	DDDD	0
ATOM	4773	03	SUL	493	36.533	-6.555	65.856	1.00109.93	DDDD	0
ATOM	4774	04	SUL	493	36.333	-8.978	65.639	1.00107.58	DDDD	0
ATOM	4775	S	SUL	494	56.567	19.753	66.302	1.00109.81	DDDD	S
ATOM	4776	01	SUL	494	56.597	19.128	67.659	1.00107.98	DDDD	0
ATOM	4777	02	SUL	494	57.964	20.027	65.795	1.00112.59	DDDD	0
ATOM	4778	03	SUL	494	55.749	21.006	66.267	1.00111.35	DDDD	0
ATOM	4779	04	SUL	494	55.886	18.792	65.379	1.00109.86	DDDD	0
ATOM	4780	S	SUL	495	34.533	11.240	75.722	1.00114.67	DDDD	S
ATOM	4781	01	SUL	495	35.274	12.213	76.595	1.00111.38	DDDD	0
ATOM	4782	02	SUL	495	35.476	10.329	74.974	1.00113.60	DDDD	0
ATOM	4783	03	SUL	495	33.552	11.860	74.748	1.00112.77	DDDD	0
ATOM	4784	04	SUL	495	33.773	10.278	76.604	1.00113.18	DDDD	0
ATOM	4785	S	SUL	496	35.466	24.844	59.093	1.00 50.73	DDDD	S
ATOM	4786	01	SUL	496	35.613	24.843	60.607	1.00 62.59	DDDD	0
ATOM	4787	02	SUL	496	36.002	23.581	58.571	1.00 48.59	DDDD	0
ATOM	4788	03	SUL	496	35.880	26.084	58.455	1.00 56.74	DDDD	0
ATOM	4789	04	SUL	496	33.958	21.953	59.034	1.00 59.34	DDDD	0
ATOM	4790	S	SUL	497	47.653	-2.303	70.199	1.00 68.98	DDDD	S
ATOM	4791	01	SUL	497	47.849	-1.058	70.996	1.00 68.52	DDDD	0
ATOM	4792	02	SUL	497	48.594	-2.509	69.072	1.00 70.94	DDDD	0
ATOM	4793	03	SUL	497	46.187	-2.393	69.810	1.00 73.47	DDDD	0
ATOM	4794	04	SUL	497	47.799	-3.446	71.129	1.00 71.33	DDDD	0
ATOM	4795	S	SUL	498	56.527	35.758	75.513	1.00 71.48	DDDD	S
ATOM	4796	01	SUL	498	55.870	35.013	76.621	1.00 72.97	DDDD	0
ATOM	4797	02	SUL	498	57.759	34.996	75.167	1.00 69.11	DDDD	0
ATOM	4798	03	SUL	498	56.619	37.237	75.785	1.00 72.45	DDDD	0
ATOM	4799	04	SUL	498	55.623	35.809	74.330	1.00 72.74	DDDD	0
ATOM	4800	S	SUL	499	40.639	27.365	69.499	1.00 74.04	DDDD	S
ATOM	4801	01	SUL	499	40.218	26.039	70.045	1.00 76.00	DDDD	0
ATOM	4802	02	SUL	499	42.089	27.608	69.835	1.00 75.15	DDDD	0
ATOM	4803	03	SUL	499	39.823	28.467	70.098	1.00 77.27	DDDD	0
ATOM	4804	04	SUL	499	40.424	27.245	68.018	1.00 75.70	DDDD	0
ATOM	4805	S	SUL	500	44.996	53.228	20.568	1.00 83.89	DDDD	S
ATOM	4806	01	SUL	500	45.080	54.400	21.461	1.00 84.79	DDDD	0
ATOM	4807	02	SUL	500	46.109	52.266	20.827	1.00 90.38	DDDD	0
ATOM	4808	03	SUL	500	45.032	53.674	19.135	1.00 92.23	DDDD	0
ATOM	4809	04	SUL	500	43.762	52.396	20.723	1.00 91.61	DDDD	0
ATOM	4810	OW	WAT	501	29.970	6.904	77.713	1.00 34.84	DDDD	0
ATOM	4813	OW	WAT	502	42.522	18.998	78.232	1.00 55.27	DDDD	0
ATOM	4816	OW	WAT	503	37.561	21.003	67.518	1.00 41.63	DDDD	0
ATOM	4819	OW	WAT	504	50.446	5.721	63.485	1.00 57.37	DDDD	0
ATOM	4822	OW	WAT	505	56.668	24.854	72.729	1.00 57.34	DDDD	0
ATOM	4825	OW	WAT	506	50.605	57.695	22.727	1.00 54.26	DDDD	0
ATOM	4828	OW	WAT	507	55.123	37.781	61.204	1.00 43.71	DDDD	0
ATOM	4831	OW	WAT	508	17.414	-9.070	74.793	1.00 48.79	DDDD	0
ATOM	4834	OW	WAT	509	44.263	20.885	63.811	1.00 28.64	DDDD	0
ATOM	4837	OW	WAT	510	45.085	19.708	84.433	1.00 49.09	DDDD	0
ATOM	4840	OW	WAT	511	33.537	1.927	71.115	1.00 60.39	DDDD	0
ATOM	4843	OW	WAT	512	19.279	4.902	75.254	1.00 55.23	DDDD	0
ATOM	4846	OW	WAT	513	11.502	-0.835	68.996	1.00 57.51	DDDD	0
ATOM	4849	OW	WAT	514	24.591	17.207	56.665	1.00 56.36	DDDD	0
ATOM	4852	OW	WAT	515	56.947	34.914	62.552	1.00 36.47	DDDD	0
ATOM	4855	OW	WAT	516	58.092	39.983	66.234	1.00 30.34	DDDD	0
ATOM	4858	OW	WAT	517	48.308	40.726	56.768	1.00 81.69	DDDD	0
ATOM	4861	OW	WAT	518	25.776	2.355	85.630	1.00 66.34	DDDD	0
ATOM	4864	OW	WAT	519	30.644	68.108	30.765	1.00 82.28	DDDD	0
ATOM	4867	OW	WAT	520	38.739	54.257	43.611	1.00 43.42	DDDD	0
ATOM	4870	OW	WAT	521	22.886	4.470	64.871	1.00 48.71	DDDD	0
ATOM	4873	OW	WAT	522	30.938	50.249	19.364	1.00 54.00	DDDD	0
ATOM	4876	OW	WAT	523	32.413	9.061	42.441	1.00 44.45	DDDD	0
ATOM	4879	OW	WAT	524	41.019	42.560	55.653	1.00 43.40	DDDD	0
ATOM	4882	OW	WAT	525	54.268	51.393	37.513	1.00 55.10	DDDD	0
ATOM	4885	OW	WAT	526	37.130	13.599	81.397	1.00 46.49	DDDD	0
ATOM	4888	OW	WAT	527	42.585	10.244	84.472	1.00 35.95	DDDD	0
ATOM	4891	OW	WAT	528	43.661	61.633	18.450	1.00 41.05	DDDD	0
ATOM	4894	OW	WAT	529	27.980	19.862	53.348	1.00 54.59	DDDD	0
ATOM	4897	OW	WAT	530	59.527	38.520	64.116	1.00 37.96	DDDD	0
ATOM	4900	OW	WAT	531	22.451	1.046	57.437	1.00 59.31	DDDD	0
ATOM	4903	OW	WAT	532	30.380	16.123	70.205	1.00 40.39	DDDD	0
ATOM	4906	OW	WAT	533	46.835	27.888	65.854	1.00 52.34	DDDD	0
ATOM	4909	OW	WAT	534	39.446	49.001	45.379	1.00 46.05	DDDD	0
ATOM	4912	OW	WAT	535	46.992	51.272	50.722	1.00 52.62	DDDD	0
ATOM	4915	OW	WAT	536	44.263	18.776	73.017	1.00 40.61	DDDD	0
ATOM	4918	OW	WAT	537	33.670	58.861	20.848	1.00 51.56	DDDD	0
ATOM	4921	OW	WAT	538	52.469	21.639	73.804	1.00 61.98	DDDD	0
ATOM	4924	OW	WAT	539	49.985	44.871	37.324	1.00 45.45	DDDD	0
ATOM	4927	OW	WAT	540	24.074	-1.791	60.677	1.00 40.40	DDDD	0
ATOM	4930	OW	WAT	541	35.207	0.714	79.039	1.00 51.34	DDDD	0
ATOM	4933	OW	WAT	542	31.231	-1.176	62.362	1.00 48.33	DDDD	0
ATOM	4936	OW	WAT	543	41.726	-5.156	55.290	1.00 60.67	DDDD	0
ATOM	4939	OW	WAT	544	48.564	37.335	72.612	1.00 71.69	DDDD	0
ATOM	4942	OW	WAT	545	49.501	40.030	67.582	1.00 44.88	DDDD	0
ATOM	4945	OW	WAT	546	54.851	7.987	60.018	1.00 49.91	DDDD	0

WO 99/28347

PCT/AU98/00998

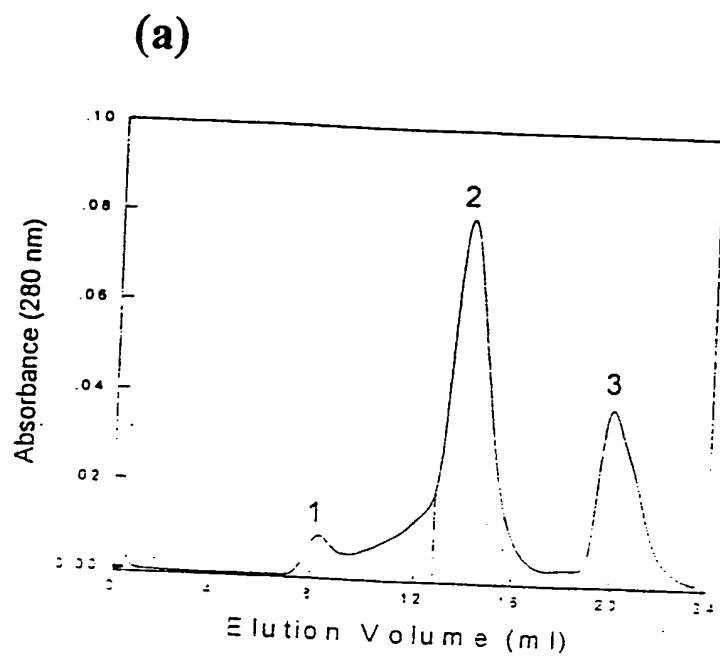
47/58

ATCH	4948	OW	WAT	547	30.459	-14.958	70.504	1.00	84.42	DDDD	o
ATCH	4951	OW	WAT	548	57.310	32.779	60.848	1.00	50.77	DDDD	o
END											

Face 1	Cleft 1	Face 2	Cleft 2	Face 3
(12D) 11N 10R 8D (6G) 5P	259E 261S 262D	305E	310T	335R
(35S) 33L 32L 30H 28Y (27G) 26E 255I	256L 263S 264E	(302C) 319M	(316S) 313S	336R
(61A) 59R 58F 56L 54Y 53E 242E 241F (274M)	276E 282I 300K	318Q	315T	338N
91E 90F 82F (88V) 83Y 80K 79W	272E 279S 298C	(322G) 321Q 347F	314V (344V)	48/58
115K 114E 112R 85Y 84N 108R	240R 270D	346Q 343E		
(140V) 138Y				

Figure 2

49/58



(b)

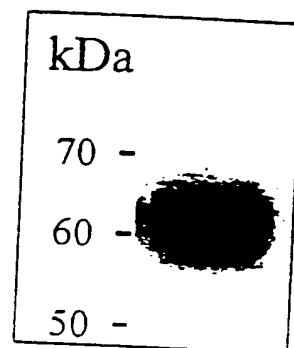
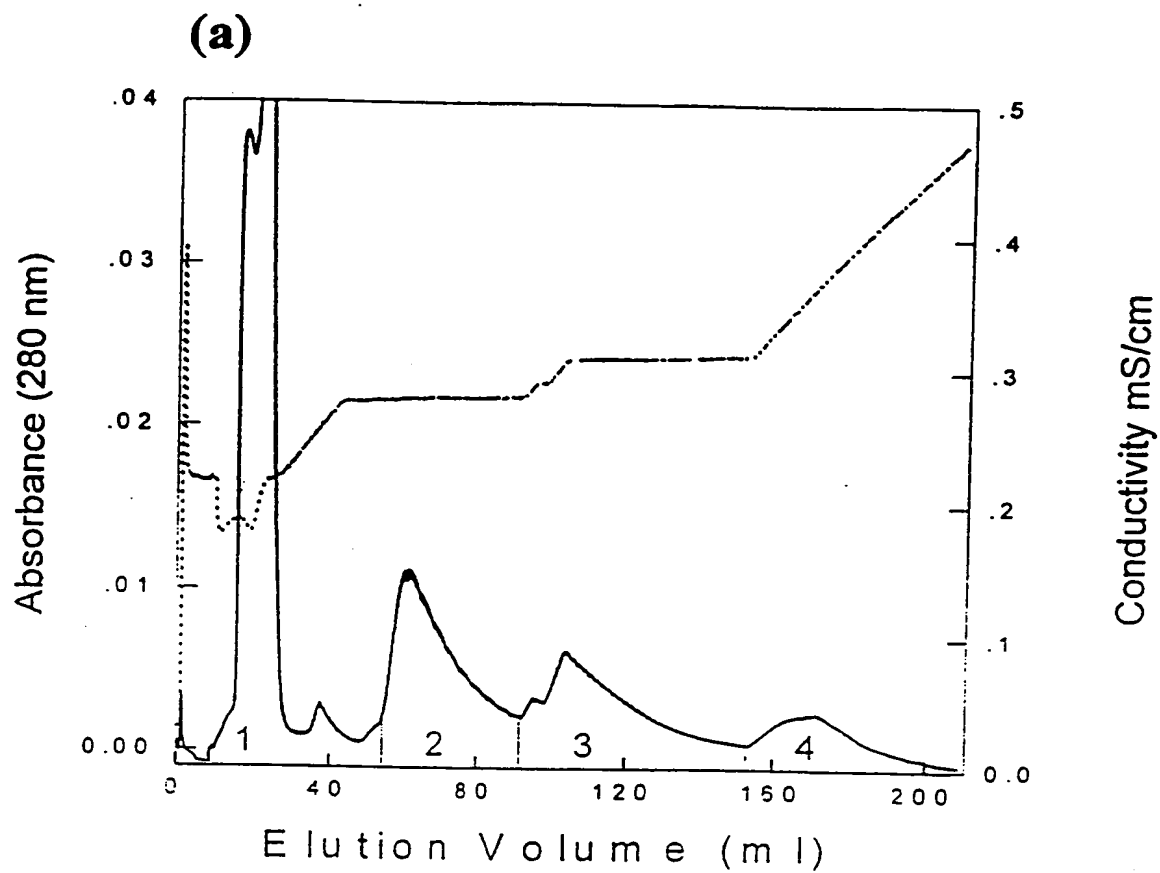
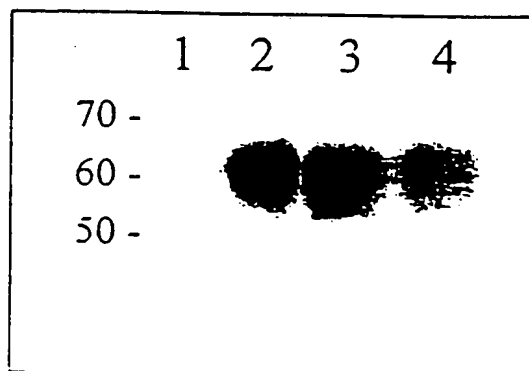


Figure 3

50/58



(b)



(c)

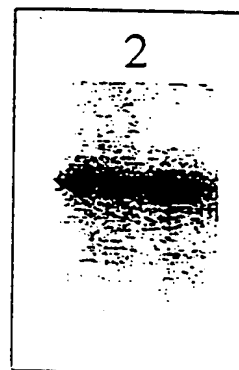


Figure 4

51/58

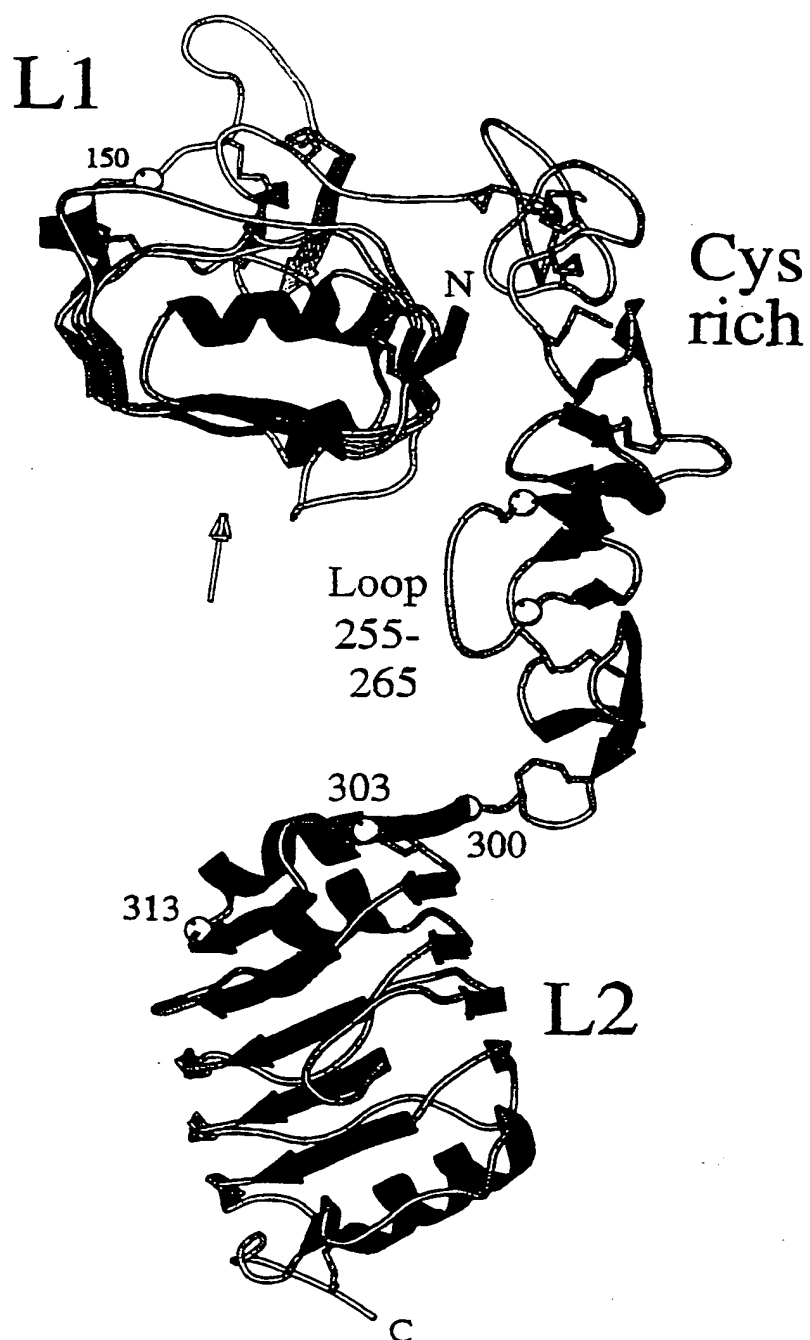
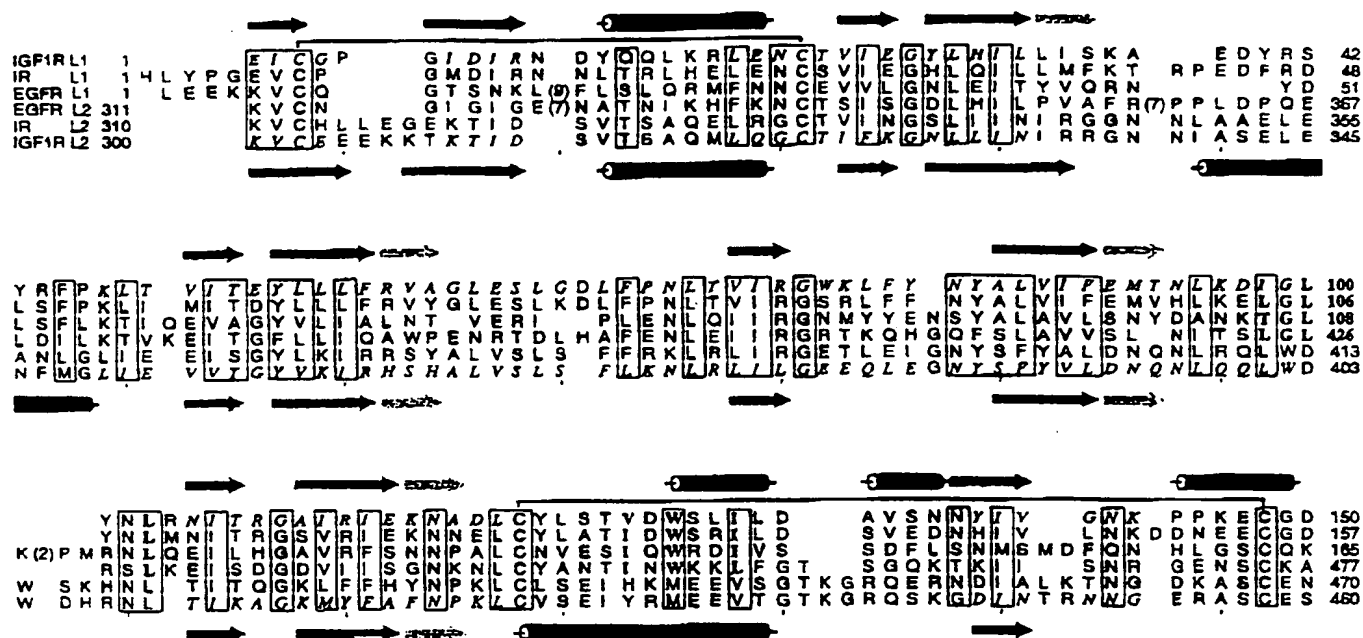


Figure 5

52/58

a



b

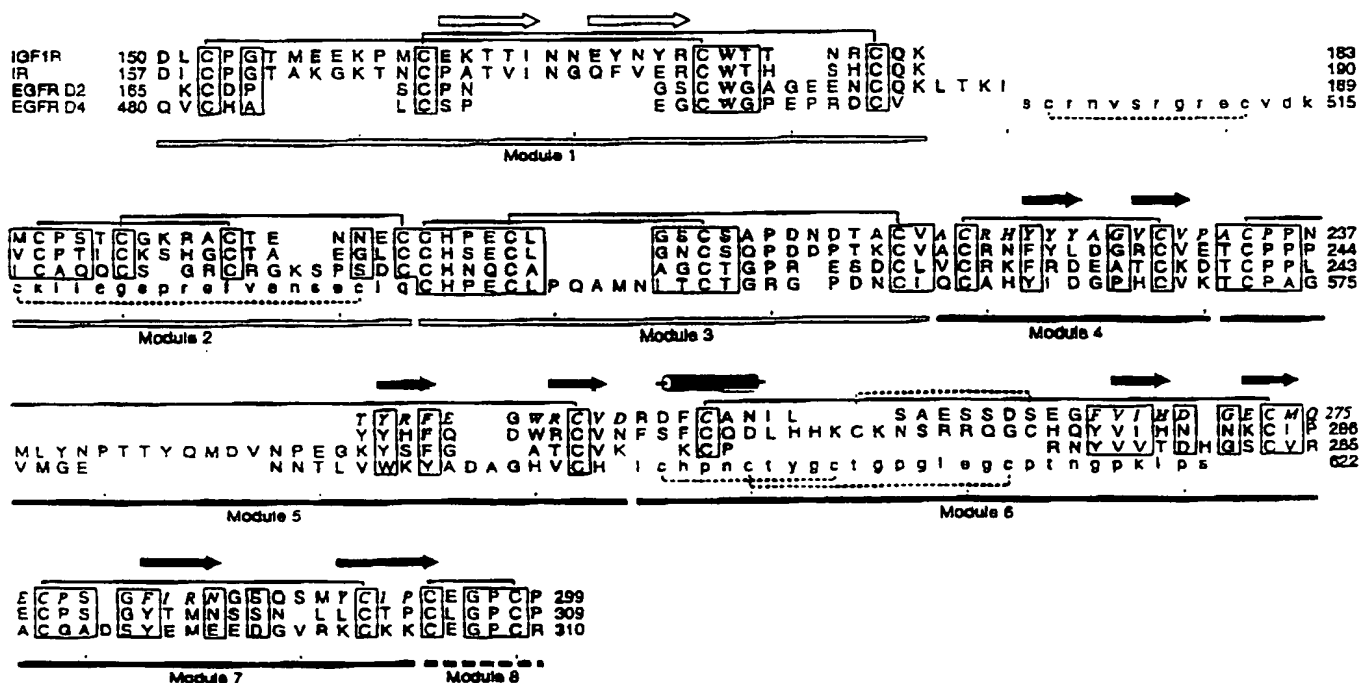


Figure 6

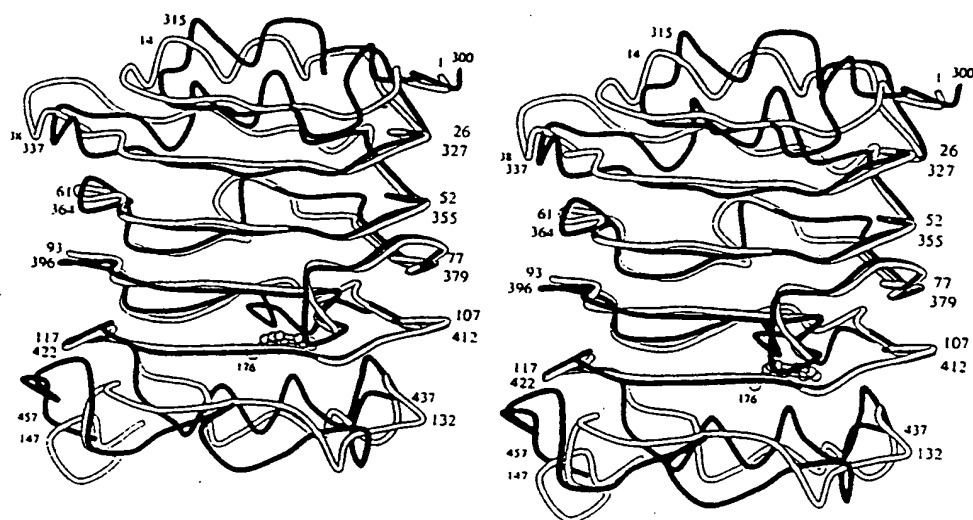


Figure 7

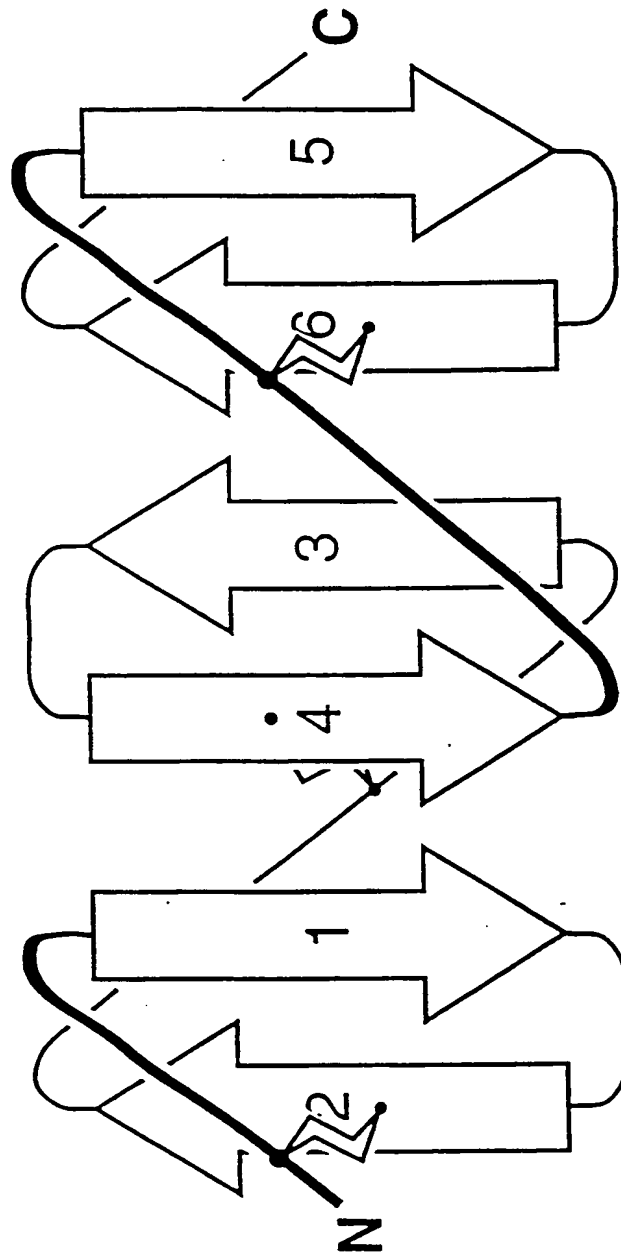


Figure 8

55/58

Figure 9: Sequence Alignment of hIGF-1R, hIR and hIRR ectodomains.

Derived by use of the PileUp program in the software package of the Genetics Computer Group, 575 Science Drive, Madison, Wisconsin, USA.

Symbol Comparison table: GenRunData:PileUpPep.Cmp CompChek: 1254

GapWeight: 3.0
GapLengthWeight: 0.1

Name: Higflr	Len: 972	CheCk: 1781	Weight: 1.00
Name: Hir	Len: 972	CheCk: 2986	Weight: 1.00
Name: Hirr	Len: 972	CheCk: 9819	Weight: 1.00

```

      *
Higflr  ....EICGP GIDIRNDYQQ LKRLNCTVI EGYLHILLIS K..AEDYRSY 43
Hir     HLYPGEVC.P GMDIRNNLTR LHELENCSVI EGHLQILLMF KTRPEDFRDL 49
Hirr    ....MNVC.P SLDIRSEVAE LRQLENCSVV EGHLQILLMF TATGEDFRGL 45

      *
Higflr  RFPKLTVITE YLLFRVAGL ESLGDLFPNL TVIRGWKLFY NYALVIFEMT 93
Hir     SFPKLIMITD YLLFRVYGL ESLKDLFPNL TVIRGSRLFF NYALVIFEMV 99
Hirr    SFPRLTQVTD YLLFRVYGL ESLRDLFPNL AVIRGTRLFL GYALVIFEMP 95

      *
Higflr  NLKDIGLYNL RNITRGAIRI EKNADLCYLS TVDWSLILDA VSNNYIVGNK 143
Hir     HLKELGLYNL MNITRGSVRI EKNNELCYLA TIDWSRILDS VEDNYIVLNK 149
Hirr    HLRDVALPAL GAVLRGAVRV EKNQELCHLS TIDWGLLQPA PGANHIVGNK 145

      *
Higflr  PPK.ECGDLC PGTMEEEKPM. CEKTTINNEY NYRCWTTNRC QKMCPSTCGK 191
Hir     DDNEECGDIC PGTAKGKTN. CPATVINGQF VERCWTHSHC QKVCPTICKS 198
Hirr    LG.EECADVC PGVLGAAGEP CAKTTFSGHT DYRCWTSSHC QRVCPCPHG. 193

      *
Higflr  RACTENNECC HPECLGSCSA PDNDTACVAC RHYYYAGVCV PACFPNTYRF 241
Hir     HGCTAEGLCC HSECLGNCSQ PDDPTKCVAC RNFYLDGRCV ETCPPPYHF 248
Hirr    MACTARGECC HTECLGGCSQ PEDPRACVAC RHLYFQGACL WACPPGTYYQY 243

      *
Higflr  EGWRCVDRDF CANILSAES. ...SDSEGFV IHDGECMQEC PSGFIRNGSQ 287
Hir     QDWRCVNFSF CQDLHHKCKN SRRQGCHQYV IHNNKCIPEC PSGYTMNSSN 298
Hirr    ESWRCVTAER CASLHSVPG. ....RASTFG IHQGSCLAQC PSGFTRNSS. 287

      *
Higflr  SMYCIPCEGP CPKVCEEEKK TKTIDSVTSA QMLQGCTIFK GNLLINIRRG 337
Hir     .LLCTPCLGP CPKVCHLLEG EKTIDSVTSA QELRGCTVIN GSLIINIRGG 347
Hirr    SIFCHKCEGL CPKECKV..G TKTIDSIQAA QDLVGCTHVE GSLILNLRQG 335

      *
Higflr  NNIASELENF MGLIEVVTGY VKIRSHALV SLSFLKNLRL ILGEEQLEGN 387
Hir     NNLAALEAN LGLIEEISGY LKIRSYALV SLSFFRKLRL IRGETLEIGN 397
Hirr    YNLEPQLQHS LGLVETITGF LKIKHSFALV SLGFFKNLKL IRGDAMVDGN 385

      *
Higflr  YSFYVLDNQN LQQLWDWDHR NLTIKAGKMY FAFNPKL CVS EIYRMEEVTG 437
Hir     YSFYALDNQN LRQLWDWSKH NLTITQGKLF FHYNPKLCLS EIHKMEEVSG 447
Hirr    YTLYVLDNQN LQQLGSWVAA GLTIPVGKIY FAFNPRLCLE HIYRLEEVTG 435

```

* !End of 1-462 fragment

BNSDOCID: <WO_____9928347A1_1_>

57/58

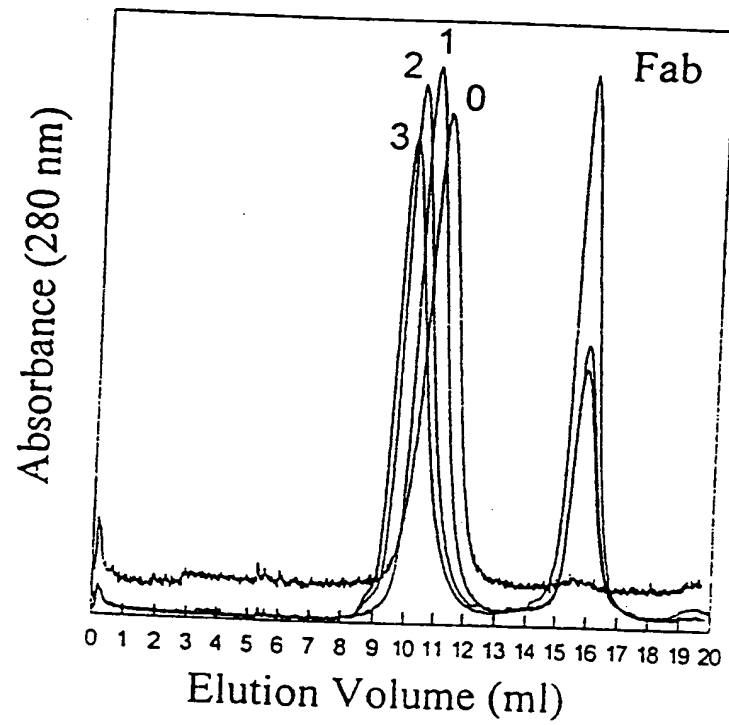


Figure 10

58/58











Schematic interpretations of EM images			
Sample	Projection along:		
	y axis	z axis	x axis
hIR			
hIR/ 83-7			
hIR/ 83-14			
hIR/ 18-44/83-14			
hIR/ 83-7/18-44			
hIR/ 83-7/83-14			

Figure 11

INTERNATIONAL SEARCH REPORT

International application No.
PCT/AU 98/00998

A. CLASSIFICATION OF SUBJECT MATTER

Int Cl⁶: C07K 14/705, 14/71; G06F 17/50, 19/00, 159:00

According to International Patent Classification (IPC) or to both national classification and IPC

B. FIELDS SEARCHED

Minimum documentation searched (classification system followed by classification symbols)

Documentation searched other than minimum documentation to the extent that such documents are included in the fields searched

Electronic data base consulted during the international search (name of data base and, where practicable, search terms used)
STN CAS-ON-LINE: keywords
MEDLINE :keywords

C. DOCUMENTS CONSIDERED TO BE RELEVANT

Category*	Citation of document, with indication, where appropriate, of the relevant passages	Relevant to claim No.
X	WO 90/00562 (DEMEYTS) 25 January 1990 See whole document	1-33
P.X	Protein Science, 1997, no. 6, pages 2663-2666 Mckern, NM et al. "Crystallization of the first 3 domains of the human idsuln-lila growth factor -1 receptor See whole document	1-33

☒ Further documents are listed in the continuation of Box C

☒ See patent family annex

* Special categories of cited documents:

"A" document defining the general state of the art which is not considered to be of particular relevance
"E" earlier application or patent but published on or after the international filing date
"L" document which may throw doubts on priority claim(s) or which is cited to establish the publication date of another citation or other special reason (as specified)
"O" document referring to an oral disclosure, use, exhibition or other means
"P" document published prior to the international filing date but later than the priority date claimed

"T" later document published after the international filing date or priority date and not in conflict with the application but cited to understand the principle or theory underlying the invention
"X" document of particular relevance: the claimed invention cannot be considered novel or cannot be considered to involve an inventive step when the document is taken alone
"Y" document of particular relevance: the claimed invention cannot be considered to involve an inventive step when the document is combined with one or more other such documents, such combination being obvious to a person skilled in the art
"&" document member of the same patent family

Date of the actual completion of the international search
12 January 1999

Date of mailing of the international search report
28 JAN 1999

Name and mailing address of the ISA/AU
AUSTRALIAN PATENT OFFICE
PO BOX 200
WODEN ACT 2606
AUSTRALIA
Facsimile No.: (02) 6285 3929

Authorized officer

OI LEE CHAI
Telephone No.: (02) 6283 2482

INTERNATIONAL SEARCH REPORT

International application No.

PCT/AU 98/00998

C (Continuation). DOCUMENTS CONSIDERED TO BE RELEVANT

Category*	Citation of document, with indication, where appropriate, of the relevant passages	Relevant to claim No.
P.X	Nature, vol 394, published 23 July 1998, pages 395-399, Garrett TPJ et al, "Crystal Structure of the first 3 domains of the type -I insulin-like growth factor-I receptor See whole document	1-33

INTERNATIONAL SEARCH REPORT

Information on patent family members

International application No
PCT/AU 98/00998

This Annex lists the known "A" publication level patent family members relating to the patent documents cited in the above-mentioned international search report. The Australian Patent Office is in no way liable for these particulars which are merely given for the purpose of information.

Patent Document Cited in Search Report		Patent Family Member					
WO	90/00562	AU	39822/89	DE	68927854	EP	378671
		JP	3501487	US	5227466		

END OF ANNEX



INTERNATIONAL APPLICATION PUBLISHED UNDER THE PATENT COOPERATION TREATY (PCT)

(51) International Patent Classification ⁶ : C07K 14/705, 14/71, G06F 17/50, 19/00, 159/00	A1	(11) International Publication Number: WO 99/28347 (43) International Publication Date: 10 June 1999 (10.06.99)
(21) International Application Number: PCT/AU98/00998 (22) International Filing Date: 27 November 1998 (27.11.98) (30) Priority Data: PP 0585 27 November 1997 (27.11.97) AU PP 2598 25 March 1998 (25.03.98) AU (71) Applicant (for all designated States except US): COMMON-WEALTH SCIENTIFIC AND INDUSTRIAL RESEARCH ORGANISATION [AU/AU]; Limestone Avenue, Campbell, ACT 2601 (AU). (71) Applicant (for US only): TULLOCH, Paul, Alexander (legal representative for the deceased inventor) [AU/AU]; 11 Kingston Court, Denmark, W.A. 6333 (AU). (72) Inventors; and (75) Inventors/Applicants (for US only): BENTLEY, John, David [AU/AU]; 85 Margaret Street, Macedon, VIC 3440 (AU). COSGROVE, Leah, Jane [AU/AU]; 22 Tarlton Street, Somerton Park, S.A. 5044 (AU). FRENKEL, Maurice, John [AU/AU]; 23 Ellington Street, South Caulfield, VIC 3162 (AU). GARRETT, Thomas, Peter, John [AU/AU]; 2 Gray Street, Brunswick, VIC 3055 (AU). LAWRENCE, Lynne, Jean [AU/AU]; 24 Cook Street, Brunswick, VIC 3055 (AU).		LOU, Meizhen [CN/AU]; 10 Roma Street, Scoresby, VIC 3179 (AU). LOVRECZ, George, Oscar [AU/AU]; 2 Tovey Street, North Balwyn, VIC 3104 (AU). McKERN, Neil, Moreton [AU/AU]; Como Road, Lilydale, VIC 3170 (AU). TULLOCH, Peter, Archibald (deceased). WARD, Colin, Wesley [AU/AU]; 903 Rathdowne Street, Carlton, VIC 3053 (AU). (74) Agent: F.B. RICE & CO.; 605 Darling Street, Balmain, NSW 2041 (AU). (81) Designated States: AL, AM, AT, AU, AZ, BA, BB, BG, BR, BY, CA, CH, CN, CU, CZ, DE, DK, EE, ES, FI, GB, GD, GE, GH, GM, HR, HU, ID, IL, IS, JP, KE, KG, KP, KR, KZ, LC, LK, LR, LS, LT, LU, LV, MD, MG, MK, MN, MW, MX, NO, NZ, PL, PT, RO, RU, SD, SE, SG, SI, SK, SL, TJ, TM, TR, TT, UA, UG, US, UZ, VN, YU, ZW, ARIPO patent (GH, GM, KE, LS, MW, SD, SZ, UG, ZW), Eurasian patent (AM, AZ, BY, KG, KZ, MD, RU, TJ, TM), European patent (AT, BE, CH, CY, DE, DK, ES, FI, FR, GB, GR, IE, IT, LU, MC, NL, PT, SE), OAPI patent (BF, BJ, CF, CG, CI, CM, GA, GN, GW, ML, MR, NE, SN, TD, TG). Published <i>With international search report.</i>
(54) Title: METHOD OF DESIGNING AGONISTS AND ANTAGONISTS TO IGF RECEPTOR (57) Abstract <p>The present invention relates to a method of designing compounds able to bind to a molecule of the insulin receptor family and to modulate the activity mediated by the receptor based on the 3-D structure coordinates of a IGF-1 receptor crystal of Figure 1.</p>		

FOR THE PURPOSES OF INFORMATION ONLY

Codes used to identify States party to the PCT on the front pages of pamphlets publishing international applications under the PCT.

AL	Albania	ES	Spain	LS	Lesotho	SI	Slovenia
AM	Armenia	FI	Finland	LT	Lithuania	SK	Slovakia
AT	Austria	FR	France	LU	Luxembourg	SN	Senegal
AU	Australia	GA	Gabon	LV	Latvia	SZ	Swaziland
AZ	Azerbaijan	GB	United Kingdom	MC	Monaco	TD	Chad
BA	Bosnia and Herzegovina	GE	Georgia	MD	Republic of Moldova	TG	Togo
BB	Barbados	GH	Ghana	MG	Madagascar	TJ	Tajikistan
BE	Belgium	GN	Guinea	MK	The former Yugoslav Republic of Macedonia	TM	Turkmenistan
BF	Burkina Faso	GR	Greece	ML	Mali	TR	Turkey
BG	Bulgaria	HU	Hungary	MN	Mongolia	TT	Trinidad and Tobago
BJ	Benin	IE	Ireland	MR	Mauritania	UA	Ukraine
BR	Brazil	IL	Israel	MW	Malawi	UG	Uganda
BY	Belarus	IS	Iceland	MX	Mexico	US	United States of America
CA	Canada	IT	Italy	NE	Niger	UZ	Uzbekistan
CF	Central African Republic	JP	Japan	NL	Netherlands	VN	Viet Nam
CG	Congo	KE	Kenya	NO	Norway	YU	Yugoslavia
CH	Switzerland	KG	Kyrgyzstan	NZ	New Zealand	ZW	Zimbabwe
CI	Côte d'Ivoire	KP	Democratic People's Republic of Korea	PL	Poland		
CM	Cameroon	KR	Republic of Korea	PT	Portugal		
CN	China	KZ	Kazakstan	RO	Romania		
CU	Cuba	LC	Saint Lucia	RU	Russian Federation		
CZ	Czech Republic	LI	Liechtenstein	SD	Sudan		
DE	Germany	LK	Sri Lanka	SE	Sweden		
DK	Denmark	LR	Liberia	SG	Singapore		
EE	Estonia						

NMR Study of the Transforming Growth Factor- α (TGF- α)-Epidermal Growth Factor Receptor Complex

VISUALIZATION OF HUMAN TGF- α BINDING DETERMINANTS THROUGH NUCLEAR OVERHAUSER ENHANCEMENT ANALYSIS*

(Received for publication, July 23, 1996, and in revised form, September 12, 1996)

Campbell McInnes†, David W. Hoyt†**, Richard N. Harkins§, Rene N. Pagila§, Maria T. Debanne¶, Maureen O'Connor-McCourt¶, and Brian D. Sykes¶

From the †Protein Engineering Network of Centres of Excellence, University of Alberta, Edmonton, Alberta T6G 2S2, Canada, §Berlex Biosciences, Richmond, California 94804, and the ¶Biotechnology Research Institute, Montreal, Quebec H4P 2R2, Canada

The study of human transforming growth factor- α (TGF- α) in complex with the epidermal growth factor (EGF) receptor extracellular domain has been undertaken in order to generate information on the interactions of these molecules. Analysis of ^1H NMR transferred nuclear Overhauser enhancement data for titration of the ligand with the receptor has yielded specific data on the residues of the growth factor involved in contact with the larger protein. Significant increases and decreases in nuclear Overhauser enhancement cross-peak intensity occur upon complexation, and interpretation of these changes indicates that residues of the A- and C-loops of TGF- α form the major binding interface, while the B-loop provides a structural scaffold for this site. These results corroborate the conclusions from NMR relaxation studies (Hoyt, D. W., Harkins, R. N., Debanne, M. T., O'Connor-McCourt, M., and Sykes, B. D. (1994) *Biochemistry* 33, 15283-15292), which suggest that the C-terminal residues of the polypeptide are immobilized upon receptor binding, while the N terminus of the molecule retains considerable flexibility, and are consistent with structure-function studies of the TGF- α /EGF system indicating a multidomain binding model. These results give a visualization, for the first time, of native TGF- α in complex with the EGF receptor and generate a picture of the ligand-binding site based upon the intact molecule. This will undoubtedly be of utility in the structure-based design of TGF- α /EGF agonists and/or antagonists.

Human TGF- α ¹ is a 50-amino acid polypeptide with 40% sequence homology to epidermal growth factor (1, 2). In addition,

the structural similarity of the two molecules results in their ability to compete for binding to the EGF receptor (3-5). Complexation of TGF- α with this receptor is believed to mediate a variety of biological effects, including embryonic development of certain tissues and wound healing (6, 7); however, the major sphere of interest of this protein lies in its role in the transformation and maintenance of various malignant tumors (8, 9).

The structural features of the homologous growth factors that contain three disulfides and hence three loops (A, B, and C) have been determined by NMR (10-13) and include a triple-stranded anti-parallel β -sheet comprising the N-terminal region, a smaller anti-parallel double hairpin in the C terminus of the molecule, and a helical segment in the A-loop in some structures. Previous studies undertaken to elucidate the structurally important residues of TGF- α (and EGF) required for complexation have implicated residues including Phe-15, Tyr-38, Arg-42, and Leu-48 (14-18). The consensus of a variety of structural studies including the use of synthetic peptide fragments (19-21), recombinant chimeric proteins (22, 23), and anti-TGF- α and anti-EGF antibodies (24, 25) is that receptor binding occurs with multiple domains of TGF- α , although conflicting results have been obtained concerning the involvement of the A-, B-, and C-loops. The multidomain binding model is consistent with the observation that, at present, it is not possible to reduce the size of the growth factor without significantly compromising its affinity for the EGF receptor. This was illustrated by deletion studies where the N-terminal residues outside the A-loop were truncated. This mutant had 3% of the binding affinity of the intact protein (20). Further data from receptor-bound TGF- α may lead to the structure-based design of reductant molecules through the precise identification of ligand binding determinants.

Hoyt *et al.* (26) have recently demonstrated, through a study of ^1H NMR transverse and longitudinal relaxation rates for the methyl resonances of TGF- α in the free state and in association with the EGFR-ED, that the C-terminal residues undergo a dramatic decrease in flexibility upon binding, while the N terminus maintains a degree of mobility similar in both bound and free forms of the ligand. The mid-portion of the molecule underwent a moderate decrease in flexibility relative to the uncomplexed polypeptide. The conclusions of this work are consistent with the previous studies, which suggest that the C-terminal residues are responsible for receptor binding, while the B-loop provides a structural scaffold for the primary site of interaction.

This study presents new insight into the components of the TGF- α structure that are requisite for complex formation from

* The costs of publication of this article were defrayed in part by the payment of page charges. This article must therefore be hereby marked "advertisement" in accordance with 18 U.S.C. Section 1734 solely to indicate this fact.

¶ To whom correspondence should be addressed: Protein Engineering Network of Centres of Excellence, 713 Heritage Medical Research Centre, University of Alberta, Edmonton, Alberta T6G 2S2, Canada. Tel.: 403-492-6540; Fax: 403-492-1473; E-mail: bds@polaris.biochem.ualberta.ca.

** Current address: Battelle-Pacific Northwest National Laboratory, Richland, WA 99352.

¹ The abbreviations used are: TGF- α , transforming growth factor- α ; EGF, epidermal growth factor; EGFR-ED, epidermal growth factor receptor extracellular domain; FID, free induction decay; NOESY, nuclear Overhauser enhancement spectroscopy; HMQC, heteronuclear multiple quantum correlation; NOE, nuclear Overhauser enhancement cross-peak; TR-NOESY, transferred nuclear Overhauser enhancement spectroscopy.

the analysis of changes in the two-dimensional ^1H NMR NOESY spectra of the ligand upon titration with the EGFR-ED (molecular mass of 85 kDa). NMR is the method of choice in the elucidation of the ligand contact sites with the receptor since it is the only technique that can give detailed information on these molecules in solution. The results suggest the involvement of residues in the A- and C-loops and C-terminal tail in the primary site of interaction of the growth factor with its receptor.

EXPERIMENTAL PROCEDURES

Expression and Purification of TGF- α —TGF- α and the EGFR-ED were prepared and purified according to previous methods (26).

NMR Sample Preparation—To a lyophilized sample of TGF- α was added 460 μl of buffer containing 50 mM potassium phosphate, 10 mM potassium chloride, 1 mM EDTA, 0.5 mM sodium azide, 0.15 mM sodium 2,2-dimethyl-2-silapentane-5-sulfonate (internal standard), and 99.9% D_2O or 90/10% (v/v) $\text{H}_2\text{O}/\text{D}_2\text{O}$. The solution was adjusted to pH 6.0 by the addition of small aliquots of 0.5 N NaOD or 0.5 N HCl, bringing the final volume to 500 μl . 230- μl aliquots of a stock EGFR-ED solution that had previously been dialyzed against the above buffer were then added successively to the TGF- α NMR sample to give concentrations of 0, 2.4, 4.9, and 6.5% EGFR-ED.

^1H NMR Spectroscopy— ^1H NMR spectra for TGF- α free in solution and in the presence of various amounts of EGFR-ED were acquired at 599.9 MHz using a Varian Unity 600 spectrometer. These included one-, two-, and three-dimensional experiments collected at 298 K, referenced relative to an internal sodium 2,2-dimethyl-2-silapentane-5-sulfonate standard and utilizing presaturation to attain suppression of the water resonance. The hypercomplex method (27) was used for acquisition of two-dimensional NOESY spectra (28–30), which incorporated 40, 64, 96, and 120 transients (for 0, 2.4, 4.9, and 6.5% EGFR-ED titration points, respectively) for each of 256 increments. NOESY spectra were recorded using 50-, 100-, and 150-ms mixing times at each receptor concentration. Each spectrum employed a spectral width of 8000 Hz and 2048 data points. The Fourier transformation of the spectra utilized shifted sinebell and zero filling to 4096 points in both dimensions. The three-dimensional ^{15}N edited NOESY (HMQC-NOESY) spectrum was acquired using a mixing time of 150 ms with the proton carrier frequency set to 4.73 ppm and a presaturation pulse to suppress the H_2O peak. The experiment was collected with sweep widths of 8000, 4000, and 1500 Hz for the ^1H , ^{15}N , and ^{15}N dimensions, respectively, with 128 (t_1), 32 (t_2), and 512 (t_3) complex points and eight scans per increment. Processing of the FID was performed using the NMRPipe program (31) and was zero-filled in F1, F2, and F3 and linear-predicted in F2 to a final size of 1024 (F_3) \times 512 (F_1) \times 64 (F_2) points. A sinebell squared weighting function shifted by 72° was applied in all three dimensions during processing.

NOEs were assigned based on the complete resonance assignment previously reported for TGF- α at pH 6.0 (26), and their volume was integrated using a combination of the NMR processing and autoassignment programs PIPP (32) and VNMR (VNMR 5.1A, Varian Associates, Palo Alto, CA). Changes in the intensity of the NOEs over the course of the receptor titration were analyzed using the program SPEAK (Robert Boyko, University of Alberta). This program ranks the NOEs in order of the increase or decrease in their volume (scaled by the average intensity for each spectrum) as a percentage of the volume for the corresponding cross-peak in the free ligand.

RESULTS

Two-dimensional ^1H NMR NOESY spectra of TGF- α free in solution and in complex with the EGF receptor at different [TGF- α]/[EGFR-ED] ratios were performed in order to generate structural information on the bound conformation of TGF- α , which could be used to determine the specific regions and residues of the ligand involved in binding. Using the transferred NOE methodology, a ligand in fast exchange with a receptor molecule is studied in excess (usually 10:1 to 20:1) over the receptor. During the course of the NOESY experiment, the bound ligand magnetization is transferred to the excess free ligand through chemical exchange, and thus, the NMR information characterizing the bound structure is observed via the sharp resonances of the free ligand. At pH 6.0, TGF- α is in fast exchange with the EGFR-ED and has an off-rate of $\geq 300 \text{ s}^{-1}$

(26), and therefore, this system has conditions amenable to study by TR-NOESY. The complete assignment of proton NMR resonances of TGF- α at pH 6.0 has been previously reported (26) and was utilized in order to assign the cross-peaks for a series of TR-NOESY spectra of TGF- α free and in the presence of 0, 2.4, 4.9, and 6.5% EGFR-ED. From the 150-ms NOESY data, of a total of 544 cross-peaks in the free ligand, 419 were assigned unambiguously. Of the 419 unambiguous cross-peaks, 404 were assigned from the two-dimensional NOESY spectrum and 15 were additionally assigned from the three-dimensional HMQC-NOESY spectrum as the latter were able to be resolved in the ^{15}N dimension from the three-dimensional spectrum.

After assignment of the TR-NOESY cross-peaks for the EGFR-ED titration series, it became apparent that very few new peaks were observed in the spectra. Due to the absence of new cross-peaks or observable chemical shift differences between the free and bound ligand, it was concluded that no major structural rearrangement of TGF- α occurs upon complexation. However, a systematic study of the spectra obtained for each point of the TGF- α /EGFR-ED titration revealed specific information on the sites of interaction of the growth factor. This was achieved by ranking the cross-peaks by the slope of the NOE intensity changes during the receptor titration series. For each spectrum in the series, the NOE volume is first divided by the average intensity in order to more accurately assess the changes between spectra. For the addition of 2.4% EGFR-ED, 524 NOEs were observed in the 150-ms NOESY spectrum, indicating that 20 peaks had disappeared. For the subsequent aliquot, bringing the receptor concentration to 4.8%, the corresponding spectrum contained 476 NOEs, and thus, 48 additional NOEs had disappeared. For the final aliquot (6.5% EGFR-ED), 434 NOEs were observed, and thus, a further 42 were absent in this spectrum. For the peaks that remained over the course of the titration, 186 increased in intensity, and 247 decreased in intensity. Fig. 1 illustrates the amide and aromatic connectivities of the TR-NOESY spectra of TGF- α , free (panel A) and in the presence of 6.5% EGFR-ED (panel B). It can be seen from these spectra that the majority of the cross-peaks decrease in intensity in the bound compared with the free ligand.

With the intention of elucidating the receptor contact sites, the NOEs that disappeared from 150-ms NOESY spectra over the course of the titration were examined. Cross-peak intensity in TR-NOESY spectra is determined by a large number of factors, including relaxation in the free and bound ligand, exchange rate, fraction bound, and NOESY mixing time. Relaxation in the free ligand is determined by internuclear distance and the rotational correlation times of the free ligand, while relaxation in the bound ligand is influenced by internuclear distance, the rotational correlation time of the complex, and additional relaxation pathways involving contact between protons in the ligand and in the target protein. In general, when the ligand is a small flexible peptide, the intrinsic NOEs in the absence of protein are small because of the short correlation time and concomitant long cross-relaxation rates. In the complex with the target protein, the ligand assumes the correlation time of the large protein and exists in the spin-diffusion limit ($\omega_0^2 \tau_c^2 > 1$) where the NOEs are large. Under these circumstances, the TR-NOESY intensities generally increase as the fraction of ligand bound increases (for small fraction bound) at constant NOESY mixing time or increase with increasing NOESY mixing time (for short τ_{mix}) at constant fraction bound (33, 34). The ranges over which these limits are observed become more stringent as the size of the target protein increases. However, the situation is more complicated when the ligand is also a protein such as TGF- α for which

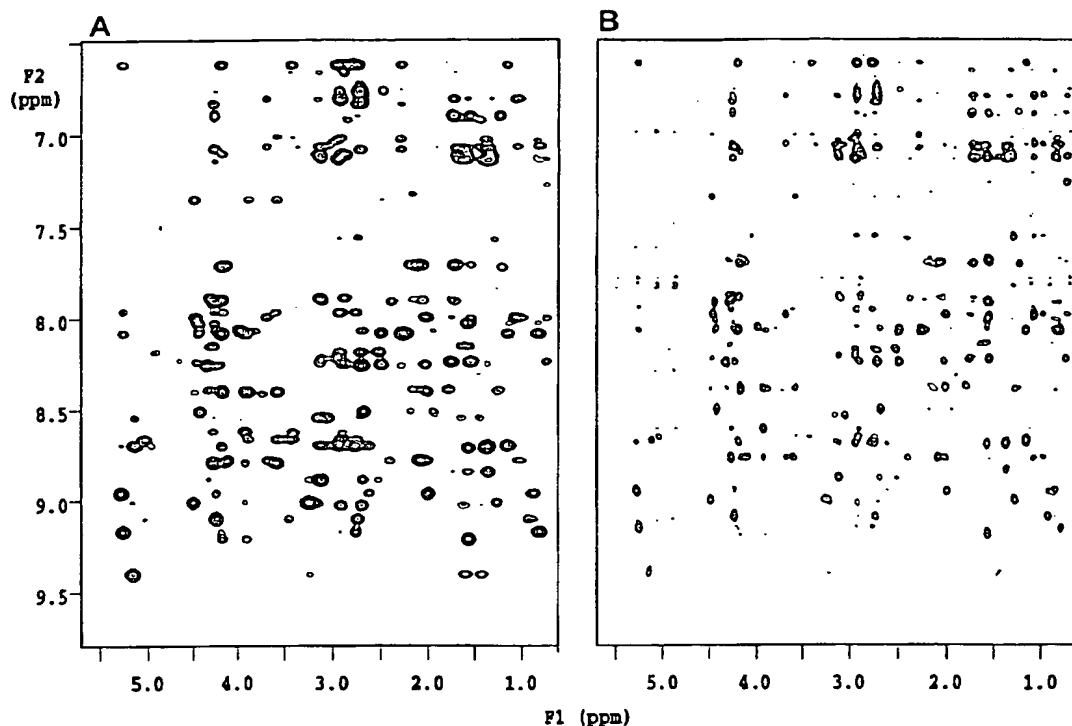


FIG. 1. TR-NOESY spectra of free TGF- α (A) and in the presence of 6.5% EGFR-ED (B) acquired at 600 MHz at 25 °C with a mixing time of 150 ms, illustrating the amide and aromatic through space connectivities of the ligand.

significant NOESY cross-peaks already exist and where differential mobility exists in both the free and bound states, as is also the case with TGF- α (26). Thus, one can expect TR-NOESY cross-peaks to both increase and decrease. *A priori*, one would expect shorter bound internuclear distance and increased correlation time to increase TR-NOESY cross-peak intensity in the limit of small fraction bound and short NOESY mixing times, but the effect can be attenuated by rapid cross-relaxation. Longer distances and additional relaxation pathways involving ligand protons would lead to a decrease in cross-peak intensity at small fraction bound and short mixing times.

To quantitate the effects of the competing influences in TR-NOESY cross-peak intensity, we have simulated spectra with estimates of the free and bound correlation times (3 and 40 ns, respectively) and exchange rates (500 s^{-1}) using a program developed for Mathematica and kindly provided by R. London (35) and subsequently modified by one of us (B. D. S.). The simulations indicate that the change in the TR-NOESY intensity is approximately linear in fraction bound for the values of fraction bound and mixing time used in this study, as is observed experimentally. Increases in intensity expected from the increased bound rotational correlation time are slight at the fraction bound used. The most striking effects come when additional relaxation pathways are considered that lead to a decrease in cross-peak intensity.

Therefore, it was decided that the most unambiguous TR-NOESY cross-peaks to focus on were those that decrease, possibly caused by increased internuclear distance, but most likely as a result of increased relaxation caused by spin-diffusion contact with protons on the target protein. Although there is an overall decrease in NOE intensity throughout the TGF- α molecule, corresponding increases in intensity of a number of cross-peaks are observed (one-third of the total number of NOEs are more intense in the TGF- α -EGFR-ED complex).

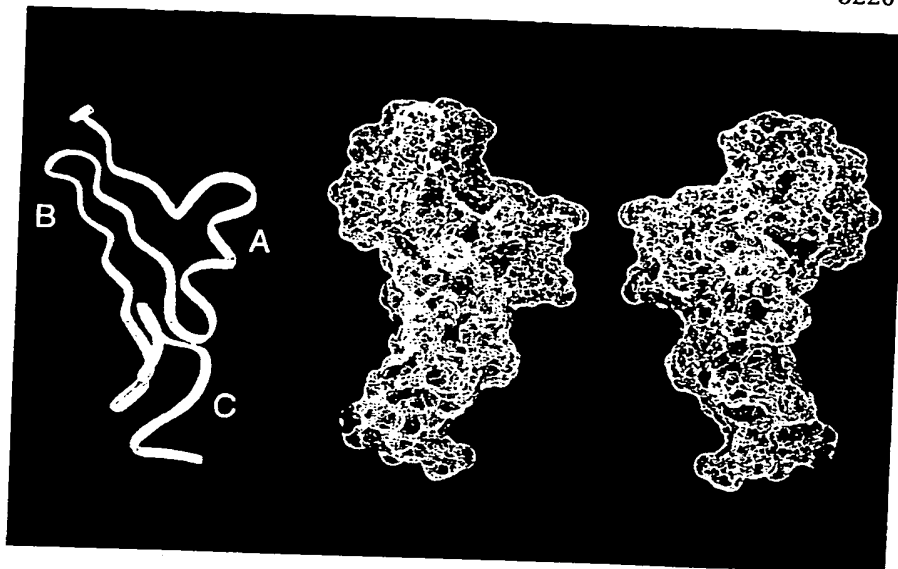
Since there are a number of pathways by which the intensity increases can occur, their interpretation is not straightforward; however, since it is probable that magnetization bleed-off occurs from ligand contact sites, it can be surmised that the atoms involved in NOEs that increase are those that either are non-surface protons or are not in contact with the EGF receptor, which typically experience the largest perturbations upon binding.

In addition to ligand magnetization loss to receptor protons, exchange broadening may play a significant role in the decreased NOE intensities. The interpretation of absent NOEs in the receptor-bound ligand is not affected in this case since these effects would be most pronounced for the residues and atoms in contact with the receptor.

For the case of the complexation of TGF- α with the EGF receptor, in which the changes in the NOE intensity from the series of NOESY spectra were examined, the most striking changes were in the number of NOEs that disappeared over the course of the receptor titration. Of a total of 544 NOEs in the uncomplexed form of TGF- α , 110 NOEs were no longer present in the bound polypeptide (*i.e.* the final receptor titration point). As discussed, the disappearance of these peaks most probably occurs as a result of magnetization bleed-off from protons of the ligand that are in direct contact with the receptor.

From the changes in the NOE intensity upon receptor addition, an understanding of the molecular nature of the interactions of the TGF- α -EGFR-ED complex can thus be deduced. As mentioned, of particular significance are the NOEs that are absent from the NOESY spectra of bound TGF- α . Fig. 2 illustrates a Connolly surface representation of the TGF- α structure and shows the atoms involved in NOEs that disappear in the NOESY spectrum of the TGF- α -6.5% EGFR-ED complex. From Fig. 2, the observation can be made that almost the whole surface of the polypeptide has atoms that lose cross-peaks, with

FIG. 2. Connolly surface representation of the TGF- α structure. The atoms involved in NOEs that disappear upon receptor binding are colored in red. Two faces of the molecule are shown (180° rotation) along with a ribbon diagram (corresponding to the left face) illustrating the loops and secondary structure. The three disulfide loops are labeled in the ribbon diagram.



the exception of the N-terminal region of the triple-stranded β -sheet. The face of the molecule displayed on the right of Fig. 2 has the greatest concentration of atoms involved in the absent NOEs, and for this face, the residues forming the C-loop predominate in this regard. This representation indicates the putative sites of contact and binding on the ligand and suggests that a large section of the protein occupies the binding pocket of the receptor.

While this manner of visualization of the receptor binding interactions is useful, it is insufficient to obtain a statistical picture of the NOEs that disappear as a particular atom can be involved in a number of absent NOEs. To address this, the number of NOEs that disappeared for each residue was determined, and the results are expressed as a percentage of NOEs per residue that were absent upon complexation *versus* the number of NOEs per residue in the free ligand. Fig. 3 (A and B) shows the total number of NOEs per residue and the percentage of absent NOEs in the receptor-bound ligand, respectively. Examination of Fig. 3B reveals some striking information on the changes that are concomitant with receptor binding. First, residues 1–4, 10, and 25–27 have no NOEs that disappear, indicating that they are not immobilized by the receptor. Interestingly, these residues are localized on the TGF- α structure at the N-terminal subdomain embodying part of the triple-stranded β -sheet. The other noticeable features of the graph in Fig. 3B are the residues for which between 40 and 60% of the free ligand NOEs are absent. These include His-12, Thr-13, Phe-15, Phe-17, Ala-31, Val-39, Gly-40, His-45, Leu-48, and Leu-49 and comprise segments of the A- and C-loops and the C-terminal tail of TGF- α . Also significant are those amino acids that lose between 20 and 40% of their cross-peaks upon complexation. If these are considered, almost all of the A-loop residues (from Ser-11 to Leu-24) are affected.

When the results shown in Fig. 3B are grouped into classes by percentage and visualized on the TGF- α structure, further insight into the ligand/receptor interactions is facilitated. Fig. 4 illustrates the NOE changes by color on the surface of TGF- α and on the secondary structure of the growth factor. The immediate observation from Fig. 4 is the localization of the different colored residues. The blue and purple colors (representing the least changes in terms of absent NOEs) are clustered, for the most part, in the N-terminal subdomain of the ligand. The white colors (indicating 20–30% of NOEs that disappear)

are more disperse throughout the molecule; however, the green residues (30–40% NOEs absent) are grouped on one face, which comprises the central region of TGF- α on the B- and C-loops. The residues involved in the highest percentage of absent NOEs in the receptor-bound state (shown in red) are clustered in two groups, the major of which also constitutes one face of TGF- α . This face consists of residues in the A- and C-loops and the C-terminal tail of the ligand. This face also includes Glu-44, which loses 30–40% of NOEs upon binding, and is contiguous with His-12, Phe-15, Phe-17, Val-39, Gly-40, and His-45 (which lose 40–60% of NOEs) on the surface of the molecule. Leucines 48 and 49 on the C-terminal tail of TGF- α both lose 50% of their NOEs, indicating that these residues play a significant role in the binding interface of the ligand-receptor complex.

Examination of the NOEs in terms of the intramolecular, intermolecular, and long-range ($i, i+2$ or further) NOEs that disappear indicates that they have similar distribution as occurs in the free ligand, *i.e.* in the NOESY spectrum of the bound ligand, 29, 36, and 39% of the intramolecular, intermolecular, and long-range NOEs, while in free TGF- α , the values are 35, 34, and 31%, respectively. This suggests that the structure is not significantly altered upon binding and that one class of NOE is not greatly more affected than another. If the case were considered where a significantly higher percentage (relative to the free ligand) of intermolecular rather than intramolecular NOEs disappeared upon binding, then this would suggest that structural perturbations rather than complexation were responsible.

Further inspection of the NOE data provides information on receptor binding that augments that previously discussed. Fig. 5 shows the number of NOEs that disappear upon addition of the first receptor aliquot. Of particular note are the most intense NOEs that are absent in the receptor-bound form. These NOEs are suggestive of the residues that form the strongest interaction with the EGF receptor since they disappear at the lowest receptor concentration. The majority of these correlate with those residues identified in the previous interpretation (Fig. 4) and thus predicate the implied binding interface.

DISCUSSION

The NOE analysis method for elucidating the receptor contact sites of the ligand is discussed in light of the current

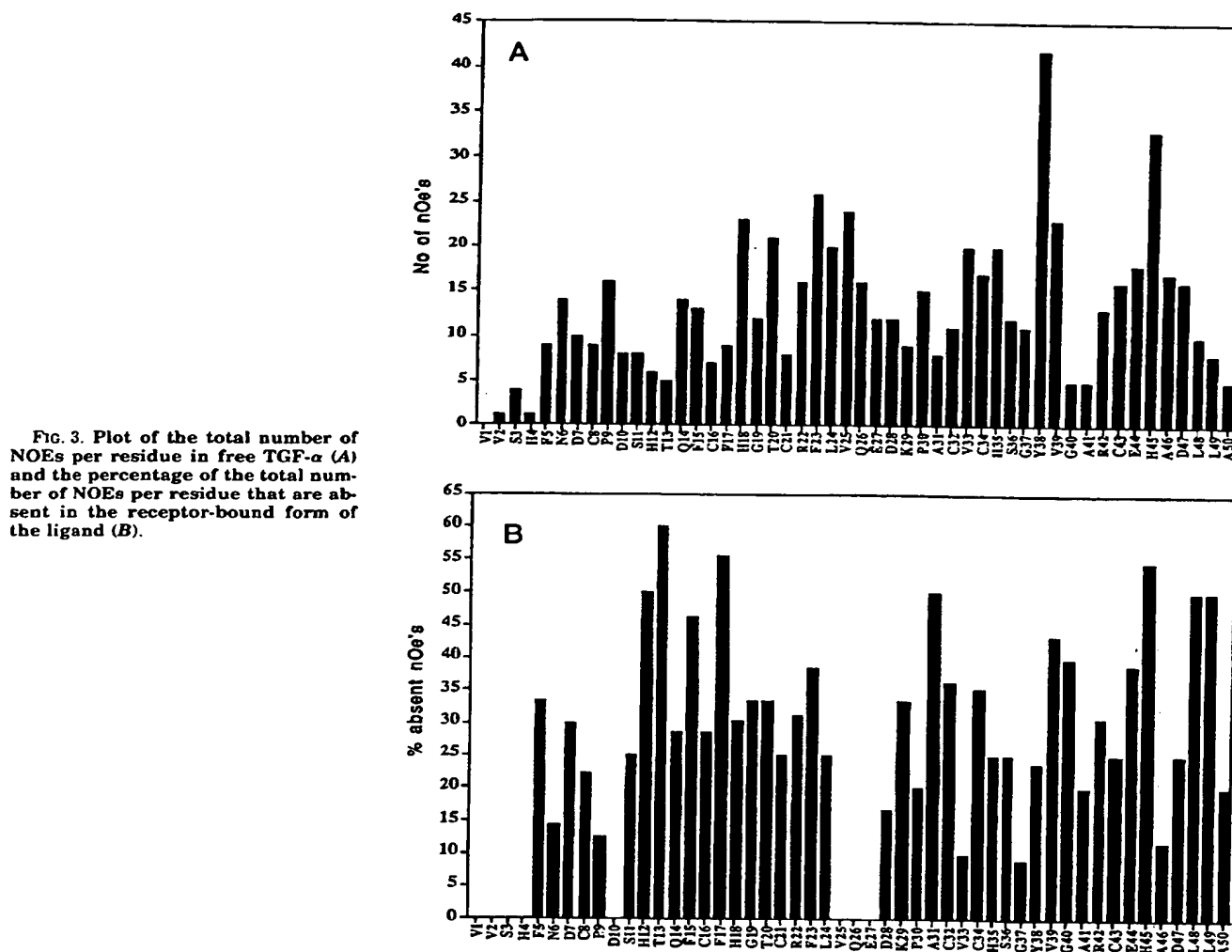


FIG. 3. Plot of the total number of NOEs per residue in free TGF- α (A) and the percentage of the total number of NOEs per residue that are absent in the receptor-bound form of the ligand (B).

understanding of the molecular requirements for TGF- α complex formation with the EGF receptor. A plethora of studies have been undertaken to determine the components of the TGF- α /EGF system that are requisite for receptor binding and activation; however, these as a whole have failed to provide a consensus as to the essential residues and regions (19–25). It has been established that a correct native fold of both growth factors is critical for biological activity since the disruption of any single disulfide results in complete loss of binding (14). Deletion studies using synthetic peptides indicate that virtually no part of these polypeptides can be removed without a significant decrease in activity. Even removal of the flexible N-terminal tail in the case of TGF- α yields an analog with only 3% of the binding affinity of the native molecule (20).

Studies of EGF and TGF- α mutants in which single amino acids are replaced in a conservative or nonconservative fashion have, for the most part, produced conflicting results. Despite this, the critical role of certain residues in receptor binding and activation has emerged, including Phe-15, Tyr-38, Arg-42, and Leu-48 (14–18).

The results obtained by the NOE analysis method support a multidomain model for receptor binding as postulated (19–25) and shown in Fig. 4. The majority of the most important residues for EGF receptor complex formation as suggested by the

residues that lose the highest percentage of NOEs are presented on a common face of TGF- α that comprises the A- and C-loops and consists of His-12, Phe-15, Phe-17, Val-39, Gly-40, and His-45, thus strongly implicating this face as a binding determinant for the ligand/receptor interaction. This postulation is corroborated by a previous study that demonstrated that antibodies specific for an epitope on the opposite face, consisting of the residues of the B-loop, were non-neutralizing in terms of receptor binding and thus proposed that the face of TGF- α including residues 12–20 and 34–43 was involved in binding (25). When the residues for which 30–40% of the NOEs were absent in the bound ligand were included in the face, a more extensive contiguous surface for receptor binding was apparent. This surface now includes two of the critical residues (Arg-42 and Phe-15) that lose 31 and 46% of their NOEs, respectively. Arg-42, which appears to be less important for binding based on the NOE criterion, may play a structural role in preserving the local conformation of Phe-15, which is a critical residue based upon the NOE data. Structural studies of the inactive R42K mutant exclude any gross conformational changes; however, do not rule out subtle effects that alter the microenvironment of the phenylalanine (17, 36).

A recent study on a chimeric growth factor consisting of the A- and C-loops of EGF and the B-loop of TGF- α concluded that,

FIG. 4. Connolly surface representation of TGF- α illustrating the percentage of absent NOEs per residue grouped into classes. 0%, blue; 0-20%, purple; 20-30%, white; 30-40%, green; and 40-60%, red.

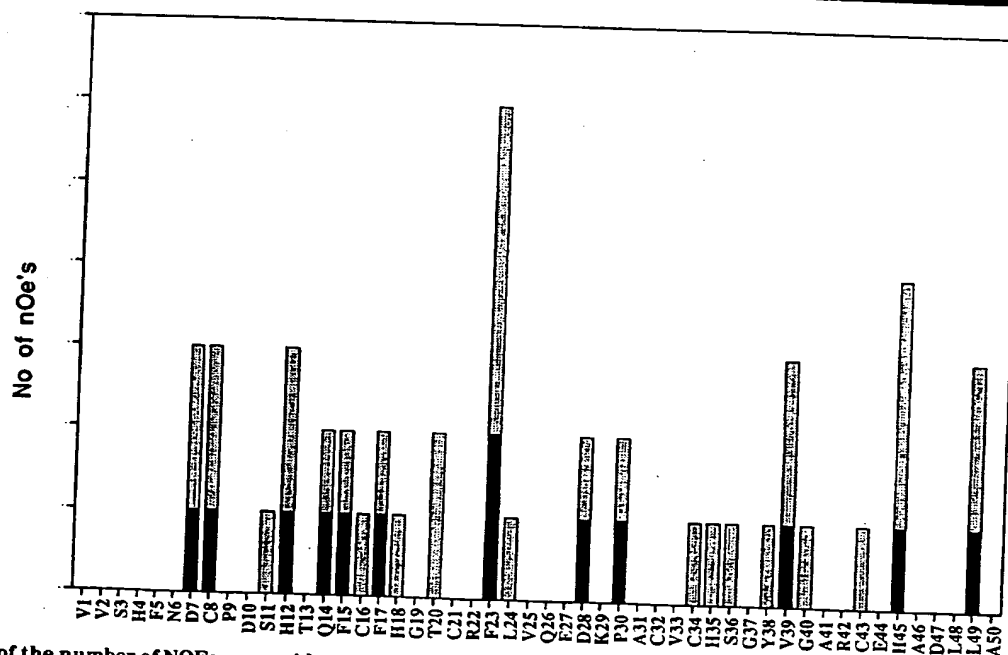
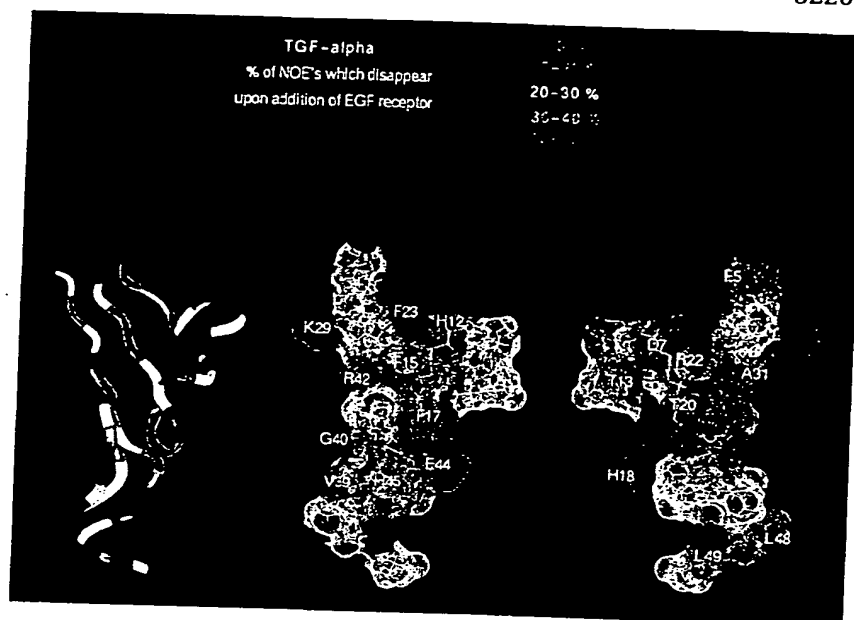


FIG. 5. Plot of the number of NOEs per residue that disappear upon addition of the first aliquot of receptor. The most intense NOEs that are absent are those in black.

since the hybrid protein exhibited enhanced binding to the receptor relative to EGF, the B-loop is an important determinant for receptor binding and mitogenic activity (22). This statement is undoubtedly true due to the multiplicity of binding domains; however, our results suggest that the B-loop plays more of a structural role in providing a molecular scaffold for presentation of the A- and C-loops to the receptor. In the case of the chimeric protein, the enhanced activity probably results from the increased stability of the A- and C-loop conformation effected by the B-loop. Another study from the same group reported mitogenic activity for a constrained B-loop analog of TGF- α (37); however, it was very low relative to the native

molecule and thus does not eliminate the role of A- and C-loop residues since the latter have been shown to contribute significantly to binding and activation of the receptor (14-18).

From Fig. 4, it is apparent that leucines 48 and 49 are immobilized in the receptor-bound ligand; however, it is also evident that these residues are not contiguous with the previously mentioned receptor interface. This observation implies that these residues provide a second interface that is integral for receptor complex formation. The impotency of the L48A analog of TGF- α (18) corroborates the role of this face as a second anchor point to the EGF receptor.

Site-directed mutagenesis of Tyr-38 in TGF- α and Tyr-37 in

FIG. 6. Comparison of the data obtained from measurement of R_2 relaxation rates ($1/T_2$) versus data from the NOE analysis displayed by color on the ribbon diagram of TGF- α . The differential mobility as suggested by the data is colored as follows: high mobility, blue; intermediate, green; low mobility, red; and no data, white.



EGF apparently gives conflicting results for the significance of this residue in the receptor interaction since it was shown to be nonessential in EGF (38) and essential in TGF- α (16). This conflict may be the consequence of a different mechanism or site of binding with the two ligands; however, our NOE data indicate that if mutation of this residue precludes binding of TGF- α , then it does so by altering the ligand conformation and thus probably does not contribute directly to the interaction.

If the NOEs that disappear upon addition of the first receptor aliquot are considered, then further insight into the receptor contacts is obtained. Of special note in the consideration of these NOEs are those of the greatest intensity that are absent in the spectrum of the first point of the titration. It can be envisaged that these NOEs belong to residues of TGF- α bound most tightly to the EGFR-ED. These residues include His-12, Phe-15, Phe-17, Phe-23, Val-39, His-45, and Leu-49 and, for the most part, predicate the postulated binding faces and the contentions of the analog studies.

It can be observed from Fig. 4 that the green residues (30–40% absent NOEs) are clustered on the view of TGF- α on the right. It is tempting to suggest that this face forms a binding interface for a second EGF receptor molecule and is of lower affinity than the face illustrated on the left Connolly surface representation in Fig. 4. Obviously, further experiments would be required to confirm this, although it has been proposed that the TGF- α /EGF/EGFR system is similar to that of human growth hormone, where one hormone binds two receptor molecules and some evidence for this mechanism has been discussed (39).

Hoyt *et al.* (26) have recently published a detailed study of methyl relaxation rates of TGF- α both free in solution and in complex with the receptor. Since these results and the current study were performed under the same conditions, congruity is to be expected between the two methods of analyzing the ligand/receptor interactions. Comparison of the transverse relaxation rates for all of the methyl-containing residues of TGF- α was used to delineate the relative mobilities of these residues within the TGF- α structure. Val-1 and Val-2 showed the highest mobility when receptor bound with virtually no enhancement of R_2 upon receptor binding. Since these two residues are flexible in both the bound and free forms, they are largely devoid of NOEs, and thus, the NOE comparison with the relaxation data cannot be made. Thr-13, Thr-20, Leu-24, Val-25, and Ala-31 all undergo intermediate loss of flexibility

as determined from the R_2 values. This compares favorably with the NOE data (Fig. 6), which suggest, with the exception of Val-25, that these residues are in contact with the receptor. Val-25, which is part of the β -turn of the β -sheet in the B-loop, does not lose any NOEs upon receptor binding, thus suggesting that this residue is not involved in receptor binding. Its methyl relaxation, however, indicates that its mobility is somewhat restricted upon complexation. A possible explanation is that its mobility is restricted compared with the very flexible N-terminal tail, but it is still flexible enough that the NOEs of this residue, which may not be in direct contact with the receptor, thus do not disappear due to magnetization bleed-off. The residues of the C-loop and C-terminal tail show strong agreement between the relaxation and NOE data as these have both the largest relaxation enhancements and the largest percentage of NOEs that disappear upon complex formation.

The results of this study demonstrate that the NOE analysis method provides a model that explicates the current understanding of TGF- α /EGF interactions with the EGF receptor in terms of a multidomain model and provides significant information on the residues contributing to binding and activation.

CONCLUSIONS

Detailed analysis of the NOEs for free and bound species of TGF- α indicates that the majority of residues of the ligand that have the highest percentage of absent NOEs in the bound form embody one face of the molecule that is composed of the A- and C-loops. A second receptor anchor point is formed by the two C-terminal leucines. The NOE analysis results are consistent with relaxation studies that indicate restricted C-terminal mobility in bound TGF- α and with structure-function studies that suggest a multidomain ligand binding model. The elucidation of the ligand interaction sites is essential for the future development of TGF- α agonists and/or antagonists using structure-based drug design methodology.

Acknowledgments—We thank Dr. Krishna Rajarathnam for critical reading of this manuscript. We thank Paul Semchuk for expert technical assistance in mass spectrometry of TGF- α . In addition, we thank Susan Smith and Susan Henry for helpful clerical assistance.

REFERENCES

1. Campbell, I. D., Cooke, R. M., Baron, M., Harvey, T. S., and Tappin, M. J. (1989) *Prog. Growth Factor Res.* 1, 13–22.
2. Simpson, R. J., Smith, J. A., Moritz, R. L., O'Hare, M. J., Rudland, P. S., Morrison, J. R., Lloyd, C. J., Grego, B., Burgess, A. W., and Nice, E. C.

- (1985) *Eur. J. Biochem.* 153, 629-637
3. Carpenter, G. (1987) *Annu. Rev. Biochem.* 56, 881-914
4. Kott, M., and Finman, J. E. (1989) *J. Biol. Chem.* 264, 14990-14999
5. Lax, I., Fischer, R., Ng, C., Segre, J., Ullrich, A., Givol, D., and Schlessinger, J. (1991) *Cell Regul.* 2, 337-345
6. Bennet, N. T., and Schultz, G. S. (1993) *Am. J. Surg.* 165, 728-737
7. Bennet, N. T., and Schultz, G. S. (1993) *Am. J. Surg.* 166, 74-81
8. Derynck, R., Goeddel, D. V., Ullrich, A., Gutterman, J. U., Williams, R. D., Bringman, T. S., and Berger, W. H. (1987) *Cancer Res.* 47, 707-712
9. ten Dijke, P., and Iwata, K. K. (1989) *Bio/Technology* 1, 793-798
10. Kohda, D., Shimada, I., Miyake, T., Fuwa, T., and Inagaki, F. (1989) *Biochemistry* 28, 953-958
11. Kline, T. P., Brown, F. K., Brown, S. C., Jeffs, P. W., Kopple, K. D., and Mueller, L. (1990) *Biochemistry* 29, 7805-7813
12. Harvey, T. S., Wilkinson, A. J., Tappin, M. J., Cooke, R. M., and Campbell, I. D. (1991) *Eur. J. Biochem.* 198, 555-562
13. Moy, F. J., Li, Y.-C., Raubenbuehler, P., Winkler, M. E., Scheraga, H. A., and Montelione, G. T. (1993) *Biochemistry* 32, 7334-7353
14. Groenen, L. C., Nice, E. C., and Burgess, A. W. (1994) *Growth Factors* 11, 235-257
15. Defeo-Jones, D., Tai, J. Y., Wegrzyn, R. J., Vuocolo, G. A., Baker, A. E., Payne, L. S., Garsky, V. M., Oliff, A., and Rieman, M. W. (1988) *Mol. Cell. Biol.* 8, 2999-3007
16. Lazar, E., Vicenzi, E., Van Obberghen-Schilling, E., Wolff, B., Dalton, S., Watanabe, S., and Sporn, M. B. (1989) *Mol. Cell. Biol.* 9, 860-864
17. Defeo-Jones, D., Tai, J. Y., Vuocolo, G. A., Wegrzyn, R. J., Scholfield, T. L., Rieman, M. W., and Oliff, A. (1989) *Mol. Cell. Biol.* 9, 4083-4086
18. Lazar, E., Watanabe, S., Dalton, S., and Sporn, M. B. (1988) *Mol. Cell. Biol.* 8, 1247-1252
19. Heath, W. P., and Merrifield, R. B. (1986) *Proc. Natl. Acad. Sci. U. S. A.* 83, 6367-6371
20. Tam, J. P., Lin, Y.-Z., Liu, W., Wang, D.-X., Ke, X.-H., and Zhang, J.-W. (1991) *Int. J. Pept. Protein Res.* 38, 204-211
21. Richter, A., Conlan, J. W., Ward, M. E., Chamberlin, S. G., Alexander, P., Richards, N. G. J., and Davies, D. E. (1992) *Biochemistry* 31, 9546-9554
22. Richter, A., Drummond, D. R., MacGarvie, J., Puddicombe, S. M., Chamberlin, S. G., and Davies, D. E. (1995) *J. Biol. Chem.* 270, 1612-1616
23. Kramer, R. H., Lenferink, A. E. G., van Bueren-Koornneef, I. L., van der Meer, A., van de Poll, M. L. M., and van Zoelen, E. J. J. (1994) *J. Biol. Chem.* 269, 8708-8711
24. Katsuura, M., and Tanaka, S. (1989) *J. Biochem. (Tokyo)* 106, 87-92
25. Hoepflich, P. D., Jr., Langton, B. C., Zhang, J., and Tam, J. P. (1989) *J. Biol. Chem.* 264, 19086-19091
26. Hoyt, D. W., Harkins, R. N., Debanne, M. T., O'Connor-McCourt, M., and Sykes, B. D. (1994) *Biochemistry* 33, 15283-15292
27. States, D. J., Haberkorn, R. A., and Ruben, D. J. (1982) *J. Magn. Reson.* 48, 286-292
28. Bodenhausen, G., Kolger, H., and Ernst, R. R. (1984) *J. Magn. Reson.* 58, 370-388
29. Kumar, A., Ernst, R. R., and Wuthrich, K. (1980) *Biochem. Biophys. Res. Commun.* 95, 1-6
30. Jeener, J., Meier, B. H., Bachmann, P., and Ernst, R. R. (1979) *J. Chem. Phys.* 71, 4546-4553
31. Delaglio, F., Grzesiek, S., Vuister, G. W., Zhu, G., Pfeifer, J., and Bax, A. (1995) *J. Biomol. NMR* 6, 277-293
32. Garrett, D. S., Powers, R., Gronenborn, A. M., and Clore, G. M. (1991) *J. Magn. Reson.* 95, 214-220
33. Campbell, A. P., and Sykes, B. D. (1993) *Annu. Rev. Biophys. Biomol. Struct.* 22, 99-122
34. Campbell, A. P., and Sykes, B. D. (1991) *J. Biomol. NMR* 1, 391-402
35. London, R. E., Perlman, M. E., and Davis, D. G. (1992) *J. Magn. Reson.* 97, 79-98
36. Engler, D. A., Montelione, G. T., and Niyogi, S. K. (1990) *FEBS Lett.* 271, 47-50
37. Chamberlin, S. G., Sargood, K. J., Richter, A., Mellor, J. M., Anderson, D. W., Richards, N. G. J., Turner, D. L., Sharma, R. P., Alexander, P., and Davies, D. E. (1995) *J. Biol. Chem.* 270, 21062-21067
38. Engler, D. A., Hauser, M. R., Cook, J. S., and Niyogi, S. K. (1991) *Mol. Cell. Biol.* 11, 2425-2431
39. Gullick, W. J. (1994) *Eur. J. Cancer* 30, 2186

XP-002190864

PROTEINS: Structure, Function, and Genetics, Suppl. 1:50-58 (1997)

Evaluation of Comparative Protein Structure Modeling by MODELLER-3

Roberto Sánchez and Andrej Šali*
The Rockefeller University, New York, New York

ABSTRACT We evaluate homology-derived 3D models of dihydrofolate reductase (DFR₁), phosphotransferase enzyme IIA domain (PTE2A₃), and mouse/human UBC9 protein (UBC9₂₄) which were submitted to the second Meeting on the Critical Assessment of Techniques for Protein Structure Prediction (CASP). The DFR₁ and PTE2A₃ models, based on alignments without large errors, were slightly closer to their corresponding X-ray structures than the closest template structures. By contrast, the UBC9₂₄ model was slightly worse than the best template due to a misalignment of the N-terminal helix. Although the current models appear to be more accurate than the models submitted to the CASP meeting in 1994, the four major types of errors in side chain packing, position, and conformation of aligned segments, position and conformation of inserted segments, and in alignment still occur to almost the same degree. The modest improvement probably originates from the careful manual selection of the templates and editing of the alignment, as well as from the iterative realignment and model building guided by various model evaluation techniques. This iterative approach to comparative modeling is likely to overcome at least some initial alignment errors, as demonstrated by the correct final alignment of the C terminus of DFR₁. *Proteins*, Suppl. 1:50-58, 1997.

© 1998 Wiley-Liss, Inc.

Key words: evaluation; comparative protein modeling; Modeller

INTRODUCTION

Protein modelers were challenged for the second time to model sequences without available 3D structures and to submit them to the CASP meeting in December 1996 (CASP; URL <http://PredictionCenter.llnl.gov/>). At the same time, the 3D structures were being determined by X-ray crystallography and NMR methods. Because the experimentally determined structures were only released at the meeting, it was possible to test the modeling methods objectively. A summary of all comparative models submitted to CASP2 can be found elsewhere in this issue (A.C.R. Martin et al.).

© 1998 WILEY-LISS, INC.

We submitted homology-derived models of three proteins: DFR₁, PTE2A₃, and UBC9₂₄; the subscript indicates the target sequence number assigned by the organizers of CASP2. All three structures have been determined by X-ray crystallography: DFR₁ at 2.6 Å resolution and R factor of 18% (U. Pieper and O. Herzberg, in preparation), PTE2A₃ at 2.4 Å resolution (K. Huang and O. Herzberg, in preparation) and UBC9₂₄ at 2.0 Å resolution and R factor of 16% (H. Tong and T. Sixma, in preparation). These three target sequences were chosen because they have a relatively low, <43% sequence identity with their templates. In this range of sequence similarity, the largest errors in comparative modeling due to misalignments begin to appear.^{1,2} It is important to concentrate on this range of sequence similarity because most of the detectable related sequence-structure pairs are related at less than 40% sequence identity level,³ despite earlier indications to the contrary.⁴

Our approach to comparative protein structure modeling is based on satisfaction of spatial restraints and is implemented in program Modeller.^{†5} This program can be used in all stages of typical comparative modeling: Finding suitable template structures in the PDB,⁶ aligning them with the sequence to be modeled, calculating the 3D model, and evaluating the model. Comparative protein modeling was recently reviewed.^{7,8}

[†]Modeller is available at URL <http://guitar.rockefeller.edu:pub/modeller> and also as part of Quanta and InsightII (MSI, San Diego, CA. E-mail: blp@msi.com).

Abbreviations: DFR₁, *Haloferax volcanii* dihydrofolate reductase; PTE2A₃, *Mycoplasma capricolum* phosphotransferase enzyme IIA domain; UBC9₂₄, mouse/human UBC9 protein; NMR, nuclear magnetic resonance; PDB, Brookhaven Protein Data Bank; RMSD, root-mean-square deviation; 3D, three-dimensional; CASP, critical assessment of techniques for protein structure prediction.

Contract grant sponsor: National Institutes of Health; Contract grant number: GM 54762; Contract grant sponsor: National Science Foundation; Contract grant number: BIR-9601845.

*Correspondence to: A. Šali, The Rockefeller University, 1230 York Avenue, New York, NY 10021.

E-mail: sali@rockvax.rockefeller.edu

Received 8 May 1997; Accepted 26 August 1997

In this article, we briefly describe the modeling method and then concentrate on evaluation of the three submitted models. In particular, we discuss the question of whether or not the models are generally closer to the X-ray structure being modeled than the template structures.

METHODS

The first step in comparative modeling of the three target proteins was identification of potential template structures. This was followed by several cycles of template selection, target-template alignment, model building, and model evaluation. The aim of the iteration was to minimize the errors in the model reported by various model evaluation techniques. This iterative process, including careful manual selection of the templates and editing of the alignments, is the main difference between the current approach and that followed two years ago for the CASP1 meeting.² The final alignments and 3D models are available from the CASP2 Web site at URL http://PredictionCenter.llnl.gov/CASP/CM_results/.

Template Selection

Proteins that have known 3D structure and are similar to the sequences being modeled had to be identified. This was achieved by searching a set of sequences representative of the whole PDB (July 1, 1996) [6], using the `SEQUENCE_SEARCH` command of Modeller.⁹ The representative set of protein structures included 916 chains whose sequence identity was less than 30% to any other chain in the set. The final templates were as follows: For DFR₁, 4DFR-B (30%, 1.4 Å, 91%), 3DFR (24%, 1.5 Å, 93%), and 8DFR (22%, 1.6 Å, 94%); for PTE2A₃, 1GPR (43%, 1.3 Å, 94%) and 1F3G (36%, 1.1 Å, 94%); and for UBC9₂₄, 1AAK (35%, 1.1 Å, 90%) and 2UCE (30%, 1.2 Å, 90%). The numbers in the parentheses are the percentage sequence identity, RMSD for C α atoms, and the fraction of the equivalent C α atoms. These were all obtained from pairwise template-target least-squares superpositions with a 3.5 Å cutoff.

Target-Template Alignment

Initial multiple template-target alignments were obtained by aligning the target sequences with the prealigned template structures, using the `ALIGN2D` command of Modeller.⁹ This command implements a global dynamic programming¹⁰ algorithm with a variable gap-penalty function that depends on the structural context of an insertion or a deletion (R. Sánchez and A. Šali, in preparation). The gap penalty is constructed such that insertions and deletions are less preferred within helices and sheets, buried regions, straight segments, and also between two residues that are distant in space. The alignments also depended on a 20 × 20 amino acid residue substitution matrix that was derived from 105 struc-

ture-structure alignments.⁴ The initial calculations were edited by hand as appropriate (below).

Model Building

The 3D models containing all nonhydrogen atoms were obtained automatically by satisfying restraints on many distances, angles, and dihedral angles. Spatial restraints were extracted from the alignment of the target sequence with the template structures^{4,5} and from the Charmm-22 force field. The whole model, including backbone, side chains, loops, and insertions, was built in one optimization. Conformation of the regions aligned with the templates was based mostly on the template structure, while the insertions were restrained mostly by preferences of the different residue types for different areas of the Ramachandran plot.

Model Evaluation

The models had to satisfy most restraints used to calculate them, especially the stereochemical restraints. These tests were done by the Model `ENERGY` command,⁹ the Procheck program,¹² and the WhatCheck program.¹³ The most important evaluation was done by "energy" profiles calculated by ProsaII, which relies on statistical potentials involving single residues and pairs of residues. Additional evaluation was done by "energy" profiles calculated from a new set of statistical potentials involving pairs of atoms.¹⁵ Side chain packing was checked by calculating cavities in the core of protein, using the Quanta Protein Health module (MSI, San Diego, CA). If any of the model evaluation tools indicated an error in the model, the model was changed manually. For example, side chains were manually repositioned to eliminate a cavity in the core. Another example is a selection of different templates and editing of the alignment around the region with a bad ProsaII profile, followed by another round of the automated model building.

RESULTS AND DISCUSSION

Although the DFR₁, UBC9₂₄, and PTE2A₃ models have good stereochemistry, they have errors in four other categories: Distortions or shifts of a region that is aligned correctly with the templates (e.g., loops, helices, strands); errors in side chain packing; distortions or shifts of a region that does not have an equivalent segment in any of the templates (e.g., inserted loops); and distortions or shifts of a region that is aligned incorrectly with the templates (e.g., loops and larger segments with low sequence identity to the templates). Examples of these errors are described in the following sections. We also discuss the lessons learned from this experiment with respect to automated template mimicking in different regions of a model; the cycle of template selection, alignment, model building, and model evaluation.

and the relative overall similarity of a model and the templates to the target X-ray structure.

Stereochemistry of the Models

The stereochemical features of the models, such as those evaluated by the Procheck¹² and WhatCheck¹³ programs, are comparable to those in the high resolution X-ray structures. These features include bond lengths, angles, improper dihedral angles, position of residues in the Ramachandran plot, peptide bonds planarity, C α tetrahedral distortion, non-bonded interactions, hydrogen bond energies, and closeness of side chain dihedral angles to ideal values. It is not surprising that the models are stereochemically correct since they were calculated partly by optimizing the stereochemical features as encoded in the Charmm-22 force field.¹¹

Errors in Side Chain Packing

The side chain rotamers were predicted surprisingly inaccurately. For example, the percentage of χ_1 angles for DFR₁, PTE2A₃, and UBC9₂₄ predicted within 30° of the target values was 42%, 48%, and 65%, respectively. Since at least the UBC9₂₄ X-ray structure has been refined at a high resolution of 2 Å and an R factor of 16%, the low prediction accuracy must reflect significant problems with our side chain modeling procedure in this range of backbone and side chain similarities. However, the mistakes made were not trivial because the models followed their templates for conserved and similar side chains, because the model rotamers were not distorted, and because the cavities in the models were not larger than those in the X-ray structures. It is not clear what kind of improvements are needed beyond a self-evident need for a more accurate energy function and perhaps a better optimizer.

The difficulty of the side chain modeling problem in this range of sequence similarity is illustrated by the fact that the template and target X-ray structures have different rotamers for up to 45% of the conserved residues. For example, DFR₁ has 125 residues with at least one side chain dihedral angle, 29 of which are conserved in one of the templates (PDB code 3DFR), but 12 of these occur in different rotamer states. A systematic analysis of this phenomenon, based on highly refined structures, would be useful. If the target and template X-ray structures are accurate and the finding proves to be general, this indicates that the side chains should be modeled on the basis of more general physical principles¹⁶⁻¹⁹ rather than by mimicking the templates,^{20,21} especially when the backbones of the target and the template have an RMSD larger than 2 Å. An additional complication for the evaluation of side chain models is that for the two targets refined at a low resolution of 2.6 Å (DFR₁) and 2.4 Å (PTE2A₃), it is not clear that all the differences between the models

and the X-ray structures are due to the mistakes in the modeling procedure.²²

Distortions or Shifts in Correctly Aligned Regions: Template Mimicking in Different Regions of a Model

For all three models, at least two template structures were used. Thus, it was possible to determine how frequently the automated model building selected the best template for a given segment where the templates shared different degrees of structural similarity with the target structure. The ability to pick locally optimal templates is important because it allows the model to be overall closer to the correct structure than any of the individual templates.

The distances of the positions of the C α atoms of the model and the templates from the equivalent atoms in the superposed target X-ray structure are shown for DFR₁ and UBC9₂₄ in Figure 1. For the correctly aligned regions, the model always follows one of the templates. When two templates differ in a given correctly aligned region, the model generally follows the template that is structurally closer to the experimental structure: Six such segments of at least three residues with distances between the templates of at least 1 Å occur in the DFR₁ and UBC9₂₄ models. For the correctly aligned regions, there are no examples of the model following a suboptimal template. As a consequence, the model is generally closer overall to the experimental structure than any of the templates (see also Fig. 4). However, for a given region, model building does not result in a model that is better than the best template in that region (Fig. 1).

These observations are a direct consequence of the form of the homology-derived distance restraints.^{4,5} The restraints are expressed as probability density functions. When several templates are aligned with a given segment in the target sequence, a restraint on an inter- or intrasegment distance has a multimodal shape with the peaks corresponding to the equivalent distances in the templates, not to the average distance. The heights and the widths of the peaks are determined by the overall and local sequence similarities between the templates and the target sequence, such that the model is most likely to resemble the template with the most similar sequence. This means that the model is generally closer to one or the other template by construction. In order to allow for the modeling of distortions or shifts relative to the template structures, a scoring function that guides the model in the correct direction from the template to the target structure is necessary. A combination of homology-derived restraints with atom based statistical potentials^{15,23-25} is perhaps one way of achieving this aim.

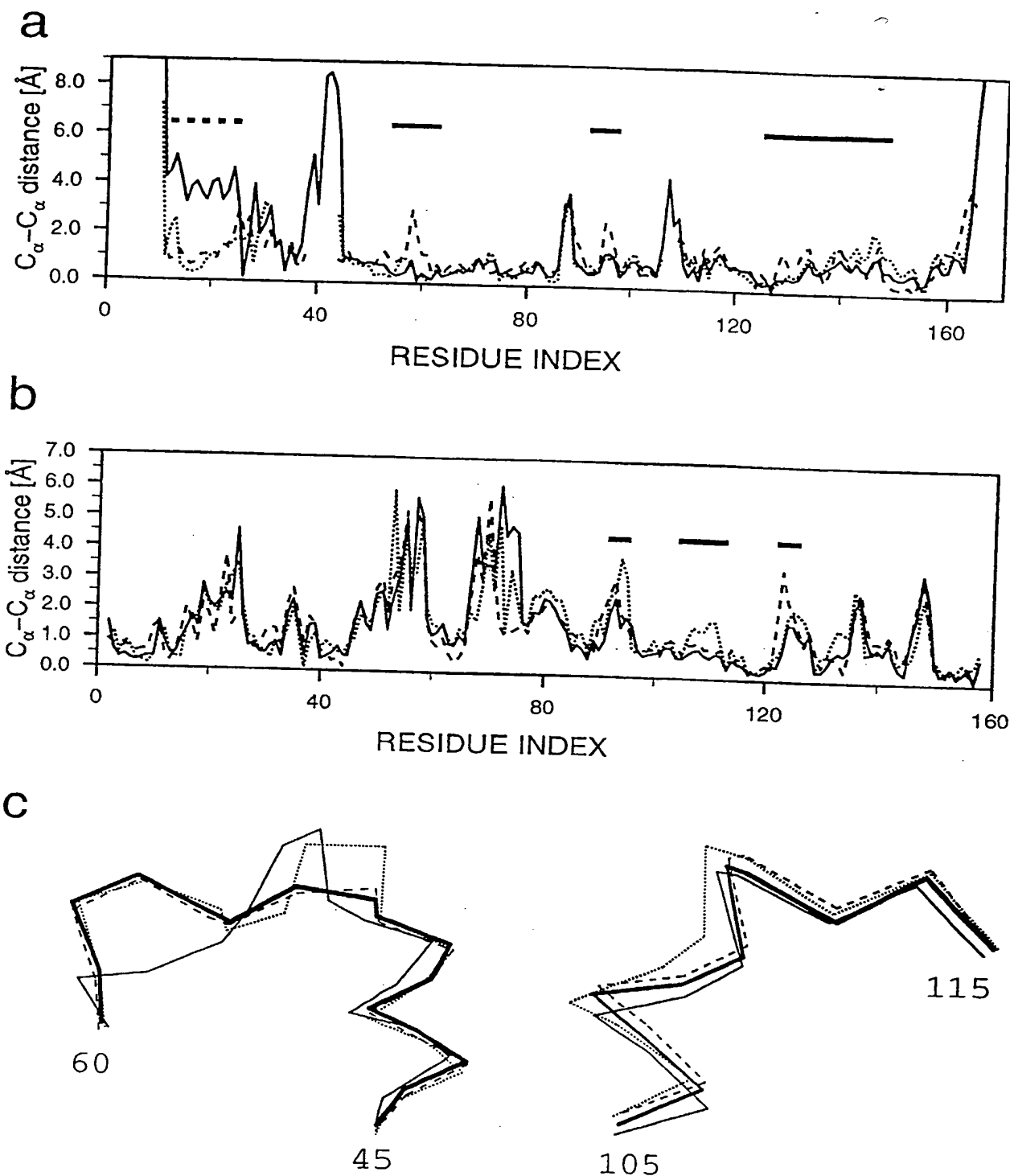


Fig. 1. Backbone errors in the UBC9₂₄ (a) and DFR₁ (b,c) models. The models and the templates are superposed as rigid bodies on the corresponding target structures using a cutoff of 3.5 Å for the equivalent C_α atoms. A curve in (a) and (b) shows the distances of the C_α atoms in the model and the templates from the equivalent atoms in the target. (a) UBC9₂₄ model - target, continuous line; template 2UCE-target, dashed line; template 1AAK-target, dotted line. (b) DFR₁ model-target, continuous line; template 4DFR-B-target, dashed line; template 3DFR-target, dotted

line. The horizontal continuous lines above the curves indicate the correctly aligned segments of at least three residues where the best template was chosen for the model. The horizontal dashed line at the N terminus in (a) indicates the 11 misaligned residues of UBC9₂₄. (c) Superposition of residues 45-60 and 105-115 of the DFR₁ model with the corresponding regions in the templates and the X-ray structure. The model, thick continuous line; X-ray structure, thin continuous line; template 3DFR, dotted line; template 4DFR-B, dashed line.

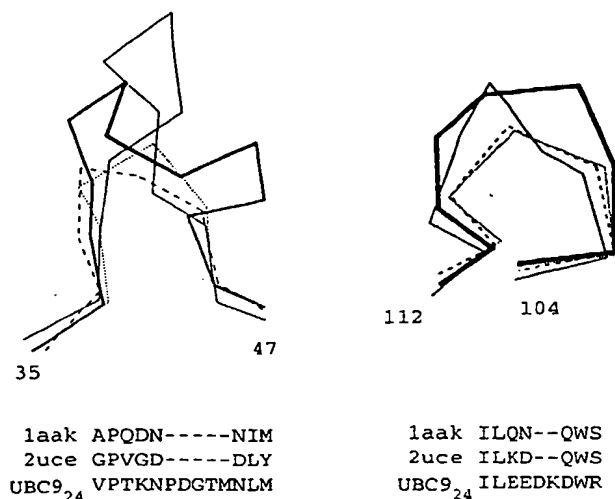


Fig. 2. Errors in the two UBC9₂₄ loop models. The loops corresponding to the two insertions in the UBC9₂₄ model (*continuous thick line*) are shown superposed with the target X-ray structure (*continuous thin line*), the templates 1AAK (*dotted line*), and 2UCE (*dashed line*). The numbers indicate the beginning and ending residues of each segment in UBC9₂₄. The corresponding regions of the modeling alignment are shown below each set of the structures.

Errors in Loops

There were only two insertions in the three models, both of them in UBC9₂₄ (Fig. 2). The longest insertion was only five residues long (residues 40–44), and the second insertion was two residues long (residues 108–109). When the whole model was superposed on the X-ray structure, the RMSD between the backbones for the five-residue loop was 6.7 Å; when the backbones of only the two loops were superposed locally, the RMSD was 1.7 Å. Thus, both the orientation and conformation of the predicted loop were incorrect. The large difference between the two numbers shows that the positioning of the loop relative to the rest of the protein can be a very important contributor to the total error even in the case of relatively short loops. The alignment in the neighborhood of the loop was correct, except perhaps

for the alignment of residue 39, which probably should not have been aligned with any residue in the templates (Fig. 2). The RMSD for the backbones of the three residues preceding (37–39) and the three residues following the loop (45–47) was 2.3 Å and 1.5 Å for the global and local superposition, respectively. The average backbone isotropic temperature factors for the five- and two-residue insertions were 24.4 Å² and 22.2 Å², respectively, compared to the slightly

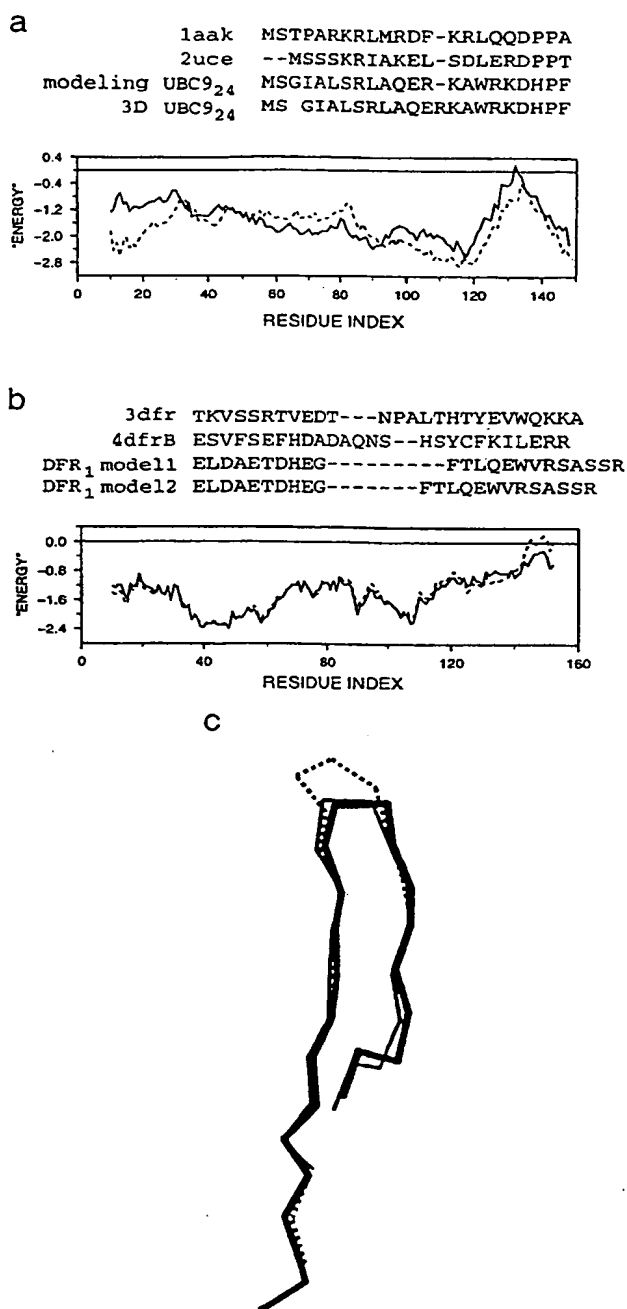
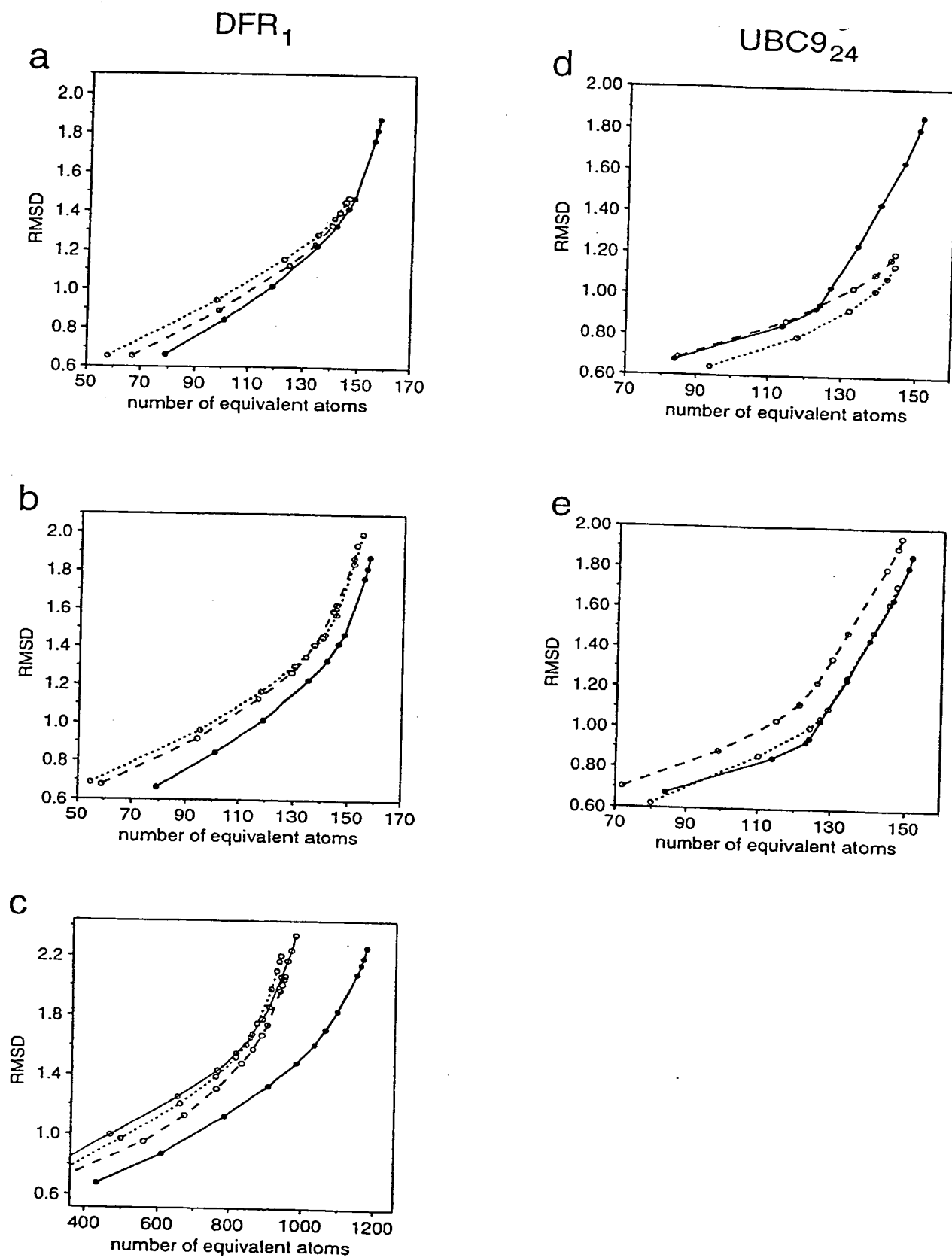


Fig. 3. Alignment problems and solutions. (a) Alignment of the N-terminal region of UBC9₂₄. The alignment used for model building (modeling) and the correct alignment derived from the superposition of the experimental structures of the templates and the target (3D) are shown. The Prosall energy profiles for the model (*continuous line*) and the target X-ray structure (*dashed line*) are shown below the alignment. Note the lower energy of the X-ray structure in the misaligned region. (b) The correct and alternative alignments for the C-terminal region of DFR₁. The Prosall energy profiles for the corresponding 3D models are shown below the alignment. The model based on the correct DFR₁ alignment, *continuous line*; the model based on the alternative alignment, *dashed line*. Note the positive energy for the alternative model in the C-terminal region. (c) Superposition of the C-terminal region of the correct (*continuous line*) and alternative model of DFR₁ (*dashed line*) with the X-ray structure (*thin line*).



lower average of 16.4 \AA^2 for the backbone of the whole protein. Thus, if the loops are not in contact with other protein molecules in the crystal, it is likely that the differences between the insertions in the crystal structure and the model reflect errors in the model.

Distortions or Shifts in Incorrectly Aligned Regions: The Cycle of Alignment, Model Building, and Model Evaluation

In the three models, there was only one secondary structure segment that was misaligned, the N-terminal helix of UBC9₂₄. In addition, there were three, zero, and one gaps in the modeling alignments for DFR₁, UBC9₂₄, and PTE2A₃, respectively, where one or a few residues were misaligned.

In the UBC9₂₄ model, the N-terminal segment of 11 residues was misaligned by one position, which resulted in large errors in the model (Fig. 1a). This misalignment was unexpected because the correct alignment corresponded to a significantly lower sequence similarity between the target and the template (Fig. 3a). For example, the number of matches between hydrophobic residues is decreased and the number of matches between hydrophobic and polar residues is increased when the incorrect alignment is corrected. The misalignment was not detected by the ProsaII profile of the model (Fig. 3a). However, the comparison of the profiles for the X-ray structure and the model shows that the X-ray structure has a lower ProsaII score in that region (Fig. 3a). This suggests that the search for the alignment with the lowest ProsaII profiles of the implied model could conceivably result in the correct alignment and thus a significantly better model in this case.

Another interesting observation is that the overall sequence identity between the target sequence and the more similar of the two templates dropped from 39% to 35% for the correct alignment. This makes the point that optimizing only sequence similarity is not always best in comparative modeling.

In the DFR₁ model, it was obviously difficult to align the last 13 residues, corresponding to the last strand of the last β hairpin (Fig. 3). Two plausible alternative alignments were generated manually by taking into account local sequence similarity, secondary structure predictions for DFR₁,²⁶⁻²⁸ and the

structures of the template proteins. The alignments were evaluated by comparing the ProsaII profiles of the models based on those alignments (Fig. 3b). One of the models had a positive profile, and the other one had a negative profile at the C terminus. A comparison of the two models with the X-ray structure showed that the model with the negative profile was indeed correctly aligned with the template (Fig. 3c).

As illustrated above, alignment errors are a major source of large errors in comparative models. We attempted to overcome this limitation by iterating through several cycles of careful manual template selection and alignment, followed by automated model building and model evaluation. This process was guided by a reduction in the errors predicted by a number of model evaluation techniques, most importantly the "energy" profiles calculated by the ProsaII program and a program of Melo and Feytmans.¹⁵ Despite our limited experience, we believe that evaluation of an alignment at the level of the implied model is likely to overcome a significant fraction of initial alignment errors, especially when better potential functions for model evaluation become available and when the iterative procedure is automated so that a larger number of alternative alignments can be explored.²⁹

Overall Accuracy of the Models: Relative Overall Similarity of a Model and the Templates to the Target X-ray Structure

We now wish to answer the question of whether the predicted structures are a better model of the experimental structures than the templates used in the calculation of the models. In other words, how much closer is a comparative model of the target sequence to the target X-ray structure than the closest template structure?

Although a single RMSD value is useful for measuring a difference between two relatively similar structures, RMSD depends on the number of equivalent atom pairs that are compared, which in turn depends on the maximal allowed distance between two equivalent atoms. This makes a single RMSD value inconvenient for comparing differences between pairs of different proteins. One solution to this problem is to define a *similarity curve* for a pairwise structure-structure comparison by plotting RMSD as a function of the number of equivalent atoms. The similarity curve is obtained by calculating RMSD at different cutoff values for equivalencing intermolecular pairs of C α atoms and plotting the resulting RMSD values against the number of equivalent positions obtained at each cutoff. Two similarity curves, instead of two single RMSD numbers, can then be inspected for a comparison of two protein-protein matches.

The similarity curves for the three pairwise comparisons of the DFR₁ model and the two templates with the target structure are plotted in Figure 4a. The curves show that over a large range of the

Fig. 4. Similarity curves for the DFR₁ (a, b, c) and UBC9₂₄ (d, e) models and templates. See the Methods section for the definition of the similarity curves. (a and d) The optimal superposition of the templates and the X-ray structure was used to define the equivalent residues. (b, c, and e) The modeling alignment was used to define the equivalences between the templates and the target. (a), (b), (d), and (e), only the C α atoms are used to calculate RMSD. (c) All atoms are used to calculate RMSD. Model-target, *thick continuous line*; template 4DFR-B-target and template 2UCE-target, *dashed line*; template-target and template 1AAK-target, *dotted line*; template 8DFR-target, *thin continuous line*.

number of equivalent atoms, the model is slightly closer to the experimental structure (lower RMSD value) than either of the two templates. In other words, at a fixed number of atoms compared, the model atoms have a lower RMSD from the X-ray structure than the template atoms; conversely, at a fixed RMSD, the model has more atoms equivalent to the X-ray structure than either of the templates. However, the differences are small, <10% over most of the similarity range.

Errors in the positioning of three gaps in the DFR₁ modeling alignment contributed to the similarity curve for the model-target comparison, but not to the template-target similarity curves in Figure 4a, which were obtained from the superposition of the crystallographic structures. In order to eliminate the contribution of the alignment errors and evaluate the model building procedure on its own, the similarity curves were recalculated using the modeling alignment for comparison of the templates with the target structure (Fig. 4b). Since the template-target comparisons now include the alignment errors, the templates are less similar to the target X-ray structure than in Figure 4a. However, the difference in how representative of the target structure are the model and the templates is still small, on the order of 10% of RMSD.

When side chain atoms were included in the calculation of the similarity curves, the DFR₁ model became an even better representation of the target structure relative to the templates (Fig. 4c). For example, the model had approximately 95% of its atoms superposed with an RMSD from the target structure of 2 Å, while the closest template only had 78% of the atoms at that level of similarity (Fig. 4c). This was expected because the templates do not share all the side chain atoms with the target structure while the model does.

In contrast to DFR₁, the UBC9₂₄ model is worse than the best template because of the alignment errors, primarily the shift for one position of the N-terminal 11 residues (Fig. 4d). The PTE2A₃ model is as close to the target structure as the best template (data not shown).

All comparative modeling methods start with an alignment of the target sequence with the template structures, followed by model building that is decoupled from the alignment procedure. Therefore, when evaluating comparative modeling methods, it is important for method developers to distinguish between errors due to misalignments and errors due to the model building procedure. This distinction is also important for the method users because the modeling alignment, not the correct alignment, would be used to extract information from the template structure in the absence of any model building. When the modeling alignment is used to compare both the model and the templates with the target structure, all three models are a better representa-

tion of the experimental structure than the templates used in their derivation (Fig. 4b,e; data not shown for PTE2A₃). This is especially true when the side chain as well as backbone atoms are compared (e.g., Fig. 4c). These comparisons suggest that it is better to use a comparative model of the target than homologous structures, unless only coarse predictions are made.

CONCLUSIONS

The modest improvement in our models relative to CASP1 probably originates from the careful manual selection of the templates and editing of the alignment, as well as from the iterative re alignment and model building. This suggests directions for future development of the algorithms that will, it is hoped, result in larger increases in the model accuracy.^{5,29-31}

ACKNOWLEDGMENTS

We thank crystallographers U. Pieper, O. Herzberg, K. Huang, H. Tong and T. Sixma for providing the structures before their release to the PDB, and F. Melo and E. Feytmans for evaluating our models with their evaluation program. R.S. is a Howard Hughes Medical Institute predoctoral fellow. A.S. is a Sinsheimer Scholar.

REFERENCES

1. Delbaere, L.T.J., Brayer, G.D., James, M.N.G. Comparison of the predicted model of fl-lytic protease with the x-ray structure. *Nature* 279:165-168, 1979.
2. Sali, A., Potterton, L., Yuan, F., van Vlijmen, H., Karplus, M. Evaluation of comparative protein modeling by MODELLER. *Proteins* 23:318-326, 1995.
3. Rost, B. Protein structures sustain evolutionary drift. *Folding Design* 2:S19-S24, 1997.
4. Sali, A. and Overington, J. Derivation of rules for comparative protein modeling from a database of protein structure alignments. *Protein Sci.* 3:1582-1596, 1994.
5. Sali, A., Blundell, T.L. Comparative protein modelling by satisfaction of spatial restraints. *J. Mol. Biol.* 234:779-815, 1993.
6. Abola, E.E., Bernstein, F.C., Bryant, S.H., Koetzle, T., Weng, J. Protein data bank. In: "Crystallographic Databases: Information, Content, Software Systems, Scientific Applications." Allen, F.H., Bergerhoff, G., Sievers, R., eds. Bonn: Data Commission of the International Union of Crystallography, 1987:107-132.
7. Johnson, M.S., Srinivasan, N., Sowdhamini, R., Blundell, T.L. Knowledge-based protein modelling. *CRC Crit. Rev. Biochem. Mol. Biol.* 29:1-68, 1994.
8. Sánchez, R., Sali, A. Advances in comparative protein-structure modeling. *Curr. Opin. Str. Biol.* 7:206-214, 1997.
9. Sánchez, R., Sali, A. Modeller, A Protein Structure Modeling Program, Release 3. URL <http://guitar.rockefeller.edu/>, 1995.
10. Needleman, S.B., Wunsch, C.D. A general method applicable to the search for similarities in the amino acid sequence of two proteins. *J. Mol. Biol.* 48:443-453, 1970.
11. Brooks, B.R., Brucoleri, R.E., Olafson, B.D., States, D.J., Swaminathan, S., Karplus, M. CHARMM: A program for macromolecular energy minimization and dynamics calculations. *J. Comp. Chem.* 4:187-217, 1983.
12. Laskowski, R.A., McArthur, M.W., Moss, D.S., Thornton, J.M. PROCHECK: A program to check the stereochemical quality of protein structures. *J. Appl. Crystallogr.* 26:283-291, 1993.

13. Hooft, R., Vriend, G., Sander, C., Abola, E. Errors in protein structures. *Nature* 381:272, 1996.
14. Sippl, M.J. Recognition of errors in three-dimensional structures of proteins. *Proteins* 17:355-362, 1993.
15. Melo, F., Feytmans, E. Novel knowledge-based mean force potential at atomic level. *J. Mol. Biol.* 267:207-222, 1997.
16. Koehl, P., Delarue, M. Application of a self-consistent mean field theory to predict protein side-chains conformation and estimate their conformational entropy. *J. Mol. Biol.* 239: 249-275, 1994.
17. Lee, C. Predicting protein mutant energetics by self consistent ensemble optimisation. *J. Mol. Biol.* 236:918-939, 1994.
18. Maeyer, M.D., Desmet, J., Lasters, I. All in one: A highly detailed rotamer library improves both accuracy and speed in the modelling of side chains by dead-end elimination. *Folding Design* 2:53-66, 1997.
19. Chung, S.Y., Subbiah, S. A structural explanation for the twilight zone of protein sequence homology. *Structure* 4:1123-1127, 1996.
20. Sutcliffe, M.J., Hayes, F.R.F., Blundell, T.L. Knowledge based modeling of homologous proteins, Part II: Rules for the conformation of substituted side-chains. *Protein Eng.* 1:385-392, 1987.
21. Summers, N.L., Karplus, M. Construction of side-chains in homology modelling: Application to the C-terminal lobe of rhizopuspepsin. *J. Mol. Biol.* 210:785-811, 1989.
22. Bower, M.J., Cohen, F.E., Dunbrack, R.L. Prediction of protein side-chain rotamers from a backbone-dependent rotamer library: A new homology modeling tool. *J. Mol. Biol.* 267:1268-1282, 1997.
23. Miyazawa, S., Jernigan, R.L. Estimation of effective inter-residue contact energies from protein crystal structures: Quasi-chemical approximation. *Macromolecules* 18:534-552, 1985.
24. Sippl, M.J. Calculation of conformational ensembles from potentials of mean force: An approach to the knowledge-based prediction of local structures in globular proteins. *J. Mol. Biol.* 213:859-883, 1990.
25. DeBolt, S.E., Skolnick, J. Evaluation of atomic level mean force potentials via inverse folding and inverse refinement of protein structures: Atomic burial position and pairwise nonbonded interactions. *Protein Eng.* 9:937-955, 1996.
26. Rost, B., Sander, C. Prediction of protein structure at better than 70% accuracy. *J. Mol. Biol.* 232:584-599, 1993.
27. Biou, V., Gibrat, J.-F., Levin, J., Garnier, J. Secondary structure prediction: Combination of three different methods. *Protein Eng.* 2:185-191, 1988.
28. Chandonia, J.M., Karplus, M. The importance of larger data sets for protein secondary structure prediction with neural networks. *Protein Sci.* 5:768-774, 1996.
29. Guenther, B., Onrust, R., Šali, A., O'Donnell, M., Kuriyan, J. Crystal structure of the δ' subunit of the clamp-loader complex of *E. coli* DNA polymerase III. *Cell* 91:335-345, 1997.
30. Šali, A. Modelling mutations and homologous proteins. *Curr. Opin. Biotech.* 6:437-451, 1995.
31. Šali, A. Protein modeling by satisfaction of spatial restraints. *Mol. Med. Today* 1:270-277, 1995.
32. Sánchez, R., Šali, A. Comparative protein modeling as an optimization problem. *J. Mol. Struct. (Theochem)* 398:469-496, 1997.

THIS PAGE BLANK (USPTO)

**This Page is Inserted by IFW Indexing and Scanning
Operations and is not part of the Official Record**

BEST AVAILABLE IMAGES

Defective images within this document are accurate representations of the original documents submitted by the applicant.

Defects in the images include but are not limited to the items checked:

- ☒ BLACK BORDERS
- ☐ IMAGE CUT OFF AT TOP, BOTTOM OR SIDES
- ☐ FADED TEXT OR DRAWING
- ☐ BLURRED OR ILLEGIBLE TEXT OR DRAWING
- ☐ SKEWED/SLANTED IMAGES
- ☒ COLOR OR BLACK AND WHITE PHOTOGRAPHS
- ☐ GRAY SCALE DOCUMENTS
- ☐ LINES OR MARKS ON ORIGINAL DOCUMENT
- ☐ REFERENCE(S) OR EXHIBIT(S) SUBMITTED ARE POOR QUALITY
- ☐ OTHER: _____

IMAGES ARE BEST AVAILABLE COPY.

As rescanning these documents will not correct the image problems checked, please do not report these problems to the IFW Image Problem Mailbox.

THIS PAGE BLANK (USPTO)